

Synthetic Studies Towards the Total Synthesis of Lancifodilactone G

Sanil Sreekumar

*Thesis submitted in accordance with the requirements for the degree
of
Doctor of Philosophy*



UNIVERSITY OF
LIVERPOOL

**Department of Chemistry
May 2011**

Doctoral Committee
23rd August 2011

Professor P. Andrew Evans
University of Liverpool, U.K.

Professor Steven V. Ley
University of Cambridge, U.K.

Professor Paul M. O'Neill
University of Liverpool, U.K.

**This thesis is dedicated to Sri Sathya Sai Institute of Higher Learning in deepest
gratitude for free university education**

Acknowledgements

First and foremost, I would like to thank my supervisor Prof. P. Andrew Evans for five years of rewarding collaboration and for his confidence in me to work on this project. I am grateful for being given the opportunity to work in his research group. He has had a tremendous impact on my growth and development as a scientist and I am truly indebted to him for that.

I am grateful to the University of Liverpool for the International Student Fellowship and for the financial support from my supervisor during the entire course of my studies in the U.K.

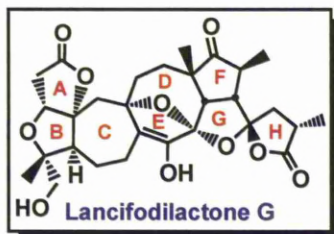
I would like to acknowledge the entire Evans group, both past and present members, for making my stay memorable in Liverpool. I would like to thank Dr. Pramod Kumar Sahu and Dr. Stephen Atkinson for my laboratory training. A special thanks to Mrs. Katie Evans for her help and support with the paperwork and other administrative issues during my studies. I would like to extend my gratitude to everyone in the department who helped me with their expertise.

I would like to thank Phillip A. Inglesby, Helen Laidlaw, Mu-hua Huang, Deju Shang, Sergio Maroto, Ryan O'Connor and my supervisor for proofreading of this thesis and providing helpful suggestions.

Finally, I would like to thank my parents, relatives, teachers and friends for their support and encouragement during the best and worst of times.

Abstract

Synthetic Studies Towards the Total Synthesis of Lancifodilactone G



This thesis presents our studies towards the first total synthesis of the novel *anti*-HIV agent lancifodilactone G, which has a highly unusual aliphatic enol. The first chapter provides a survey of architecturally diverse nortriterpenoids that were isolated from the Schisandraceae family. A proposed biosynthetic pathway for lancifodilactone G and closely related natural products provides a rationale for the formation of the consecutive 7/8/5 fused carbocycles that are unique to *Schisandra* nortriterpenoids. Chapter 1 goes on to outline the reported strategies to access the core of lancifodilactone G and concludes with a retrosynthetic analysis proposed by the Evans group, which includes a biosynthetically inspired single-pot polycyclisation reaction.

Chapter 2 describes the highly stereocontrolled synthesis of the eastern fragment (F-G rings) using transition metal-mediated Pauson-Khand reaction. This chapter also reviews the metal-mediated diastereoselective Pauson-Khand reaction directed by the stereogenic centre at C2, with the ample illustration to total synthesis. Attempted strategies for the assembly of the bicyclic cyclopentanone motif *via* a dienyl Pauson-Khand reaction of silicon- and oxygen-tethered diene-enes are presented. The failure of these strategies at different stages of the synthesis resulted in the exploration of a classical Pauson-Khand approach, which successfully furnished the eastern fragment. Finally, a second-generation synthesis is

described which provided the fully functionalised eastern fragment with improved efficiency and overall yield.

Chapter 3 discusses the successful synthesis of the western fragment (B-C rings) using a diastereoselective [4+3] cycloaddition strategy. Attempted strategies for the synthesis of the key 2,3-disubstituted furan derivative are presented, which was achieved *via* a hetero Pauson-Khand reaction. This chapter includes a brief account of the classical [4+3] cycloaddition reactions of furans using an *in situ* generated oxyallyl cation and also employing vinyl carbenoids in the metal-catalysed version. The review also highlights the application of the [4+3] cycloaddition reaction in the expeditious assembly of functionalised 7-membered rings that occur in a number of important biologically active natural products. The third chapter goes on to describe the application of these cycloaddition reactions in the synthesis of the fully functionalised western fragment of Lancifodilactone G.

Chapter 4 describes a model study aimed at expediting the synthesis of the western fragment using a rhodium-catalysed allylic substitution reaction. A brief mechanistic discussion on unique aspects of the allylic alkylation reaction is illustrated. Chapter 4 concludes by outlining the coupling strategy for eastern and western fragments and the end game studies for the completion of the synthesis of lancifodilactone G.

<i>Abstract</i>	v
<i>List of Schemes</i>	xii
<i>List of Figures</i>	xvii
<i>List of Tables</i>	xviii
<i>List of Abbreviations</i>	xix

Chapter 1

Nortriterpenoids Isolated From the Genus *Schisandra* and Studies Towards the Total Synthesis of Lancifodilactone G

1.1	Introduction	1
1.1.1	Types of <i>Schisandra</i> Nortriterpenoids	2
1.1.2	Schisanartane Type	2
1.1.3	Schiartane Type	4
1.1.4	18-Norschiartane and 18(13→14)- <i>abeo</i> -Schiartane Types	4
1.1.5	Pre-schisanartane and Wuweiziartane Types	5
1.2	Proposed Biosynthetic Route for Lancifodilactone G and for Related Schisanartane Type of Nortriterpenoids	6
1.3	Insights into the Stability of the Aliphatic Enol Functionality at the core of Lancifodilactone G	7
1.4	Synthetic Approaches Towards the Core of Lancifodilactone G	8
1.4.1	The Paquette's Approach	8
1.4.2	Anderson's Approach	13
1.5	Original Retrosynthetic End Game for Lancifodilactone G	15
1.6	References	17

Chapter 2

Synthesis of the Eastern Fragment (F-G Rings) of Lancifodilactone G

2.1	Introduction	19
2.1.1	Previous Synthetic Work	19
2.1.1.1	The Paquette Approach	19
2.2	Results and Discussion	22
2.2.1	Retrosynthetic Analysis	22
2.3	An Overview on the Metal-Mediated Diastereoselective Pauson-Khand Reaction	23
2.3.1	Stoichiometric Cobalt-Mediated PK Reaction	23
2.3.1.1	Proposed Mechanism for the Cobalt-Mediated PK Reaction	24
2.3.1.2	Diastereoselectivity in Cobalt-Mediated PK Reaction	25
2.3.2	Stoichiometric Molybdenum-Mediated PK Reaction	27
2.3.3	Transition Metal-Catalysed Diastereoselective PK Reaction	27
2.3.3.1	Cobalt-Catalysed PK Reaction	27
2.3.3.2	Rhodium-Catalysed PK Reaction	28
2.3.3.2.1	Diastereoselectivity in Rhodium(I)-Catalysed PK Reaction	29
2.3.3.3	Other Transition Metal-Catalysed PK Reaction	33
2.4	Temporary Silicon-Tethered Approach	35
2.4.1	Contributions from the Evans Group	35
2.4.1.1	TST-RCM Cross-Coupling Reaction	35
2.4.1.2	Rhodium-Catalysed TST-[4+2+2] Cycloisomerisation Reaction	38
2.5	Synthesis of Allyl Alcohol Fragment 24	40
2.6	Attempted Routes Towards the Synthesis of the Eastern Fragment	42
2.6.1	Model Study on TST- Pauson-Khand Reaction	42
2.6.2	Oxygen Tethered Rhodium-Catalysed Dienyl PK Strategy	45

2.7	Completion of the Synthesis of the Eastern Fragment	49
2.7.1	First Generation Synthesis	49
2.7.2	Second-Generation Synthesis	54
2.8	Conclusion	57
2.9	Experimental	58
2.9.1	General	58
2.9.2	Experimental Procedures	59
2.10	References	82
2.11	Appendix	86
2.11.1	Mosher Ester Analysis for Allylic Alcohol 24	86
2.11.2	One-Dimensional ¹ H-nOe Data: Proof of Relative Configuration for Compounds 118 and 137	87

Chapter 3

Synthesis of the Western Fragment (B-C Rings) of Lancifodilactone G

3.1	Introduction	95
3.1.1	Previous Synthetic Work	95
3.1.1.1	The Paquette Approach	95
3.1.1.2	The Ghosh Approach	98
3.2	Results and Discussions	101
3.2.1	Retrosynthetic Analysis	101
3.2.2	Attempted Strategies Towards the Synthesis of 2,3-Disubstituted Furan Derivative 44	102
3.2.3	Revised Strategy Towards the Synthesis of 2,3-Disubstituted Furan 44	108
3.2.4	Synthesis of 2,3-Disubstituted Bicyclic Furan Derivative 44	109
3.3	An Overview on Diastereoselective [4+3] Cycloaddition Reactions of Furans for the Synthesis of 8-Oxabicycles	113

3.3.1	Oxyallyl Cations Generated from the Reduction of Polyhalogenated Ketones	114
3.3.2	[4+3] Cycloadditions of Oxygen-Stabilised Oxyallyl Cations	119
3.3.3	[4+3] Cycloadditions of Oxyallyl Cations Derived From Epoxides	121
3.3.4	Rhodium(II)-Catalysed [4+3] Cycloadditions of VinylCarbenoids	122
3.4	Diastereoselective [4+3] Cycloaddition Reaction	127
3.4.1	Substrate-Controlled [4+3] Cycloaddition Reaction	127
3.4.2	Revised End Game Strategy For Lancifodilactone G	128
3.4.3	Catalyst-Controlled [4+3] Cycloaddition Reaction	130
3.5	Conclusion	131
3.6	Experimental	132
3.6.1	General	132
3.6.2	Experimental Procedures	133
3.7	References	157
3.8	Appendix	160
3.8.1	One-Dimensional ^1H -nOe Data: Proof of Relative Configuration for Compound 71	160

Chapter 4

Model Study for the Second-Generation Synthesis of the Western Fragment and Plans for the Completion of the Synthesis of Lancifodilactone G

4.1	Second-Generation Strategy for the Western Fragment	163
4.2	Development and Mechanism of Rhodium(I)-catalysed Allylic Substitution Reaction	164
4.2.1	Regiospecificity	164
4.2.2	Enantiospecificity	166
4.3	Rhodium(I)-Catalysed Allylic Etherification	167

4.3.1	Background	167
4.3.2	Rhodium(I)-Catalysed Etherification: Model Study	168
4.4	Future Studies	169
4.4.1	Second-Generation Synthesis of the Western Fragment	169
4.4.2	End Game Strategy	170
4.5	Experimental	164
4.5.1	General	172
4.5.2	Experimental Procedures	172
4.6	References	178

List of Schemes

Chapter 1

Nortriterpenoids Isolated From the Genus *Schisandra* and Studies Towards the Total Synthesis of Lancifodilactone G

Scheme 1.1 <i>Proposed Biosynthetic Pathways for Schisanartane Nortriterpenoids.</i>	6
Scheme 1.2 <i>Relative Stabilities of the Enol Versus Keto Tautomer.</i>	8
Scheme 1.3 <i>Retrosynthetic Strategy for Tricycle 37.</i>	10
Scheme 1.4 <i>Synthesis of Dialdehyde 44 and the Attempted Macrocyclisation Reaction.</i>	10
Scheme 1.5 <i>Synthesis of Tricyclic Derivative 37.</i>	11
Scheme 1.6 <i>Synthesis of Enol Ether 52.</i>	12
Scheme 1.7 <i>Claisen Ring Expansion Reaction of Enol Ether 52.</i>	13
Scheme 1.8 <i>Anderson's Retrosynthetic Strategy.</i>	14
Scheme 1.9 <i>Synthesis of Tricycle 58.</i>	14
Scheme 1.10 <i>Retrosynthetic Analysis of Lancifodilactone G 5.</i>	15

Chapter 2

Synthesis of the Eastern Fragment (F-G Rings) of Lancifodilactone G

Scheme 2.1 <i>Paquette's Retrosynthetic Analysis.</i>	19
Scheme 2.2 <i>Preparation of Vinyl Triflate 4.</i>	20
Scheme 2.3 <i>Synthesis of Bromoacetal 15.</i>	20
Scheme 2.4 <i>Synthesis of Aldehyde 2.</i>	21
Scheme 2.5 <i>Retrosynthetic Analysis for the Eastern Fragment 20.</i>	22
Scheme 2.6 <i>Mechanism for the Cobalt-Mediated PK Reaction.</i>	24

Scheme 2.7 <i>Magnus Formal Synthesis of Coriolin 33.</i>	25
Scheme 2.8 <i>Models for 1,3- and 1,2-Stereinduction in the Cobalt-Mediated PKR Reaction.</i>	26
Scheme 2.9 <i>Application of Cobalt-Mediated PK Reaction in Total Synthesis.</i>	26
Scheme 2.10 <i>Molybdenum-Mediated PK Reaction of Alkynyl Allenes.</i>	27
Scheme 2.11 <i>Cobalt-Catalysed PK Reaction Nitrogen-Tethered Enyne.</i>	28
Scheme 2.12 <i>Rhodium(I)-Catalysed PK Reaction.</i>	28
Scheme 2.13 <i>Catalytic Cycle for the Rhodium-Catalysed PK Type Reaction.</i>	29
Scheme 2.14 <i>Rhodium(I)-Catalysed Diastereoselective Synthesis of Bicyclic Enone.</i>	30
Scheme 2.15 <i>Rhodium-Catalysed Tandem Allylic Alkylation/PK Reaction.</i>	30
Scheme 2.16 <i>Catalytic Cycle for Four- and Five-Coordinate Rhodium Complexes.</i>	32
Scheme 2.17 <i>Diastereoselective Titanium-, Palladium-, and Ruthenium-Catalysed PK Reaction.</i>	34
Scheme 2.18 <i>Synthesis of C₂-Symmetric Silaketals 67.</i>	35
Scheme 2.19 <i>Preparation of D-Altritol 72.</i>	36
Scheme 2.20 <i>Enantioselective Synthesis of (–)-Mucocin 77.</i>	37
Scheme 2.21 <i>Long Range Asymmetric Induction Using TST-RCM Reaction.</i>	37
Scheme 2.22 <i>Synthesis of Trans-Silaketals 86.</i>	38
Scheme 2.23 <i>Rhodium(I)-Catalysed [4+2+2] TST-Cycloisomerisation Reaction.</i>	39
Scheme 2.24 <i>Synthesis of TIPS Allyl Ether 105.</i>	40
Scheme 2.25 <i>Synthesis of TIPS Allyl Alcohol Fragment 24 and Mechanism for the Corey Bakshi-Shibata (CBS) Reduction of Ketone.</i>	41
Scheme 2.26 <i>Rhodium(I)-Catalysed [2+2+1] Dienyl Pauson-Khand Reaction.</i>	42
Scheme 2.27 <i>Synthesis of Model Substrate 113 for the TST-PK Reaction.</i>	43
Scheme 2.28 <i>Revised Retrosynthetic Analysis For the Eastern Fragment.</i>	45
Scheme 2.29 <i>Synthesis of Bicyclic Ketones 119 and 126.</i>	47
Scheme 2.30 <i>Attempted Exo-Deconjugative Methylation Reaction.</i>	48
Scheme 2.31 <i>Revised Route for the Installation of Quaternary Stereogenic Centre.</i>	49

Scheme 2.32 <i>Deconjugative Methylation Strategy in the Schreiber's Epoxydictymene Synthesis.</i>	50
Scheme 2.33 <i>Diastereoselective Synthesis of Bicyclic Ketone 118.</i>	50
Scheme 2.34 <i>First Generation Synthesis of the Eastern Fragment.</i>	53
Scheme 2.35 <i>Second Generation Synthesis of the Eastern Fragment.</i>	56
Scheme 2.36 <i>Summary and Outlook.</i>	57

Chapter 3

Synthesis of the Western Fragment (B-C Rings) of Lancifodilactone G

Scheme 3.1 <i>Paquette's Retrosynthetic Analysis.</i>	95
Scheme 3.2 <i>Synthesis of Hydroxyl Enyne 6.</i>	96
Scheme 3.3 <i>Attempted RCM of Enyne 6.</i>	96
Scheme 3.4 <i>Synthesis of Diol 17.</i>	97
Scheme 3.5 <i>Completion of the Western Fragment.</i>	97
Scheme 3.6 <i>Synthesis of Cycloheptenone Derivative 30.</i>	99
Scheme 3.7 <i>Synthesis of C5-epi-ABC Subunit 38.</i>	100
Scheme 3.8 <i>Retrosynthetic Analysis for the Western Fragment.</i>	101
Scheme 3.9 <i>Attempted Routes Towards the Synthesis of 2,3-Disubstituted Furan 44.</i>	103
Scheme 3.10 <i>Attempted Intramolecular Oxy-Michael Cyclisation of 48.</i>	104
Scheme 3.11 <i>Intramolecular Oxy-Michael Cyclisation of 59.</i>	105
Scheme 3.12 <i>Intramolecular Radical Cyclisation of 46.</i>	106
Scheme 3.13 <i>Attempted Intramolecular Epoxide Opening Reaction of 50.</i>	107
Scheme 3.14 <i>Attempted Intramolecular Iodo-Etherification Reaction of 52.</i>	107
Scheme 3.15 <i>Revised Route Towards 2,3-Disubstituted Furan Derivative 44.</i>	108
Scheme 3.16 <i>Crimmins Alkylation Reaction of 75.</i>	108
Scheme 3.17 <i>Synthesis of Alkynyl Alcohol Derivative 74.</i>	109

Scheme 3.18 <i>Synthesis of Glycolate 84.</i>	110
Scheme 3.19 <i>Elaboration of Enyne 84 to Alcohol 86.</i>	111
Scheme 3.20 <i>Synthesis of 2,3-Disubstituted Furan 44.</i>	112
Scheme 3.21 <i>[4+3] Cycloaddition Reaction of Chloroketone 87.</i>	113
Scheme 3.22 <i>Types of [4+3] Cycloaddition Reactions.</i>	115
Scheme 3.23 <i>Proposed Models for the [4+3] Cycloaddition Reaction.</i>	116
Scheme 3.24 <i>Diastereoselective [4+3] Cycloaddition Reaction of 109.</i>	117
Scheme 3.25 <i>[4+3] Cycloaddition Reaction of Bromo Oxonitrile 113.</i>	117
Scheme 3.26 <i>Solvent Effect in the [4+3] Cycloaddition Reaction of 116.</i>	118
Scheme 3.27 <i>[4+3] Cycloaddition Reaction of 121 With TCA 122 in TFE.</i>	119
Scheme 3.28 <i>Base and Lewis Acid mediated [4+3] Cycloaddition Reactions.</i>	119
Scheme 3.29 <i>[4+3] Cycloaddition in the Synthesis of (–)-Colchicine 140.</i>	120
Scheme 3.30 <i>[4+3] Cycloaddition of Silyloxy Acrolein 141.</i>	121
Scheme 3.31 <i>[4+3] Cycloaddition of Amidoallene 145.</i>	122
Scheme 3.32 <i>[4+3] Cycloaddition of Epoxy Enolsilane 150 and Furan.</i>	122
Scheme 3.33 <i>Mechanisms for Rh(II)-Catalysed [4+3] Cycloaddition of Vinylcarbenoid.</i>	124
Scheme 3.34 <i>[4+3] Cycloaddition of Vinyl diazocarbene 163 and Cyclopentadiene 164.</i>	125
Scheme 3.35 <i>Model for the Stereoselectivity in the Cyclopropanation Step.</i>	125
Scheme 3.36 <i>[4+3] Cycloaddition in the Total Synthesis of (–)-Englerin A 174.</i>	126
Scheme 3.37 <i>Diastereoselective Synthesis of Tricycle 43.</i>	127
Scheme 3.38 <i>Diastereoselective Hydrogenation Reaction and Attempted Ring-Opening of 42.</i>	128
Scheme 3.39 <i>Revised End Game Strategy for Lancifodilactone G 1.</i>	129
Scheme 3.40 <i>Rhodium(II)-Catalysed [4+3] Cycloaddition Reaction of Bicyclic Furan 44.</i>	130
Scheme 3.41 <i>Summary and Outlook.</i>	131

Chapter 4

Model Study for the Second-Generation Synthesis of the Western Fragment and Plans for the Completion of the Synthesis of Lancifodilactone G

Scheme 4.1 <i>First-Generation Synthesis of the Western Fragment.</i>	163
Scheme 4.2 <i>Second Generation Plan for the Western Fragment.</i>	164
Scheme 4.3 <i>Tsuji's Regiospecific Allylic Substitution Reaction.</i>	164
Scheme 4.4 <i>Metal Effect on Regiospecific Allylic Substitution Reaction.</i>	165
Scheme 4.5 <i>Evans' Regioselective Allylic Substitution Reaction.</i>	165
Scheme 4.6 <i>Enantiospecific Allylic Substitution Reaction.</i>	166
Scheme 4.7 <i>Origin of Stereospecificity in the Allylic Substitution Reaction.</i>	167
Scheme 4.8 <i>Rhodium(I)-Catalysed Allylic Etherification of Secondary and Tertiary Alcohols.</i>	168
Scheme 4.9 <i>Role of Excess Phosphite in the Rhodium(I)-Catalysed Allylic Etherification.</i>	168
Scheme 4.10 <i>Synthesis of Model Compound 28 Via Rhodium(I)-Catalysed Etherification Reaction.</i>	169
Scheme 4.11 <i>Synthesis of Carbonate 4.</i>	169
Scheme 4.12 <i>Synthesis of Tertiary Alcohol 6.</i>	170
Scheme 4.13 <i>Nickel(II)-Catalysed Radical Cyclisation Reaction of 35.</i>	170
Scheme 4.14 <i>End Game for Lancifodilactone G 41.</i>	161

List of Figures

Chapter 1

Nortriterpenoids Isolated From the Genus *Schisandra* and Studies Towards the Total Synthesis of Lancifodilactone G

Figure 1.1 <i>Representative Examples of Schisanartane Nortriterpenoids.</i>	3
Figure 1.2 <i>Members of Schiartane Nortriterpenoids.</i>	4
Figure 1.3 <i>Representative Examples for 18-Norschiartane and 18(13→14)-abeo-Schiartane.</i>	5
Figure 1.4 <i>Representative Examples for Pre-schisanartane and Wuweiziartane Types.</i>	5

Chapter 2

Synthesis of the Eastern Fragment (F-G Rings) of Lancifodilactone G

Figure 2.1 <i>Proposed Mechanistic Hypothesis in the Rhodium-Catalysed PK Reaction.</i>	31
Figure 2.2 <i>Reaction Energy Profiles for the Rhodium(I)-Catalysed PK Reaction.</i>	32
Figure 2.3 <i>Proposed Model for the Rhodium(I)-Catalysed PK Reaction.</i>	55

Chapter 3

Synthesis of the Western Fragment (B-C Rings) of Lancifodilactone G

Figure 3.1 <i>Transition States for Oxy-Michael Cyclisation of Rac-48.</i>	103
Figure 3.2 <i>Transition States for the 5-exo-trig Radical Cyclisation of Rac-46.</i>	105

List of Tables

Chapter 2

Synthesis of the Eastern Fragment (F-G Rings) of Lancifodilactone G

Table 2.1. <i>Effect of CO Pressure on the Diastereoselectivity in the PK Reaction.</i>	33
Table 2.2 <i>Rhodium(I)-Catalysed TST Dienyl Pauson-Khand Reaction.</i>	44
Table 2.3 <i>Rhodium(I)-Catalysed Dienyl Pauson-Khand Reaction: Spartan Calculations.</i>	45
Table 2.4 <i>Rhodium(I)-Catalysed Oxygen-Tethered Dienyl PK Reaction: Model Study.</i>	47
Table 2.5 <i>Attempted Functionalisation of the Bicyclic Alkene 118.</i>	52
Table 2.6 <i>Optimisation of Rhodium(I)-Catalysed Pauson-Khand Reaction.</i>	55
Table 2.7 $\Delta\delta = \delta_S - \delta_R$ <i>Data for the (S)- and (R)-Mosher Ester of Allylic Alcohol 24.</i>	86

Chapter 3

Synthesis of the Western Fragment (B-C Rings) of Lancifodilactone G

Table 3.1 <i>Reagent Controlled [4+3] Cycloaddition Reaction.</i>	115
Table 3.2 <i>[4+3] Cycloaddition between Furan Derivative and Vinyl diazomethane.</i>	123
Table 3.3 <i>Rhodium(II)-Catalysed [4+3] Cycloaddition Reaction of Bicyclic Furan 44.</i>	130

LIST OF ABBREVIATIONS

Å	angstrom
APT	attached proton test
Bn	benzyl
Bz	benzoyl
BINAP	2,2'- <i>bis</i> (diphenylphosphino)-1,1'-binaphthyl
BOC	<i>tert</i> -butoxycarbonyl
BOC-ON	2-(<i>tert</i> -butoxycarbonyloxyimino)-2-phenylacetonitrile
9-BBN	9-borabicyclononane
brsm	based on recovered starting material
ⁿ Bu	butyl
ⁱ Bu	<i>iso</i> -butyl
^t Bu	<i>tert</i> -butyl
<i>c</i>	concentration
°C	degree Celcius
<i>cee</i>	conservation of enantiomeric excess
CI	chemical ionisation
CO	carbon monoxide
COD	1,5-cyclooctadiene
Cp	cyclopentadienyl
Cy	cyclohexyl
DCE	1,2-dichloroethane
DCM	dichloromethane
DFT	density functional theory
DEAD	diethyl azodicarboxylate

DIBAL-H	diisobutylaluminium hydride
DMAP	4-dimethylaminopyridine
DME	ethylene glycol dimethyl ether
DMF	<i>N,N</i> -dimethylformamide
DMSO	dimethyl sulfoxide
dppb	1,4- <i>bis</i> (diphenylphosphino)butane
dppe	1,2- <i>bis</i> (diphenylphosphino)ethane
dppp	1,3- <i>bis</i> (diphenylphosphino)propane
dr	diastereomeric ratio
ds	diastereoselectivity
EA	ethyl acetate
<i>e.e.</i>	enantiomeric excess
ESI	electron spray ionisation
<i>ent</i>	enantiomer
Et	ethyl
FTIR	fourier transform infra-red
g	gram
GC	gas chromatography
¹³ C _{Hex}	cyclohexyl
HMDS	1,1,1,3,3,3-hexamethyldisilazane
HMPA	hexamethylphosphoramide
HPLC	high performance liquid chromatography
HRMS	high-resolution mass spectrometry
IBX	2-iodoxybenzoic acid
IR	infrared
L	ligand

LAB	lithium amidoborane
LDA	lithium diisopropylamine
Lg	leaving group
L _n	ligand set
M	metal
Me	methyl
mg	milligram
MHz	megahertz
mL	millilitre
mmol	millimole
MOM	methoxymethyl
NaH	sodium hydride
NBS	<i>N</i> -bromosuccinimide
NCS	<i>N</i> -chlorosuccinimide
NMM	<i>N</i> -methyl morpholine
NMO	<i>N</i> -methyl morpholine- <i>N</i> -oxide
NMR	nuclear magnetic resonance
nOe	nuclear Overhauser effect
Pd	palladium
PCC	pyridinium chlorochromate
Ph	phenyl
piv	pivaloyl
PK	Pauson-Khand
PMB	<i>para</i> -methoxybenzyl
PMP	<i>para</i> -methoxyphenyl
PPTS	pyridinium <i>p</i> -toluenesulphonate

ⁱ Pr	isopropyl
ⁿ Pr	propyl
RCM	ring closing metathesis
rs	regioselectivity
RT	room temperature
TBAF	tetrabutylammonium fluoride
TBAI	tetrabutylammonium iodide
TBDPS	<i>tert</i> -butyldiphenylsilyl
TBHP	<i>tert</i> -butyl hydroperoxide
TBS	<i>tert</i> -butyldimethylsilyl
TEA	triethylamine
TES	triethylsilyl
Tf	trifluoromethanesulfonyl
TFA	trifluoroacetic acid
TFE	2,2,2-trifluoroethanol
THF	tetrahydrofuran
THP	tetrahydropyran
TIPS	triisopropylsilyl
TMANO	trimethylamine <i>N</i> -oxide
TMS	trimethylsilyl
TMTU	tetramethylthiourea
TPAP	tetra- <i>n</i> -propylammonium perruthenate
<i>t</i> _R	retention time
TRIBAL	triisobutylaluminum
Ts	toluenesulphonyl
μL	microlitre

Chapter 1

Nortriterpenoids Isolated From the Genus *Schisandra* and Studies Towards the Total Synthesis of Lancifodilactone G

1.1 Introduction

The plant family Schisandraceae comprises of climbing and flowering plants that belong to the order Austrobaileyales and contain the genera *Schisandra* and *Kadsura*. Nearly 50 species of plants belonging to these genera have significant economical and medicinal value and are predominantly indigenous to Southeast Asia and North America. Several species of plants have an array of biological activities such as *anti*-hepatotoxic, *anti*-asthmatic, *anti*-tussive, *anti*-fatigue, *anti*-oxidant, *anti*-cancer, sedative, immunostimulant, liver protecting properties and have been used extensively in traditional Chinese medicines for the treatment of common ailments.¹ For example, the dried berries from *Schisandra chinensis* commonly known in China as “wu-wei zi” have been used as a remedy for hepatitis and other disorders for more than 2000 years. In addition to medicinal properties, some species of this family have been utilised in the food and beverage industry as an important ingredient in wine, fruit juice, jelly and other edible products. Consequently, species of the Schisandraceae family have evoked considerable interest within the phytochemical community which has led to the isolation of 70 highly oxygenated triterpenoids with varying scaffold specifically from the stem, root and leaf extracts of plants belonging to *Schisandra* and *Kadsura* genera. These triterpenoids from Schisandraceae family, based on different carbon skeletons, can be broadly divided into three categories: (i)

lanostane, (ii) cycloartane and (iii) *Schisandra* nortriterpenoids. Considering several comprehensive reviews on the isolation, classification, structural elucidation of triterpenoids from Schisandraceae,^{1,2} the following section will outline the salient features of *Schisandra* nortriterpenoids that have been recently discovered and are a current focus of study within the Evans group.

1.1.1 Types of *Schisandra* Nortriterpenoids

Schisandra nortriterpenoids are a family of highly oxygenated polycyclic natural products that have been proposed to be biosynthetically derived from cycloartane.¹ These compounds are isolated from plants of genus *Schisandra*, some of which show potent *anti*-HIV activity with low levels of cytotoxicity. Triterpenoids from *Schisandra* nortriterpenoids are further classified into six types depending on carbon connectivities: (i) schisanartane (ii) schiartane (iii) 18-norschiartane (iv) 18(13→14)-*abeo*-schiartane (v) pre-schisanartane and (vi) wuweiziartane.

1.1.2 Schisanartane Type

The schisanartane nortriterpenoids are the main constituents of the *Schisandra* genus. As illustrated in Figure 1.1, the novel triterpenoids of this series possess an unprecedented 7/8/5 fused carbocycle with more than twelve stereogenic centres and an octacyclic backbone. The unusual skeletal pattern found in the schisanartane class was first observed in the isolation of micrandilactone A from the stems and leaves of *Schisandra micrantha* in 2003.³

Following the isolation of micrandilactone A, a series of architecturally related nortriterpenoids have been discovered in recent years, as exemplified by the micrandilactones (D-G),⁴ lancifodilactones (B-E),⁵ lancifodilactone G,⁶ lancifodilactones (I-N),⁷ henridilactones (A-D),⁸ propindilactones (A-D),⁹ rubriflorins (A-J),¹⁰ schindilactones (A-G),¹¹ sphenadilactones (A-B),¹² and sphenalactone (A-D)¹³ (Figure 1.1). Interestingly, triterpenoids depicted in Figure 1.1 are not specific to a particular plant of *Schisandra* genus. For instance, micrandilactone A was isolated from *Schisandra micrantha*, *Schisandra propinque* var.

propinqua, *Schisandra lancifolia* and *Schisandra rubriflora*. Hence, these compounds presumably arise *via* related biosynthetic pathways.

Among the plethora of triterpenoids isolated from the plants of *Schisandra*, lancifodilactone G **5** is unique. This agent was isolated from the leaves and stems of *Schisandra lancifolia*, and demonstrated minimal cytotoxicity against C8166 cells ($CC_{50} > 200$ $\mu\text{g/mL}$) and modest *anti*-HIV activity with an EC_{50} value of 95.5 ± 14.2 $\mu\text{g/mL}$.⁶

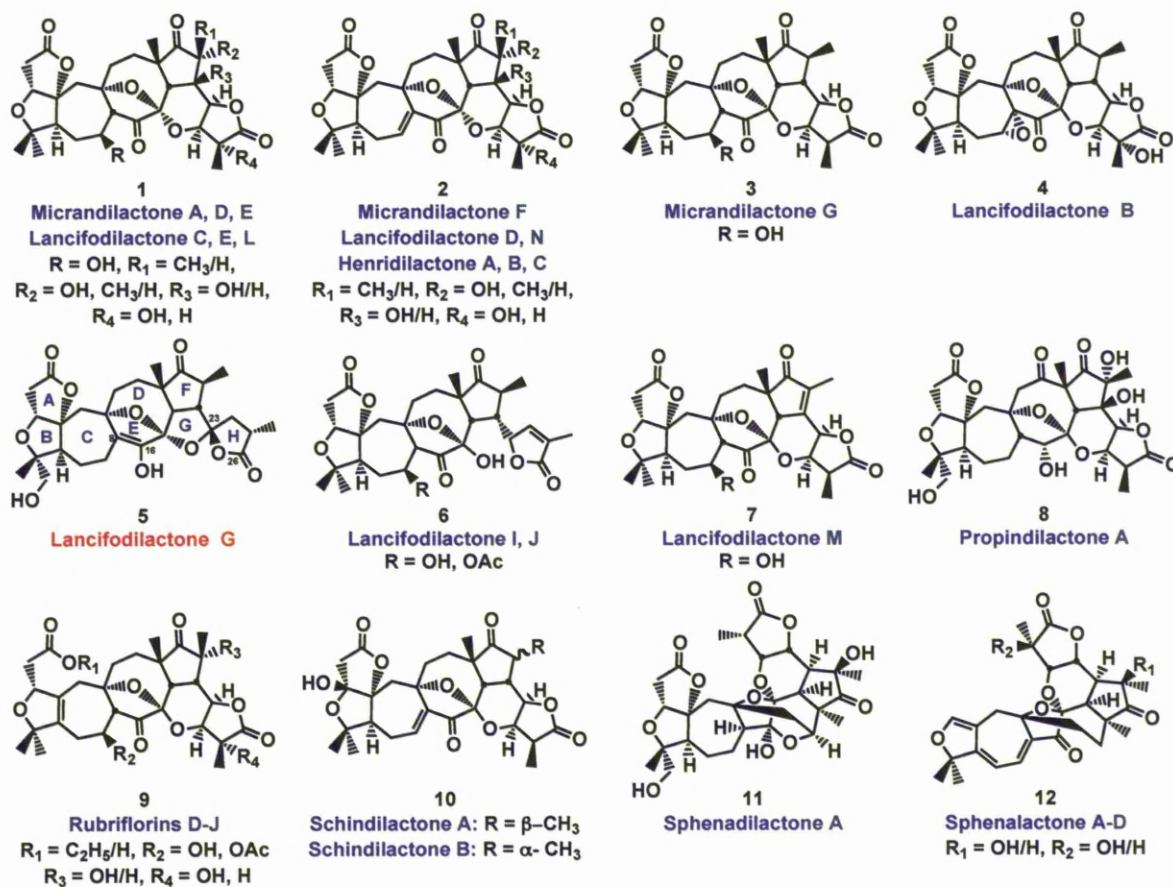


Figure 1.1 Representative Examples of Schisanartane Nortriterpenoids.

Nevertheless, a key feature of this natural product is that it contains a stable aliphatic enol functionality devoid of enol stabilising groups, such as a conjugated aromatic ring or a 1,3-diketone unit. Hence, the atypical norcycloartane skeleton, decorated with twelve stereogenic centers, ten oxygenated carbons, two quaternary carbons and a spirocyclic acetal at C23 and the unusual enol at C8-C16 makes it a challenging and structurally interesting synthetic target.

The structural elucidation and relative stereochemistry in lancifodilactone **5** was accomplished using extensive NMR analysis and single-crystal X-ray crystallography, while the absolute configuration was extrapolated from the biogenetic connectivity to its congener micrandilactone B, a schiartane type of triterpenoid described in the next section.

1.1.3 Schiartane Type

Micrandilactone B and C are the only triterpenoids known to possess schiartane skeleton.¹⁴ A characteristic feature of this class of triterpenoids is the absence of C28 methyl group compared to its biogenetic cycloartane congener (Figure 1.2). These highly oxygenated nortriterpenoids were isolated from the stem and leaf of *Schisandra micranta*. The carbon connectivity and the relative configuration were unambiguously determined using extensive NMR spectroscopy and X-ray crystallography. The absolute configuration of **13** was established using the Mosher protocol. Although micrandilactone C **14** has promising *anti*-HIV activity ($EC_{50} = 7.71 \mu\text{g/mL}$), triterpenoid **13** however showed weak *anti*-HIV activity.



Figure 1.2 Members of Schiartane Nortriterpenoids.

1.1.4 18-Norschiartane and 18(13→14)-abeo-Schiartane Types

18-Norschiartanes is a family of bisnortriterpenoids that are derived from the cycloartane class of natural products, albeit with the absence of methyl groups at C18 and C28 (Figure 1.3). Lancifodilactone A **16** is representative example of this group, which was isolated from the stems and leaves of *Schisandra lancifolia*.¹⁵ 18(13→14)-abeo-Schiartane is a very small group of nortriterpenoids with the methyl group at C14 having an unusual β -orientation. There are only four natural products in this category namely wuweizidilactones C-F that were isolated from *Schisandra chinensis* (Figure 1.3).¹⁶

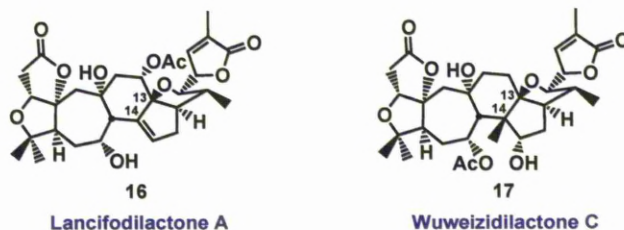


Figure 1.3 Representative Examples for 18-Norschiartane and 18(13→14)-abeo-Schiartane.

1.1.5 Pre-schisanartane and Wuweiziartane Types

Pre-schisanartane A **18** along with pre-schisanartane B were isolated from *Schisandra chinensis*.^{1,17} They are believed to be the biosynthetic precursor of the schisanartane triterpenoids (Figure 1.4). These natural products contain a 7/8/3 fused carbocycle and are also produced with the schisanartane family of triterpenoids within the same plant.

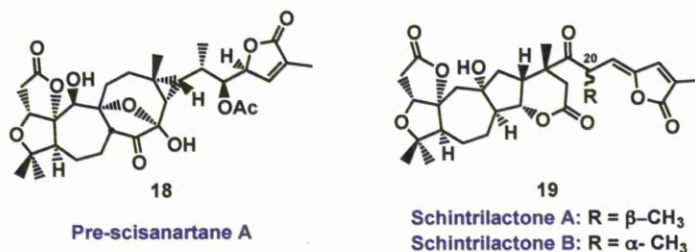


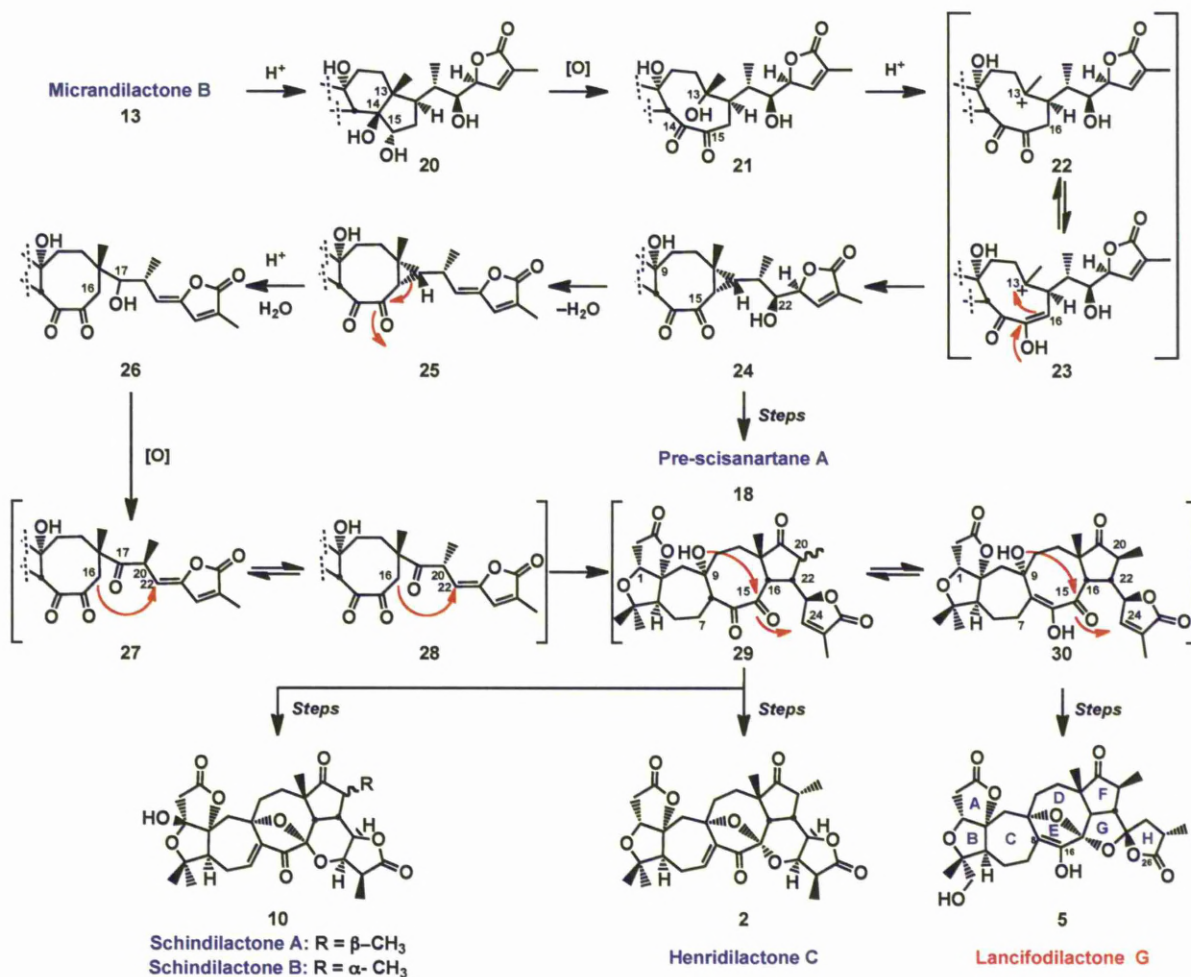
Figure 1.4 Representative Examples for Pre-schisanartane and Wuweiziartane Types.

Schintrilactones A and B **19** belong to wuweiziartane type of triterpenoids which were isolated from *Schisandra chinensis*.¹⁸ These natural products were found to be configurationally unstable at C20 and epimerised slowly in solution. Additionally, triterpenoids **19** also possessed a modified 5-membered D ring at the core and a conjugated δ -butenolide moiety differing from other related natural products in the Schisandraceae family.

In the following section, a hypothetical biosynthetic pathway proposed by Sun and co-workers for Lancifodilactone G **5** and structurally related triterpenoids of schisanartane category will be described.^{1,14,19}

1.2 Proposed Biosynthetic Route for Lanicifodilactone G and for Related Schisanartane Type of Nortriterpenoids

The following biosynthetic proposal is based on the fact that the cycloartane core is retained in micrandilactone B **13** and the 28-nor-14,15-epoxy moiety is commonly found in the naturally occurring triterpenoids. Hence, Sun and co-workers hypothesised the schiartane scaffold is formed early in the biosynthetic pathway of the schisanartane type of



Scheme 1.1 *Proposed Biosynthetic Pathways for Schisanartane Nortriterpenoids.*

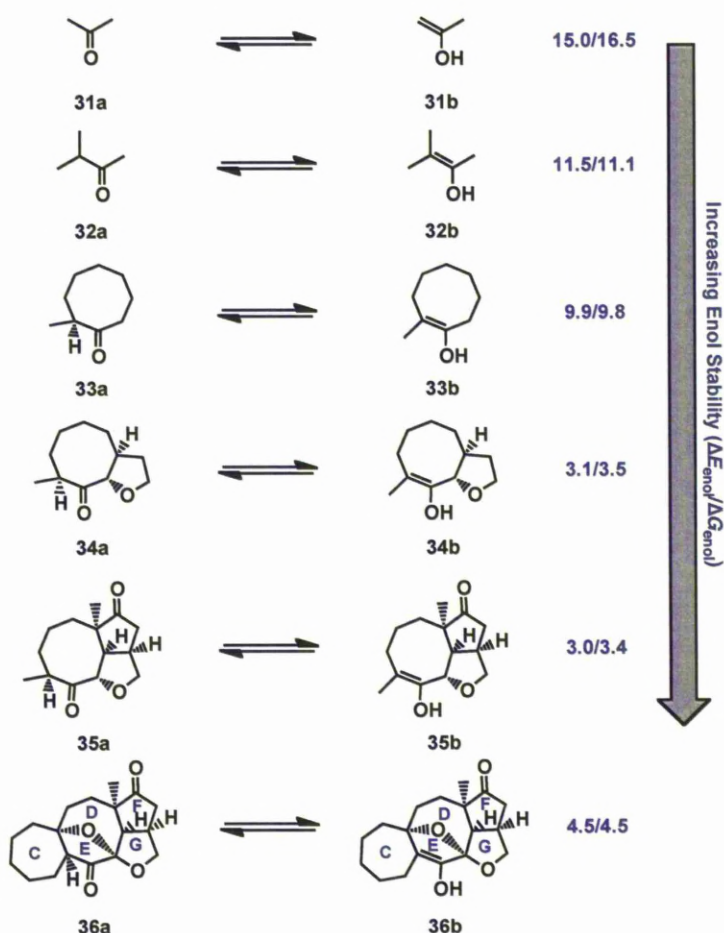
nortriterpenoids (Scheme 1.1). Tetraol **20** was proposed to arise *via* enzymatic opening of the epoxy ring in **13**. Oxidative cleavage of the C13-C14 bond followed by selective oxidation of the secondary hydroxyl groups at C14 and C15 was envisioned to furnish the nine-membered diketone derivative **21**. They proposed that the unprecedented 7/8/3 fused carbocycle present in pre-schisanartane triterpenoids could be formed by selective protonation of the tertiary

alcohol at C13 in **21** to form a stable carbocation **22**. Successive enolisation at C16 followed by nucleophilic attack at C13 could lead to intermediate **24**. Under acidic conditions, cyclopropyl ketone **24** was predicted to furnish the biogenetically related pre-schisanartane A **18** upon intramolecular hemiketalisation of the tertiary alcohol at C9 and ketone at C15 followed by two additional steps involving acetylation of the alcohol at C22 and hydroxylation of the seven-membered ring. Intermediate **24** is also susceptible to the acid-mediated elimination of secondary hydroxyl group at C22, which could afford the conjugated butenolide **25**. Compound **25** can be converted to **26** upon cleavage of the cyclopropane moiety followed by trapping of resulting carbocation at C17 by water. Oxidation of the C17 hydroxyl group in **26** could trigger epimerisation of the α -methyl group at C20 to afford an epimeric mixture of **27** and **28**, which presumably undergo conjugate addition between C16 and C22 to furnish a mixture of cyclopentanones **29**. The hexacyclic intermediate **29** provides a common precursor to schisanartane skeletons through divergent reaction pathways. While the intramolecular ketalisation/Michael addition cascade between the 9-OH, and the ketone at C15 and the enoate at C24 followed by oxidation state adjustment was envisioned to deliver schindilactones **10** and henridilactone C **2**, Lancifodilactone G **5** was hypothesised to arise from enol **30** by similar ring-closure followed by C-H activation and additional oxidative ring-closure event.

1.3 Insights into the Stability of the Aliphatic Enol Functionality at the Core of Lancifodilactone G

Most stable enols derive their stability from the conjugation of enolic double bond with a bulky aromatic or a 1,3-diketone unit. Lancifodilactone G **5** represents a rare class of a nonresonance stabilised enols that draws its stability from the architectural organisation of the polycyclic rings. Goddard *et. al.*, in their recent computational study have provided some insights into the thermodynamic stability of the keto versus enol form of lancifodilactone G **5** and have suggested a plausible mechanism for the interconversion between the two

tautomers.²⁰ In this study, DFT calculations were performed on keto and enol forms of compounds **31-36** in order to determine the structural features responsible for the stabilisation of the enol tautomer (Scheme 1.2). While the simple aliphatic enol **31b** derived from acetone was thermodynamically disfavoured by 15.0 kcal/mol, a combination of tetrasubstitution and incorporating the enolic double bond into a eight-membered ring found in lancifodilactone **G** lowers the energy of enol **33b** to 9.9 kcal/mol. A dramatic drop in the energy of enol **34b** was observed when the cyclooctane moiety was fused with the tetrahydrofuran ring ($\Delta E_{\text{enol}} = 3.1$ kcal/ mol) (Scheme 1.2). Although the addition of the cyclopentanone ring has minimal



Scheme 1.2 Relative Stabilities of the Enol Versus Keto Tautomer.

influence on enol stability, the addition of a bridged ether and rigidification of the cyclooctane ring by the incorporation of C ring had a destabilising effect on the enol **36b** ($\Delta E_{\text{enol}} = 4.5$

kcal/mol). Interestingly, the natural product **5** has a large increase in the stabilisation of enol form ($\Delta E_{\text{enol}} = 0.6$ kcal/mol), which results in the near isoenergetic keto-enol ground state. Overall, the unusual thermodynamic stability of the enol tautomer in lancifodilactone G **5** was attributed to the tetrasubstitution of the double bond, geometric constraints imposed by the cyclooctane ring, rigidification of the cyclooctane moiety by C-, F- and G-rings coupled with transannular effects of the A-, B-, and H-rings.

In addition to these findings, the group also ruled out the possibility of [1,3]-hydrogen shift enolisation mechanism that was earlier proposed by Sun and co-workers due to very high high-energy barrier ($\Delta E^\ddagger = 75.7$ kcal/mol).^{6b} Nevertheless, DFT studies predicted a dramatic reduction of enolisation barrier by as much as $\Delta\Delta E^\ddagger = 37$ kcal/mol for the concerted water-catalysed process, thus indicating a substantial effect on the kinetic barrier for the keto-enol tautomerisation. However, the conventional stepwise mechanisms along with acid- and base-catalysed processes cannot be precluded to describe the kinetics of tautomerisation mechanism since the barrier of 37 kcal/mol is still very high.

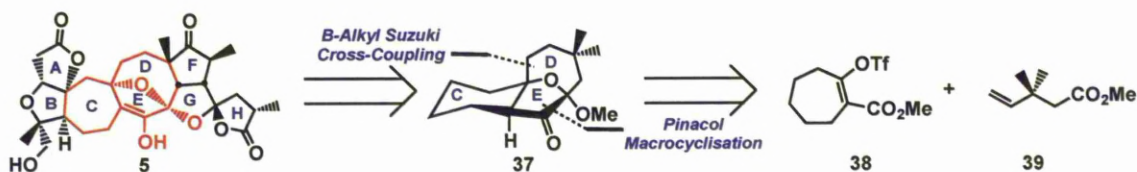
1.4 Synthetic Approaches Towards the Core of Lancifodilactone G

The total synthesis of lancifodilactone G **5** has not been reported at this juncture. However, the intriguing architecture of lancifodilactone G **5** has drawn considerable interest within the synthetic community to establish a viable route towards this natural product.²¹ The following section will outline strategic approaches towards the core of lancifodilactone G **5**. Discussions pertaining to the synthesis of eastern and western fragments of the natural product are presented in Chapters 2 and 3 respectively (*vide infra*).

1.4.1 The Paquette's Approach

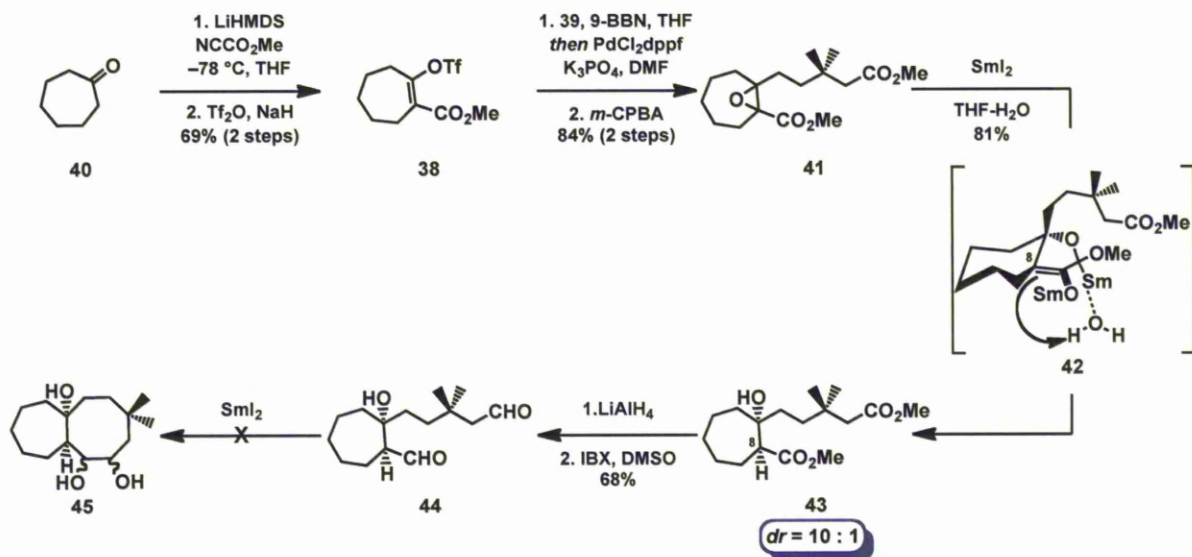
In 2008, Paquette and Lai disclosed their first approach towards the assembly of CDE core of lancifodilactone G **5** (Scheme 1.3).²² The synthesis utilised SmI_2 -mediated intramolecular pinacol coupling for the construction of eight-membered diketone core,²³

which was assembled by a sp^2 - sp^3 *B*-alkyl Suzuki-Miyaura cross-coupling between a terminal olefin and vinyl triflate **38**.²⁴



Scheme 1.3 Retrosynthetic Strategy for Tricycle **37**.

The preparation of enol triflate **38** for the Suzuki-Miyaura cross coupling reaction was initiated from the cycloheptenone **40**, which was first converted to the β -ketoester under standard conditions and later subjected to the triflation reaction employing NaH and $\text{ Tf}_2\text{O}$ (Scheme 1.4). The key palladium-catalysed *B*-alkyl Suzuki-Miyaura reaction involved the hydroboration of *gem*-dimethyl alkene **39** with 9-BBN to generate *B*-alkyl species followed by transmetalation with palladium, to provide the diester **41** in excellent overall yield after epoxidation of tetrasubstituted olefin.²⁴ Treatment of the α,β -epoxy diester **41** with SmI_2 ,



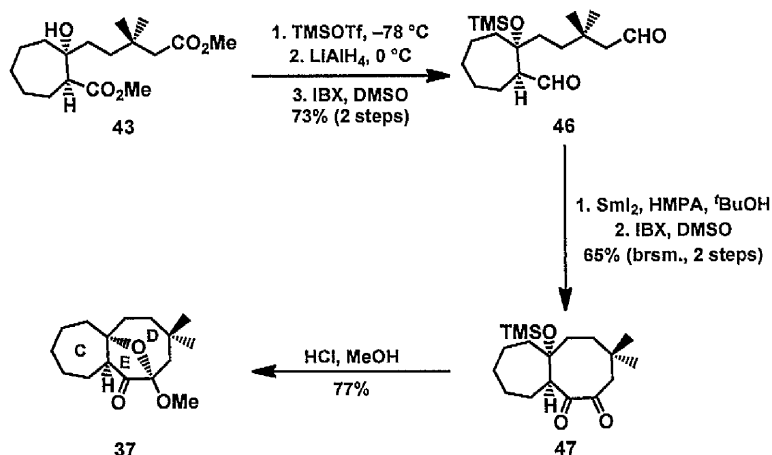
Scheme 1.4 Synthesis of Dialdehyde **44** and the Attempted Macrocyclisation Reaction.

furnished the hydroxy-diester **43** in 81% yield with a good diastereoselectivity ($dr = 10 : 1$) using water as the proton source.²⁵ The observed diastereocontrol at C8 was rationalised using **42**, where the internal delivery of the proton from water coordinated to the Sm(III) -alkoxide is

delivered to the α -face of the Sm(III)-enolate (Scheme 1.4). The oxidation state of the diester **43** was adjusted to the dialdehyde **44** using a standard reduction/oxidation sequence, employing LiAlH_4 and IBX, respectively.

With dialdehyde **44** in hand, attention turned towards the critical pinacol cyclisation for the construction of the eight-membered carbocycle (Scheme 1.4). All efforts to affect the key macrocyclisation employing SmI_2 at either ambient or low temperatures furnished the undesired monocyclic triol derivative from dialdehyde reduction. The exhaustive reduction of dialdehydes in **44** was attributed to the presence of the free hydroxyl group, which could presumably increase the reduction potential of SmI_2 after displacing the labile iodide ligand. Consequently, it was envisioned that masking the hydroxyl group would overcome the undesired reduction.

Towards this end, the cycloheptenol derivative **43** was protected as a trimethylsilyl ether, and the oxidation state of the diester was adjusted as described earlier to furnish the



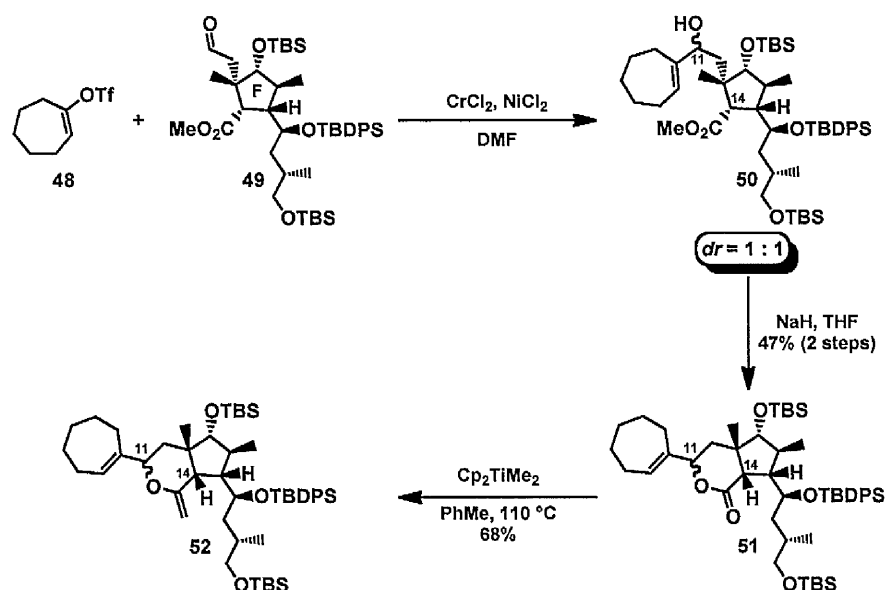
Scheme 1.5 *Synthesis of Tricyclic Derivative 37.*

dialdehyde **46** in 73% overall yield (Scheme 1.5). Gratifyingly the pinacol coupling reaction of **46** under high dilution conditions using SmI_2 in conjunction with HMPA afforded a inconsequential diastereomeric mixture of bicyclic diols, which were oxidised to the diketone **47** in 32% (65% brsm) overall yield.²³ Finally, the oxabridge in **37** was installed in the

presence of acidic methanol, which cleaved the TMS protecting group and concomitantly facilitated methoxy ketalisation to furnish tricyclic core **37** in 77% yield.

In 2009, Paquette and Lai published an alternative approach towards the synthesis of the 7/8/5 fused skeleton of Lancifodilactone G **5**.²⁶ The synthesis displays the utility of a Nozaki-Hiyama-Kishi (NHK) cross-coupling reaction inconjunction with the Petasis-Claisen ring expansion process for the stereocontrolled assembly of CDEF framework of the natural product.

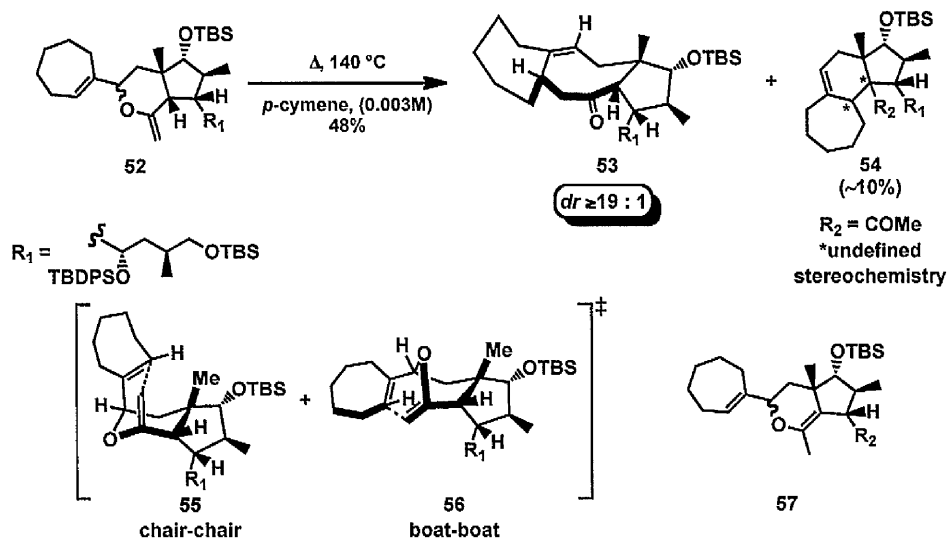
As illustrated in Scheme 1.6, the model study commenced with the union of their fully functionalised eastern fragment **49** (*vide infra*) with organochromium derivative generated from the vinyl triflate **48** to afford an inconsequential 1 : 1 diastereomeric mixture of allylic



Scheme 1.6 *Synthesis of Enol Ether 52.*

alcohols **50** along with inseparable lactone **51**. Treatment of the crude reaction mixture with excess NaH completed the conversion to the lactone **51** in 47% overall yield, which was epimeric at C11 but without any trace of epimerisation at C14. Methylenation of the six-membered lactone **51** using Petasis-Tebbe reagent furnished the desired enol ether **52** in 68% yield.

With compound **52** in hand, studies were initiated to probe the pivotal Claisen ring expansion reaction (Scheme 1.7). Preliminary experiments involving the treatment of the acid sensitive **52** to the TRIBAL-mediated Claisen rearrangement reaction only furnished complex

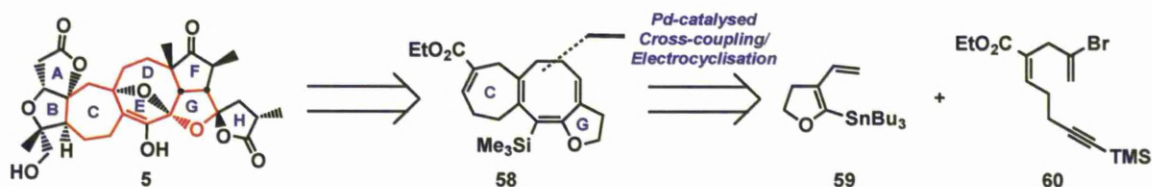


Scheme 1.7 Claisen Ring Expansion Reaction of Enol Ether **52**.

by-products. Nevertheless, thermolysis of **52** in a solution of *p*-cymene furnished the desired tricyclic enone in 48% yield with excellent diastereoselectivity (Scheme 1.7). The complete diastereocontrol observed in the reaction of **52** was rationalised on the basis of chair-chair **55** and boat-boat **56** transition states, which provided the enone **53** with the identical stereochemical outcome. The minor tricyclic by-product **54** was speculated to originate by the Claisen rearrangement of **57**, which in turn arises *via* a competitive [1,3]-hydrogen shift of the *exo*-methylene moiety in **52**.

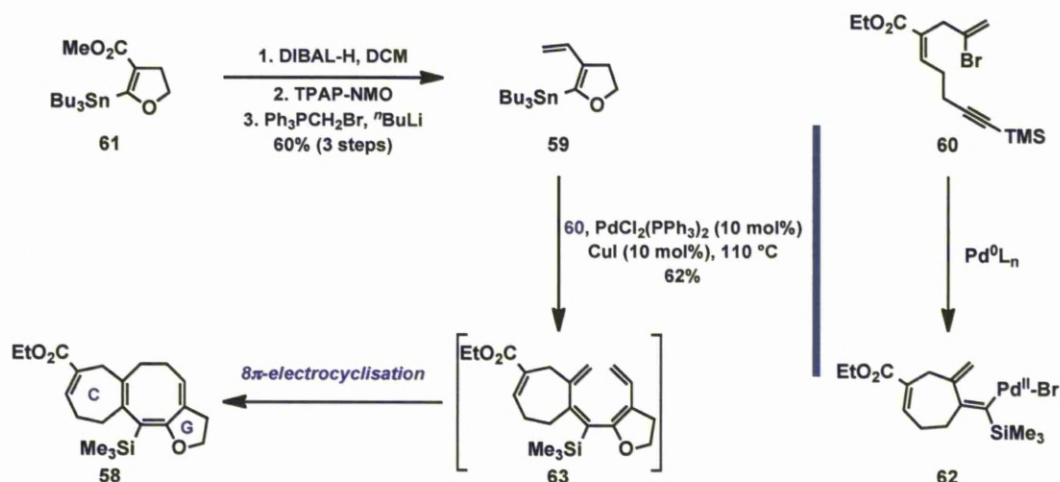
1.4.2 Anderson's Approach

In 2008, Anderson and co-workers reported a palladium-catalysed cascade cyclisation reaction for the construction of 7/8 and 7/6 fused ring skeletons from acyclic alkenylstannane and bromo enyne precursors.^{28a} Hence, the rapid assembly of tricyclic 7/8/5 core of lancifodilactone **5** was prepared *via* a novel cyclisation/cross-coupling/electrocyclisation sequence using model compounds **59** and **60** (Scheme 1.8).^{28b}



Scheme 1.8 Anderson's Retrosynthetic Strategy.

As illustrated in Scheme 1.9, the synthesis of dienyl stannane **59** was achieved in 3 steps in 60% overall yield from the known methyl ester **61**. DIBAL reduction of the ester followed by a ruthenium-catalysed oxidation²⁹ of the resulting alcohol and Wittig methylenation of the aldehyde provided the target vinyl stannane **59**. With **59** in hand, the cascade cyclisation was examined using the bromo dienyne **60** and catalytic $\text{Pd}(\text{PPh}_3)_2\text{Cl}_2$, which furnished the desired tricyclic intermediate **58** in 62% yield. The polycyclisation reaction is worthy of further comment. Oxidative addition of $\text{Pd}(0)$, which is formed *in situ*, with alkenyl bromide **60** initially affords a organopalladium species which undergoes an intramolecular *syn*-carbopalladation with the resident alkyne to afford palladium-bound triene **62**. A bulky silyl group at the terminus of the alkyne is crucial to preclude the undesired *syn*-



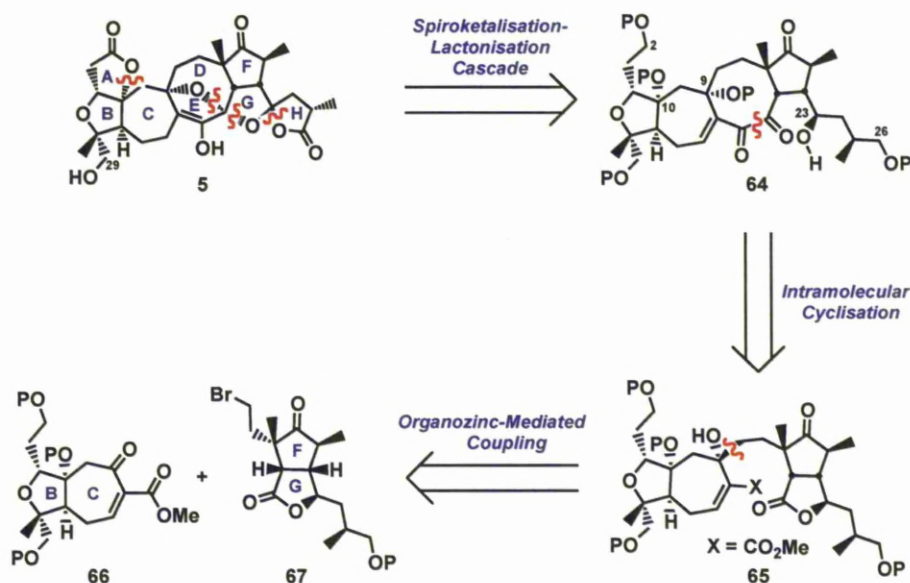
Scheme 1.9 Synthesis of Tricycle **58**.

anti isomerisation of the resulting alkenylpalladium intermediate **62**.^{28b} Stille cross-coupling of **62** with vinyl stannane **59** generated the bicyclic pentaene derivative **63** which underwent 8π -electrocyclisation reaction to deliver the desired tricycle **58**. Additionally, the addition of catalytic copper(I) iodide was essential to increase the rate of transmetallation of

dihydrofuranylstannane **59**, presumably resulting in formation of the vinyl-copper(I) species upon preliminary transmetallation between organostannane **59** and copper(I) iodide.³⁰

1.5 Original Retrosynthetic End Game for Lancifodilactone G

At the outset of our synthetic studies, we were prompted to design a fairly flexible retrosynthetic pathway that would also enable the strategy to be modified to prepare other structurally similar bioactive natural products in the *Schisandra* genus. Towards this end, a highly convergent retrosynthetic analysis for lancifodilactone G **5** was proposed based on the biosynthetic sequence described earlier in Section 1.2 (*vide supra*).^{1,14,19} As outlined in Scheme 1.10, we anticipate that lancifodilactone G **5** could be obtained by the hydrogenolysis of benzyl ether precursor at C29, which in turn was envisaged to arise *via* a biomimetic polycyclisation reaction of the silylated tetracyclic intermediate **64**. The critical cascade



Scheme 1.10 Retrosynthetic Analysis of Lancifodilactone G **5**.

reaction would initially involve an oxidative global silyl deprotection of **64** to provide the corresponding carboxylic acid and ketone functionalities at C2, C26, and C23.³¹ A tandem spiroketalisation-lactonisation sequence triggered by the tertiary hydroxyl groups at C9 and C10 was envisioned to deliver the octacyclic natural product precursor. We envisioned that the flexibility in the final stage would also allow the investigation of the rate of keto-enol

tautomerisation of this unique enolic natural product. The eight-membered ring in **64** could be assembled using an unprecedented acyloin condensation between methyl ester and lactone functionalities, however, there are several other possibilities such as intramolecular benzoin condensation, pinacol-coupling or ring closing metathesis-dihydroxylation sequence in an event that acyloin reaction is unsuccessful. The tertiary alcohol **65** could be traced back to the advanced intermediates **66** and **67** by means of organozinc-mediated intramolecular diastereoselective cross-coupling reaction.

Efforts towards highly stereocontrolled synthesis of eastern and western fragments **67** and **66** are described in Chapter 2 and 3, respectively (*vide infra*). Based on some interesting insights in the construction of the western fragment, an alternative end game of lancifodilactone G can also be envisioned, which will be discussed in Chapter 3.

1.6 References

- 1 Xiao, W. L.; Li, R. T.; Huang, S. X.; Pu, J. X.; Sun, H. D. *Nat. Prod. Rep.* **2008**, *25*, 871, and pertinent references cited therein.
- 2 For reviews on Schisandraceae triterpenoids, see: (a) D. F. Chen, *Zhongguo Tianran Yaowu*, **2007**, *5*, 15. (b) Chang, J. B.; Reiner, J.; Xie, J. X. *Chem. Rev.* **2005**, *105*, 4581. (c) Y. G. Chen, G. W. Qin and Y. Y. Xie, *Huaxue Yanjiu Yu Yingyong*, **2001**, *13*, 363. (d) J. F. Zhao, B. C. Shen, Q. M. Yuan, Z. H. Jin and L. Li, *Tianran Chanwu Yanjiu Yu Kaifa*, **2000**, *12*, 101. (e) Ward, R. S. *Nat. Prod. Rep.* **1999**, *16*, 75. (f) Ward, R. S. *Nat. Prod. Rep.* **1997**, *14*, 43. (g) Ward, R. S. *Nat. Prod. Rep.* **1995**, *12*, 183. (h) Ward, R. S. *Nat. Prod. Rep.* **1993**, *10*, 1. (i) Whiting, D. A. *Nat. Prod. Rep.* **1990**, *7*, 349. (j) Whiting, D. A. *Nat. Prod. Rep.* **1987**, *4*, 499. (k) Whiting, D. A. *Nat. Prod. Rep.* **1985**, *2*, 191. (l) Ward, R. S. *Chem. Soc. Rev.* **1982**, *11*, 75.
- 3 Li, R. T.; Zhao, Q. S.; Li, S. H.; Han, Q. B.; Sun, H. D.; Lu, Y.; Zhang, L. L.; Zheng, Q. T. *Org. Lett.* **2003**, *5*, 1023.
- 4 (a) Li, R. T.; Xiao, W. L.; Shen, Y. H.; Zhao, Q. S.; Sun, H. D. *Chem. Eur. J.* **2005**, *11*, 6763. (b) Li, R. T.; Xiao, W. L.; Shen, Y. H.; Zhao, Q. S.; Sun, H. D. *Chem. Eur. J.* **2005**, *11*, 2989.
- 5 Li, R. T.; Xiang, W.; Li, S. H.; Lin, Z. W.; Sun, H. D. *J. Nat. Prod.* **2004**, *67*, 94.
- 6 (a) Xiao, W. L.; Zhu, H. J.; Shen, Y. H.; Li, R. T.; Li, S. H.; Sun, H. D.; Zheng, Y. T.; Wang, R. R.; Lu, Y.; Wang, C.; Zheng, Q. T. *Org. Lett.* **2006**, *8*, 801. (b) Xiao, W. L.; Zhu, H. J.; Shen, Y. H.; Li, R. T.; Li, S. H.; Sun, H. D.; Zheng, Y. T.; Wang, R. R.; Lu, Y.; Wang, C.; Zheng, Q. T. *Org. Lett.* **2005**, *7*, 2145.
- 7 Xiao, W. L.; Huang, S. X.; Zhang, L.; Tian, R. R.; Wu, L.; Li, X. L.; Pu, J. X.; Zheng, Y. T.; Lu, Y.; Li, R. T.; Zheng, Q. T.; Sun, H. D. *J. Nat. Prod.* **2006**, *69*, 650.
- 8 Li, R. T.; Shen, Y. H.; Xiang, W.; Sun, H. *Eur. J. Org. Chem.* **2004**, 807.
- 9 Lei, C.; Huang, S. X.; Chen, J. J.; Pu, J. X.; Li, L. M.; Xiao, W. L.; Liu, J. P.; Yang, L. B.; Sun, H. D. *Helv. Chim. Acta* **2007**, *90*, 1399.
- 10 (a) Xiao, W. L.; Li, X. L.; Wang, R. R.; Yang, L. M.; Li, L. M.; Huang, S. X.; Pu, J. X.; Zheng, Y. T.; Li, R. T.; Sun, H. D. *J. Nat. Prod.* **2007**, *70*, 1056. (b) Xiao, W. L.; Pu, J. X.; Wang, R. R.; Yang, L. M.; Li, X. L.; Li, S. H.; Li, R. T.; Huang, S. X.; Zheng, Y. T.; Sun, H. D. *Helv. Chim. Acta* **2007**, *90*, 1505.
- 11 (a) Huang, S. X.; Han, Q. B.; Lei, C.; Pu, J. X.; Xiao, W. L.; Yu, J. L.; Yang, L. M.; Xu, H. X.; Zheng, Y. T.; Sun, H. D. *Tetrahedron* **2008**, *64*, 4260. (b) Huang, S. X.; Li, R. T.; Liu, J. P.; Lu, Y.; Chang, Y.; Lei, C.; Xiao, W. L.; Yang, L. B.; Zheng, Q. T.; Sun, H. D. *Org. Lett.* **2007**, *9*, 2079.
- 12 (a) Xiao, W. L.; Pu, J. X.; Chang, Y.; Li, X. L.; Huang, S. X.; Yang, L. M.; Li, L. M.; Lu, Y.; Zheng, Y. T.; Li, R. T.; Zheng, Q. T.; Sun, H. D. *Org. Lett.* **2006**, *8*, 4669. (b) Xiao, W. L.; Pu, J. X.; Chang, Y.; Li, X. L.; Huang, S. X.; Yang, L. M.; Li, L. M.; Lu, Y.; Zheng, Y. T.; Li, R. T.; Zheng, Q. T.; Sun, H. D. *Org. Lett.* **2006**, *8*, 1475.

- 13 Xiao, W. L.; Yang, L. M.; Li, L. M.; Pu, J. X.; Huang, S. X.; Weng, Z. Y.; Lei, C.; Liu, J. P.; Wang, R. R.; Zheng, Y. T.; Li, R. T.; Sun, H. D. *Tetrahedron Lett.* **2007**, *48*, 5543.
- 14 Li, R. T.; Han, Q. B.; Zheng, Y. T.; Wang, R. R.; Yang, L. M.; Lu, Y.; Sang, S. Q.; Zheng, Q. T.; Zhao, Q. S.; Sun, H. D. *Chem. Commun.* **2005**, 2936.
- 15 Li, R. T.; Li, S. H.; Zhao, Q. S.; Lin, Z. W.; Sun, H. D.; Lu, Y.; Wang, C.; Zheng, Q. T. *Tetrahedron Lett.* **2003**, *44*, 3531.
- 16 Huang, S. X.; Yang, L. B.; Xiao, W. L.; Lei, C.; Liu, J. P.; Lu, Y.; Weng, Z. Y.; Li, L. M.; Li, R. T.; Yu, J. L.; Zheng, Q. T.; Sun, H. D. *Chem. Eur. J.* **2007**, *13*, 4816.
- 17 Huang, S. X.; Li, R. T.; Liu, J. P.; Lu, Y.; Chang, Y.; Lei, C.; Xiao, W. L.; Yang, L. B.; Zheng, Q. T.; Sun, H. D. *Org. Lett.* **2007**, *9*, 2079.
- 18 Huang, S. X.; Yang, J.; Huang, H.; Li, L. M.; Xiao, W. L.; Li, R. T.; Sun, H. D. *Org. Lett.* **2007**, *9*, 4175.
- 19 Xiao, W. L.; Lei, C.; Ren, J.; Liao, T. G.; Pu, J. X.; Pittman, C. U.; Lu, Y.; Zheng, Y. T.; Zhu, H. J.; Sun, H. D. *Chem. Eur. J.* **2008**, *14*, 11584.
- 20 Chenoweth, D. M.; Chenoweth, K.; Goddard, W. A. *J. Org. Chem.* **2008**, *73*, 6853.
- 21 For the fragment synthesis of lancifodilactone G, see: (a) Maity, S.; Matcha, K.; Ghosh, S. *J. Org. Chem.* **2010**, *75*, 4192. (b) Lai, K. W.; Paquette, L. A. *Org. Lett.* **2008**, *10*, 2115. (c) Paquette, L. A.; Lai, K. W. *Org. Lett.* **2008**, *10*, 2111.
- 22 Paquette, L. A.; Lai, K. W. *Org. Lett.* **2008**, *10*, 3781, and pertinent references cited therein.
- 23 For a review on SmI₂-mediated intramolecular cyclisation reactions, see: Edmonds, D. J.; Johnston, D.; Procter, D. J. *Chem. Rev.* **2004**, *104*, 3371.
- 24 Miyaura, N.; Ishiyama, T.; Sasaki, H.; Ishikawa, M.; Satoh, M.; Suzuki, A. *J. Am. Chem. Soc.* **1989**, *111*, 314.
- 25 Otsubo, K.; Inanaga, J.; Yamaguchi, M. *Tetrahedron Lett.* **1987**, *28*, 4437.
- 26 Paquette, L. A.; Lai, K. W. *Heterocycles* **2009**, *79*, 299, and pertinent references cited therein.
- 27 Paquette, L. A., In *Stereocontrolled Organic Synthesis*; ed. by B. M. Trost; Blackwell Scientific Publications: Oxford, England, 1994; pp 313-336.
- 28 (a) Kan, S. B. J.; Anderson, E. A. *Org. Lett.* **2008**, *10*, 2323. (b) Cordonnier, M. C. A.; Kan, S. B. J.; Anderson, E. A. *Chem. Commun.* **2008**, 5818.
- 29 Ley, S. V.; Norman, J.; Griffith, W. P.; Marsden, S. P. *Synthesis* **1994**, 639.
- 30 Corey, E. J.; Han, X. J.; Stoltz, B. M. *J. Am. Chem. Soc.* **1999**, *121*, 7600.
- 31 Evans, P. A.; Roseman, J. D.; Garber, L. T. *Synth. Commun.* **1996**, *26*, 4685.

Chapter 2

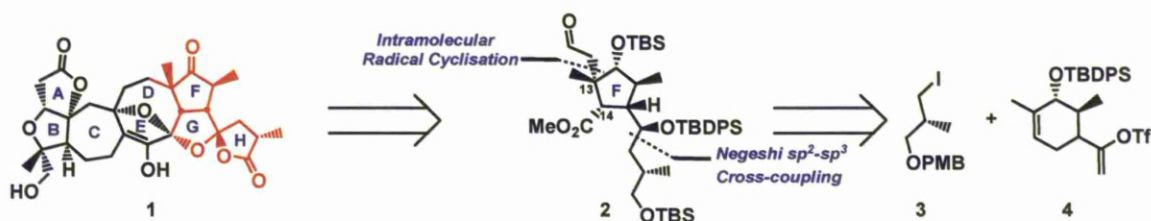
Synthesis of the Eastern Fragment (F-G Rings) of Lancifodilactone G

2.1 Introduction

2.1.1 Previous Synthetic Work

2.1.1.1 The Paquette Approach

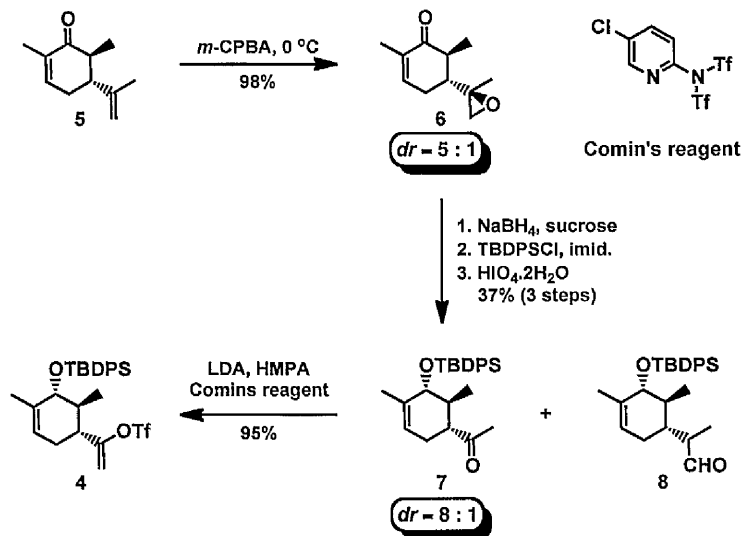
In 2008, Paquette and co-workers reported the only synthesis to date of the eastern fragment using a stereochemically linear strategy to construct the congested F ring of Lancifodilactone G **1**.¹ As outlined in Scheme 2.1, the key disconnections on the advanced intermediate **2** involve an intermolecular free-radical cyclisation reaction² envisioned to install the challenging quaternary stereogenic centre at C13 and a sp^2 - sp^3 Negishi cross-



Scheme 2.1 Paquette's Retrosynthetic Analysis.

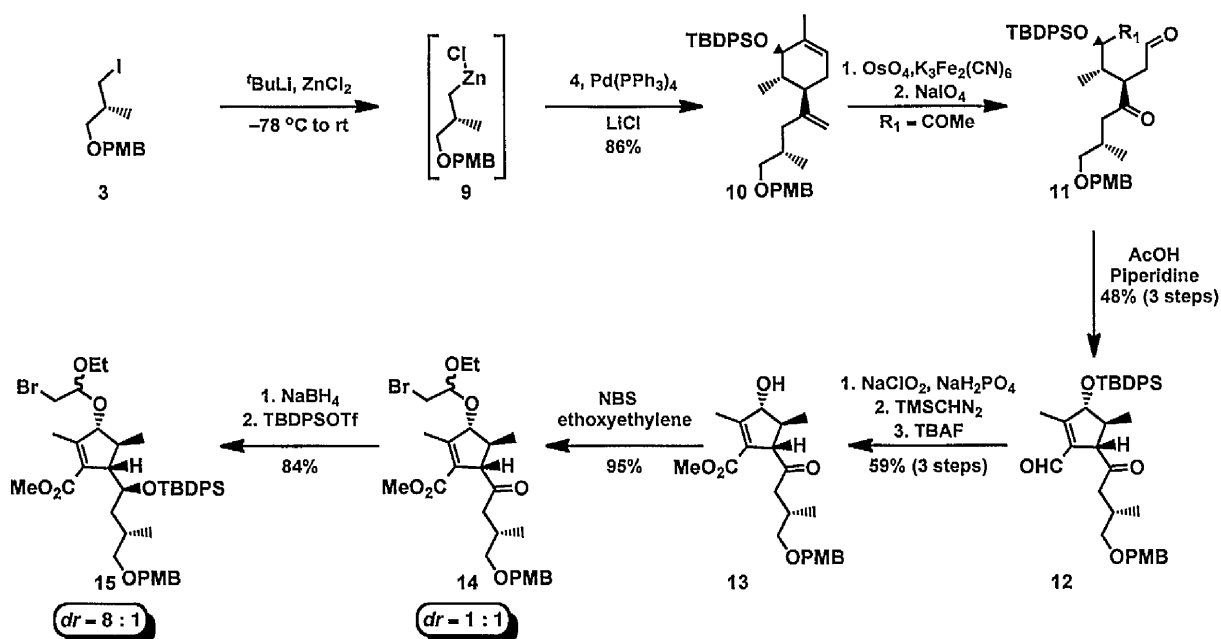
coupling reaction³ to connect the side chain **3** to the vinyl triflate **4**. The synthesis commenced with the substrate controlled stereoselective epoxidation of the readily available carvone derivative **5** to afford mixture of epoxides **6** in an excellent yield, albeit with 5 : 1 diastereoselectivity (Scheme 2.2). A two-step reagent directed stereoselective hydride reduction-silyl protection sequence⁴ on the epoxide **6** afforded the corresponding epoxy-silyl ether, which on exposure to periodic acid underwent oxidative cleavage to generate the desired methyl ketone **7** in low yield. The reaction also led to the concomitant formation of

the undesired aldehyde **8** originating from a [1,2] hydride shift.⁵ The conversion of the ketone **7** to the vinyl triflate **4** was then achieved in 95% yield using the Comins's reagent in conjunction with LDA and HMPA.⁶ Having secured access to the vinyl triflate **4**, the modified palladium-catalysed Negishi cross-coupling reaction³ was carried out with the



Scheme 2.2 Preparation of Vinyl Triflate **4**.

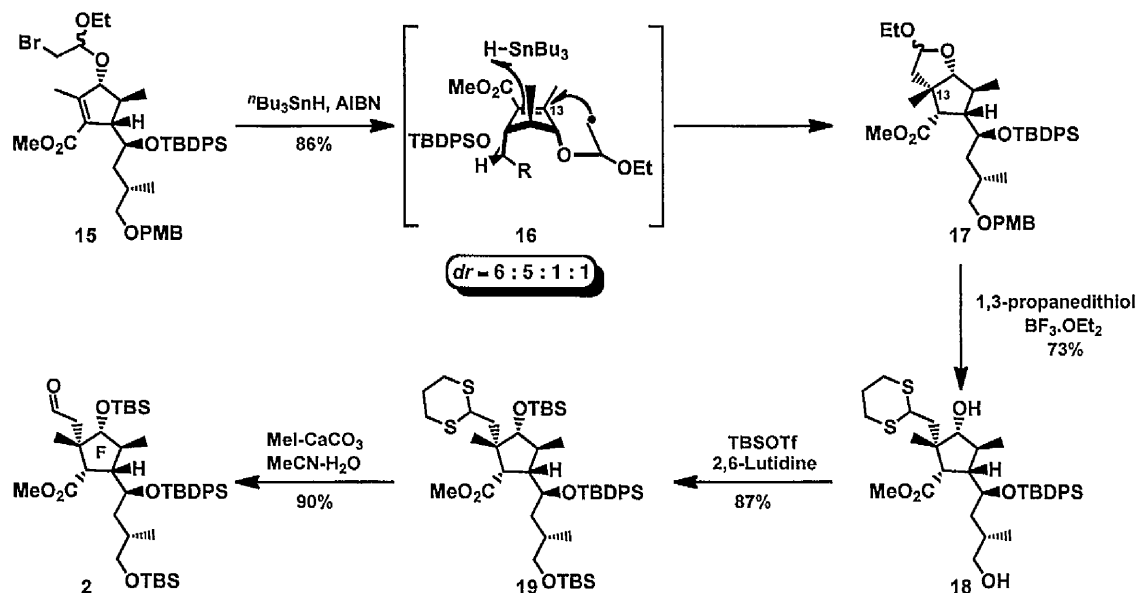
putative organozinc species **9** to afford diene **10** in 86% yield (Scheme 2.3). During the optimisation study, it was found that premixing the iodide **3** with ZnCl_2 prior to the addition of three equivalents of $t\text{BuLi}$ to form the organozinc species **9** was a critical factor



Scheme 2.3 Synthesis of Bromoacetal **15**.

in achieving a high yield.^{7a} Additionally, the utilisation of LiCl also had a beneficial effect in the reaction, which presumably favours the lithium-zinc transmetallation step by generating a highly soluble $RZnX \cdot LiCl$ complex^{7b} post halogen-lithium exchange of the alkyl halide **3**. The six-membered ring in **10** was then subjected to a ring-contraction to afford five-membered keto-aldehyde **12** in 48% yield using a three-step sequence involving *bis*-dihydroxylation of the diene **10**, oxidative cleavage of the resulting tetraol and intramolecular aldol cyclisation-elimination. The aldehyde **12** was converted to the hydroxy ester **13** in three steps using standard transformations, which was subsequently elaborated to the bromoacetal **14** in excellent yield. Chelation-controlled hydride reduction of the ketone **14** followed by silyl protection afforded the advanced intermediate **15** required for the free radical reaction.

Treatment of the bromide **15** with tributyltin hydride and AIBN promoted the intramolecular radical cyclisation², which installed the two contiguous stereocentres at C13 and C14 with moderate diastereoselectivity (Scheme 2.4). The stereoselectivity in this



Scheme 2.4 *Synthesis of Aldehyde 2.*

reaction can be rationalised from the intermediate **16** wherein the pendent radical side chain approaches from the bottom face to the acceptor π -bond to set up the quaternary stereocentre

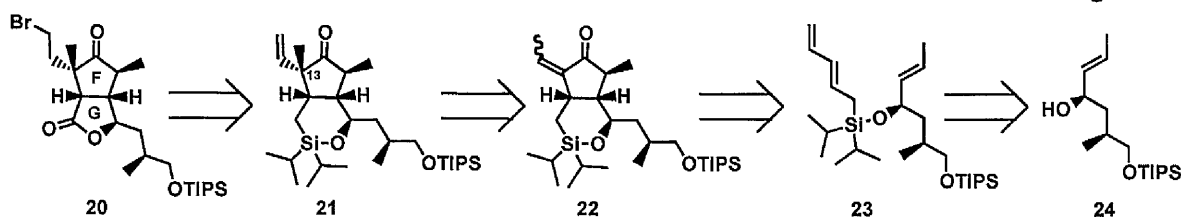
at C13 followed by reduction from the more accessible convex face. In the next step, the dithioketal **18** was formed using 1,3-propanedithiol and $\text{BF}_3 \cdot \text{Et}_2\text{O}$, which also deprotected the primary PMB group. Subsequent *bis*-TBS protection of the diol **18** followed by dethioacetalisation of **19** furnished the target aldehyde **2** in 78% yield over two steps.

In conclusion, the Paquette's group accomplished their synthesis in 19 linear steps with 3% overall yield. Despite the successful development of a route for the eastern fragment, the synthesis has a number of problems, which emanate from modest selectivity in the critical stereoselective reactions.

2.2 Results and Discussion

2.2.1 Retrosynthetic Analysis

In planning our synthetic strategy to the eastern fragment, our main priority was to identify an approach that would deliver an efficient and scalable synthetic route to the intermediate **20** with the requisite functional group handle to test the critical coupling reaction with the western intermediate. Our initial retrosynthetic analysis for the eastern fragment is illustrated in Scheme 2.5, which involves functional group interconversion of the bromide side chain in **20** to the terminal alkene. Initial consideration includes a single-



Scheme 2.5 Retrosynthetic Analysis for the Eastern Fragment **20**.

pot hydrozirconation-bromination sequence¹⁰ or a two-step hydroboration-oxidation reaction followed by the bromination of the primary alcohol. Retrosynthetic disconnection of the five-membered ring after the oxidation state adjustment of the bicyclic lactone **20** unveiled the 1,4-diol functionality which would be derived after the Tamao-Kumada oxidation reaction of temporary silicon-tethered bicyclic alkene **21**.¹¹ We envisioned the quaternary stereogenic centre at C13 would be controlled by the facial bias of the *cis*-fused bicyclic

enolate formed from a *exo*-deconjugative methylation reaction of **22**, which should preferentially methylate from the more accessible convex face. The diastereoselective temporary silicon-tethered (TST) rhodium-catalysed dienyne Pauson-Khand reaction¹² was envisioned to provide the bicyclic ketone **22** in an expeditious manner. The differentially substituted silicon tether **23** could be in turn be assembled from the allyl alcohol fragment **24** in a relatively standard manner.

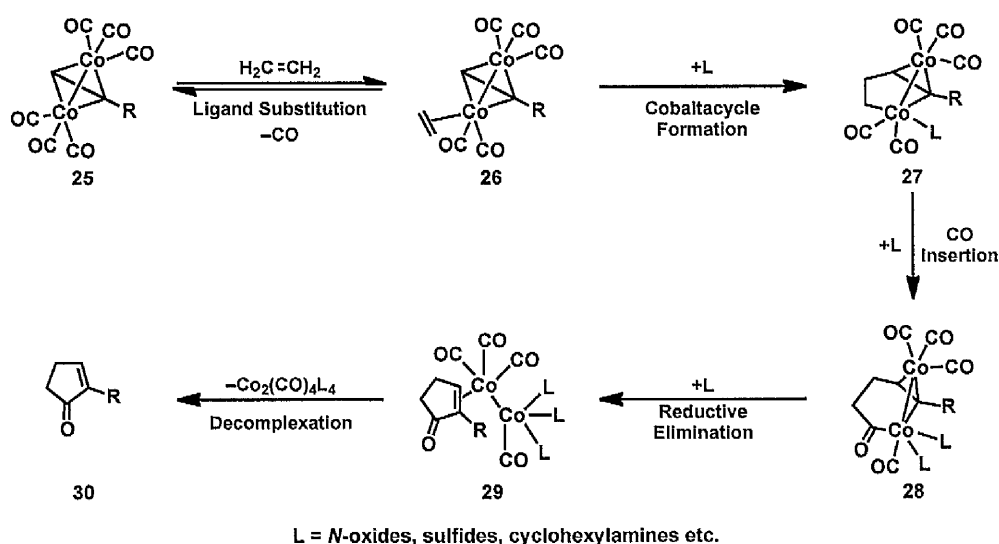
2.3 An Overview on the Metal-Mediated Diastereoselective Pauson-Khand Reaction

2.3.1 Stoichiometric Cobalt-Mediated PK Reaction

The Pauson-Khand (PK) reaction is a transition metal-assisted three-component carbonylation of an alkyne, an alkene and carbon monoxide widely utilised in the convergent synthesis of functionalised cyclopentenones that are commonly found in biologically active natural products. Since the first report of the intermolecular process between norbornadiene and hexacarbonyldicobalt complex disclosed by Pauson and Khand,¹³ the PK reaction has been the focus of intense attention over the past two decades. The studies have addressed drawbacks associated with the reaction's scope and efficiency. A key improvement in the original transformation is the intramolecular variant of the cobalt-mediated PK reaction that solved the regioselectivity issues associated with unsymmetrical alkynes and poor reactivity of unstrained alkenes.¹⁴ Other notable variations that have evolved over the years also include the use of different transition metals and promoters,¹⁵ which were aimed at accomplishing a catalytic version and mitigate the harsh conditions often employed in the PK reaction. As a result of these findings, the PK annulation reaction has emerged as a strategic transformation for the construction of five-membered carbocycles in the context of total synthesis. The PK reaction has been the subject of several comprehensive reviews,¹⁶ and hence, the current discussion would be limited to the metal-mediated diastereoselective PK reactions having a stereogenic centre at C2.

2.3.1.1 Proposed Mechanism for the Cobalt-Mediated Pauson-Khand Reaction

The mechanistic pathway proposed by Magnus and co-workers for the PK reaction has gained universal acceptance despite the lack of experimental evidence, which can be attributed to the difficulty in detecting intermediates during the cyclisation sequence.¹⁷ Nevertheless, the proposed mechanism accounts for several experimental observations and makes it possible to perform DFT calculations on the rate-determining step to further understand the mechanism.^{17a} As illustrated in Scheme 2.6, the sequence begins with the alkene-CO ligand exchange on a cobalt atom to furnish the corresponding complex **26**. This step is a highly endothermic process and computed to be the rate-determining step in the PK reaction. The promoters such as tertiary amine-*N*-oxides, DMSO etc. are speculated to accelerate the stoichiometric cobalt-mediated PK reactions by facilitating the oxidative



Scheme 2.6 Mechanism for the Cobalt-Mediated PK Reaction.

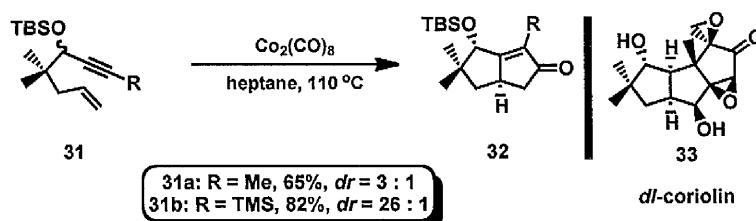
removal of CO, which creates a vacant site on the metal centre for coordination with the reacting alkene thereby lowering the activation energy of the ligand substitution reaction.¹⁵

In the second step, a σ -C-C bond is formed between the alkene and the less hindered terminus of the cobalt complexed alkyne **26** to form the five-membered metallacycle **27**. The regioselectivity in the intermolecular PK reaction with unsymmetrically substituted alkynes places the less hindered end of the alkene into the less hindered Co-C bond. Following the

formation of the cobaltacycle **27**, the second carbon-carbon bond is formed after the migratory insertion of the metal-bound CO to generate the six-membered metallacycle **28**. The resulting cobaltacycle **28** undergoes reductive elimination to form the final carbon-carbon bond in complex **29** and ensuing decomplexation of the metal cluster releases the cyclopentenone **30**.

2.3.1.2 Diastereoselectivity in Cobalt-Mediated PK Reaction

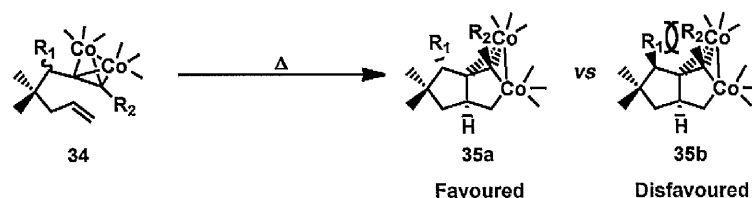
In 1985, Magnus and co-workers proposed a working mechanistic hypothesis to explain the origins of the observed 1,2- and 1,3-*cis*-stereoselectivity in the PK reaction



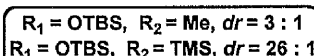
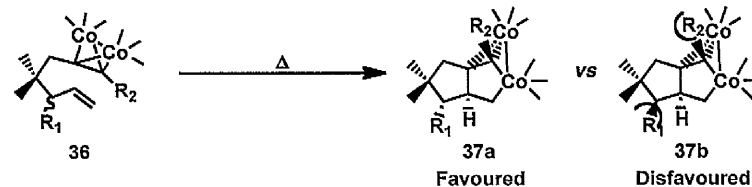
Scheme 2.7 Magnus Formal Synthesis of Coriolin **33**.

en route to the formal synthesis of coriolin **33** (Scheme 2.7).^{17e,f} During the course of their study, the group observed a modest diastereoselectivity of 3 : 1 favouring the *cis*-isomer **32a** for the PK reaction of the enyne **31a** bearing a methyl substituent at the alkyne terminus. Interestingly, an excellent selectivity of 26 : 1 was obtained when the methyl substituent was replaced with a bulky TMS group (Scheme 2.7). The stereochemical outcome in the synthesis of bicyclopentenones **32** was rationalised during the metallacycle formation based on models depicted in Scheme 2.8. In this model, the bulky group on the alkyne terminus magnifies the pseudo diaxial interactions in the disfavoured transition states **35b** and **37b**, which results in superior levels of diastereocontrol with the more bulky TMS group over the methyl substituent. The mechanistic insights that were gleaned by the Magnus group during the total synthesis of coriolin **33** were later successfully extended to the syntheses of other biologically active natural products such as hirsutene, hirsutic acid and (±)-quadrone.^{17e-g}

1,3-Induction

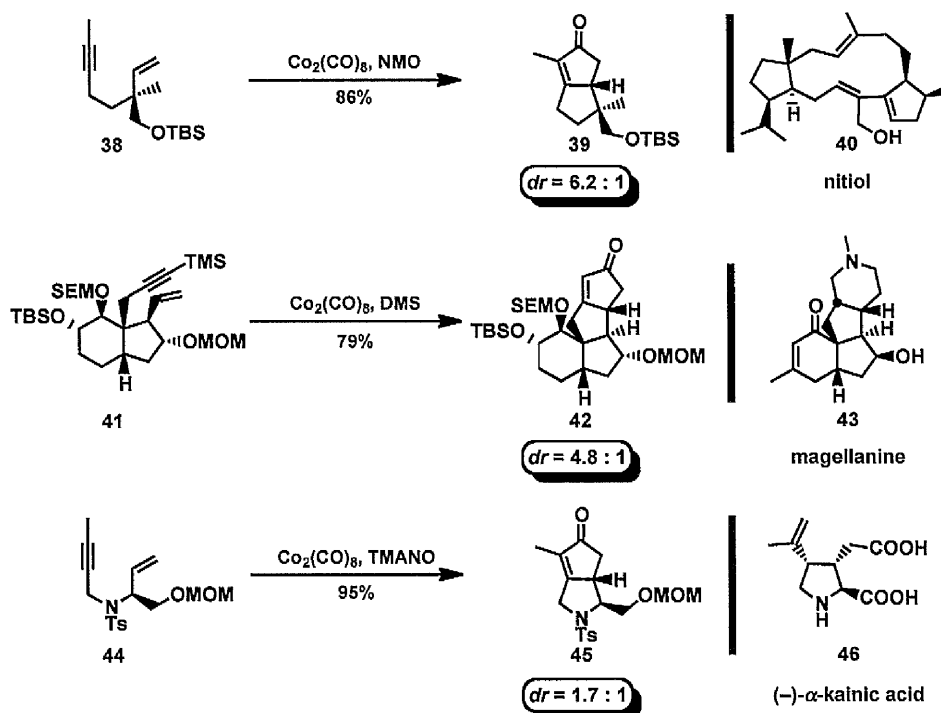


1,2-Induction



Scheme 2.8 Models for 1,3- and 1,2-Stereoinduction in the Cobalt-Mediated PKR Reaction.

Following the pioneering report of Magnus, the cobalt-mediated diastereoselective PKR reaction has emerged as a robust and valuable reaction for the stereoselective construction of bicyclic fused ring systems. Representative examples for the application of diastereoselective PK reactions in several total syntheses are outlined in Scheme 2.9.¹⁸

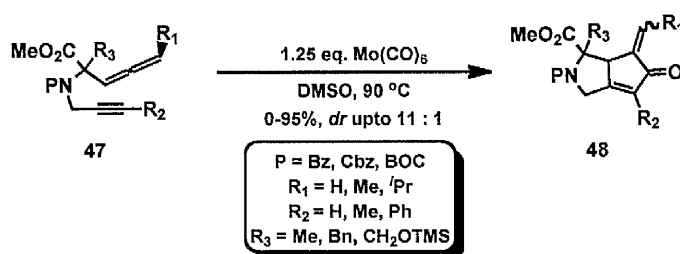


Scheme 2.9 Application of Cobalt-Mediated PK Reaction in Total Synthesis.

Although the proposed model by Magnus serves as an excellent mnemonic for predicting the facial selectivity of the major diastereoisomer in the PK reaction, the cobalt-mediated cyclisation continues to be plagued with the issues of low to moderate diastereocontrol with several substrates despite considerable efforts in this area during the last decade.

2.3.2 Stoichiometric Molybdenum-Mediated PK Reaction

In 2004, Brummond and co-workers reported the first diastereoselective molybdenum-mediated PK reaction of functionalised alkynyl allenes **47** for the construction of α -alkylidene cyclopentenones **48** (Scheme 2.10).¹⁹ During the examination of the allenic PK reaction, the group discovered divergent reaction pathways leading to the selective formation of 5,5- and 5,6-azabicycles, resulting from the selective participation of the



Scheme 2.10 Molybdenum-Mediated PK Reaction of Alkynyl Allenes.

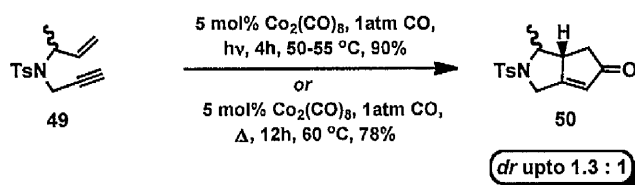
proximal and distal double bond of the allene **47**, respectively, depending using either stoichiometric molybdenum hexacarbonyl or [Rh(CO)₂Cl] complex. While the reaction has been found to be very effective with wide range of substrates in the carbocyclisation reaction, the problems of low diastereocontrol, poor *E/Z* stereoselectivity and the use of stoichiometric molybdenum or rhodium complexes make this methodology unattractive in comparison with the cobalt-mediated PK reaction.

2.3.3 Transition Metal-Catalysed Diastereoselective PK Reaction

2.3.3.1 Cobalt-Catalysed PK Reaction

Since the initial report on the catalytic PK reaction by Pauson and co-workers,^{13b} significant advances have been made in the catalytic adaptation for the PK reaction. For

example, Rautenstrauch,²⁰ Livinghouse,²¹ Jeong,²² and Krafft²³ have independently employed cobalt complexes to achieve an atom economical carbonylative process for enyne cyclisation. Despite significant progress in identifying a suitable catalytic system that provides excellent yield with a broad substrate scope, a practical catalytic version for the diastereoselective PK reaction using cobalt complexes still remains elusive. For example, the Livinghouse group published on a photochemically and thermally promoted cobalt-catalysed intramolecular PK reaction using 1 atmosphere of carbon monoxide pressure with the enyne **49** to furnish the bicyclic enone **50** in excellent yield, albeit with almost no diastereocontrol (Scheme 2.11).²¹ While cobalt complexes continue to be thoroughly

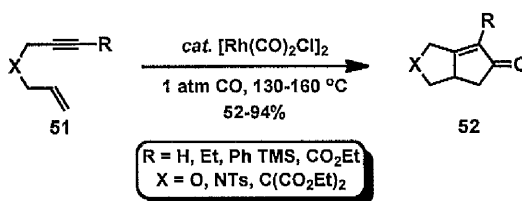


Scheme 2.11 Cobalt-Catalysed PK Reaction Nitrogen-Tethered Enyne.

investigated in the stereoselective PK reaction, the development of for a general catalytic system has expanded into other transition metals, such as rhodium,²⁴ titanium,²⁵ ruthenium,²⁶ chromium,²⁷ iron,²⁸ nickel,²⁹ zirconium,³⁰ molybdenum,¹⁹ palladium,³¹ tungsten,³² and iridium.³³

2.3.3.2 Rhodium-Catalysed PK Reaction

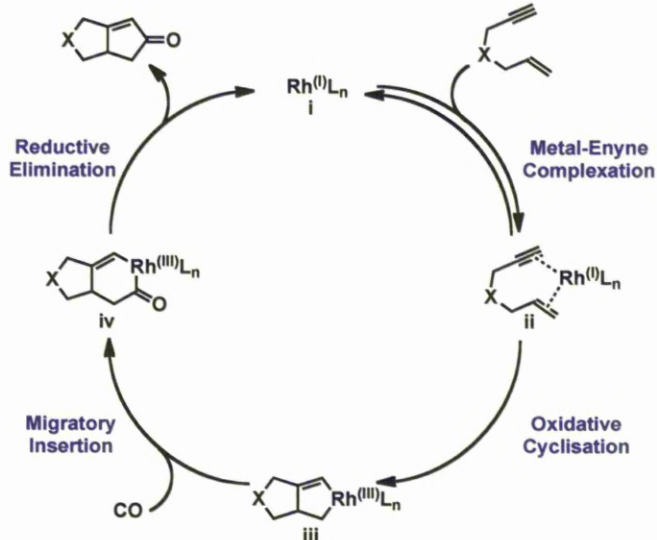
The intramolecular rhodium-catalysed [2+2+1] reaction of enynes and carbon monoxide was first accomplished by Narasaka and co-workers in 1998 employing $[\text{Rh}(\text{CO})_2\text{Cl}]_2$ (Scheme 2.12).^{24a,b} The dirhodium carbonyl complex exhibited remarkable



Scheme 2.12 Rhodium(I)-Catalysed PK Reaction.

catalytic activity in the PK reaction with carbon and heteroatom-tethered enynes, to furnish the corresponding bicyclic cyclopentenones using 2 mol% catalyst in the presence of 1 atmosphere of carbon monoxide.

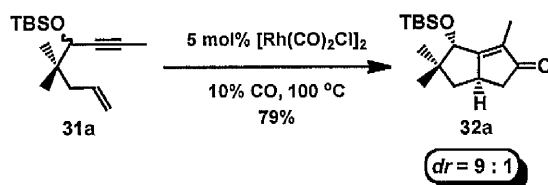
A general catalytic cycle for the rhodium-catalysed PK reaction using 1,6-enynes is outlined in Scheme 2.13.³⁴ In the first step of the catalytic cycle, the rhodium(I) catalyst **i** reversibly binds to the enyne to form the metal-enyne complex **ii**, which then undergoes the rate-determining oxidative cyclisation to irreversibly generate the rhodium metallacycle **iii**. Migratory insertion of metal-bound CO into the rhodium-sp³ carbon bond in **iii** gives rise to a 5,6-fused bicyclic rhodacycle **iv**, which subsequently undergoes reductive elimination to release the requisite bicyclic enone and regenerate rhodium(I) catalyst **i**.



Scheme 2.13 Catalytic Cycle for the Rhodium-Catalysed PK Type Reaction.

2.3.3.2.1 Diastereoselectivity in Rhodium(I)-Catalysed PK Reaction

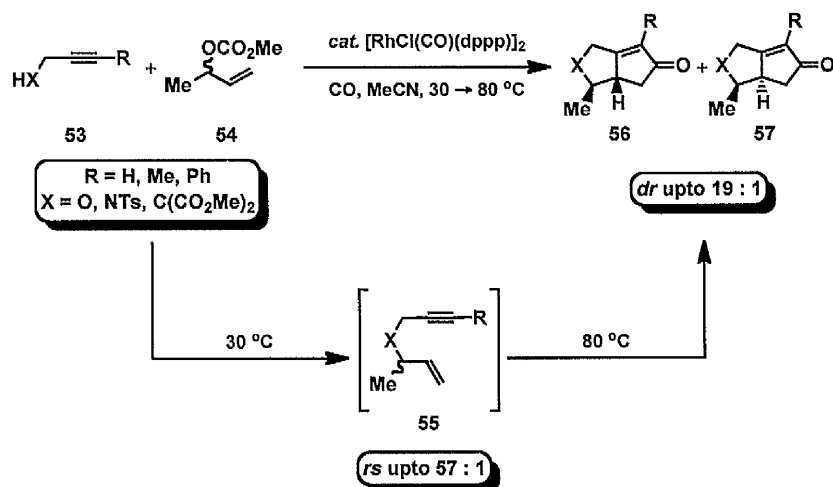
Narasaka *et al.* also examined the effect of reducing the carbon monoxide concentration in an analogous manner to the titanium-catalysed version of the PK reaction.^{24b} Interestingly, the reaction under 0.1 atmosphere of carbon monoxide proceeded faster compared to the reaction under 1 atmosphere, which enabled the reaction to be performed at a lower temperature, albeit with longer reaction time. Furthermore, as illustrated in Scheme 2.14, the modified conditions were employed in the diastereoselective



Scheme 2.14 Rhodium(I)-Catalysed Diastereoselective Synthesis of Bicyclic Enone.

synthesis of the key intermediate **32a** which was earlier reported in the total synthesis of *dl*-coriolin **33** (Scheme 2.7) by Magnus (*vide supra*).^{17e, f} The enyne **31a** furnished improved efficiency and diastereocontrol in the rhodium(I)-catalysed PK reaction as compared to the stoichiometric cobalt-mediated version.

In a first study of its kind, Evans and Robinson reported one-pot sequential allylic alkylation/PK reaction facilitated by a single metal-catalyst to construct complex bicyclic enones in a regio- and diastereoselective manner.^{35c} This transformation represents the first instance to address the issues of diastereoselectivity in the rhodium-catalysed PK reaction. Contrary to the approach of Jeong, wherein dual metal-catalysts in the form of $[\text{Pd}_2(\text{dba})_3]$ and $[\text{RhCl}(\text{CO})\text{dppp}]$ were utilised to effect the sequential allylic alkylation/PK reaction, the Evans group sought to carry out this challenging transformation using temperature to modulate the catalytic activity of the π -acidic rhodium(I) catalyst (Scheme 2.15). The multicomponent annulation reaction initially involved a highly regioselective allylic



Scheme 2.15 Rhodium-Catalysed Tandem Allylic Alkylation/PK Reaction.

substitution reaction of the pronucleophiles **53** with the secondary allylic carbonates **54** at 30 °C under 1 atmosphere of carbon monoxide, which furnished the carbon and heteroatom-tethered enynes **55** in a highly regioselective manner. The 1,6-enynes **55** were then subjected to the diastereoselective PK reaction by simply raising the reaction temperature to afford the desired bicyclopentenone **56** in a diastereoselective manner. The stereochemical outcome in the reaction is analogous to the cobalt-mediated PK reaction wherein the major diastereoisomer possessed a *cis*-relationship of the C3 bridgehead proton with the C2 alkyl substituent. The origin of stereocontrol in the reaction was rationalised by invoking a face selective binding of rhodium(I) catalyst to the enyne **i**, which would presumably result in the siphoning of the major diastereoisomer from the isomeric mixture of **ii** and **iii** through a pathway devoid of destabilising non-bonding interaction between the bulky metal complex and the alkyl substituent at C2 (Figure 2.1).

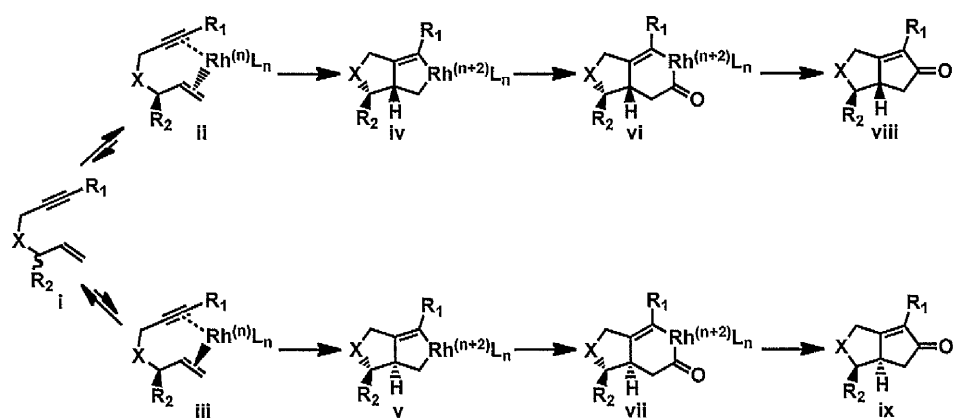
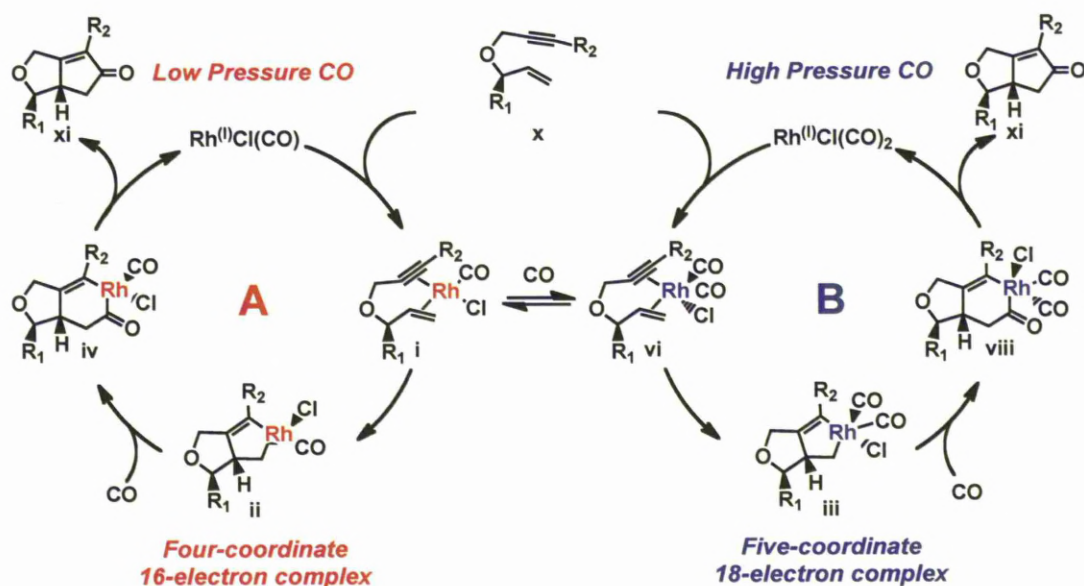


Figure 2.1 *Proposed Mechanistic Hypothesis in the Rhodium-Catalyzed PK Reaction.*

In order to gain further insight into the origin of diastereoselectivity in the PK reaction, Evans and Baik undertook a computational study to understand the role of coordination number for governing the stereocontrol.^{35a,b} This study probed catalytic systems originating from $[\text{Rh}^{\text{I}}\text{Cl}(\text{CO})]$ and $[\text{Rh}^{\text{I}}\text{Cl}(\text{CO})_2]$ which were speculated to be the active catalysts in the PK reaction.^{35b} Hence, the catalysts formed π -complexes with enyne **x** to furnish a 16-electron square planar adduct **i** and an 18-electron trigonal-bipyramidal organorhodium complex **vi** (Scheme 2.16). Examination of the free-energy profile for the

square planar complex revealed the energy difference of 1.2 kcal mol⁻¹ between the *cis*- and the *trans*-diastereoisomer for the rate-determining oxidative cyclisation step (Figure 2.2). This in turn predicts a maximum of 10 : 1 diastereomeric ratio (*d.r.*) in the reaction contrary



Scheme 2.16 Catalytic Cycle for Four- and Five-Coordinate Rhodium Complexes.

to the observed selectivity of $\geq 99 : 1$ for the oxygen tethered enynes at 1 atmosphere of carbon monoxide. Surprisingly, for the trigonal-bipyramidal complex, the *cis*-isomer was favoured by 7.0 kcal mol⁻¹ (*dr* $\geq 99 : 1$) over the *trans*-diastereoisomer, which accounts for

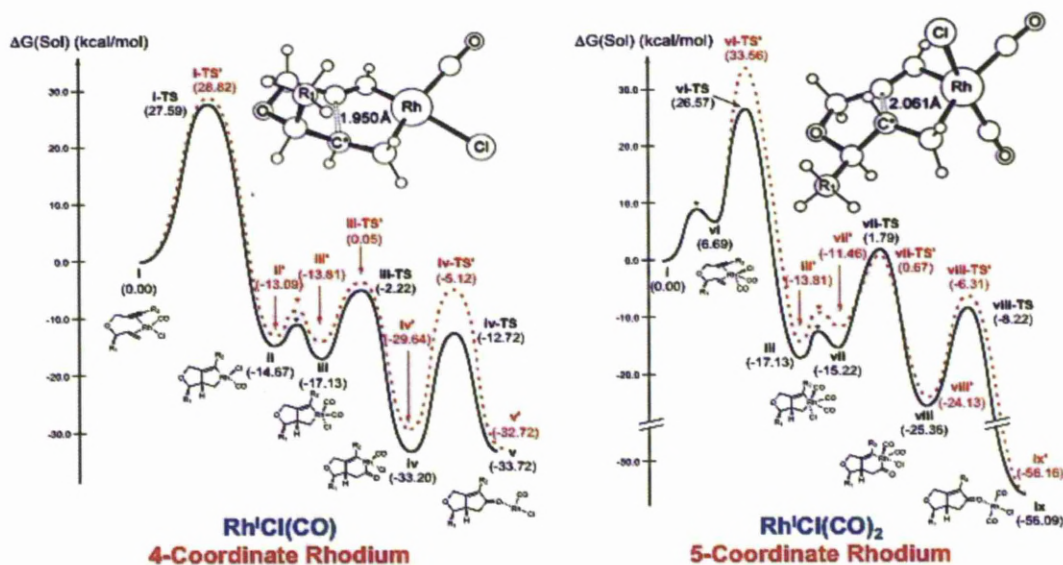


Figure 2.2 Reaction Energy Profiles for the Rhodium(I)-Catalysed PK Reaction.

the excellent diastereoselectivity observed in the PK reaction (Figure 2.2). Thus, the study implicates concentration of carbon monoxide on the rate determining oxidative cyclisation step and also suggests the formation of the thermodynamically disfavoured five-coordinate trigonal-bipyramidal complex **vi** to be the critical factor for attaining high levels of diastereocontrol in the PK reaction. These theoretical findings were put to test by performing PK reactions with varying compositions of carbon monoxide with the aim of altering the equilibrium ratio between the square planar **i** and the trigonal bipyramidal organorhodium complexes **vi**. As shown in Table 1, the excellent diastereoselectivity that was observed at 1 atmosphere of carbon monoxide was diminished to mediocre levels when it was reduced (Table 2.1, Entry 1 vs 2 and 3). Additionally, the theoretical predictions were further corroborated when the PK reaction of oxygen-tethered enyne **58** was catalysed by the $[\text{RhCl}(\text{CO})(\text{dppp})]_2$ complex, which contained a bidentate phosphine ligands, which enforces a trigonal-bipyramidal geometry thereby affording excellent yield and selectivity at low carbon monoxide concentration (Table 2.1, Entries 5 and 6).

Entry	Rhodium complex	CO : Ar (atm.)	Yield (%)	dr (59 : 60)
1	$[\text{RhCl}(\text{CO})_2]_2$	1.00 : 0.00	81	22 : 1
2	$[\text{RhCl}(\text{CO})_2]_2$	0.10 : 0.90	64	10 : 1
3	$[\text{RhCl}(\text{CO})_2]_2$	0.05 : 0.95	57	6 : 1
4	$[\text{RhCl}(\text{CO})(\text{dppp})]_2$	1.00 : 0.00	88	≥ 99 : 1
5	$[\text{RhCl}(\text{CO})(\text{dppp})]_2$	0.10 : 0.90	51	58 : 1
6	$[\text{RhCl}(\text{CO})(\text{dppp})]_2$	0.05 : 0.95	44	57 : 1

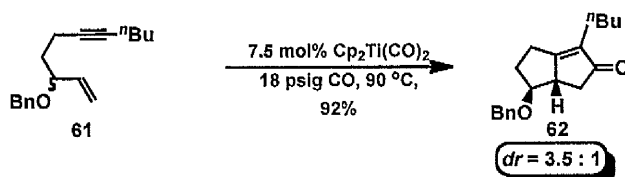
Table 2.1. *Effect of CO Pressure on the Diastereoselectivity in the PK Reaction.*

2.3.3.3 Other Transition Metal-Catalysed PK Reaction

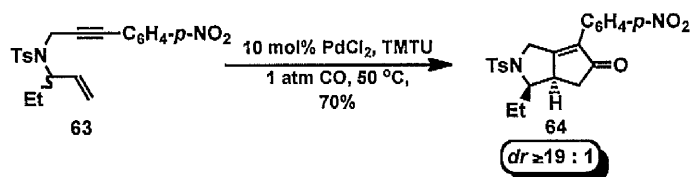
Several other transition metal carbonyl complexes are known to catalyse the diastereoselective PK reaction. However, they tend to be more limited in the context of poor

diastereoselection, substrate scope and generality. Additionally, these processes rely on high carbon monoxide pressure and elevated temperature, which makes these metal-catalysed processes less desirable to the rhodium and cobalt assisted carbocyclisation. Notable examples for some of these metal-catalysed reactions are illustrated in the following Scheme 2.17.

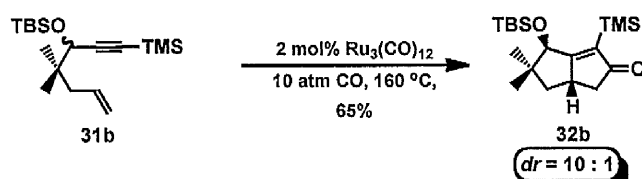
▪ **Titanium-Catalysed PK Reaction by Buchwald and Co-workers**²⁴



▪ **Palladium-Catalysed PK Reaction by Yang and Co-workers**³¹



▪ **Ruthenium-Catalysed PK Reaction by Murai and Co-workers**²⁶



Scheme 2.17 Diastereoselective Titanium-, Palladium-, and Ruthenium-Catalysed PK Reaction.

2.4 Temporary Silicon-Tethered Approach

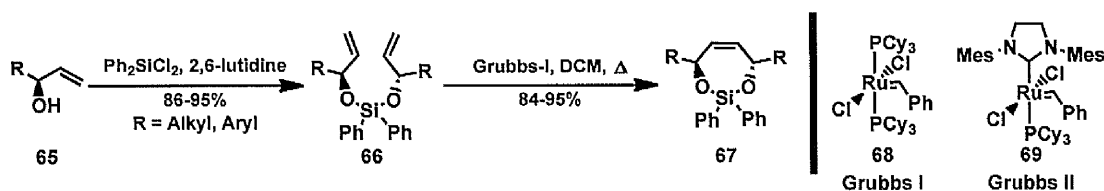
The concept of temporary silicon-tethered (TST) in transforming intermolecular reactions into the corresponding intramolecular variant is well established and also has been the subject of comprehensive reviews.³⁶ This strategy continues to find extensive application in organic transformations because of its attractive features such as readily accessibility of suitable coupling partners, stability of the tether to a variety of reaction conditions and finally, the tether can be selectively removed from the product or can be functionalised under a wide range of reaction conditions.³⁷ These reactions often proceed with high degrees of regio-, chemo- and stereoselectivity thereby overcoming the limitations of corresponding intermolecular reactions. Hence, temporary silicon tethers have been utilised as versatile disposable linkers in a myriads of reactions since the seminal work of Nishiyama and Stork in the area of free radical cyclisation reactions.³⁸

2.4.1 Contributions from the Evans Group

Development of novel TST transition metal-catalysed higher order $[m+n+o]$ carbocyclisation reactions³⁹ and its application to the synthesis of challenging natural products is an on-going area of research within the Evans group. The following section will discuss some of the methodology and its application in the total synthesis of natural product that were conducted within the group.

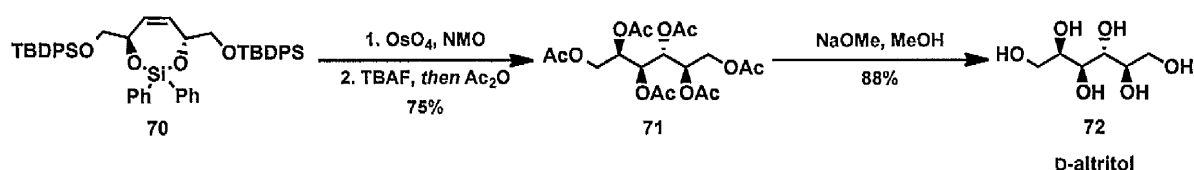
2.4.1.1 TST-RCM Cross-Coupling Reaction

In 1998, Evans and Murthy described the combination of the temporary silicon-tether with ring closing metathesis, utilising several optically enriched allylic alcohols for the



Scheme 2.18 Synthesis of C_2 -Symmetric Silaketals **67**.

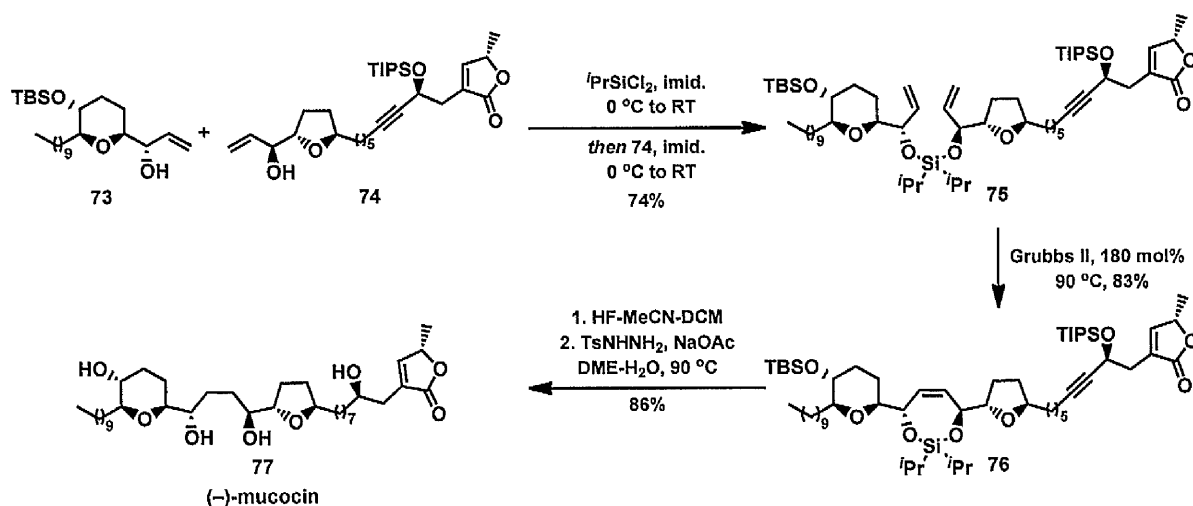
preparation of C_2 -symmetric diols.^{40, 41} In this study, as depicted in Scheme 2.18, a series of *bis*-alkoxysilanes **66** were prepared by treatment of allylic alcohols **65** with diphenyldichlorosilane and 2,6-lutidine. The resulting acyclic dienyl diphenylsilaketals **66** were converted to the corresponding cyclic diphenylsilaketals **67** by ring closing metathesis employing Grubbs 1st generation catalyst **68**. The C_2 -symmetric silaketals such as **67** can be readily transformed to a number of valuable intermediates. Towards this end, the Evans group applied this methodology in the preparation of reduced carbohydrate D-altritol **72**.⁴⁰ As illustrated in Scheme 2.19, the diphenyl silaketal **70** was subjected to the standard dihydroxylation reaction followed by fluoride mediated silyl deprotection to furnish D-altritol **72** which was peracetylated *in situ* to expedite isolation. Saponification of the hexaacetate **71** afforded D-altritol **72** in 88% yield.



Scheme 2.19 Preparation of D-Altritol **72**.

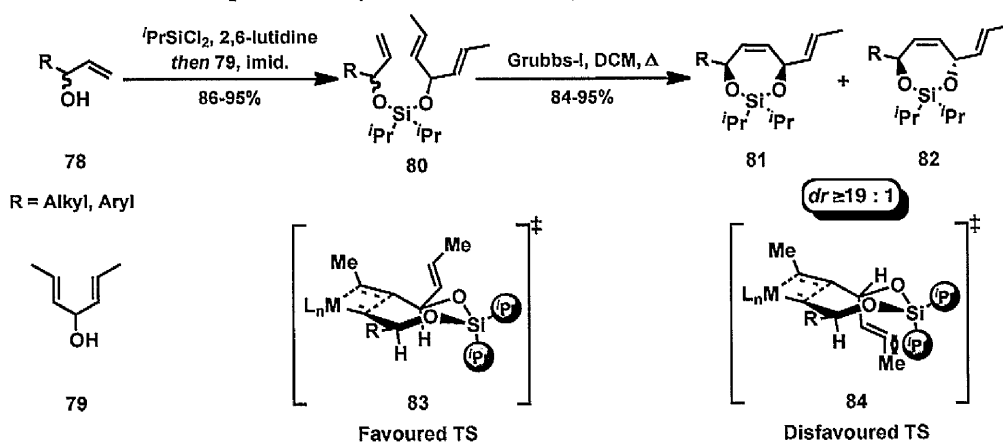
In 2003, Evans and co-workers elegantly incorporated the TST-RCM methodology in the asymmetric synthesis of the potent antitumour agent (–)-mucocin **77** (Scheme 2.20).⁴² As illustrated in Scheme 2.20, the differentially substituted dienyl *bis*-alkoxysilane **75** was prepared by the addition of the allyl alcohol **74** to the preformed solution of monochlorosilane derived from the TBS protected allyl alcohol **73**. The *bis*-alkoxysilane **75** underwent cyclisation on treatment with an excess of Grubbs II catalyst **69** to deliver the cyclic silaketal **76** in 83% yield. Stoichiometric amounts and slow addition of the active ruthenium carbene catalyst using syringe pump were critical factors in order to drive the reaction to completion and also to suppress the competing side reactions in this challenging transformation. Global silyl deprotection followed by the chemoselective reduction of the

alkyne and alkene in **76** using diimide completed the expeditious synthesis of the annonaceous acetogenin (–)-mucocin **77** in a 12 step sequence in 13.6% overall yield.⁴²



Scheme 2.20 Enantioselective Synthesis of (–)-Mucocin **77**.

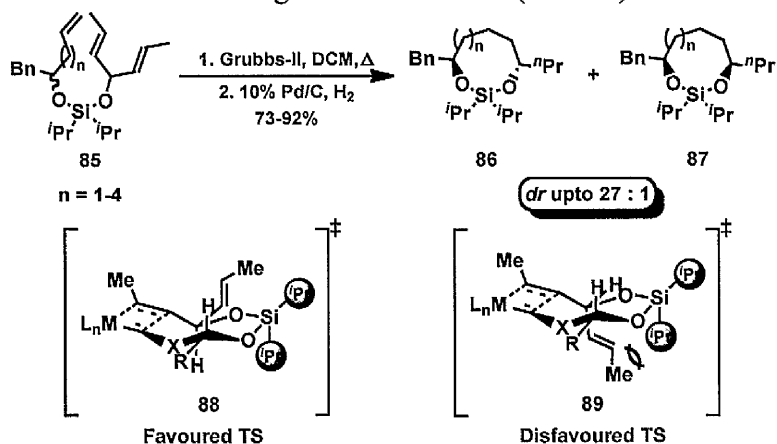
Building on the TST-RCM methodology for the enantioselective construction of C₂-symmetrical 1,4-diols, the Evans group employed this strategy for controlling long-range asymmetric induction for the diastereoselective syntheses of 1,4-, 1,5- and 1,6-silaketals,⁴³ wherein one of the tethered alkene partners is derived from a prochiral alcohol **79**. As outlined in Scheme 2.21, preliminary studies investigated the steric effect imposed by the



Scheme 2.21 Long Range Asymmetric Induction Using TST-RCM Reaction.

alkyl substituents on the silicon in which the diisopropyl tether provided the *bis*-alkoxysilane **81** in excellent yield and with impressive levels of 1,4-stereocontrol in the reaction of acyclic silaketal **80**. The *cis*-selectivity in the reaction can be rationalised from

the favoured transition state **83** (Scheme 2.21) in which the propenyl moiety adopts the pseudoequatorial orientation in order to minimise the non-bonding interactions with the bulky isopropyl substituent as shown in the disfavoured transition state **84**. Interestingly, a switch in the selectivity favouring the *trans*-isomer was observed when the reaction was extended to the construction of homologated silaketals **86** ($n = 1-4$)⁴³. As shown in Scheme



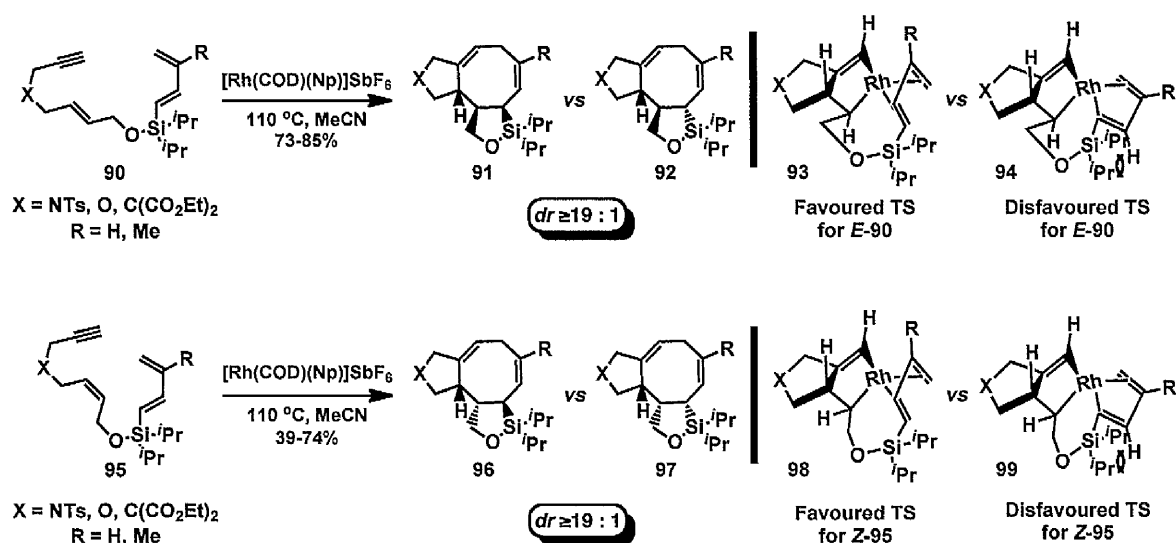
Scheme 2.22 Synthesis of *Trans*-Silaketals **86**.

2.22), the propenyl substituent occupies the pseudoequatorial position in the favoured transition state **88** to avoid steric clash with the axial isopropyl group on silicon. Hence, the origin of diastereoselectivity outlined in Scheme 2.22 is consistent with the previous model, albeit the pseudoaxial and pseudoequatorial positions are reversed in the medium size rings.

2.4.1.2 Rhodium-Catalysed TST-[4+2+2] Cycloisomerisation Reaction

In 2004, Evans and Baum reported the first intramolecular TST rhodium-catalysed cycloisomerisation of trienynes that proceeded in exquisite levels of regioselectivity and diastereoselectivity (Scheme 2.23).^{44a} A striking feature with this transformation is the stereochemistry of the olefin in trienynes **90** and **95** are transferred to tricyclic octanoids **91** and **96** stereospecifically with high levels of fidelity. Thus, the complimentary diastereoselection observed in this reaction can be exploited in the target-directed synthesis of cyclooctanoid containing natural products. A variety of carbon and heteroatom tethers were successfully employed in the cycloisomerisation reaction which were either unreactive or afforded mixture of regioisomers in the intermolecular variant reported by the group in

2002.^{44b} The excellent facial selectivity observed during the carbometallation step involving initially formed metallacyclopentene and the tethered diene is in agreement with the

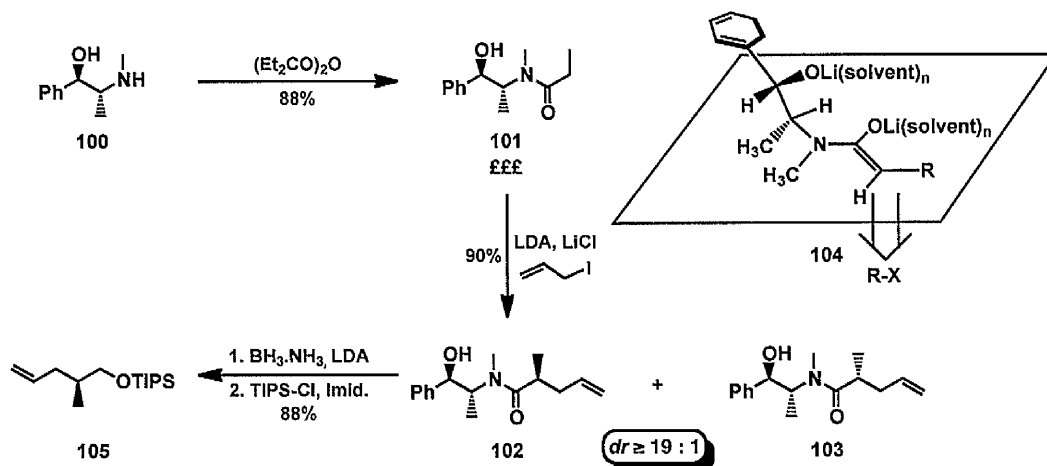


Scheme 2.23 Rhodium(I)-Catalysed [4+2+2] TST-Cycloisomerisation Reaction.

identical orientation of the diene in both cases. This preference can be attributed to a nonbonding interaction between one of the isopropyl groups on silicon and the C2 proton on the 1,3-butadiene derivative, a phenomenon also observed in the study of long-range asymmetric induction described in the section 2.4.1.1.

2.5 Synthesis of Allyl Alcohol Fragment 24

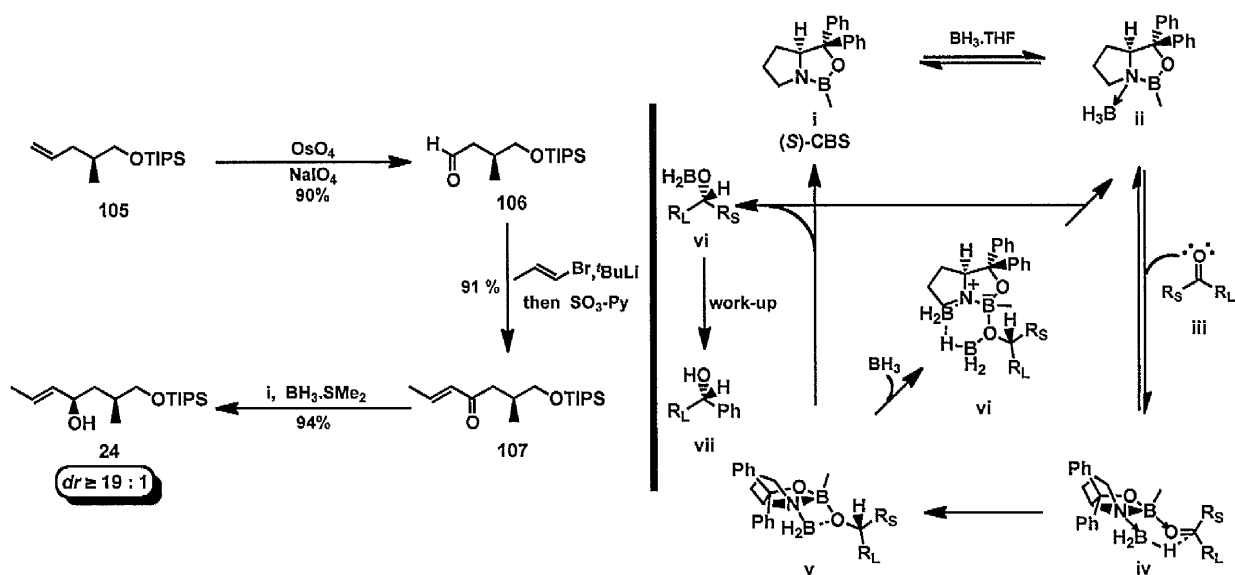
Our efforts towards the synthesis of the allyl alcohol fragment **24** commenced with the multigram synthesis of allyl pseudoephedrine propionamide derivative **102** (Scheme 2.24) according to the procedure developed by Myers *et. al.*⁴⁵ The excellent diastereoselectivity in the allylation of the pseudoephedrine amide enolate can be rationalised by invoking the model **104**, wherein the solvent molecules (THF) and



Scheme 2.24 Synthesis of TIPS Allyl Ether **105**.

diisopropylamine associated with the lithium alkoxide provide a steric blockade to the β -face of the (*Z*)-enolate thereby forcing the allylation to occur from the α -face. Subsequent LAB cleavage of the chiral auxiliary in **102** followed by TIPS protection of the resulting alcohol afforded the known compound **105** in 88% overall yield.⁴⁶ The enantiopurity of the allyl ether **105** was tentatively determined by comparing its specific rotation with the literature reported value (experimental value $[\alpha]_D^{20} -1.9$ ($c = 1.18$, $CHCl_3$), reported value $[\alpha]_D^{20} -2.0$ ($c = 0.96$, $CHCl_3$).⁴⁶ The allyl ether **105** was readily converted to the aldehyde **106** by Johnson-Lemieux oxidation⁴⁷ in excellent yield (Scheme 2.25). Thereafter, the aldehyde **106** was treated with (*E*)-propenyllithium, formed *in situ* by the halogen-lithium exchange reaction between (*E*)-propenyl bromide and *tert*-butyllithium to provide the corresponding allyl alcohol,⁴⁸ which was oxidised to

the allyl ketone derivative **107** in 91% overall yield in an one-pot operation. Finally, the CBS^{49a} reduction of enone **107** furnished the desired allyl alcohol fragment **24** in



Scheme 2.25 Synthesis of TIPS Allyl Alcohol Fragment **24** and Mechanism for the Corey Bakshi-Shibata (CBS) Reduction of Ketone.

excellent yield with $\geq 19:1$ diastereoselectivity (by ^1H NMR spectroscopy). To confirm the absolute configuration of the allylic alcohol **24**, a diastereomeric pair of Mosher esters was prepared and their ^1H NMR spectra were analysed by the subtraction protocol of the advanced Mosher method (Appendix 2.11.1).⁵⁰

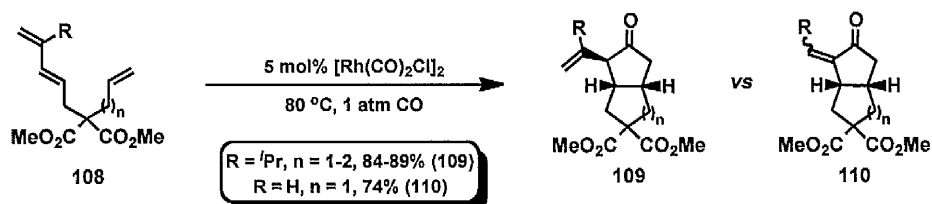
At this point it is pertinent to discuss the mechanism of the CBS reduction of ketones.^{49b} A plausible catalytic cycle with the oxazaborolidine catalyst **i** is illustrated in Scheme 2.25. In the first step, the electrophilic BH_3 reversibly binds to the Lewis basic nitrogen atom on the α -face of oxazaborolidine **i** to form the *cis*-fused oxazaborolidine-borane complex **ii**. The coordination in turn polarises the nitrogen-endocyclic boron bond in **ii** thereby activating the BH_3 as a hydride donor and increasing the Lewis acidity of the endocyclic boron. In the next step, the strongly Lewis acidic complex **ii** readily binds to the ketone **iii** at the more sterically accessible electron lone pair and *cis* to the vicinal BH_3 group. In this step the bulky alkyl chain prefers to point away from the oxazaborolidine in **iv** in order to minimize unfavourable steric interaction. This mode of alignment of the ketone

to the oxazaborolidine enables intramolecular face-selective hydride transfer *via* a six-membered transition state to form the reduction product **v**. Thus the polarisation of endocyclic boron-nitrogen bond in **ii** on coordination of the BH₃ to the oxazaborolidine **i** is the primary reason for the rate enhancement in the CBS reduction reaction. The intermediate **v** can regenerate the active oxazaborolidine catalyst after liberating the borinate **vi** by two reaction pathways. This can either happen by cycloelimination of the alkoxide ligand attached to the endocyclic boron and the BH₂ attached to the nitrogen to produce **i** directly or by the addition of BH₃ to the **v** to form a six-membered BH₃ bridged species **vi** which undergoes decomplexation to afford *cis*-fused oxazaborolidine-borane complex **ii**.

2.6 Attempted Routes Towards the Synthesis of the Eastern Fragment

2.6.1 Model Study on TST- Pauson-Khand (PK) Reaction

Having successfully developed a scalable and high-yielding route for the synthesis of allyl alcohol **24**, our next task was to investigate the critical diastereoselective TST-dienyl PK reaction. Wender *et al* first demonstrated the intramolecular rhodium(I)-catalysed [2+2+1] PK reaction with the diene-enes **108** in the presence of carbon monoxide for the construction of bicyclopentanones (Scheme 2.26).⁵¹ The reaction showed broad scope with respect to the diene substitution and different heteroatom linkers. Depending upon the

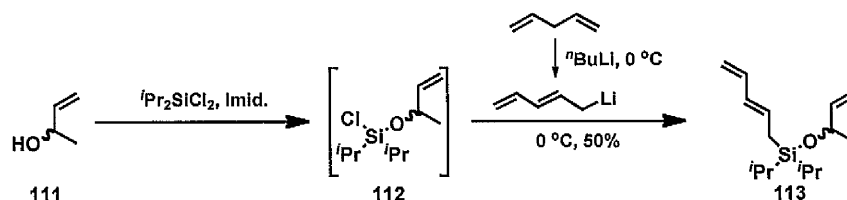


Scheme 2.26 Rhodium(I)-Catalysed [2+2+1] Dienyl Pauson-Khand Reaction.

substitution on the diene, the reaction generated cyclopentanone **109** as a single diastereoisomer or the *E*- and *Z*-geometrical isomeric cyclopentanones **110** in good yields. The dienyl PK reaction differs from the conventional PK reaction in the sense that the former utilises dienes as one of the two carbon components instead of alkynes. In a control experiment, it was unambiguously demonstrated that the dienyl moiety was crucial for the

success of this transformation since the analogous tethered *bis*-ene substrate failed to cyclise under the reaction condition. Later Baik and co-workers delineated the role of dienes using DFT calculations.⁵² The computational studies revealed that the additional π -component in the diene moiety facilitates the oxidative cyclisation step with a low energy barrier by transforming the 14-electron d^8 $[\text{Rh}(\text{CO})_2\text{Cl}]$ into a co-ordinatively saturated 18-electron species after the expulsion of a CO ligand. *Bis*-enes, on the other hand, lack viable π -base fragments that can undergo rearrangement to facilitate CO loss.

In the context of our eastern fragment of Lancifodilactone **1**, two pivotal questions needed to be examined. Firstly, could the Si-O linker be employed in Wender's [2+2+1] PK reaction since the previous feasibility study with cobalt and molybdenum mediated TST-PK reaction by Brummond's group were either unsuccessful or inefficient.^{12d} Secondly, could the dienyl tether bearing a methyl substituent on the alkene component be utilised, since it was prone to undergo the undesired ene-cycloisomerisation *via* a common rhodium metallacycle at elevated temperature. Additionally, there were very few examples of tethers with a substituted alkenes employed in rhodium(I)-catalysed PK reactions. Hence, dienylalkoxysilane **113** was initially selected as a model substrate to explore the efficacy of the TST in the rhodium(I)-catalysed PK reactions. As shown in Scheme 2.27, the synthesis of the model TST-PK precursor **113** was achieved by the initial treatment of the allylic alcohol **111** with diisopropyldichlorosilane to furnish the moisture sensitive alkoxychlorosilane **112**, which was not isolated. The intermediate **112** was sequentially



Scheme 2.27 Synthesis of Model Substrate **113** for the TST-PK Reaction.

treated with the *in situ* generated dienyllithium to afford the desired dienylalkoxysilane **113** in moderate yield.^{42,53} With compound **113** in hand, our attention turned towards identifying

the optimum conditions for the carbocyclisation reaction (Table 2.2). Treatment of the silane **113** under the optimised condition for the dienyl PK reaction reported by Wender and co-workers⁵¹ did not afford any of the desired cyclopentenone **114** (Table 2.2, Entry 1). Performing the reaction with higher catalyst loading (Table 2.2, Entry 2) or with the monomeric rhodium complex with a triphenyl phosphine ligand (Table 2.2, Entry 3) led to

Reaction scheme: Silane **113** (a dienylalkoxysilane with two isopropyl groups on the silicon) reacts under 1 atm CO to form cyclopentenone **114** (a five-membered ring with a ketone and a silyl ether substituent). The reaction is marked with a large 'X' over the arrow, indicating it failed.

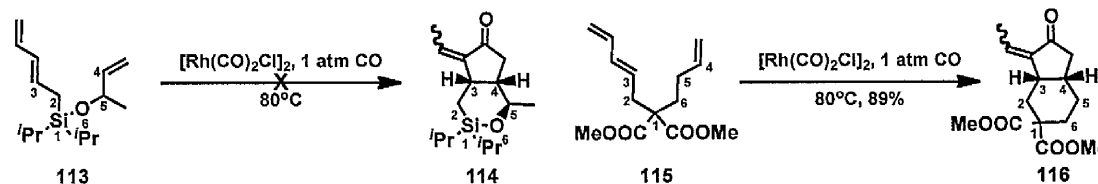
Entry	Catalyst	Cat. load (mol%)	Additive	Temp (°C)	Result
1	[Rh(CO) ₂ Cl] ₂	0.05	none	80	SM ^a
2	“	0.13	“	“	“
3	Rh(CO)Cl(PPh ₃)	0.1	“	“	“
4	[Rh(CO) ₂ Cl] ₂	“	AgOTf	“	“
5	“	“	AgSbF ₆	“	“

^aStarting material.

Table 2.2 Rhodium(I)-Catalysed TST Dienyl Pauson-Khand Reaction.

the similar unproductive outcome. It is well established that the cationic rhodium(I) complex formed after the abstraction of the chloride ligand on a neutral rhodium(I) complex opens a coordination site thereby improving the reactivity in the transition metal-catalysed carbocyclisation reactions. Despite attempts to modify the active catalyst with triflate and hexafluoroantimonate counter ions with Ag(I) salts (Table 2.2, Entries 4 and 5) did not furnish any of the desired cyclisation reaction and merely led to the recovery of starting material **113**. In order to gain insight into the possible reasons for the failure of the TST-PK reaction, Spartan calculations compared bond lengths and angles for the starting material **113** and the product **114** in the TST-PK reaction with the corresponding carbon-tethered substrates **115** and **116**, which were known to undergo carbocyclisation under Wender's reaction conditions.⁵¹ As tabulated in the Table 2.3, the Si-C₂ and the Si-O bond lengths in the dienylalkoxysilane **113** were significantly longer than the C1-C2 and the C1-C6 bonds in

the diene-ene **115** by 0.4 and 0.1 Å respectively. Interestingly, the bond angle difference between the starting material and products of both systems was even more dramatic, in which the angle between **115** to **116** for C₁-C₆-C₅ was estimated to be 4°, compared to 11° for the TST systems **113** to **114** for the C₅-O-Si. This suggested that the silane **113** was too substrate-like, which disfavoured the oxidative cyclisation with the rhodium(I) catalyst. Thus the computed data demonstrated a very good agreement with the TST-PK reaction and indicates that the presence of Si-O linker has a detrimental effect on the cyclisation.



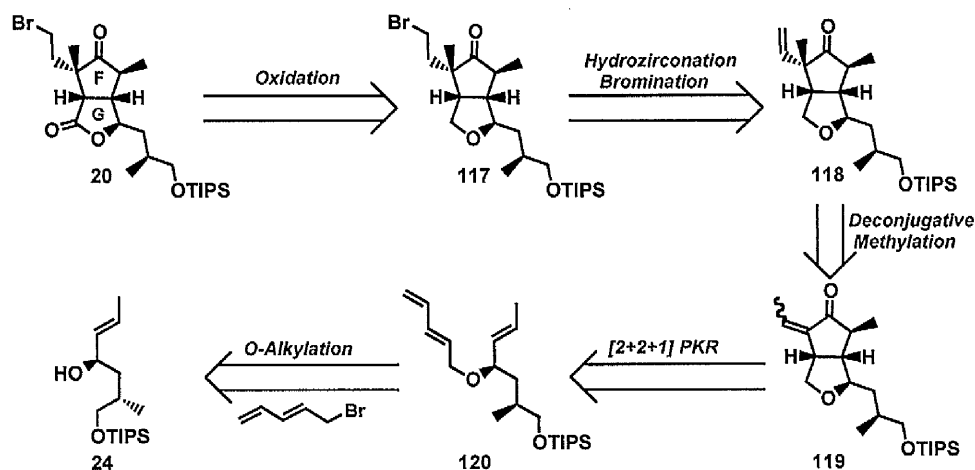
Entry ^a	Si-C ₂	C ₂ -C ₃	Si-O	O-C ₅	C ₅ -C ₄	O-Si-C ₂	C ₅ -O-Si	C ₁ -C ₂	C ₂ -C ₃	C ₁ -C ₆	C ₆ -C ₅	C ₅ -C ₄	C ₂ -C ₁ -C ₆	C ₁ -C ₆ -C ₅
SM	1.892	1.512	1.648	1.444	1.508	104.96	137.13	1.557	1.509	1.548	1.549	1.509	111.26	115.04
Product	1.885	1.552	1.648	1.540	1.542	102.19	126.32	1.542	1.536	1.542	1.534	1.535	111.18	111.18

^aBond length and bond angle in angstroms and degrees respectively.

Table 2.3 Rhodium(I)-Catalysed Dienyl Pauson-Khand Reaction: Spartan Calculations.

2.6.2 Oxygen Tethered Rhodium-Catalysed Dienyl Pauson-Khand Strategy

As a result of the failure of the TST-PK reaction approach for the synthesis of the core of the eastern fragment, an alternate strategy was proposed. The new approach takes advantage of the oxygen-tethered dienyl ethers that undergo Pauson-Khand reaction very efficiently.⁵¹ As illustrated in Scheme 2.28, the lactone functionality in the advanced



Scheme 2.28 Revised Retrosynthetic Analysis For the Eastern Fragment.

intermediate **20** was envisaged to come directly from a C-H oxidation reaction of the methylene unit of the five-membered ether ring in **117**. As previously described in Scheme 2.5, the pendant alkene in the compound **118** could be elaborated to the primary bromide **117** by well established synthetic procedures¹⁰ and the installation of the quaternary stereogenic centre in the cyclopentanone **118** could be accomplished by an *exo*-deconjugative methylation reaction of bicyclopentenone **119**. The rhodium(I)-catalysed [2+2+1] reaction on dienyl ether **120** was envisioned to generate bicyclopentenone **119** with very high diastereoselectivity in accordance with studies in the Evans group.³⁵ Finally, PK precursor **120** could be derived after the etherification reaction of the allylic alcohol **24**, which was used in the previous approach (*vide supra*), with the known dienyl bromide (Scheme 2.28).⁵¹

Before embarking on the new route for the synthesis of the eastern fragment, a model study was initiated in order to optimise the dienyl PK reaction with methyl substitution on the terminal alkene. For this purpose, the oxygen tethered dienyl ethers **121** and **122** bearing a C₂-methyl substituent were readily prepared *via* an alkylation reaction employing 3-buten-2-ol and 3-penten-2-ol with 5-bromo-1,3-pentadiene.⁵¹ Treatment of the dienyl ether **121** under the optimal reaction conditions furnished a 1 : 1 mixture of *E* and *Z* isomeric cyclopentanones **123** in 75% combined yield, with excellent diastereoselectivity (Table 2.4, Entry 1). Under similar reaction conditions, albeit with prolonged heating, compound **122** bearing an additional methyl group on the terminal alkene, afforded complex mixture of nonpolar cycloisomerised compounds without incorporation of CO. Efforts to optimise the reaction by changing rhodium(I) catalyst or by modifying the active catalyst using silver salts (Table 2.4, Entries 3-5) furnished only trace amounts of desired product under these conditions. In an effort to suppress the undesired cycloisomerisation reaction, the PK reaction was carried out at 60 °C with 10 mol% [Rh(CO)₂Cl]₂ (Table 2.4, Entry 6) which resulted in 50% conversion to the desired mixture of products **123**, **124** and **125** after 15 hours. Finally,

90% conversion to the cyclopentanones **123**, **124** and **125** was achieved after increasing the catalyst loading and reaction time to 20 mol% and 48 hours (Table 2.4, Entry 7).

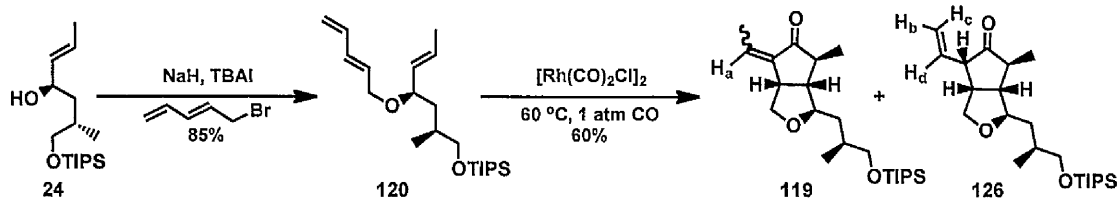
Entry	R	Catalyst (mol%)	Additive	Temp (°C)	Time (hr)	Conv. ^a (%)
1	H	[Rh(CO) ₂ Cl] ₂ (10)	none	80	3	100 ^b
2	Me	"	"	"	6	100 ^c
3	"	Rh(IMes)(CO) ₂ Cl (10)	"	"	24	Trace ^d
4	"	Rh(PPh ₃) ₂ (CO)Cl (10)	"	"	"	"
5	"	"	AgSbF ₆	"	"	"
6	"	[Rh(CO) ₂ Cl] ₂ (10)	"	60	15	50
7	Me	[Rh(CO) ₂ Cl] ₂ (20)	"	60	48	90

^aConversion based on ¹H NMR. ^b75% isolated yield. ^cMixture of cycloisomerised products.

^dMainly starting material.

Table 2.4 Rhodium(I)-Catalysed Oxygen-Tethered Dienyl PK Reaction: Model Study.

With the optimised condition for dienyl PK reaction in hand, our attention turned towards the synthesis of the parent PK precursor **120** which was readily achieved by the etherification reaction of the allylic alcohol **24** with 5-bromo-1,3-pentadiene to afford **120** in 85% yield, which was also contaminated with small amounts of inseparable dialkylated by-products resulting after the TIPS group cleavage during the alkylation reaction (Scheme

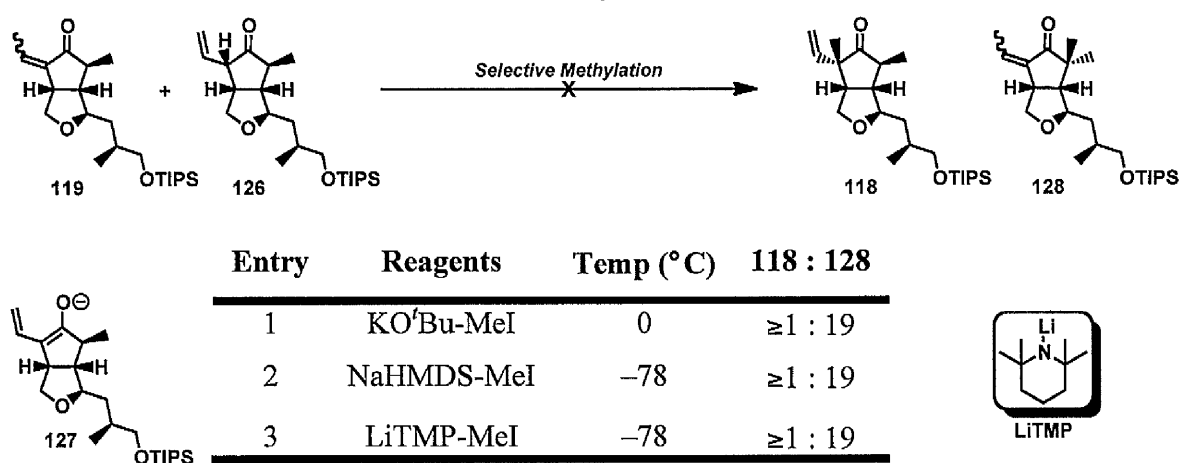


Scheme 2.29 Synthesis of Bicyclic Ketones **119** and **126**.

2.29). Nevertheless, in line with the model studies, treatment of the dienyl ether **120** under the optimised PK reaction conditions furnished a mixture (3.8 : 1 : 1.3) of *E*- and *Z*-geometric alkenes **119** in addition to the positional isomer **126** in 60% yield in a highly diastereoselective manner ($\geq 19 : 1$ by ¹H NMR) (Scheme 2.29). The complete

characterisation of bicyclic cyclopentanones **119** and **126** could not be achieved at this stage since they were inseparable by silica-gel chromatography. However, on careful analysis of coupling constants in the ^1H NMR of the mixture, five sets of distinct proton signals were distinguishable in the alkene region (7-5 ppm) which were assigned to the *E*-(H_a , qd, $J = 7.3$, 1.9 Hz), *Z*-isomers (H_a , qd, $J = 7.3$, 2.2 Hz) of **119** and positional isomer **126** (H_d , ddd, $J = 16.8$, 10.5, 6.8 Hz), (H_b , d, $J = 10.5$ Hz) and (H_c , d, $J = 16.8$ Hz). It is worthy to note that the PK reaction controls the relative configuration of four contiguous stereocentres in excellent diastereoselectivity ($\geq 19 : 1$ by ^1H NMR) in a single operation.

Having assembled the cyclopentanone core of the eastern fragment, the next step in the synthesis was to install the challenging quaternary stereogenic centre in the bicyclic cyclopentanone **118** using an *exo*-deconjugative methylation reaction (Scheme 2.30).⁵⁴ This reaction relies on the initial formation of the bicyclic enolate **127** after the chemoselective



Scheme 2.30 Attempted *Exo*-Deconjugative Methylation Reaction.

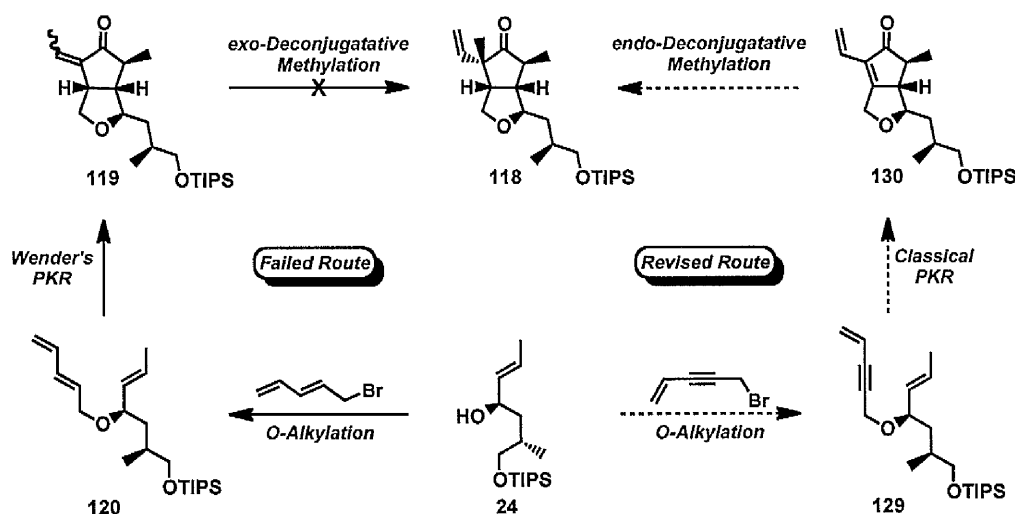
deprotonation of the γ -proton over the sterically hindered α -proton of the major isomers **119**. The minor isomer **126** is also expected to favour the formation of enolate **127** after the deprotonation of the more acidic α -allylic proton. The enolate **127** should then trap the electrophile from the less hindered β -face to furnish the kinetically favoured β,γ -unsaturated bicyclic ketone **118**. Despite several attempts to effect such a transformation on the mixture of **119** and **126**, the reaction furnished isomeric mixture of *gem*-dimethylated bicyclopentanones **128** instead of the desired bicyclic ketone **118** even after employing

sterically bulky bases (Scheme 2.30). In light of the unsuccessful efforts to install the desired quaternary stereogenic in the eastern fragment, a minor revision was sought in order to circumvent the aforementioned problems, as outlined in the following section.

2.7 Completion of the Synthesis of the Eastern Fragment

2.7.1 First Generation Synthesis

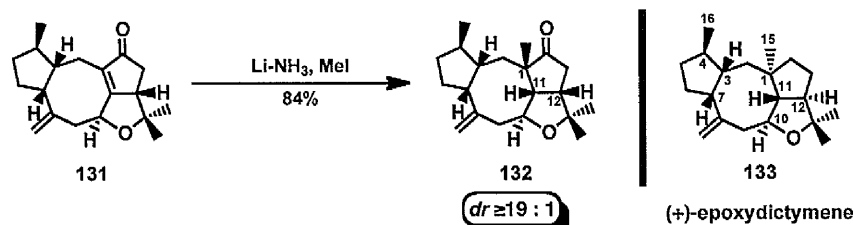
As an alternative to the *exo*-deconjugative methylation reaction, an *endo*-deconjugative methylation of vinyl cyclopentenone **130** was envisioned to generate the enolate **127**, which could be utilised in the β -face selective methylation reaction to install the quaternary stereogenic centre in the eastern fragment (Scheme 2.31). The synthesis of compound **130** requires a more classical Pauson-Khand reaction employing oxygen tethered enyne **129**,³⁵ which in turn could be prepared *via* an etherification reaction between the



Scheme 2.31 Revised Route for the Installation of Quaternary Stereogenic Centre.

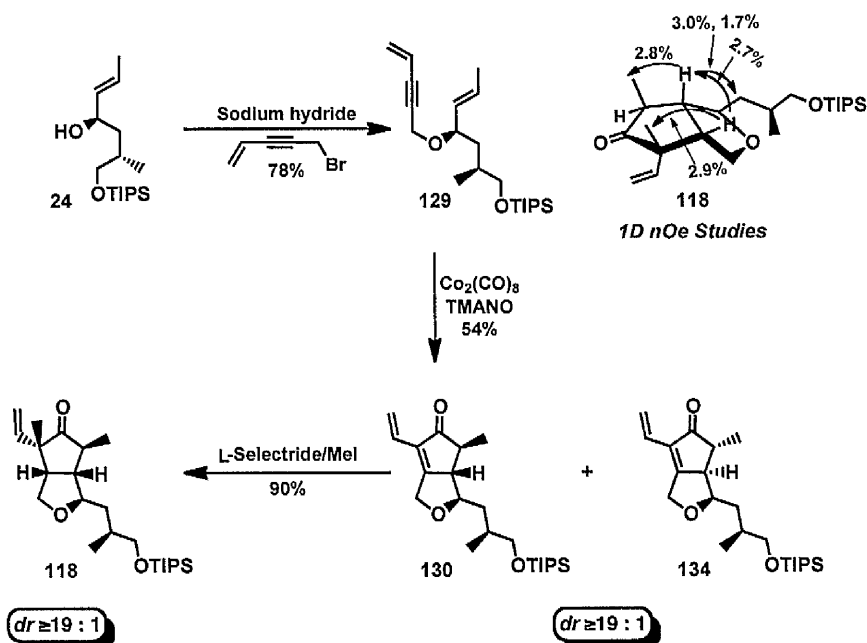
allylic alcohol **24** and vinyl propargyl bromide. It is worth mentioning that the idea of using the *endo*-deconjugative methylation reaction for the installation of the quaternary stereogenic centre is related to that described in Schreiber's total synthesis of epoxydictymene⁵⁵ **133**, wherein the quaternary stereogenic centre at C1 was installed with the α -orientation using dissolving metal reduction-methylation sequence as outlined in Scheme 2.32. The reaction furnished 5,5-*cis*-fused C1-*epi*-tetracyclic ketone **132** with

opposite configuration at C1 centre that was incorrect for epoxydictymene **133**, albeit with complete diastereocontrol. Hence, we anticipated the methylation of bicyclic enolate **127** would proceed from the convex face due to the inherent facial bias in the 5,5-*cis*-fused bicyclic ring in an analogous manner.



Scheme 2.32 Deconjugative Methylation Strategy in the Schreiber's Epoxydictymene Synthesis.

In light of the overall efficiency and the ease with which the compound **132** was formed in the deconjugative methylation reaction of **131**, we resumed our pursuit towards installing the quaternary stereogenic centre in the eastern fragment. Etherification reaction between the allylic alcohol **24** and 1-bromo-4-penten-2-yne⁵⁶ afforded the desired PK precursor **129** in 78% yield with the concurrent formation of the dialkylated by-product, which was inseparable by column chromatography (Scheme 2.33). Treatment of the mixture of compounds **129** to the optimised rhodium(I)-catalysed dienyl PK reaction conditions at



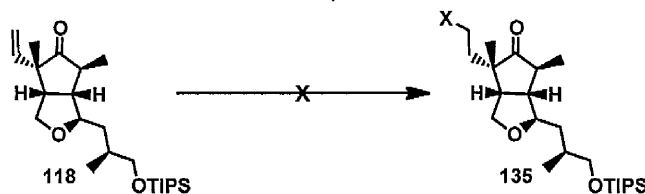
Scheme 2.33 Diastereoselective Synthesis of Bicyclic Ketone **118**.

60 °C, furnished only a trace amount of bicyclic cyclopentenone **130**, albeit as a single diastereoisomer. Increasing the reaction temperature led to the complete decomposition of the desired product **130** probably due to the instability of the conjugated vinyl cyclopentenone functionality in **130** to the thermal conditions. The enyne **129** was transformed to the desired vinyl bicyclic enone **130** in 54% yield with $\geq 19 : 1$ diastereoselectivity (by ^1H NMR) upon sequential treatment with stoichiometric $\text{Co}_2(\text{CO})_8$ at room temperature followed by excess amounts of TMANO at $-20\text{ }^\circ\text{C}$.^{18a} The bicycle **130** was unstable at room temperature over long periods of time, which was used immediately in the next step or stored in benzene at $-30\text{ }^\circ\text{C}$ in order to prevent decomposition.

Following the synthesis of bicyclic enone **130**, our entire endeavour focused towards the installation of the quaternary stereogenic centre in **118** using an *endo*-deconjugative methylation reaction (Scheme 2.33). Preliminary experiments using an Li-NH_3 reduction-methylation sequence afforded the desired bicyclic cyclopentanone **118** in low yield.⁵⁵ However, after undertaking extensive optimisation studies to improve the efficiency of the reaction, the combination of L-selectride with methyl iodide as the internal quench delivered the cyclopentanone derivative **118** in 90% yield with excellent diastereoselectivity.^{18a} The relative configuration of the stereocentres in the newly formed bicyclic ketone **118** was ascertained using one-dimensional ^1H -nOe experiments as illustrated in the Scheme 2.33 (Appendix 2.11.2).

The successful installation of the quaternary stereogenic centre prompted the completion of the fragment with the conversion of the bicyclic alkene **118** to the corresponding halide **135**. This task proved far from trivial since attempts to halogenate the terminal alkene **118** using the commercially available Schwartz reagent failed to effect the zirconation reaction.¹⁰ Instead, the bicyclic methyl ketone **118** either underwent epimerisation at the α -stereogenic centre or provided recovered starting material (Table 2.5, Entry 1-2). Additional studies focussed on a two-step hydroboration-oxidation/bromination

sequence. Unfortunately, efforts to secure access to the alcohol derivative using number of dialkyl boranes led to the quantitative recovery of **118** (Table 2.5, Entry 3-6), which was attributed to the presence of ketone functionality in **118**.⁵⁷ We envisioned that the β -face



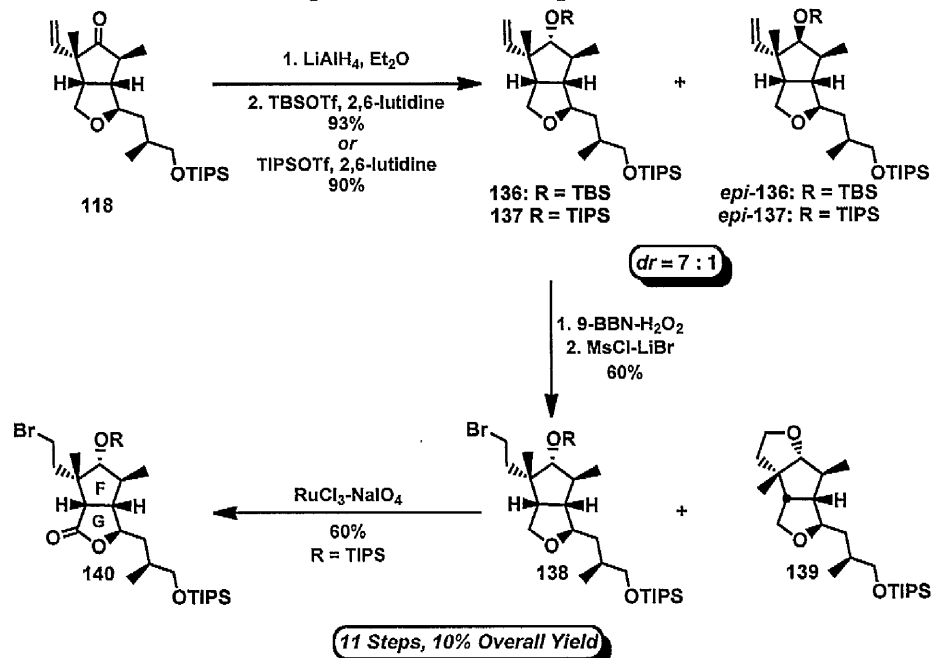
Entry	Condition	X	Result
1	Cp ₂ ZrHCl-NBS	Br	Epimerisation
2	Cp ₂ ZrCl ₂ -DIBAL-I ₂	I	SM ^a
3	Catechol borane, Rh(PPh ₃) ₃ Cl	OH	“
4	9-BBN	“	“
5	Cy ₂ BH	“	“
6	BH ₃ .DMS	“	“

^aStarting material.

Table 2.5 Attempted Functionalisation of the Bicyclic Alkene **118**.

selective hydride reduction of the bicyclic ketone **118** followed by the protection of the resulting hydroxyl functionality with a silyl group could overcome this problem. In order to test this hypothesis, cyclopentanone **118** was reduced under standard conditions (Scheme 2.34) to generate an inconsequential 7 : 1 mixture of secondary alcohols, which was protected as the TIPS ether **137**. The relative configuration of the newly formed stereocentre in the major isomer **137** was confirmed by one-dimensional nOe experiments (Appendix 2.11.2). Treatment of the bicyclic alkene **137** with an excess of 9-BBN followed by oxidation of the resulting bicyclic alkyl borane with NaOH-H₂O₂, provided the desired primary alcohol, which was subsequently converted to the corresponding primary bromide **138** in 60% overall yield. The choice of silyl group utilised for protecting the secondary alcohol after the hydride reduction of **118** played a significant role in the efficiency of hydroboration-oxidation and bromination reactions. For example, the TBS protected derivative **136** underwent the hydroboration reaction at room temperature with excellent

conversion. However, the resulting alcohol derivative was not stable to the bromination reaction conditions and the secondary TBS protected substrate predominantly generated undesired 5,5,5-*cis*-fused tricyclic pentanoid **139**. In the case of the ditriisopropylsilyl ether **137**, the hydroboration reaction required elevated temperatures, however, the TIPS ether



Scheme 2.34 First Generation Synthesis of the Eastern Fragment.

group was relatively stable to protodesilylation during the bromination reaction. Additionally, the facile formation of 5,5,5-*cis*-fused pentanoid **139** also corroborates the nOe studies, which supports the assignment of the relative configuration of the quaternary stereogenic centre of cyclopentanone **118**. Finally, ruthenium-catalysed C-H oxidation of the tetrahydrofuran ring in **138** delivered the desired bicyclic lactone derivative **140** in 60% yield⁵⁸ thereby completing the synthesis of the eastern fragment in 11 steps and 10% overall yield (Scheme 2.34).

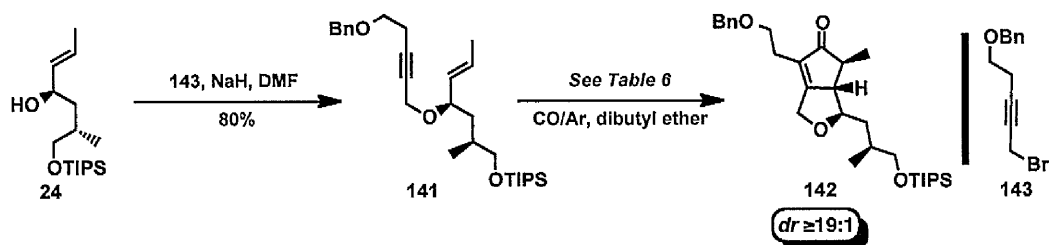
The successful construction of the eastern fragment **140** after circumventing several pitfalls during the course of the synthesis was a significant milestone towards realising the first chemical synthesis of Lancifodilactone G **1**. However, our quest to further improve the overall efficiency of the eastern fragment synthesis ultimately led to the development of a

concise and scalable route for the synthesis of the congested F-G rings, which would be discussed in the next following section.

2.7.2 Second-Generation Synthesis

The poor reactivity of the bicyclic alkene **118** in the hydrometallation reactions unexpectedly resulted in the addition of two extra steps in the synthesis. We sought to address this problem by using the benzyloxy protected propargyl bromide **143**⁵⁹ in place of the vinyl propargyl bromide in the etherification reaction, which would install the requisite side chain in the correct oxidation state as well being easily functionalised to the desired bromide derivative upon debenylation. The presence of the benzyloxy side chain was also anticipated to alleviate the problems associated with the instability of the PK product at elevated temperatures. Additionally, it was anticipated that this would provide an opportunity to explore the rhodium(I)-catalysed PK reaction in second generation synthesis.

Towards this end, the requisite bromide **143** was prepared in three steps using the literature procedure⁵⁹ and subjected to the propargylic etherification reaction with the allylic alcohol **24** to furnish the enyne derivative **141** as a single compound in 80% yield. This set the stage to reexamine the oxygen-tethered enynyl ether **141** in the rhodium(I)-catalysed PK reaction (Table 2.6). At high concentration of carbon monoxide in the presence of the rhodium(I) catalyst, the enynyl ether **141** afforded the desired bicyclic enone **142** with excellent stereocontrol, albeit in very low yield (Table 2.6, Entry 1). Systematically varying the catalyst loading, reaction temperature, time and modifying the nature of rhodium(I) catalyst did not improve the efficiency of the reaction (Table 2.6, Entries 2-5). Surprisingly, a dramatic increase in the rate and yield of the PK reaction was observed when the reaction was conducted with a 10% carbon monoxide-argon mixture with 10 mol% [Rh(CO)₂Cl]₂ catalyst at 100 °C (Table 2.6, Entry 6). However, decreasing the temperature to 80 °C had a detrimental effect on the efficiency of the PK reaction (Table 2.6, Entry 7). The significant increase in yield on lowering the carbon monoxide concentration in the PK reaction of enyne



Entry	Catalyst (mol%)	Additive	Temp (°C)	Time (hr)	CO : Ar (atm.)	Yield ^a
1	[Rh(CO) ₂ Cl] ₂ (10)	none	100	18	1.0 : 0.0	14
2	[Rh(CO) ₂ Cl] ₂ (20)	“	130	48	“	27 ^b
3	[RhCOCl dppp] ₂ (10)	“	“	18	“	15
4	[Rh(COD)Cl] ₂ (10)	dppp	“	“	“	11
5	Rh(PPh ₃) ₂ COCl (10)	none	“	“	“	8
6	[Rh(CO)₂Cl]₂ (10)	“	100	12	0.1 : 0.9	86^b
7	[Rh(CO) ₂ Cl] ₂ (10)	“	80	18	0.1 : 0.9	21

^aHPLC yield. ^bIsolated Yield.

Table 2.6 Optimisation of Rhodium(I)-Catalysed Pauson-Khand Reaction.

141 was an unexpected result since earlier work within the group had shown that lowering the carbon monoxide concentration in the reaction led to a diminished yield and lowered the level of stereocontrol.^{35b} The transition states **144** and **145** depicted in Figure 2.3 provide a rationale to explain the observed efficiency of the PK reaction at low carbon monoxide pressure. In line with these potential transition states, at high carbon monoxide concentration, the rhodium(I) complex prefers a trigonal bipyramidal geometry in which

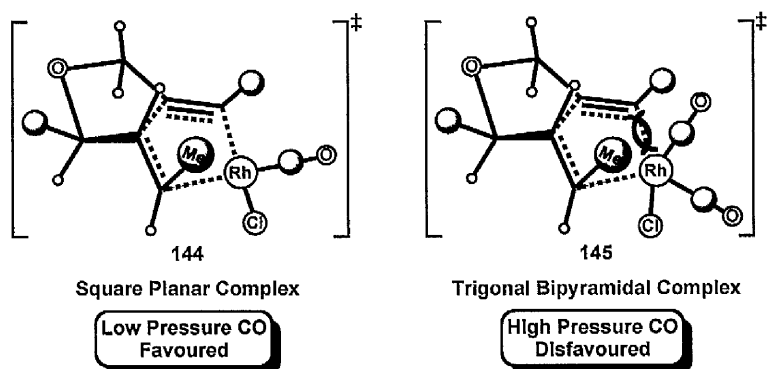
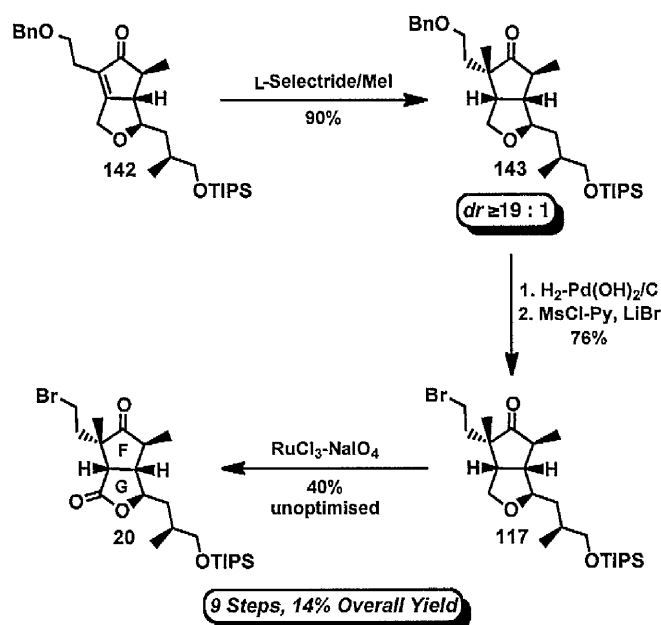


Figure 2.3 Proposed Model for the Rhodium(I)-Catalysed PK Reaction.

one of the carbonyl ligands and the chlorido ligand occupy axial positions and the methyl group on the terminal alkene is stereospecifically placed in a β -orientation by the virtue of the alkene geometry. In this arrangement, a steric clash between the methyl group and the axial ligand disfavours the oxidative addition step, which result in the lowering of chemical yield. In contrast, the low carbon monoxide concentration prefers a square planar configuration, which alleviates the steric clash between the methyl group and axial ligand, thereby favouring the oxidative cyclisation.

Having established a viable route to prepare multigram quantities of advanced intermediate **142**, the bicyclic enone **142** was taken forward in the synthesis in a similar fashion to the previously optimised *endo*-deconjugative methylation reaction, which uneventfully led to the bicyclic ketone **143** in 90% yield and with excellent



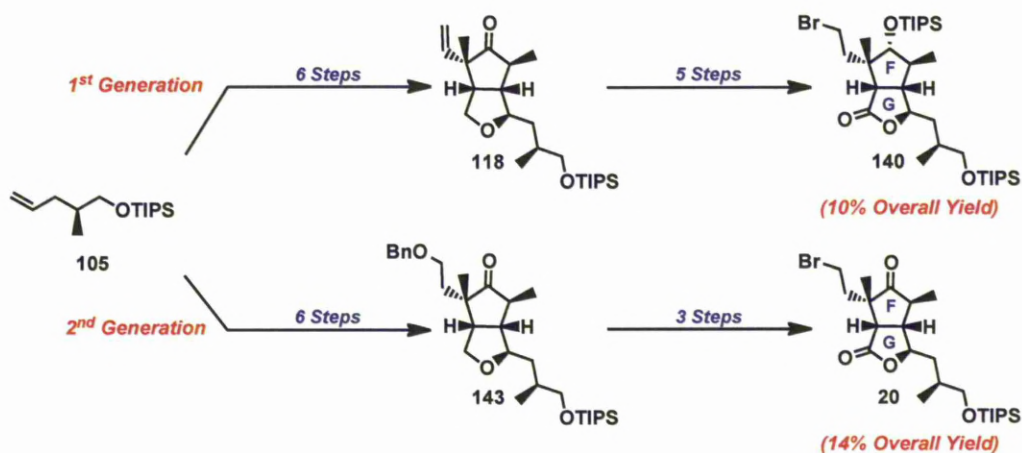
Scheme 2.35 Second Generation Synthesis of the Eastern Fragment.

diastereoselectivity (Scheme 2.35). Following standard procedures, the primary benzyl group in the compound **143** was hydrogenolysed and the resulting alcohol was converted to the corresponding primary bromide **117** in 76% overall yield. Finally, ruthenium-catalysed C-H oxidation of the five-membered ring of the bicyclic bromo ketone **117** afforded the

desired keto-lactone **20** in modest yield,⁵⁸ thereby completing the second generation synthesis of eastern fragment in 9 steps and with 14% overall yield (Scheme 2.35).

2.8 Conclusion

The construction of eastern fragment of Lancifodilactone G **1** required the exploration of several strategies, which ultimately culminated in the development of a concise route towards the synthesis of the sterically congested F-G rings (Scheme 2.36). The first



Scheme 2.36 Summary and Outlook.

generation synthesis of the eastern fragment was achieved in 11 steps (longest linear sequence) and in 10% overall yield whereas the second route is much more practical, providing the ketone **20** in 9 steps with 14% overall yield (longest linear sequence).

2.9 Experimental

2.9.1 General

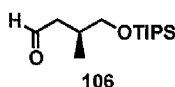
All reactions were performed in oven-dried (125 °C) or flame-dried glassware under an inert atmosphere of nitrogen or argon. Syringes were oven-dried (125 °C) and then cooled in a desiccator. The following reaction solvents were dried using an alumina column solvent system: toluene (PhMe), diethyl ether (Et₂O) and dichloromethane (DCM) were dried over alumina column solvent system using the method of Grubbs.⁶⁰ The following reaction solvents were distilled from the indicated drying agents: tetrahydrofuran (THF) (sodium, benzophenone), hexanes (CaH₂), benzene (PhH) (sodium) and acetonitrile (MeCN) (CaH₂). Triethyl amine (Et₃N) was distilled from CaH₂. Brine refers to a saturated solution of NaCl. All starting material and reagents were purchased from Acros, Aldrich, Alfa Aesar, Fluka, and Strem chemical companies and were used without further purification unless noted otherwise.

Analytical thin layer chromatography (TLC) was performed on Merck 60 F₂₅₄ precoated silica-gel plates. Visualization was accomplished with a UV light and/or a KMnO₄, or *p*-anisaldehyde solution. Flash column chromatography (FCC) was performed by the method of Still with Merck Silica-gel 60 (230-400 mesh). Solvents for extraction and FCC were technical grade. Reported solvent mixtures for both TLC and FCC were volume/volume mixtures. Infrared spectra (IR) were obtained on a Perkin-Elmer spectrum one series FTIR spectrophotometer. Peaks are reported in cm⁻¹ with the following relative intensities: s (strong), m (medium), w (weak). The Liverpool University Mass Spectroscopy Centre and EPSRC National Spectrometry Centre, Swansea, recorded Mass spectra. High-resolution electron-impact electrospray (ESI) mass spectra were obtained on a Micromass LCT Mass spectrometer and LTQ Orbitrap XL. The specific rotation was measured with a PerkinElmer Model 343 Plus polarimeter.

^1H -NMR and ^{13}C -NMR were recorded on a Bruker DRX-500 MHz NMR spectrometer in the indicated deuterated solvents. For ^1H -NMR, CDCl_3 and C_6D_6 were set to 7.26 ppm (CDCl_3 singlet) and 7.16 (C_6D_6 singlet) respectively and for ^{13}C -NMR, CDCl_3 and C_6D_6 were set to 77.16 ppm (CDCl_3 center of triplet) and 128.06 ppm (C_6D_6 center of triplet) respectively. All values for ^1H -NMR and ^{13}C -NMR chemical shifts for deuterated solvents were obtained from Cambridge Isotope Labs. Data are reported in the following order: chemical shift in ppm (δ) (multiplicity, which are indicated by br (broadened), s (singlet), d (doublet), t (triplet), q (quartet), quint (quintet), m (multiplet)); assignment of 2nd order pattern, if applicable; coupling constants (J , Hz); integration. All ^{13}C -NMR spectra were reported using the descriptor (o) and (e) referring to whether the peak is odd or even, respectively, and correlate to an attached proton test (ATP) experiment.

2.9.2 Experimental Procedures

(*S*)-3-Methyl-4-((triisopropylsilyl)oxy)butanal



To a solution of alkene **105**⁴⁶ (7.00 g, 27.30 mmol) and 4-methylmorpholine *N*-oxide (6.40 g, 54.6 mmol) in 4 : 1 acetone- H_2O (90 mL) was added osmium tetroxide (6.60 mL, 0.33 mmol, 0.05 M in water) at room temperature and stirred for 12 hours. The reaction mixture was quenched with saturated aqueous $\text{Na}_2\text{S}_2\text{O}_3$ and diluted with brine. The reaction mixture was partitioned with diethyl ether and the phases were separated. The combined organic phases were dried over MgSO_4 and concentrated under *vacuo* to afford the crude oil, which was redissolved in a 4 : 1 of $\text{MeOH-H}_2\text{O}$ (55 mL). The reaction mixture was treated with sodium periodate (11.68 g, 54.6 mmol) and the solution was stirred for 4 hours at room temperature. The reaction mixture was partitioned with diethyl ether and the phases were separated. The combined organic phases were dried over MgSO_4 and concentrated under

vacuo to afford the crude oil. Purification by flash chromatography over silica-gel (10% Et₂O-hexanes as eluent) afforded the (*S*)-**106** as a colourless oil (6.35 g, 90%).

$[\alpha]_D^{20}$ -5.6 (*c* = 0.45, CHCl₃).

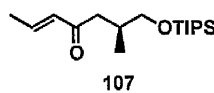
¹H NMR (500 MHz, CDCl₃) δ 9.78 (app. t, *J* = 2.2 Hz, 1H), 3.65 (dd, A of ABX, *J*_{AB} = 9.6 Hz, *J*_{AX} = 4.8 Hz, 1H), 3.44 (dd, B of ABX, *J*_{AB} = 9.6 Hz, *J*_{BX} = 7.4 Hz, 1H), 2.57 (ddd, *J* = 15.7, 5.8, 2.3 Hz, 1H), 2.31-2.22 (m, 2H), 1.07-1.02 (m, 21H), 0.95 (d, *J* = 6.7 Hz, 3H).

¹³C NMR (125 MHz, CDCl₃) δ 203.18 (o), 68.16 (e), 48.37 (e), 31.77 (o), 18.12 (o), 16.87 (o), 11.97 (o).

IR (Neat) 2943 (s), 2866 (s), 1727 (s), 1463 (m), 1384 (w), 1099 (s), 882 (s).

HRMS (ESI, [M + Na]⁺) calcd for C₁₄H₃₀O₂NaSi 281.1913, found 281.1913.

(*S,E*)-6-Methyl-7-((triisopropylsilyl)oxy)hept-2-en-4-one



A pentane solution of *tert*-butyllithium (0.072 mL, 1.14 mmol, 1.6 M) was added dropwise a solution of *trans*-1-bromo-1-propene (0.061 mL, 0.71 mmol), THF (0.35 mL) and Et₂O (0.35 mL) at -100 °C. After stirring for 15 minutes, the reaction was warmed to -78 °C and further stirred at the same temperature for 3 hours whereupon a solution of (*S*)-**106** (0.05 g, 0.19 mmol) in THF (0.44 mL) and Et₂O (0.44 mL) was added dropwise over 10 minutes. The resulting solution was slowly warmed to room temperature overnight whereupon the reaction mixture was concentrated under *vacuo*. The crude allylic alcohol was redissolved in 1.3 : 1 DCM-DMSO (0.4 mL) and the reaction mixture was cooled to 0 °C. Triethylamine (0.31 mL, 2.23 mmol) followed by SO₃.Py (0.29 mg, 1.84 mmol) were added in a single portion. After stirring for an hour at 0 °C, the reaction was diluted with water (5 mL) and Et₂O (5 mL). The reaction mixture was partitioned with diethyl ether and the phases were separated. The combined organic phases were dried over MgSO₄ and concentrated under

vacuo to afford the crude oil Purification by flash chromatography over silica-gel (5% diethyl ether-hexanes as eluent) afforded the allylic ketone **107** as a colourless oil (0.053 g, 91%).

$[\alpha]_D^{20} -0.7$ ($c = 1.44$, CHCl_3).

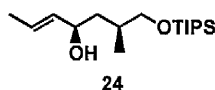
$^1\text{H NMR}$ (500 MHz, CDCl_3) δ 6.77 (dq, $J = 15.7, 6.9$ Hz, 1H), 6.04 (dq, $J = 15.7, 1.6$ Hz, 1H), 3.50 (dd, A of ABX, $J_{AB} = 9.6$ Hz, $J_{AX} = 5.1$ Hz, 1H), 3.40 (dd, B of ABX, $J_{AB} = 9.6$ Hz, $J_{BX} = 6.3$ Hz, 1H), 2.71 (dd, $J = 15.0, 4.9$ Hz, 1H) 2.21-2.10 (m, 2H), 1.80 (dd, $J = 6.9, 1.7$ Hz, 3H), 0.99-0.95 (m, 21H), 0.83 (d, $J = 6.6$ Hz, 3H).

$^{13}\text{C NMR}$ (125 MHz, CDCl_3) δ 200.16 (e), 142.17 (o), 132.39 (o), 67.83 (e), 43.54 (e), 32.77 (o), 18.13 (o), 17.97 (o), 16.74 (o), 11.92 (o).

IR (Neat) 2942 (s), 2866 (s), 1698 (m), 1673 (m), 1634 (m), 1462 (m), 1098 (s), 881 (s).

HRMS (ESI, $[\text{M} + \text{Na}]^+$) calcd for $\text{C}_{17}\text{H}_{34}\text{O}_2\text{NaSi}$ 321.2226, found 321.2225.

(4*R*,6*S*,*E*)-6-Methyl-7-((triisopropylsilyl)oxy)hept-2-en-4-ol



A flame-dried 250 ml RBF was charged with allylic ketone **107** (5.30 g 17.75 mmol) in THF (88 ml). The vessel was cooled to -30 °C and (*S*)-methyl-CBS-oxazaborolidine (17.60 mL, 17.75 mmol, 1M in toluene) was added. Borane-methyl sulfide complex (11.80 mL, 124.0 mmol) was slowly added over 15 minutes. The reaction stirred for 2 hours at this temperature before being slowly quenched with 5 mL of methanol over 30 minutes. The reaction was warmed to room temperature, and after the majority of gas evolution subsided, the reaction was diluted with water (20 mL) and ethyl acetate (20 mL). The reaction mixture was partitioned with ethyl acetate and the phases were separated. The combined organic phases were dried over MgSO_4 and concentrated under *vacuo* to afford the crude oil.

Purification by flash chromatography over silica-gel (10% EtOAc-hexanes as eluent) furnished the allylic alcohol **24** as a colourless oil (5.0 g, 94%, $dr \geq 19 : 1$ by $^1\text{H-NMR}$).

$[\alpha]_{\text{D}}^{20} +2.1$ ($c = 1.19$, CHCl_3).

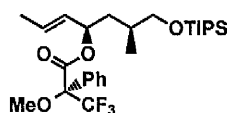
$^1\text{H NMR}$ (500 MHz, CDCl_3) δ 5.67 (dq, $J = 15.0, 6.4, 0.9$ Hz, 1H), 5.48 (ddq, $J = 15.3, 7.0, 1.5$ Hz, 1H), 4.22-4.18 (m, 1H), 3.60 (dd, A of ABX, $J_{AB} = 9.7$ Hz, $J_{AX} = 4.6$ Hz, 1H), 3.53 (dd, B of ABX, $J_{AB} = 9.8$ Hz, $J_{BX} = 7.0$ Hz, 1H), 1.88-1.78 (m, 1H), 1.70-1.68 (m, 3H), 1.60 (ddd, $J = 13.7, 6.9, 5.7$ Hz, 1H), 1.51 (ddd, $J = 13.6, 7.3, 6.2$ Hz, 1H), 1.15-1.04 (m, 21H), 0.91 (d, $J = 6.9$ Hz, 3H).

$^{13}\text{C NMR}$ (125 MHz, CDCl_3) δ 134.49 (o), 126.24 (o), 70.73 (o), 68.86 (e), 42.16 (e), 32.55 (o), 18.06 (o), 17.75 (o), 17.54 (o), 12.01 (o).

IR (Neat) 3336 (br, w), 2942 (m), 2865 (m), 1462 (m), 1382 (w), 1099 (s), 882 (s).

HRMS (ESI, $[\text{M} + \text{Na}]^+$) calcd for $\text{C}_{17}\text{H}_{36}\text{O}_2\text{NaSi}$ 323.2382, found 323.2382.

(*S*)-(4*R*,6*S*,*E*)-6-Methyl-7-((triisopropylsilyl)oxy)hept-2-en-4-yl-3,3,3-trifluoro-2-methoxy -2-phenylpropanoate



To a stirred solution of allyl alcohol **24** (0.019 g, 0.07 mmol) in dry pyridine (0.65 mL) was added (*R*)-(+)- α -methoxy- α -(trifluoromethyl)phenylacetic acid chloride (0.015 mL, 0.081 mmol) at 0 °C under argon. After being stirred for 48 h at the same temperature, the reaction mixture was partitioned between ethyl acetate (5 mL) and water (5 mL). The phases were separated and the combined extracts dried over anhydrous MgSO_4 , filtered and evaporated under *vacuo*. Purification by flash chromatography over silica-gel (10% EtOAc-hexanes as eluent) afforded the (*S*)-Mosher ester as a colourless oil (0.027 g, 81%).

$[\alpha]_{\text{D}}^{20} -34.6$ ($c = 0.33$, CHCl_3).

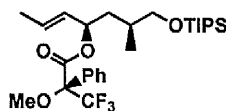
¹H NMR (500 MHz, CDCl₃) δ 7.50-7.49 (m, 2H), 7.39-7.35 (m, 3H), 5.81 (dq, *J* = 15.2, 6.6 Hz, 1H), 5.51 (app. q, *J* = 7.6 Hz, 1H), 5.35-5.29 (m, 1H), 3.57-3.53 (m, 4H), 3.51 (dd, *J* = 9.6, 5.8 Hz, 1H), 1.82 (ddd, *J* = 13.4, 7.7, 5.8 Hz, 1H), 1.71-1.61 (m, 1H), 1.55-1.50 (m, 1H), 1.12-1.01 (m, 21H), 0.93 (d, *J* = 6.7 Hz, 3H).

¹³C NMR (125 MHz, CDCl₃) δ 165.89 (e), 132.54 (e), 131.61 (o), 129.60 (o), 128.50 (o), 128.37 (o), 127.58 (o), 123.48 (e), 84.39 (e) 77.11 (o), 68.09 (e), 55.60 (o) 37.82 (e), 32.57 (o), 18.15 (o), 17.84 (o), 17.00 (o), 12.09 (o).

IR (Neat) 2943 (m), 2866 (m), 1745 (s), 1462 (w), 1254 (m), 1167 (s), 1105 (s), 881 (m).

HRMS (ESI, [M + Na]⁺) calcd for C₂₇H₄₃O₄F₃NaSi 539.2780, found 539.2784.

(*R*)-(4*R*,6*S*,*E*)-6-Methyl-7-((triisopropylsilyl)oxy)hept-2-en-4-yl-3,3,3-trifluoro-2-methoxy -2-phenylpropanoate



(*R*)-Mosher ester was synthesised in an analogous manner to (*S*)-Mosher ester by reacting allylic alcohol **24** with (*S*)-(-)- α -methoxy- α -(trifluoromethyl)phenylacetic acid chloride in place of (*R*)-(+)- α -methoxy- α -(trifluoromethyl)phenylacetic acid chloride.

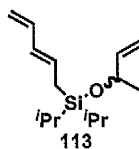
$[\alpha]_D^{20}$ +32.0 (*c* = 0.35, CHCl₃).

¹H NMR (500 MHz, CDCl₃) δ 7.52-7.49 (m, 2H), 7.40-7.35 (m, 3H), 5.88 (dq, *J* = 15.2, 6.6 Hz, 1H), 5.53 (app. q, *J* = 7.4 Hz, 1H), 5.47-5.42 (m 1H), 3.55 (s, 3H), 3.52 (dd, A of ABX, *J*_{AB} = 9.7 Hz, *J*_{AX} = 5.4 Hz, 1H), 3.46 (dd, B of ABX, *J*_{AB} = 9.6 Hz, *J*_{BX} = 5.4 Hz, 1H), 1.77-1.67 (m, 4H), 1.56-1.50 (m, 1H), 1.47(app. dt, *J* = 13.3, 7.3 Hz, 1H), 1.10-1.02 (m, 21H), 0.87 (d, *J* = 6.6 Hz, 3H).

¹³C NMR (125 MHz, CDCl₃) δ 166.01 (e), 132.77 (e), 131.89 (o), 129.59 (o), 128.77 (o), 128.41 (o), 127.46 (o), 123.54 (e), 84.50 (e) 77.09 (o), 67.85 (e), 55.55 (o) 37.62 (e), 32.36 (o), 18.16 (o), 17.90 (o), 17.46 (o), 12.10 (o).

IR (Neat) 2944 (m), 2866 (m), 1745 (s), 1462 (w), 1247 (m), 1168 (s), 1105 (s), 881 (m).

(E)-(But-3-en-2-yloxy)diisopropyl(penta-2,4-dien-1-yl)silane



Dichlorodiisopropylsilane (0.35 g, 1.90 mmol) was added to imidazole (0.64 g, 9.40 mmol) in anhydrous THF (8 mL) at 0 °C under an atmosphere of argon. The solution was stirred for *ca.* 5 minutes, then the allylic alcohol **111** (0.14 g, 1.90 mmol) in THF (2 mL) was added *via* syringe pump over *ca.* 2 hours at 0 °C. The reaction mixture was then allowed to warm up to room temperature and stirred for 2 hours. In a separate flask, to a solution of *n*-butyllithium (0.75 mL 1.90 mmol, 2.5 M in hexane) in anhydrous THF (2 mL) at –78 °C was added 2,4-pentadiene (0.20 mL, 1.90 mmol) dropwise. The cooling bath was removed and the reaction mixture was stirred for 30 minutes at room temperature before cooling to 0 °C. The solution of preformed monochlorosilane was then added *via* Teflon cannula to the solution of lithiated 2,4-pentadiene. The reaction mixture was stirred at 0 °C for 1 hour and further stirred at room temperature for 2 hours whereupon the reaction mixture was quenched with brine (10 mL) and diluted with ethyl acetate (10 mL). The reaction mixture was partitioned with ethyl acetate and the phases were separated. The combined organic phases were dried with MgSO₄, filtered, and concentrated under *vacuo*. Purification by flash chromatography over silica-gel (hexanes as eluent) afforded the dienyloxyalkoxysilane **113** as a colourless oil (0.24 g, 50%)

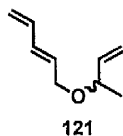
¹H NMR (500 MHz, CDCl₃) δ 6.28 (app. dt, *J* = 17.0, 10.3 Hz, 1H), 6.00 (dd, *J* = 15.1, 10.6 Hz, 1H), 5.85 (ddd, *J* = 16.1, 10.5, 5.6 Hz, 1H), 5.76 (app. dt, *J* = 15.0, 8.4 Hz, 1H), 5.16 (app. dt, *J* = 17.2, 1.4 Hz, 1H), 5.01-4.98 (m, 2H), 4.86 (d, *J* = 10.3 Hz, 1H), 4.35 (quint, *J* = 6.0 Hz, 1H), 1.74 (d, *J* = 8.3 Hz, 2H), 1.23 (d, *J* = 6.3 Hz, 3H), 1.03-1.02 (m, 14H).

^{13}C NMR (125 MHz, CDCl_3) δ 142.92 (o), 137.68 (o), 131.68 (o), 130.64 (o), 113.01 (e), 112.75 (e), 69.96 (o), 24.61 (o), 18.27 (e) 17.67 (o), 17.63 (o), 12.94 (o) 12.91 (o).

IR (Neat) 2944 (s), 2867 (s), 1745 (s), 1644 (w), 1463 (w), 1151 (m), 1088 (s), 1000 (s), 882 (s).

HRMS (ESI, $[\text{M} + \text{Na}]^+$) calcd for $\text{C}_{15}\text{H}_{28}\text{ONaSi}$ 275.1807, found 275.1806.

(*E*)-5-(But-3-en-2-yloxy)penta-1,3-diene



General Procedure for the Preparation of Oxygen-Tethered Enynes: Sodium hydride (0.72 g, 17.89 mmol, 60% in oil) was weighed into a 25 mL single-necked round-bottom flask under argon. The solids were suspended in DMF (10 mL) and the reaction mixture was cooled to 0 °C. 3-buten-2-ol (0.43 g, 5.96 mmol) in DMF (10 mL) was added dropwise. The reaction was stirred for 45 minutes before (*E*)-5-bromopenta-1,3-diene (2.63 g, 17.89 mmol) was added dropwise followed by addition of TBAI (0.60 g, 0.22 mmol) in a single portion. The reaction was allowed to gradually warm to room temperature and was stirred for 18 hours. The reaction was quenched with water (15 mL) and diluted with Et_2O (10 mL). The reaction mixture was partitioned with diethyl ether and the phases were separated. The organic phases was combined, washed with brine, dried over MgSO_4 and filtered. The solvent was removed under *vacuo* to afford a crude oil. Purification by flash chromatography over silica-gel (5% Et_2O -hexanes as eluent) afforded the desired dienyl ether **121** (0.50 g, 60%).

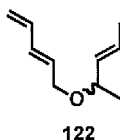
^1H NMR (500 MHz, CDCl_3) δ 6.31 (app. dt, $J = 16.8, 10.3$ Hz, 1H), 6.23 (dd, $J = 15.0, 10.7$ Hz, 1H), 5.79-5.68 (m, 2H), 5.21-5.12 (m, 3H), 5.07 (d, $J = 10.1$ Hz, 1H), 4.05 (dd, $J = 12.9, 5.6$ Hz, 1H), 3.90-3.84 (m, 2H), 1.25 (d, $J = 6.4$ Hz, 3H).

^{13}C NMR (125 MHz, CDCl_3) δ 140.22 (o), 136.53 (o), 132.95 (o), 130.57 (o), 117.42 (e), 116.17 (e), 76.43 (o), 68.22 (e), 21.46 (o).

IR (Neat) 3087 (w), 2977 (w), 2855 (w), 1604 (w), 1369 (w), 1316 (w), 1097 (s), 1002 (s), 901 (s).

HRMS (ESI, $[\text{M} + \text{H}]^+$) calcd for $\text{C}_9\text{H}_{15}\text{O}$ 139.1117, found 139.1117.

(*E*)-5-((*E*)-Pent-3-en-2-yloxy)penta-1,3-diene



Compound **122** was synthesised in an analogous manner to **121** by the use of (*E*)-pent-3-en-2-ol in place 3-buten-2-ol.

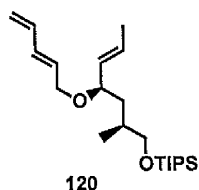
^1H NMR (500 MHz CDCl_3) δ 6.34 (app. dt, $J = 16.9, 10.3$ Hz, 1H), 6.23 (dd, $J = 15.2, 10.6$ Hz, 1H), 5.77 (app. dt, $J = 15.1, 6.1$ Hz, 1H), 5.61 (dq, $J = 15.2, 6.6$ Hz, 1H), 5.36 (ddq, $J = 15.3, 8.0, 1.6$ Hz, 1H), 5.19 (d, $J = 16.4$ Hz, 1H), 5.07 (d, $J = 10.1$ Hz, 1H), 4.03 (dd, $J = 13.5, 5.5$ Hz, 1H), 3.88-3.80 (m, 2H), 1.71 (dd, $J = 6.5, 1.6$ Hz, 3H), 1.23 (d, $J = 6.3$ Hz, 3H).

^{13}C NMR (125 MHz, CDCl_3) δ 136.54 (o), 133.22 (o), 132.72 (o), 130.76 (o), 127.71 (o), 117.16 (e), 75.93 (o), 67.83 (e), 21.65(o), 17.70 (o).

IR (Neat) 3088 (w), 2974 (w), 2856 (w), 1605 (w), 1448 (w), 1369 (w), 1100 (s), 1002 (s), 968 (s), 900 (s).

HRMS (ESI, $[\text{M} + \text{H}]^+$) calcd for $\text{C}_{10}\text{H}_{17}\text{O}$ 153.1274, found 153.1277.

Triisopropyl(((2*S*,4*R*,*E*)-2-methyl-4-((*E*)-penta-2,4-dien-1-yloxy)hept-5-en-1-yl)oxy) silane



Compound **120** was synthesised in an analogous manner to **121** by the use of allylic alcohol **24** in place of 3-buten-2-ol.

$[\alpha]_D^{20} +14.3$ (c = 0.42, CHCl₃).

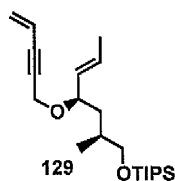
¹H NMR (500 MHz, CDCl₃) δ 6.33 (app. dt, *J* = 16.9, 10.3 Hz, 1H), 6.22 (dd, *J* = 15.2, 10.6 Hz, 1H), 5.76 (app. dt, *J* = 15.2, 6.1 Hz, 1H), 5.60 (dq, *J* = 15.3, 6.5 Hz, 1H), 5.26 (ddq, *J* = 15.5, 8.4, 1.6 Hz, 1H), 5.19 (d, *J* = 16.7 Hz, 1H), 5.06 (d, *J* = 9.8 Hz, 1H), 4.05 (dd, A of ABX, *J*_{AB} = 13.0, *J*_{AX} = 5.6 Hz, 1H), 3.82 (dd, B of ABX, *J*_{AB} = 13.0, *J*_{BX} = 6.6 Hz, 1H), 3.75-3.70 (m, 1H), 3.54 (dd, *J* = 9.5, 5.5 Hz, 1H), 3.50-3.47 (m, 1H), 1.75-1.67 (m, 4H), 1.59 (ddd, *J* = 13.6, 7.4, 6.1 Hz, 1H), 1.44-1.39 (m, 1H), 1.12-1.03 (m, 21H), 0.91 (d, *J* = 6.7 Hz, 3H).

¹³C NMR (125 MHz, CDCl₃) δ 136.70 (o), 132.82 (o), 132.33 (o), 130.99 (o), 128.83 (o), 117.21 (e), 78.95 (o), 68.46 (e), 67.98 (e), 39.25 (e), 32.62 (o), 18.20 (o), 17.88 (o), 17.38 (o), 12.13 (o).

IR (Neat) 2942 (m), 2865 (m), 1604 (w), 1462 (m), 1382 (w), 1098 (s), 1002 (s), 882 (s).

HRMS (ESI, [M + Na]⁺) calcd for C₂₂H₄₂O₂NaSi 389.2852, found 389.2860.

Triisopropyl(((2*S*,4*R*,*E*)-2-Methyl-4-(pent-4-en-2-yn-1-yloxy)hept-5-en-1-yl)oxy) silane



Compound **129** was synthesised in an analogous manner to **121** by the use of allylic alcohol

24 (0.3 g, 0.99 mmol) and 5-bromopent-1-en-3-yne (0.43 g, 30.0 mmol) in the place of 3-buten-2-ol and (*E*)-5-bromopenta-1,3-diene respectively to afford enyne **129** as a yellow oil (0.28 g, 78%).

$[\alpha]_{\text{D}}^{20} +60.5$ ($c = 0.58$, CHCl_3).

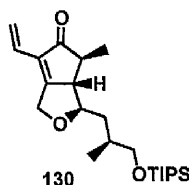
^1H NMR (500 MHz, CDCl_3) δ 5.81 (app. ddt, $J = 17.6, 11.0, 1.9$ Hz, 1H), 5.71-5.61 (m, 2H), 5.46 (dd, $J = 11.1, 2.2$ Hz, 1H), 5.23 (ddq, $J = 15.3, 8.7, 1.6$ Hz, 1H), 4.26 (dd, A of ABX, $J_{AB} = 15.9, J_{AX} = 1.9$ Hz, 1H), 4.11 (dd, B of ABX, $J_{AB} = 15.8, J_{BX} = 1.9$ Hz, 1H), 3.90 (app. dt, $J = 8.6, 7.1$ Hz, 1H), 3.54 (d, $J = 5.7$ Hz, 2H), 1.75-1.70 (m, 4H), 1.62 (ddd, $J = 13.3, 6.9, 6.3$ Hz, 1H), 1.42 (app. dt, $J = 13.6, 7.3$ Hz, 1H), 1.10-1.03 (m, 21H), 0.92 (d, $J = 6.7$ Hz, 3H).

^{13}C NMR (125 MHz, CDCl_3) δ 131.27 (o) 130.13 (o), 127.31 (e), 116.96 (o), 86.72 (e), 84.25 (e), 78.36 (o), 68.14 (e), 55.45 (e), 38.88 (e), 32.52 (o), 18.19 (o), 17.93 (o) 17.32 (o), 12.08 (o).

IR (Neat) 2941 (m), 2865 (m), 1462 (w), 1259 (m), 1060 (s), 1033 (s), 968 (m), 881 (m).

HRMS (ESI, $[\text{M} + \text{Na}]^+$) calcd for $\text{C}_{22}\text{H}_{40}\text{O}_2\text{NaSi}$ 387.2695, found 387.2688.

(3*R*,3*aS*,4*S*)-4-Methyl-3-((*S*)-2-methyl-3-((triisopropylsilyl)oxy)propyl)-6-vinyl-3*a*,4-dihydro-1*H*-cyclopenta[*c*]furan-5(3*H*)-one



To a suspension of flame-dried 4Å molecular sieves (2 g) in DCM (2 mL) was added a solution of enyne **129** (0.26 g, 0.71 mmol) in DCM (16 mL) followed by dicobalt octacarbonyl (0.28 g, 0.82 mmol) in a single portion under argon. The reaction mixture was stirred at room temperature for 2 hours after which the solution was cooled to -20 °C. TMANO (0.43 g, 5.68 mmol) was added in small portions over 10 minutes whereupon a

stream of air was bubbled through the dark solution for 20 min before stirring was continued for 16 hours at room temperature (open flask). The blue-coloured cobalt by-products were filtered through a plug of silica aided by Et₂O. The reaction mixture was concentrated under *vacuo* and the crude oil was purified by silica-gel chromatography (10% Et₂O-hexanes as eluent) to afford the bicyclic cyclopentenone **130** as a light brown oil (0.15 g, 54%) with *dr* $\geq 19 : 1$ (by ¹H NMR).

$[\alpha]_D^{20}$ -38.0 (c = 0.42, CHCl₃).

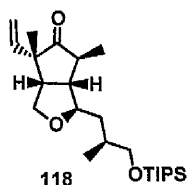
¹H NMR (500 MHz, C₆D₆) δ 6.35 (dd, *J* = 17.8, 11.2 Hz, 1H), 5.75 (d, *J* = 18.0 Hz, 1H), 5.20 (d, *J* = 11.2 Hz, 1H), 4.30 (d, A of AB, *J*_{AB} = 16.7 Hz, 1H), 4.19 (d, B of AB, *J*_{AB} = 17.1 Hz, 1H), 3.56 (dd, A of ABX, *J*_{AB} = 9.6, *J*_{AX} = 5.3 Hz, 1H), 3.50 (dd, B of ABX, *J*_{AB} = 9.5, *J*_{BX} = 5.6 Hz, 1H), 3.19 (ddd, *J* = 10.2, 8.1, 3.9 Hz, 1H), 1.98 (br d, *J* = 9.3 Hz, 1H), 1.94-1.86 (m, 2H), 1.83 (qd, *J* = 7.2, 4.0 Hz, 1H), 1.52-1.46 (m, 1H), 1.17 (d, *J* = 7.3 Hz, 3H), 1.14-1.04 (m, 21H), 1.02 (d, *J* = 6.7 Hz, 3H).

¹³C NMR (125 MHz, C₆D₆) δ 207.53 (e), 175.23 (e), 131.54 (e), 126.24 (o), 119.95 (e), 82.08 (o), 68.36 (e), 65.89 (e), 57.94 (o), 46.37 (o), 38.49 (e), 34.19 (o), 18.31 (o), 17.86 (o), 13.84 (o), 12.33 (o).

IR (Neat) 2941 (m), 2865 (s), 1714 (s), 1664 (w), 1461 (m), 1098 (s), 997 (s), 882 (s).

HRMS (ESI, [M + Na]⁺) calcd for C₂₃H₄₀O₃NaSi 415.2644, found 415.2635.

(1*R*,3*aS*,4*S*,6*S*,6*aR*)-4,6-Dimethyl-1-((*S*)-2-methyl-3-((triisopropylsilyl)oxy)propyl)-4-vinyltetrahydro-1*H*-cyclopenta[*c*]furan-5(3*H*)-one



L-Selectride (0.026 mL, 0.026 mmol, 1.0M in THF) was added dropwise to a solution of the bicyclic enone **130** (0.01 g, 0.025 mmol) in THF (0.26 mL) at -78 °C and the reaction

mixture was stirred at the same temperature for 10 minutes. Iodomethane (0.048 mL, 0.76 mmol) was added dropwise and the reaction mixture was warmed to 0 °C over 1.5 hours followed by stirring at 0 °C for further 6 hours. The reaction mixture was quenched with water (1 mL) and was partitioned with ethyl acetate. The phases were separated and the combined organic phases were dried over MgSO₄ and concentrated under *vacuo* to afford a clear oil. Purification by silica-gel chromatography (10% Et₂O-hexanes) afforded **118** as a colourless oil (0.0094 g, 90%) with *dr* ≥ 19 : 1 (by ¹H NMR).

$[\alpha]_D^{20} +31.0$ (c = 0.83, CHCl₃).

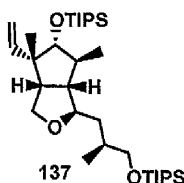
¹H NMR (500 MHz, C₆D₆) δ 5.77 (dd, *J* = 17.6, 10.8 Hz, 1H), 5.03 (dd, *J* = 17.6, 1.1 Hz, 1H), 4.96 (dd, *J* = 10.9, 1.1 Hz, 1H), 3.96 (ddd, *J* = 8.0, 6.0, 1.9 Hz, 1H), 3.87 (dd, *J* = 9.2, 8.3 Hz, 1H), 3.65 (dd, A of ABX, *J*_{AB} = 9.5, *J*_{AX} = 5.3 Hz, 1H), 3.54 (dd, B of ABX, *J*_{AB} = 9.6, *J*_{BX} = 5.6 Hz, 1H), 3.49 (app. t, *J* = 9.2 Hz, 1H), 2.36 (app. q, *J* = 8.4 Hz, 1H), 2.01-1.95 (m, 1H), 1.92-1.86 (m, 2H), 1.69 (app. dt, *J* = 13.4, 6.2 Hz, 1H), 1.41 (app. dt, *J* = 13.6, 7.7 Hz, 1H), 1.17-1.09 (m, 21H), 1.07 (d, *J* = 7.1 Hz, 3H), 1.04 (d, *J* = 6.8 Hz, 3H), 1.00 (s, 3H).

¹³C NMR (125 MHz, C₆D₆) δ 218.10 (e), 138.97 (o), 115.19 (e), 83.47 (o), 69.53 (e), 68.10 (e), 54.33 (e), 51.59 (o), 50.55 (o), 47.35 (o), 39.56 (e), 33.80 (o), 25.05 (o), 18.34 (o), 17.81 (o), 15.12 (o), 12.35 (o).

IR (Neat) 2941 (s), 2865 (s), 1742 (s), 1636 (w), 1460 (m), 1382 (w), 1097 (s), 1052 (s), 882 (s).

HRMS (ESI, [M + Na]⁺) calcd for C₂₄H₄₄O₃NaSi 431.2957, found 431.2937.

(((1*R*,3*aS*,4*S*,5*R*,6*S*,6*aR*)-4,6-Dimethyl-1-((*S*)-2-methyl-3-((triisopropylsilyl)oxy)propyl)-4-vinylhexahydro-1*H*-cyclopenta[*c*]furan-5-yl)oxy)triisopropylsilane



To a solution of **118** (0.112 g, 0.27 mmol) in ether (5.5 mL) at $-10\text{ }^{\circ}\text{C}$ was added LAH (7.6 mg, 0.20 mmol). The solution was stirred at same temperature for 16 hours. The reaction mixture was diluted with Rochelle salt (5 mL) and was stirred at room temperature for 10 minutes. The reaction mixture was partitioned with ethyl acetate and the phases were separated. The combined organic phases were dried over MgSO_4 and concentrated in *vacuo* to afford the crude oil which was directly used in the next step (*dr* = 7 : 1 from the crude ^1H -NMR).

2,6-Lutidine (0.16 mL, 1.38 mmol) and TIPSOTf (0.22 mL, 0.83 mmol) were sequentially added to a solution of crude bicyclic alcohol (0.113 g, 0.28 mmol) in DCM (5 mL) at $0\text{ }^{\circ}\text{C}$. The reaction mixture was warmed to room temperature and stirred for 15 hours before being quenched by the addition of MeOH (1 mL). The reaction mixture was partitioned with ethyl acetate and the phases were separated. The combined organic phases were dried over MgSO_4 and concentrated under *vacuo* to afford the crude oil. The residue was purified by silica gel column chromatography (20% Et_2O -hexanes) to afford **137** as a colourless oil (0.13 g, 90%).

$[\alpha]_{\text{D}}^{20} +11.3$ ($c = 1.04$, CHCl_3).

^1H NMR (500 MHz, CDCl_3) δ 6.04 (dd, $J = 17.6, 11.1$ Hz, 1H), 5.13 (dd, $J = 11.0, 1.5$ Hz, 1H), 4.97 (dd, $J = 17.6, 1.6$ Hz, 1H), 3.85 (ddd, $J = 8.1, 5.9, 4.0$ Hz, 1H), 3.80 (dd, A of ABX, $J_{AB} = 9.1, J_{AX} = 5.0$ Hz, 1H), 3.72 (dd, B of ABX, $J_{AB} = 9.2, J_{BX} = 7.7$ Hz, 1H), 3.62 (dd, A of ABX, $J_{AB} = 9.6, J_{AX} = 5.2$ Hz, 1H), 3.56 (d, $J = 8.2$ Hz, 1H), 3.50 (dd, B of ABX, $J_{AB} = 9.6, J_{BX} = 5.5$ Hz, 1H), 2.35 (ddd, $J = 9.9, 7.6, 5.0$ Hz, 1H), 1.96-1.92 (m, 1H), 1.81

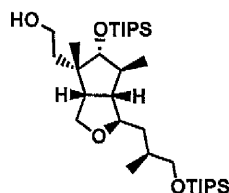
(ddd, $J = 9.9, 8.0, 4.0$ Hz, 1H), 1.74-1.68 (m, 1H), 1.62 (app. dt, $J = 13.2, 6.2$ Hz, 1H), 1.25 (app. dt, $J = 13.6, 7.5$ Hz, 1H), 1.16 (s, 3H), 1.12 (d, $J = 6.8$ Hz, 3H), 1.11-1.02 (m, 42H), 0.95 (d, $J = 6.8$ Hz, 3H).

^{13}C NMR (125 MHz, CDCl_3) δ 141.05 (o), 114.32 (e), 89.69 (o), 84.81 (o), 68.42 (e), 67.84 (e), 54.19 (o), 52.86 (o), 50.58 (e), 46.02 (o), 38.70 (e), 33.46 (o), 24.59 (o), 19.21 (o), 18.47 (o), 18.45 (o), 18.20 (o), 17.68 (o), 13.30 (o), 12.15 (o).

IR (Neat) 2943 (m), 2866 (s), 1636 (s), 1462 (m), 1383 (w), 1100 (s), 1066 (s), 880 (s), 678 (s).

HRMS (ESI, $[\text{M} + \text{Na}]^+$) calcd for $\text{C}_{33}\text{H}_{66}\text{O}_3\text{NaSi}_2$ 589.4448, found 589.4454.

2-((1*R*,3*aS*,4*S*,5*R*,6*S*,6*aR*)-4,6-Dimethyl-1-((*S*)-2-methyl-3-((triisopropylsilyl)oxy)propyl)-5-((triisopropylsilyl)oxy)hexahydro-1*H*-cyclopenta[*c*]furan-4-yl)ethanol



To a solution of **137** (0.142 g, 0.25 mmol) in dry THF (2.5 mL) was added 9-BBN dimer (0.30 mg, 1.25 mmol) at room temperature under argon. The reaction mixture was refluxed for 3 hours before allowing the solution to cool to room temperature. After addition of a 1 : 1 premixed solution of 3N NaOH and 30% H_2O_2 (1.7 mL), the resulting mixture was stirred for an additional 30 minutes. The mixture was diluted with water (5 mL) and partitioned with ethyl acetate. The combined organic phases were dried over MgSO_4 and filtered. After concentration under *vacuo*, the residue was diluted with diethyl ether (5 mL) and refrigerated at -30°C for 24 h. The reaction mixture was filtered and the solid was washed successively with cold ether (3 X 5 mL). After concentration under *vacuo* the residue was purified by silica gel column chromatography (10% EtOAc-Hex) to provide the bicyclic alcohol as a colourless oil (0.117 g, 80 %).

$[\alpha]_D^{20} +1.3$ ($c = 0.75$, CHCl_3).

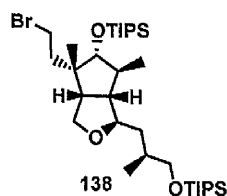
^1H NMR (500 MHz, CDCl_3) δ 3.95-3.89 (m, 2H), 3.83 (app. t, $J = 8.4$ Hz, 1H), 3.76 (app. dt, $J = 10.5, 7.3$ Hz, 1H), 3.65 (app. dt, $J = 10.6, 7.0$ Hz, 1H), 3.59 (dd, A of ABX, $J_{AB} = 9.4$, $J_{AX} = 5.4$ Hz, 1H), 3.56 (d, $J = 5.0$, 1H), 3.49 (dd, B of ABX, $J_{AB} = 9.6$, $J_{BX} = 5.7$ Hz, 1H), 2.37 (app. q, $J = 8.1$ Hz, 1H), 2.00-1.93 (m, 1H), 1.88 (app. dt, $J = 8.4, 3.1$ Hz, 1H), 1.75 (app. dt, $J = 7.2, 1.5$ Hz, 1H), 1.70-1.65 (m, 1H), 1.61 (app. dt, $J = 12.9, 6.4$ Hz, 1H), 1.27 (app. dt, $J = 13.6, 7.1$ Hz, 1H), 1.15 (d, $J = 7.2$ Hz, 3H), 1.12-1.03 (m, 42H), 1.01 (s, 3H), 0.94 (d, $J = 6.7$ Hz, 3H).

^{13}C NMR (125 MHz, CDCl_3) δ 89.82 (o), 85.23 (o), 68.79 (e), 68.05 (e), 60.27 (e), 55.94 (o), 54.57 (o), 48.42 (o), 46.41 (e), 39.70 (e), 36.62 (e), 33.57 (o), 26.57 (o), 20.61 (o), 18.50 (o), 18.44 (o), 18.20 (o), 17.47 (o), 13.11 (o), 12.14 (o).

IR (Neat) 3420 (br, w), 2943 (m), 2866 (s), 1462 (m), 1383 (w) 1245 (w), 1089 (s), 1064 (s), 881 (s), 678 (s).

HRMS (ESI, $[\text{M} + \text{Na}]^+$) calcd for $\text{C}_{33}\text{H}_{68}\text{O}_4\text{NaSi}_2$ 607.4554, found 607.4534.

(((1*R*,3*aS*,4*S*,5*R*,6*S*,6*aR*)-4-(2-Bromoethyl)-4,6-dimethyl-1-((*S*)-2-methyl-3-((triisopropylsilyl)oxy)propyl)hexahydro-1*H*-cyclopenta[*c*]furan-5-yl)oxy)triisopropylsilane



To a stirred solution of bicyclic alcohol (0.005 mg, 8.55 μmol) in THF (0.18 mL) at room temperature under argon was added triethylamine (2.98 μL , 0.021 mmol) methanesulfonyl chloride (1.5 μL , 0.019 mmol). The reaction mixture was stirred at room temperature for 2 hours whereupon LiBr (0.0015 g, 0.017 mmol) was added in single portion and was refluxed under argon for 3 hours. The reaction mixture was quenched with saturated aqueous Na_2CO_3 solution (1 mL) and the residue was diluted with diethyl ether (5 mL) and water (5 mL). The

reaction mixture was partitioned with diethyl ether and the phases were separated. The combined organic phases were dried over MgSO_4 and concentrated under *vacuo* to afford the crude oil. Purification by silica-gel chromatography (5% Et_2O -hexanes) to furnished **138** as a colourless oil (0.0043 g, 75%).

$[\alpha]_{\text{D}}^{20} -0.3$ ($c = 0.43$, CHCl_3).

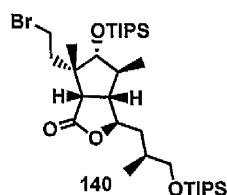
^1H NMR (500 MHz, C_6D_6) δ 4.05 (ddd, $J = 8.4, 5.6, 2.9$, 1H), 4.00 (app. t, $J = 8.5$ Hz, 1H), 3.80 (app. t, $J = 8.4$ Hz, 1H), 3.68 (dd, A of ABX, $J_{AB} = 9.5$, $J_{AX} = 5.4$ Hz, 1H), 3.56 (dd, B of ABX, $J_{AB} = 9.5$, $J_{BX} = 5.5$ Hz, 1H), 3.47 (d, $J = 4.2$ Hz, 1H), 3.33 (ddd, $J = 11.9, 9.5, 5.4$ Hz, 1H), 3.13 (ddd, $J = 12.0, 9.5, 5.4$ Hz, 1H), 2.25-2.08 (m, 3H), 2.02-1.93 (m, 2H), 1.79-1.71 (m, 2H), 1.44 (app. dt, $J = 13.7, 7.6$ Hz, 1H), 1.16-1.01 (m, 48H), 0.69 (s, 3H).

^{13}C NMR (125 MHz, C_6D_6) δ 90.13 (o), 85.08 (o), 68.83 (e), 68.21 (e), 56.67 (o), 54.56 (o), 49.37 (o), 48.61 (e), 40.04 (e), 38.46 (e), 33.94 (o), 30.26 (e), 26.13 (o), 20.81 (o), 18.60 (o), 18.52 (o), 18.38 (o), 17.95 (o), 13.33 (o), 12.40 (o).

IR (Neat) 2943 (m), 2866 (s), 1462 (m), 1383 (w), 1090 (s), 1064 (s), 881 (s), 679 (m).

HRMS (ESI, $[\text{M} + \text{Na}]^+$) calcd for $\text{C}_{33}\text{H}_{67}\text{O}_3\text{NaSi}_2^{79}\text{Br}$ 669.3710, found 669.3726, (ESI, $[\text{M} + \text{Na}]^+$) calcd for $\text{C}_{33}\text{H}_{67}\text{O}_3\text{NaSi}_2^{81}\text{Br}$ 671.3689, found 671.3688.

(3*R*,3*aS*,4*S*,5*R*,6*S*,6*aS*)-6-(2-Bromoethyl)-4,6-dimethyl-3-((*S*)-2-methyl-3-((triisopropylsilyl)oxy)propyl)-5-((triisopropylsilyl)oxy)hexahydro-1*H*-cyclopenta[*c*]furan-1-one



A mixture of **138** (0.010 g, 0.015 mmol), ruthenium trichloride (0.0018 mg, 8.49 μmol), and sodium metaperiodate (0.026 mg, 0.12 mmol) in 2:2:1 $\text{MeCN}/\text{CCl}_4/\text{H}_2\text{O}$ (0.4 mL) was stirred for 3 hours at room temperature (TLC control). The reaction mixture was diluted with water (5 mL) and was partitioned with DCM. The phases were separated and the combined

organic phases were dried over MgSO_4 and concentrated under *vacuo* to afford a black residue. Purification by silica-gel chromatography (10% Et_2O -hexanes) delivered **140** as a colourless oil (0.0061 g, 60%).

$[\alpha]_{\text{D}}^{20} +1.1$ ($c = 0.27$, CHCl_3).

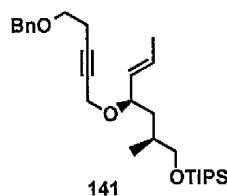
$^1\text{H NMR}$ (500 MHz C_6D_6) δ 4.32 (ddd, $J = 9.1, 4.8, 2.9$ 1H), 3.83 (ddd, $J = 12.2, 9.1, 5.1$ Hz, 1H), 3.62 (dd, A of ABX, $J_{AB} = 9.8, J_{AX} = 4.7$ Hz, 1H), 3.44 (ddd, $J = 12.3, 9.1, 4.8$ Hz, 1H), 3.39 (dd, B of ABX, $J_{AB} = 9.8, J_{BX} = 5.3$ Hz, 1H), 3.33 (d, $J = 4.7$ Hz, 1H), 2.77 (ddd, $J = 13.5, 12.6, 5.1$ Hz, 1H), 2.31 (ddd, $J = 13.7, 12.3, 4.9$ Hz, 1H), 2.19 (d, $J = 9.3$ Hz, 1H) 1.94-1.87 (m, 1H), 1.84-1.78 (m, 1H), 1.69 (ddd, $J = 9.2, 6.3, 2.8$ Hz, 1H), 1.62 (ddd, $J = 13.8, 7.4, 5.0$ Hz, 1H), 1.26 (ddd, $J = 14.1, 9.3, 6.3$ Hz, 1H), 1.14-0.99 (m, 42H), 0.97 (d, $J = 7.4$ Hz, 3H), 0.91 (d, $J = 6.9$ Hz, 3H), 0.79 (s, 3H).

$^{13}\text{C NMR}$ (125 MHz, C_6D_6) δ 175.35 (e), 88.38 (o), 84.00 (o), 67.47 (e), 51.09 (o), 50.83 (o), 49.60 (o), 40.96 (e), 37.03 (e), 32.87 (o), 30.24 (e), 29.99 (e), 24.89 (o), 20.05 (o), 18.46 (o), 18.41 (o), 18.33 (o), 17.87 (o), 13.31 (o), 12.32 (o).

IR (Neat) 2943 (s), 2866 (s), 1766 (m), 1463 (m), 1385 (w), 1093 (m), 1066 (m), 882 (m), 798 (m), 680 (m).

HRMS (ESI, $[\text{M} + \text{Na}]^+$) calcd for $\text{C}_{33}\text{H}_{65}\text{O}_4\text{NaSi}_2^{79}\text{Br}$ 683.3502, found 683.3470, (ESI, $[\text{M} + \text{Na}]^+$) calcd for $\text{C}_{33}\text{H}_{67}\text{O}_3\text{NaSi}_2^{81}\text{Br}$ 685.3482, found 685.3499.

(9*R*,11*S*)-14,14-Diisopropyl-11,15-dimethyl-1-phenyl-9-((*E*)-prop-1-en-1-yl)-2,8,13-trioxa-14-silahexadec-5-yne



Compound **141** was synthesised in an analogous manner to **121** by employing allylic alcohol **24** (0.50 g, 1.67 mmol) and propargyl bromide **143** (1.27 g, 5.02 mmol) in the place of 3-

buten-2-ol and (*E*)-5-bromopenta-1,3-diene respectively to afford enyne **141** as a colourless oil (0.64 g, 80%).

$[\alpha]_D^{20} +42.7$ ($c = 0.43$, CHCl_3).

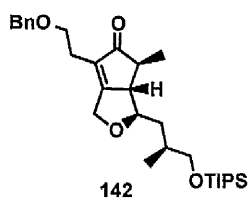
$^1\text{H NMR}$ (500 MHz, CDCl_3) δ 7.37-7.27 (m, 5H), 5.64 (dq, $J = 15.3, 6.5$ Hz, 1H), 5.21 (ddq, $J = 15.4, 8.6, 1.6$ Hz, 1H), 4.54 (s, 2H), 4.13 (app. dt, $J = 15.2, 2.2$ Hz, 1H), 3.95 (app. dt, $J = 15.1, 2.1$ Hz, 1H), 3.88-3.83 (m, 1H), 3.58 (t, $J = 7.2$ Hz, 2H), 3.52 (d, $J = 5.7$ Hz, 2H), 2.54 (tt, $J = 7.2, 2.1$ Hz, 2H), 1.71-1.68 (m, 4H), 1.61 (ddd, $J = 13.3, 7.4, 5.8$ Hz, 1H), 1.41 (ddd, $J = 13.6, 7.9, 6.7$ Hz, 1H), 1.09-1.03 (m, 21H), 0.90 (d, $J = 6.7$ Hz, 3H).

$^{13}\text{C NMR}$ (125 MHz, CDCl_3) δ 138.09 (e), 131.38 (o), 129.73 (o), 128.45 (o), 127.73 (o), 82.56 (e), 78.11 (o), 77.81 (e), 72.99 (e), 68.44 (e), 68.17 (e), 55.27 (e), 38.83 (e), 32.49 (o), 20.29 (e), 18.12 (o), 17.80 (o), 17.23 (o), 12.02 (o).

IR (Neat) 2941 (m), 2865 (m), 1455 (m), 1362 (w), 1100 (s), 1063 (s), 968 (m), 882 (m).

HRMS (ESI, $[\text{M} + \text{Na}]^+$) calcd for $\text{C}_{29}\text{H}_{48}\text{O}_3\text{NaSi}$ 495.3270, found 495.3267.

(3*R*,3*aS*,4*S*)-6-(2-(Benzyloxy)ethyl)-4-methyl-3-((*S*)-2-methyl-3-((triisopropylsilyl)oxy)propyl)-3*a*,4-dihydro-1*H*-cyclopenta[*c*]furan-5(3*H*)-one



$[\text{Rh}(\text{CO})_2\text{Cl}]_2$ (0.0082 mg, 0.021 mmol) was weighed into a flame dried reaction tube under argon atmosphere. After the flask was evacuated and backfilled three times with 10% carbon monoxide, dibutyl ether (2.1 mL) followed by the enyne ether **141** (0.10 g, 0.21 mmol) were added from a tared syringe and the reaction was heated at 100 °C and stirred for 12 h under 10% carbonmonoxide. The reaction mixture was filtered through a pad of silica aided by diethylether and was concentrated under *vacuo*. The crude residue was purified by flash

chromatography (20% Et₂O-hexanes as eluent) to furnish the bicyclic enone **142** (0.091 mg, 86%) with *dr* ≥ 19 : 1 (by ¹H NMR).

[α]_D²⁰ -49.6 (c = 0.46, CHCl₃).

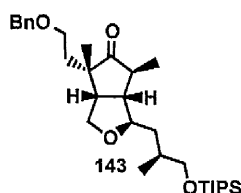
¹H NMR (500 MHz, CDCl₃) δ 7.35-7.25 (m, 5H), 4.63 (d, A of AB, *J*_{AB} = 16.1 Hz, 1H), 4.54 (d, B of AB, *J*_{BA} = 16.1 Hz, 1H), 4.47 (s, 2H), 3.64-3.59 (m, 2H), 3.53-3.48 (m, 3H), 2.58 (app. dt, *J* = 14.8, 5.9 Hz, 1H), 2.46-2.39 (m, 2H), 2.09 (qd, *J* = 7.2, 3.3 Hz, 1H), 1.98 (ddd, *J* = 13.8, 6.3, 4.8 Hz, 1H), 1.86-1.80 (m, 1H), 1.52 (app. dt, *J* = 13.8, 7.5 Hz, 1H), 1.24 (d, *J* = 7.3 Hz, 3H), 1.09-1.03 (m, 21H), 0.98 (d, *J* = 6.8 Hz, 3H).

¹³C NMR (125 MHz, CDCl₃) δ 210.83 (e), 177.24 (e), 138.21 (e), 132.54 (e), 128.53 (o), 127.79 (o), 127.77 (o), 82.20 (o), 73.05 (e), 68.05 (e), 67.83 (e), 65.95 (e), 58.17 (o), 45.58 (o), 38.32 (e), 33.63 (o), 25.07 (e), 18.17 (o), 17.82 (o), 13.87 (o), 12.05 (o).

IR (Neat) 2942 (m), 2865 (m), 1714 (s), 1678 (m), 1455 (m), 1364 (w), 1098 (s), 996 (s), 882 (s).

HRMS (ESI, [M + Na]⁺) calcd for C₃₀H₄₈O₄NaSi 523.3220, found 523.3220.

(1*R*,3*aS*,4*S*,6*S*,6*aR*)-4-(2-(Benzyloxy)ethyl)-4,6-dimethyl-1-((*S*)-2-methyl-3-(((triisopropylsilyl)oxy)propyl)tetrahydro-1*H*-cyclopenta[*c*]furan-5(3*H*)-one



L-Selectride (0.021 mL, 0.021 mmol, 1.0 M solution in THF) was added dropwise to a solution of the bicyclic enone **142** (0.011 g, 0.021 mmol) in THF (0.21 mL) at -78 °C and the reaction mixture was stirred at the same temperature for 3 hours. Iodomethane (0.039 mL, 0.63 mmol) was added dropwise and the reaction mixture was slowly warmed to room temperature overnight. The reaction mixture was diluted with water (1 mL) and partitioned diethylether. The phases were separated and the combined organic extracts were dried over

MgSO₄, filtered and concentrated under *vacuo* to yield a clear colourless oil. The crude oil was purified by silica-gel column chromatography (20% Et₂O-hexanes) to yield **143** (0.0098 g, 90%) with *dr* ≥ 19 : 1 (by ¹H NMR).

$[\alpha]_D^{20} +23.8$ (c = 0.40, CHCl₃).

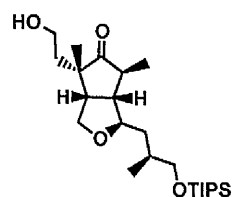
¹H NMR (500 MHz, CDCl₃) δ 7.35-7.27 (m, 5H), 4.49 (d, A of AB, *J*_{AB} = 12.0 Hz, 1H), 4.45 (d, B of AB, *J*_{AB} = 11.9 Hz, 1H), 4.07-4.01 (m, 2H), 3.62 (dd, *J* = 9.6, 4.8 Hz, 1H), 3.59-3.55 (m, 1H), 3.53-3.48 (m, 3H), 2.72-2.67 (m, 1H), 1.91 (app. dt, *J* = 14.5, 5.6 Hz, 1H), 1.73-1.67 (m, 2H), 1.59 (app. dt, *J* = 14.5, 7.4 Hz, 1H), 1.37-1.31 (m, 1H), 1.19 (d, *J* = 7.0 Hz, 3H), 1.18-1.04 (m, 21H), 1.02 (s, *J* = 3H), 0.96 (d, *J* = 6.5 Hz, 3H).

¹³C NMR (125 MHz, CDCl₃) δ 222.63 (e), 138.34 (e), 128.46 (o), 127.66 (o), 127.62 (o), 83.29 (o), 73.17 (e), 69.17 (e), 67.82 (e), 66.40 (e), 51.19 (o), 50.41 (o), 50.15 (e), 47.05 (o), 39.08 (e), 33.43 (o), 32.98 (e), 22.93 (o), 18.15 (o), 17.36 (o), 15.73 (o), 12.00 (o).

IR (Neat) 2941 (m), 2865 (s), 1737 (s), 1455 (m), 1365 (w), 1099 (s), 995 (m), 882 (m).

HRMS (ESI, [M + Na]⁺) calcd for C₃₁H₅₂O₄NaSi 539.3533, found 539.3532.

(1*R*,3*aS*,4*S*,6*S*,6*aR*)-4-(2-Hydroxyethyl)-4,6-dimethyl-1-((*S*)-2-methyl-3-((triisopropylsilyloxy)propyl)tetrahydro-1*H*-cyclopenta[*c*]furan-5(3*H*)-one



Compound **143** (0.18 g, 0.35 mmol) was dissolved in MeOH (12 mL) and Pd(OH)₂/C on carbon (0.12 g, 20 wt.%) was added in a single portion. The reaction mixture was stirred at room temperature for 30 minutes under an atmosphere of hydrogen gas whereupon, the suspension was filtered through a pad of celite aided by ethyl acetate. The filtrate was concentrated under *vacuo* to afford the bicyclic alcohol as a colourless oil (0.15 g, quant.)

$[\alpha]_D^{20} +25.7$ (c = 0.38, CHCl₃).

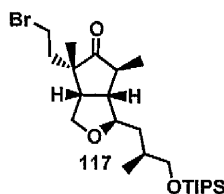
¹H NMR (500 MHz, CDCl₃) δ 4.06-4.03 (m, 2H), 3.88-3.82 (m, 1H), 3.70-3.65 (m, 1H), 3.62 (dd, A of ABX, $J_{AB} = 9.5$, $J_{AX} = 4.9$ Hz, 1H), 3.55 (app. t, $J = 9.6$ Hz, 1H), 3.49 (dd, B of ABX, $J_{BA} = 9.6$, $J_{BX} = 5.6$ Hz, 1H), 2.75 (br dd, $J = 7.1$, 2.8 Hz, 1H), 2.69-2.64 (m, 1H), 2.27-2.24 (m, 1H), 2.21-2.15 (m, 1H), 1.84 (ddd, $J = 14.3$, 7.9, 6.0 Hz, 1H), 1.73-1.65 (m, 2H), 1.51 (app. dt, $J = 14.7$, 5.4 Hz, 1H), 1.37-1.31 (m, 1H), 1.20 (d, $J = 7.2$ Hz, 3H), 1.13 (s, 3H), 1.07-0.99 (m, 21H), 0.96 (d, $J = 6.5$ Hz, 3H).

¹³C NMR (125 MHz, CDCl₃) δ 224.54 (e), 83.46 (o), 68.84 (e), 67.80 (e), 58.72 (e), 51.32 (o), 51.21 (o), 50.94 (e), 47.40 (o), 39.15 (e), 35.69 (e), 33.44 (o), 22.95 (o), 18.15 (o), 17.34 (o), 15.77 (o), 12.01 (o).

IR (Neat) 3453 (br, w), 2940 (m), 2866 (s), 1737 (m), 1460 (m), 1382 (w), 1098 (s), 1051 (s), 882 (s).

HRMS (ESI, $[M + Na]^+$) calcd for C₂₄H₄₆O₄NaSi 449.3063, found 449.3062.

(1*R*,3*aS*,4*S*,6*S*,6*aR*)-4-(2-Bromoethyl)-4,6-dimethyl-1-((*S*)-2-methyl-3-((triisopropyl silyl) oxy)propyl)tetrahydro-1*H*-cyclopenta[*c*]furan-5(3*H*)-one



To a stirred solution of bicyclic alcohol (0.005 g, 0.012 mmol) in THF (0.23 mL) at room temperature under argon was added triethylamine (4.08 μ L, 0.029 mmol) and methanesulfonyl chloride (2.01 μ L, 0.026 mmol). The reaction mixture was stirred at room temperature for 2 hours whereupon LiBr (0.006 g, 0.059 mmol) was added in single portion and was refluxed under argon for 3 hours. The reaction mixture was quenched with saturated aqueous Na₂CO₃ solution (1 mL) and the residue was diluted with diethyl ether (5 mL) and water (5 mL). The reaction mixture was partitioned with diethyl ether and the phases were separated. The combined organic phases were dried over MgSO₄ and concentrated under

vacuo to afford the crude oil. Purification by silica-gel chromatography (10% Et₂O-hexanes) to furnished **117** as a colourless oil (0.0042 g, 76%).

$[\alpha]_D^{20} +38.4$ ($c = 0.21$, CHCl₃).

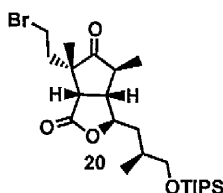
¹H NMR (500 MHz, CDCl₃) δ 4.08 (app. t, $J = 8.7$ Hz, 1H), 4.04-4.01 (m, 1H), 3.61 (dd, $J = 9.6, 4.8$ Hz, 1H), 3.56 (app. dt, $J = 10.2, 4.7$ Hz, 1H), 3.52-3.45 (m, 2H), 3.32 (app. dt, $J = 10.2, 6.9$ Hz, 1H), 2.71 (app. dt, $J = 9.6, 7.8$ Hz, 1H), 2.26 (ddd, $J = 14.7, 10.2, 4.6$ Hz, 1H), 2.20 (ddd, $J = 9.0, 7.2, 1.0$ Hz, 1H), 2.15-2.09 (m, 1H), 1.79 (ddd, $J = 14.5, 10.4, 6.8$ Hz, 1H), 1.72-1.64 (m, 2H), 1.37-1.31 (m, 1H), 1.18 (d, $J = 7.1$ Hz, 3H), 1.06 (s, 3H), 1.04-1.02 (m, 21H), 0.95 (d, $J = 6.6$ Hz, 3H).

¹³C NMR (125 MHz, CDCl₃) δ 221.59 (e), 83.39 (o), 68.65 (e), 67.81 (e), 51.61 (e), 51.16 (o), 50.00 (o), 47.13 (o), 39.06 (e), 36.92 (e), 33.45 (o), 28.41 (e), 22.51 (o), 18.18 (o), 17.35 (o), 15.73 (o), 12.02 (o).

IR (Neat) 2941 (m), 2866 (s), 1737 (s), 1461 (m), 1382 (w), 1096 (s), 1052 (s), 882 (s).

HRMS (ESI, $[M + Na]^+$) calcd for C₂₄H₄₅O₃NaSi⁷⁹Br 511.2219, found 511.2236, (ESI, $[M + Na]^+$) calcd for C₂₄H₄₅O₃NaSi⁸¹Br 513.2199, found 513.2211.

(3*R*,3*aS*,4*S*,6*S*,6*aS*)-6-(2-Bromoethyl)-4,6-dimethyl-3-((*S*)-2-methyl-3-((triisopropyl silyl)oxy)propyl)tetrahydro-1*H*-cyclopenta[*c*]furan-1,5(3*H*)-dione



A mixture of **117** (0.014 g, 0.027 mmol), ruthenium trichloride (0.0031 mg, 0.015 mmol), sodium bicarbonate (0.005 mg, 0.054 mmol) and sodium metaperiodate (0.43 mL, 0.28 mmol, 0.5M in water) in ethyl acetate (0.68 mL) was stirred for 5 h at room temperature (TLC control). The reaction mixture was diluted with water (5 mL) and was partitioned with ethyl acetate. The phases were separated and the combined organic extracts were dried on

MgSO₄, and filtered and concentrated under *vacuo*. The black residue was purified by silica-gel chromatography (20% Et₂O-hexanes) to afford the bicyclic lactone **20** (0.0058 mg, 40%).

$[\alpha]_D^{20} +13.1$ (c = 0.29, CHCl₃).

¹H NMR (500 MHz, CDCl₃) δ 4.52 (ddd, *J* = 7.9, 6.0, 1.8 Hz, 1H), 3.71 (dd, A of ABX, *J*_{AB} = 9.8, *J*_{AX} = 4.4 Hz, 1H), 3.60 (ddd, *J* = 11.4, 9.7, 5.5 Hz, 1H), 3.50 (dd, B of ABX, *J*_{AB} = 9.7, *J*_{BX} = 6.2 Hz, 1H), 3.43 (ddd, *J* = 11.2, 9.6, 5.0 Hz, 1H), 2.98 (d, *J* = 8.4 Hz, 1H), 2.44-2.40 (m, 1H), 2.26-2.23 (m, 1H), 2.21-2.17 (m, 1H), 1.91-1.86 (m, 2H), 1.62-1.53 (m, 2H), 1.21 (d, *J* = 7.1 Hz, 3H), 1.17 (s, 3H), 1.07-1.04 (m, 21H), 0.98 (d, *J* = 6.7 Hz, 3H).

¹³C NMR (125 MHz, CDCl₃) δ 217.55 (e), 174.66 (e), 82.58 (o), 68.73 (e), 67.48 (e), 48.95 (o), 47.15 (o), 46.87 (o), 38.87 (e), 36.90 (e), 32.67 (o), 27.81 (e), 23.36 (o), 18.19 (o), 17.52 (o), 14.40 (o), 11.99 (o).

IR (Neat) 2928 (s), 2865 (s), 1767 (m), 1741 (m), 1464 (m), 1183 (w), 880 (w).

HRMS (ESI, [M + Na]⁺) calcd for C₂₄H₄₃O₄NaSi⁷⁹Br 525.2012, found 525.2015, (ESI, [M + Na]⁺) calcd for C₂₄H₄₃O₄NaSi⁸¹Br 527.1991, found 527.2012.

2.10 References

- 1 Lai, K. W.; Paquette, L. A. *Org. Lett.* **2008**, *10*, 2115.
- 2 (a) Stork, G.; Mook, R.; Biller, S. A.; Rychnovsky, S. D. *J. Am. Chem. Soc.* **1983**, *105*, 3741. (b) Jasperse, C. P.; Curran, D. P.; Fevig, T. L. *Chem. Rev.* **1991**, *91*, 1237.
- 3 (a) Negishi, E.; Valente, L. F.; Kobayashi, M. *J. Am. Chem. Soc.* **1980**, *102*, 3298. (b) Negishi, E. I. *Acc. Chem. Res.* **1982**, *15*, 340.
- 4 Denis, C.; Laignel, B.; Plusquellec, D.; LeMarouille, J. Y.; Botrel, A. *Tetrahedron Lett.* **1996**, *37*, 53.
- 5 Davisson, V. J.; Neal, T. R.; Poulter, C. D. *J. Am. Chem. Soc.* **1993**, *115*, 1235.
- 6 Comins, D. L.; Dehghani, A. *Tetrahedron Lett.* **1992**, *33*, 6299.
- 7 (a) Smith, A. B.; Beauchamp, T. J.; LaMarche, M. J.; Kaufman, M. D.; Qiu, Y. P.; Arimoto, H.; Jones, D. R.; Kobayashi, K. *J. Am. Chem. Soc.* **2000**, *122*, 8654. (b) Krasovskiy, A.; Malakhov, V.; Gavryushin, A.; Knochel, P. *Angew Chem Int Ed.* **2006**, *45*, 6040.
- 8 Poss, C. S.; Schreiber, S. L. *Acc. Chem. Res.* **1994**, *27*, 9.
- 9 Corey, E. J.; Danheiser, R. L.; Chandrasekaran, S.; Keck, G. E.; Gopalan, B.; Larsen, S. D.; Siret, P.; Gras, J. L. *J. Am. Chem. Soc.* **1978**, *100*, 8034.
- 10 (a) Smith, A. B.; Bosanac, T.; Basu, K. *J. Am. Chem. Soc.* **2009**, *131*, 2348. (b) Hart, D. W.; Schwartz, J. *J. Am. Chem. Soc.* **1974**, *96*, 8115.
- 11 (a) Robertson, J.; Hall, M. J.; Stafford, P. M.; Green, S. P. *Org. Biomol. Chem.* **2003**, *1*, 3758. (b) Tamao, K.; Kakui, T.; Akita, M.; Iwahara, T.; Kanatani, R.; Yoshida, J.; Kumada, M. *Tetrahedron* **1983**, *39*, 983.
- 12 For silicon-tethered Pauson-Khand reactions, see: (a) Dobbs, A. P.; Miller, I. J.; Martinovic, S. *Beilstein J. Org. Chem.* **2007**, *3*. (b) Reichwein, J. F.; Iacono, S. T.; Patel, M. C.; Pagenkopf, B. L. *Tetrahedron Lett.* **2002**, *43*, 3739. (c) Reichwein, J. F.; Iacono, S. T.; Pagenkopf, B. L. *Tetrahedron* **2002**, *58*, 3813. (d) Brummond, K. M.; Sill, P. C.; Rickards, B.; Geib, S. J. *Tetrahedron Lett.* **2002**, *43*, 3735.
- 13 (a) Pauson, P. L. *Tetrahedron* **1985**, *41*, 5855. (b) Khand, I. U.; Knox, G. R.; Pauson, P. L.; Watts, W. E. *J. Chem. Soc., Perkin Trans., 1* **1973**, 975. (c) Khand, I. U.; Knox, G. R.; Pauson, P. L.; Watts, W. E.; Foreman, M. I. *J. Chem. Soc., Perkin Trans. 1* **1973**, 977. (d) Khand, I. U.; Knox, G. R.; Pauson, P. L.; Watts, W. E. *J. Chem. Soc., Chem. Comm.* **1971**, 36.
- 14 Schore, N. E.; Croudace, M. C. *J. Org. Chem.* **1981**, *46*, 5436.
- 15 (a) Jeong, N.; Chung, Y. K.; Lee, B. Y.; Lee, S. H.; Yoo, S. E. *Synlett* **1991**, 204. (b) Shambayati, S.; Crowe, W. E.; Schreiber, S. L. *Tetrahedron Lett.* **1990**, *31*, 5289.
- 16 For reviews on PK reactions, see: (a) Lee, H. W.; Kwong, F. Y. *Eur. J. Org. Chem.*

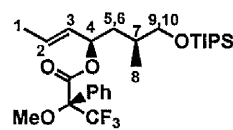
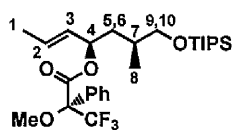
- 2010**, 789. (b) Shibata, T. *Adv. Synth. Catal.* **2006**, 348, 2328. (c) Bonaga, L. V. R.; Krafft, M. E. *Tetrahedron* **2004**, 60, 9795. (d) Blanco-Urgoiti, J.; Anorbe, L.; Perez-Serrano, L.; Dominguez, G.; Perez-Castells, J. *Chem. Soc. Rev.* **2004**, 33, 32. (e) Rivero, M. R.; Adrio, J.; Carretero, J. C. *Eur. J. Org. Chem.* **2002**, 2881. (f) Sugihara, T.; Yamaguchi, M.; Nishizawa, M. *Chem. Eur. J.* **2001**, 7, 1589. (g) Fletcher, A. J.; Christie, S. D. R. *J. Chem. Soc. Perkin Trans. 1* **2000**, 1657. (h) Brummond, K. M.; Kent, J. L. *Tetrahedron* **2000**, 56, 3263. (i) Chung, Y. K. *Coord. Chem. Rev.* **1999**, 188, 297. (j) Geis, O.; Schmalz, H. G. *Angew. Chem. Int. Ed.* **1998**, 37, 911.
- 17 For the mechanism of cobalt-mediated PK reaction, see: (a) Pericas, M. A.; Balsells, J.; Castro, J.; Marchueta, I.; Moyano, A.; Riera, A.; Vazquez, J.; Verdager, X. *Pure Appl. Chem.* **2002**, 74, 167. (b) Krafft, M. E.; Scott, I. L.; Romero, R. H.; Feibelman, S.; Vanpelt, C. E. *J. Am. Chem. Soc.* **1993**, 115, 7199. (c) Krafft, M. E. *J. Am. Chem. Soc.* **1988**, 110, 968. (d) Krafft, M. E. *Tetrahedron Lett.* **1988**, 29, 999. (e) Magnus, P.; Principe, L. M. *Tetrahedron Lett.* **1985**, 26, 4851. (f) Magnus, P.; Exon, C.; Albaughrobertson, P. *Tetrahedron* **1985**, 41, 5861. (g) Magnus, P.; Principe, L. M.; Slater, M. J. *J. Org. Chem.* **1987**, 52, 1483.
- 18 (a) Wilson, M. S.; Woo, J. C. S.; Dake, G. R. *J. Org. Chem.* **2006**, 71, 4237. (b) Kozaka, T.; Miyakoshi, N.; Mukai, C. *J. Org. Chem.* **2007**, 72, 10147. (c) Yoo, S. E.; Lee, S. H. *J. Org. Chem.* **1994**, 59, 6968.
- 19 Brummond, K. M.; Mitasev, B. *Org. Lett.* **2004**, 6, 2245.
- 20 Rautenstrauch, V.; Megard, P.; Conesa, J.; Kuster, W. *Angew. Chem. Int. Ed.* **1990**, 29, 1413.
- 21 (a) Belanger, D. B.; Livinghouse, T. *Tetrahedron Lett.* **1998**, 39, 7641. (b) Belanger, D. B.; O'Mahony, D. J. R.; Livinghouse, T. *Tetrahedron Lett.* **1998**, 39, 7637. (c) Pagenkopf, B. L.; Livinghouse, T. *J. Am. Chem. Soc.* **1996**, 118, 2285.
- 22 (a) Jeong, N.; Hwang, S. H.; Lee, Y. S.; Chung, Y. K. *J. Am. Chem. Soc.* **1994**, 116, 3159. (b) Lee, B. Y.; Chung, Y. K.; Jeong, N.; Lee, Y. S.; Hwang, S. H. *J. Am. Chem. Soc.* **1994**, 116, 8793.
- 23 (a) Krafft, M. E.; Hirosawa, C.; Bonaga, L. V. R. *Tetrahedron Lett.* **1999**, 40, 9177. (b) Krafft, M. E.; Bonaga, L. V. R.; Hirosawa, C. *Tetrahedron Lett.* **1999**, 40, 9171.
- 24 For rhodium-catalysed PK reactions, see: (a) Kobayashi, T.; Koga, Y.; Narasaka, K. *J. Organomet. Chem.* **2001**, 624, 73. (b) Koga, Y.; Kobayashi, T.; Narasaka, K. *Chem. Lett.* **1998**, 249. (c) Jeong, N.; Lee, S.; Sung, B. K. *Organometallics* **1998**, 17, 3642.
- 25 For titanium-catalysed PK reactions, see: (a) Hicks, F. A.; Kablaoui, N. M.; Buchwald, S. L. *J. Am. Chem. Soc.* **1999**, 121, 5881. (b) Hicks, F. A.; Kablaoui, N. M.; Buchwald, S. L. *J. Am. Chem. Soc.* **1999**, 121, 5881.
- 26 For ruthenium-catalysed PK reactions, see: (a) Kondo, T.; Suzuki, N.; Okada, T.; Mitsudo, T. *J. Am. Chem. Soc.* **1997**, 119, 6187. (b) Morimoto, T.; Chatani, N.; Fukumoto, Y.; Murai, S. *J. Org. Chem.* **1997**, 62, 3762.
- 27 For a chromium-promoted PK reaction, see: Jordi, L.; Segundo, A.; Camps, F.; Ricart, S.; Moreto, J. M. *Organometallics* **1993**, 12, 3795.

- 28 For iron-promoted PK reactions, see: (a) Pearson, A. J.; Dubbert, R. A. *Organometallics* **1994**, *13*, 1656. (b) Pearson, A. J.; Dubbert, R. A. *J. Chem. Soc., Chem Comm* **1991**, 202.
- 29 For nickel-catalysed PK reactions, see: (a) Zhang, M. H.; Buchwald, S. L. *J. Org. Chem.* **1996**, *61*, 4498. (b) Tamao, K.; Kobayashi, K.; Ito, Y. *Synlett.* **1992**, 539. (c) Pages, L.; Llebaria, A.; Camps, F.; Molins, E.; Miravittles, C.; Moreto, J. M. *J. Am. Chem. Soc.* **1992**, *114*, 10449.
- 30 For zirconium-promoted PK reactions, see: (a) Negishi, E.; Holmes, S. J.; Tour, J. M.; Miller, J. A.; Cederbaum, F. E.; Swanson, D. R.; Takahashi, T. *J. Am. Chem. Soc.* **1989**, *111*, 3336. (b) Negishi, E.-I. in *Comprehensive Organic Synthesis* (Eds.: Trost, B. M.; Fleming), Pergamon, Oxford, **1991**, Vol. 5, p. 1163-1188.
- 31 For a palladium-catalysed PK reaction, see: Tang, Y. F.; Deng, L. J.; Zhang, Y. D.; Dong, G. B.; Chen, J. H.; Yang, Z. *Org. Lett.* **2005**, *7*, 1657.
- 32 For tungsten-mediated PK reactions, see: (a) Shiu, Y. T.; Madhushaw, R. J.; Li, W. T.; Lin, Y. C.; Lee, G. H.; Peng, S. M.; Liao, F. L.; Wang, S. L.; Liu, R. S. *J. Am. Chem. Soc.* **1999**, *121*, 4066. (b) Hoye, T. R.; Suriano, J. A. *J. Am. Chem. Soc.* **1993**, *115*, 1154.
- 33 For iridium-catalysed PK reactions, see: (a) Shibata, T.; Takagi, K. *J. Am. Chem. Soc.* **2000**, *122*, 9852. (b) Shibata, T.; Toshida, N.; Yamasaki, M.; Maekawa, S.; Takagi, K. *Tetrahedron* **2005**, *61*, 9974.
- 34 Leahy, D. K.; Evans, P. A. in *Modern Rhodium-Catalyzed Organic Reactions* (Ed.: Evans, P. A.), Wiley-VCH: Weinheim, **2005**, Ch. 11, pp 216-217.
- 35 (a) Baik, M. H.; Mazumder, S.; Ricci, P.; Sawyer, J. R.; Song, Y. G.; Wang, H.; Evans, P. A. *J. Am. Chem. Soc.* **2011**, *133*, 7621. (b) Wang, H.; Sawyer, J. R.; Evans, P. A.; Baik, M. H. *Angew. Chem. Int. Ed.* **2008**, *47*, 342. (c) Evans, P. A.; Robinson, J. E. *J. Am. Chem. Soc.* **2001**, *123*, 4609.
- 36 For reviews on silicon-tether reactions, see (a) Marciniak, B.; Pietraszuk, C. *Curr. Org. Chem.* **2003**, *7*, 691. (b) Cox, L. R.; Ley, S. V. Use of the Temporary Connection in Organic Synthesis. In *Templated Organic Synthesis*; Diederich, F.; Stang, P. J., Eds.; Wiley-VCH: Weinheim, 1999; pp 275-395. (c) Fensterbank, L.; Malacria, M.; Sieburth, S. M. *Synthesis* **1997**, 813. (d) Bols, M.; Skrydstrup, T. *Chem. Rev.* **1995**, *95*, 1253.
- 37 For selective deprotection of silyl ethers, see (a) Crouch, R. D. *Tetrahedron* **2004**, *60*, 5833. (b) Nelson, T. D.; Crouch, R. D. *Synthesis-Stuttgart* **1996**, 1031.
- 38 (a) Stork, G.; Chan, T. Y.; Breault, G. A. *J. Am. Chem. Soc.* **1992**, *114*, 7578. (b) Stork, G.; Kim, G. *J. Am. Chem. Soc.* **1992**, *114*, 1087. (c) Nishiyama, H.; Kitajima, T.; Matsumoto, M.; Itoh, K. *J. Org. Chem.* **1984**, *49*, 2298.
- 39 For recent advances in TST-metal mediated reactions, see (a) Bracegirdle, S.; Anderson, E. A. *Chem. Soc. Rev.* **2010**, *39*, 4114. (b) For stereoselective transition metal-catalysed higher-order carbocyclisation reactions see Inglesby, P. A.; Evans, P. A. *Chem. Soc. Rev.* **2010**, *39*, 2791.

- 40 Evans, P. A.; Murthy, V. S. *J. Org. Chem.* **1998**, *63*, 6768.
- 41 Fu, G. C.; Grubbs, R. H. *J. Am. Chem. Soc.* **1992**, *114*, 5426.
- 42 Evans, P. A.; Cui, J.; Gharpure, S. J.; Polosukhin, A.; Zhang, H. R. *J. Am. Chem. Soc.* **2003**, *125*, 14702.
- 43 Evans, P. A.; Cui, B.; Buffone, G. P. *Angew Chem Int Ed.* **2003**, *42*, 1734.
- 44 (a) Evans, P. A.; Baum, E. W. *J. Am. Chem. Soc.* **2004**, *126*, 11150. (b) Evans, P. A.; Robinson, J. E.; Baum, E. W.; Fazal, A. N. *J. Am. Chem. Soc.* **2003**, *125*, 14648.
- 45 Myers, A. G.; Yang, B. H.; Chen, H.; McKinsty, L.; Kopecky, D. J.; Gleason, J. L. *J. Am. Chem. Soc.* **1997**, *119*, 6496.
- 46 Fettes, A.; Carreira, E. M. *J. Org. Chem.* **2003**, *68*, 9274.
- 47 Pappo, R.; Allen, D. S.; Lemieux, R. U.; Johnson, W. S. *J. Org. Chem.* **1956**, *21*, 478.
- 48 Lebsack, A. D.; Overman, L. E.; Valentekovich, R. J. *J. Am. Chem. Soc.* **2001**, *123*, 4851.
- 49 (a) Evans, M. A.; Morken, J. P. *Org. Lett.* **2005**, *7*, 3371. (b) Corey, E. J.; Helal, C. J. *Angew Chem Int Ed.* **1998**, *37*, 1987.
- 50 Hoye, T. R.; Jeffrey, C. S.; Shao, F. *Nat. Protoc.* **2007**, *2*, 2451.
- 51 Wender, P. A.; Croatt, M. P.; Deschamps, N. M. *J. Am. Chem. Soc.* **2004**, *126*, 5948.
- 52 Pitcock, W. H.; Lord, R. L.; Baik, M. H. *J. Am. Chem. Soc.* **2008**, *130*, 5821.
- 53 Schlosser, M.; Zellner, A.; Leroux, F. *Synthesis* **2001**, 1830.
- 54 Castro, J. M.; Linares-Palomino, P. J.; Salido, S.; Altarejos, J.; Nogueras, M.; Sanchez, A. *Tetrahedron* **2005**, *61*, 11192.
- 55 (a) Jamison, T. F.; Shambayati, S.; Crowe, W. E.; Schreiber, S. L. *J. Am. Chem. Soc.* **1997**, *119*, 4353. (b) Jamison, T. F.; Shambayati, S.; Crowe, W. E.; Schreiber, S. L. *J. Am. Chem. Soc.* **1994**, *116*, 5505.
- 56 Park, J.; Kim, S. H.; Lee, P. H. *Org. Lett.* **2008**, *10*, 5067.
- 57 (a) Reisman, S. E.; Ready, J. M.; Weiss, M. M.; Hasuoka, A.; Hirata, M.; Tamaki, K.; Ovaska, T. V.; Smith, C. J.; Wood, J. L. *J. Am. Chem. Soc.* **2008**, *130*, 2087. (b) McIntosh, J. M.; Cassidy, K. C.; Matassa, L. C. *Tetrahedron* **1989**, *45*, 5449.
- 58 Carlsen, P. H. J.; Katsuki, T.; Martin, V. S.; Sharpless, K. B. *J. Org. Chem.* **1981**, *46*, 3936.
- 59 Wu, Y.; Carroll, P. J.; Quintana, W. *Polyhedron* **1998**, *17*, 3391.
- 60 Pangborn, A. B.; Giardello, M. A.; Grubbs, R. H.; Rosen, R. K.; Timmers, F. J. *Organometallics* **1996**, *15*, 1518.

2.11 Appendix

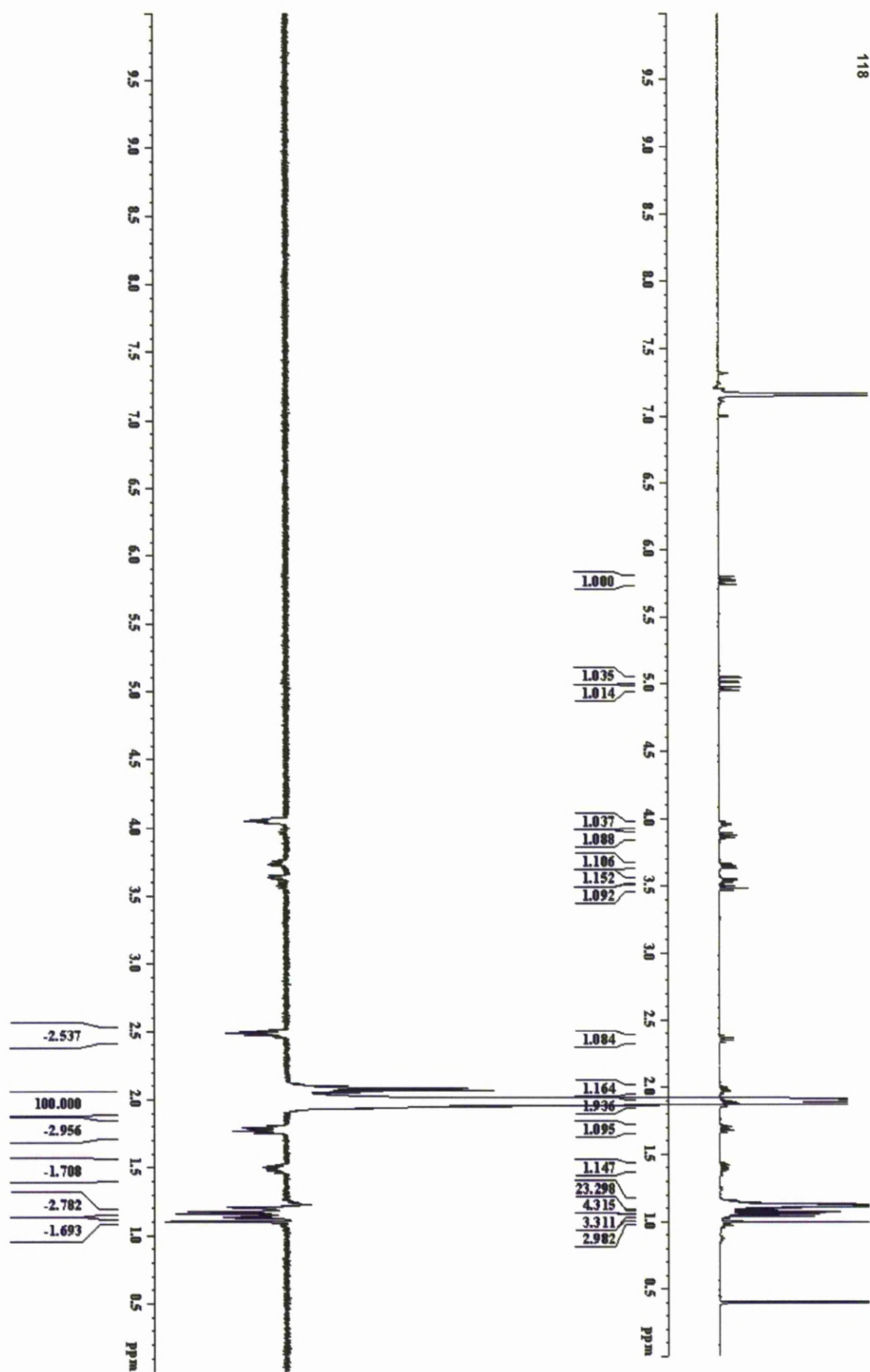
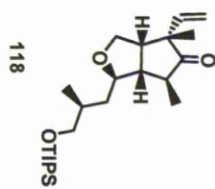
2.11.1 Mosher Ester Analysis for Allylic Alcohol 24

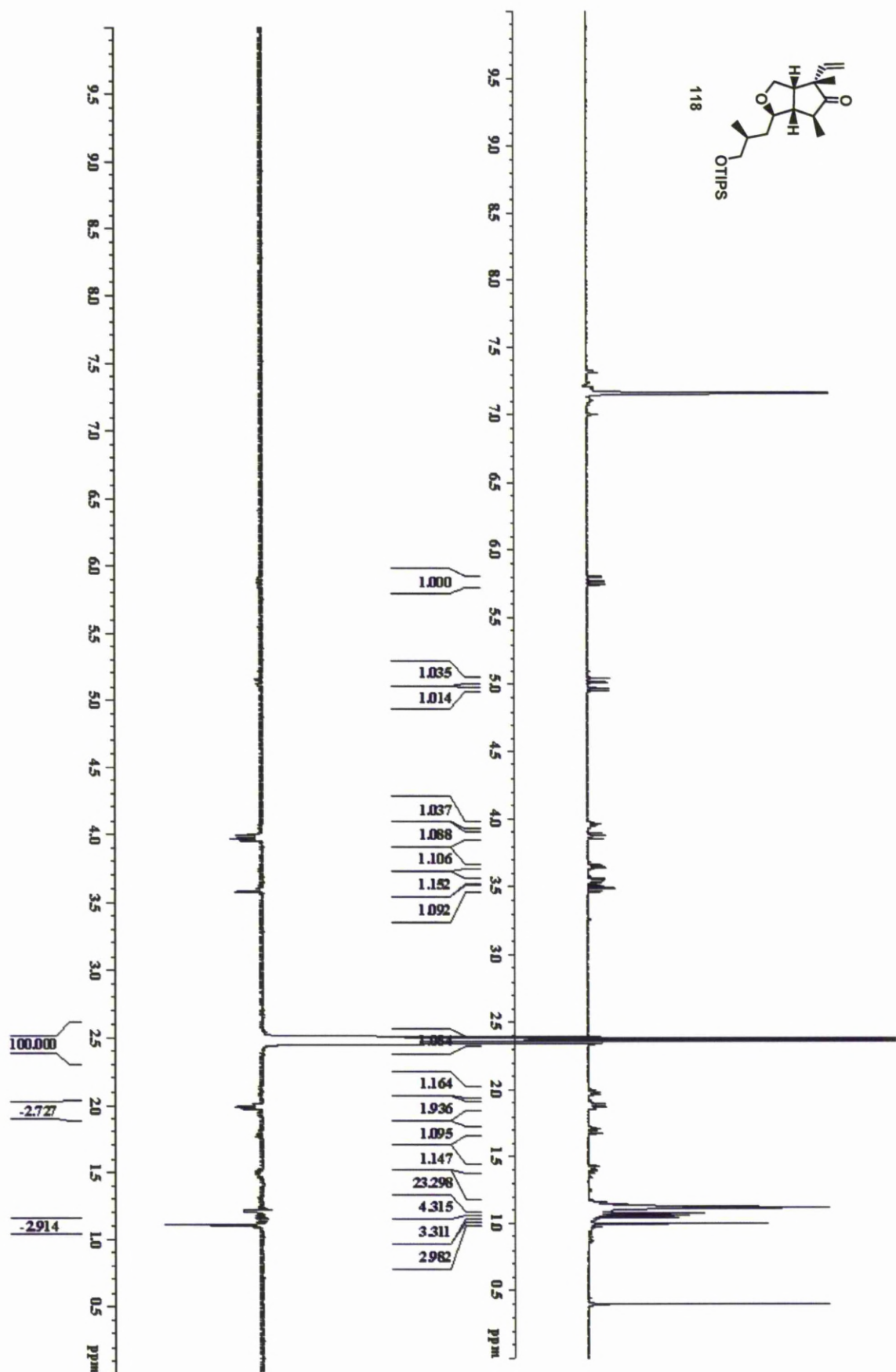
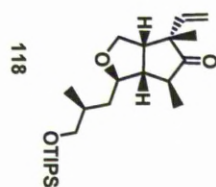


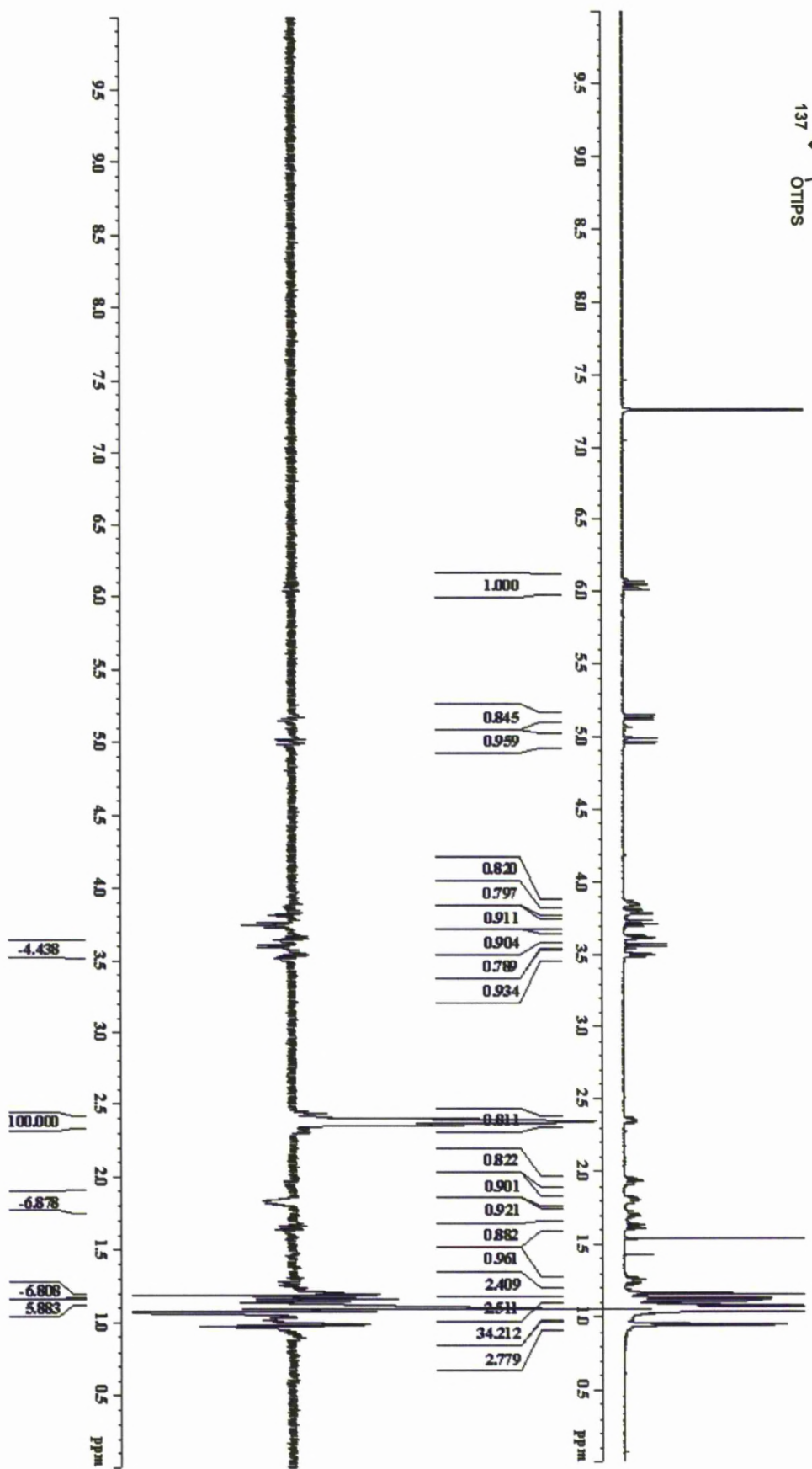
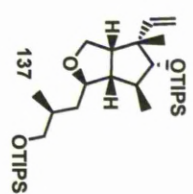
Entry	Proton	(<i>S</i>)-Ester δ_S (ppm)	(<i>R</i>)-Ester δ_R (ppm)	$\Delta\delta = \delta_S - \delta_R$ (ppm)	Hz (500 MHz)
1	H ₁	1.677	1.715	-0.038	-19
2	H ₂	5.319	5.441	-0.122	-61
3	H ₃	5.806	5.876	-0.070	-35
4	H ₄	5.506	5.534	-0.028	-14
5	H ₅	1.815	1.533	+0.282	+141
6	H ₆	1.518	1.464	+0.054	+27
7	H ₈	0.930	0.868	+0.062	+31
8	H ₉	3.544	3.517	+0.027	+13.5
9	H ₁₀	3.499	3.461	+0.036	+18

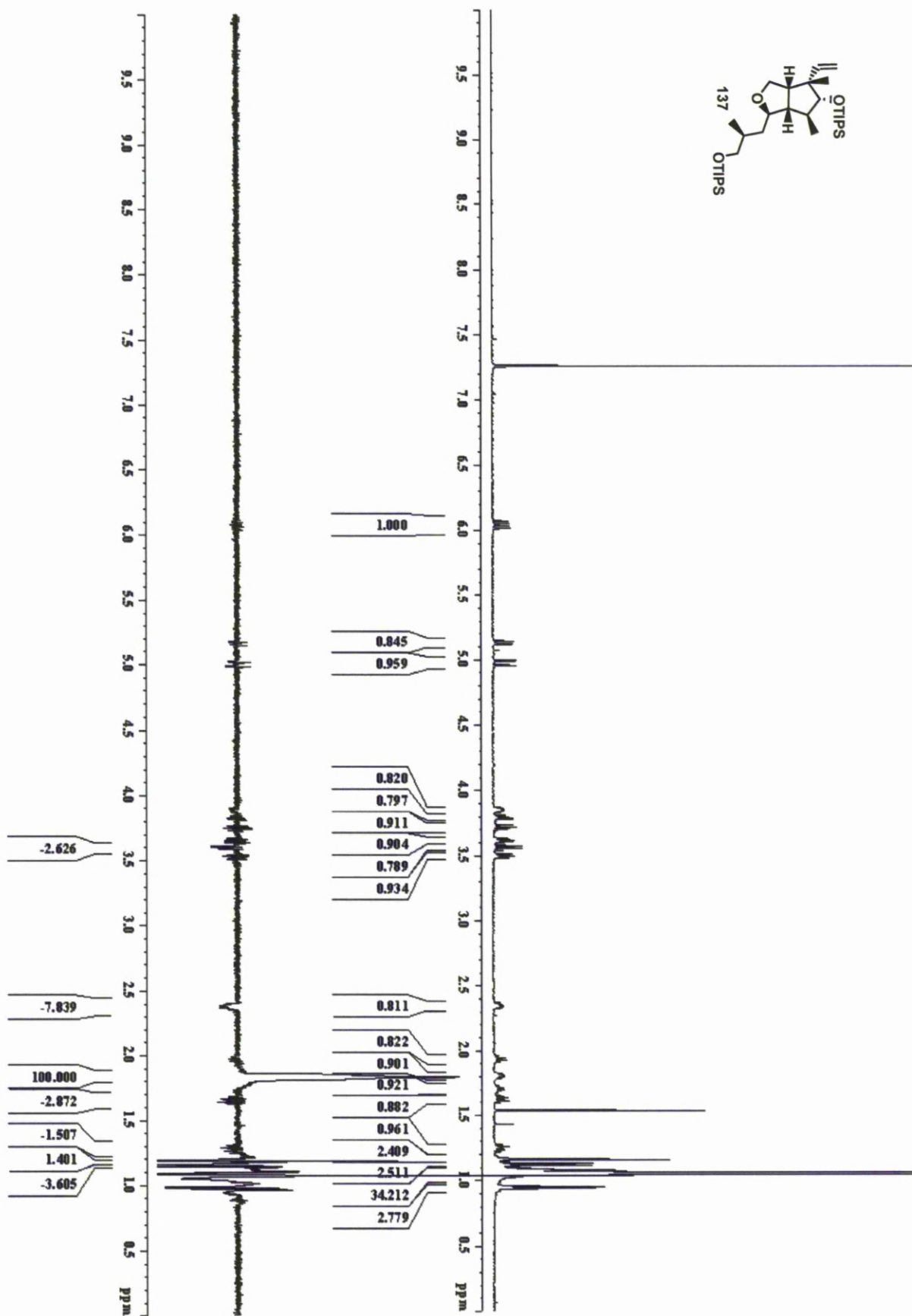
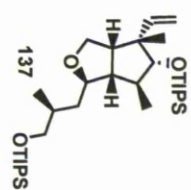
Table 2.7 $\Delta\delta = \delta_S - \delta_R$ Data for the (*S*)- and (*R*)-Mosher Ester of Allylic Alcohol 24.

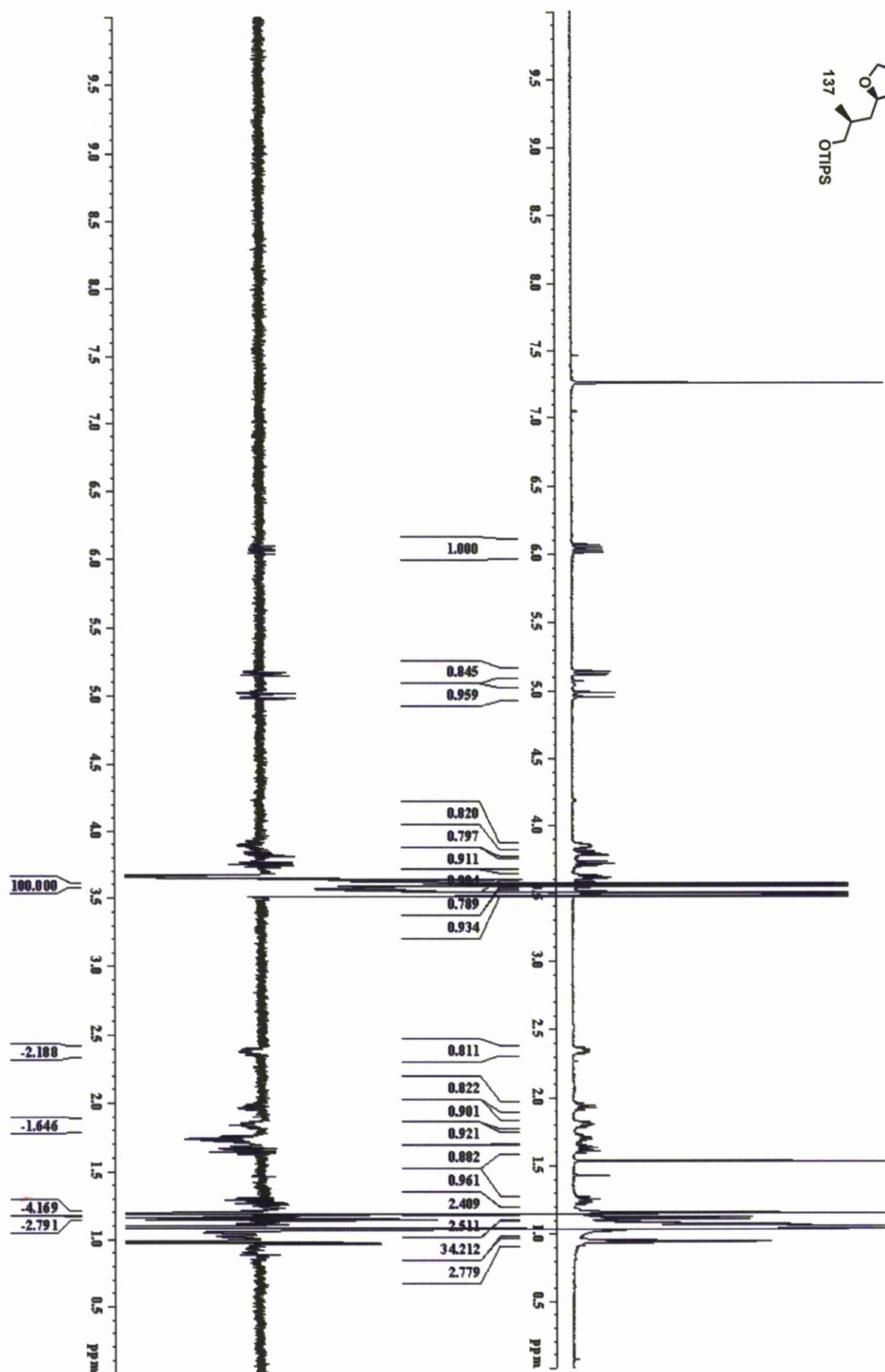
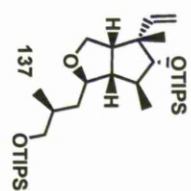
2.11.2 One-Dimensional ^1H -nOe Data: Proof of Relative Configuration for Compounds 118 and 137

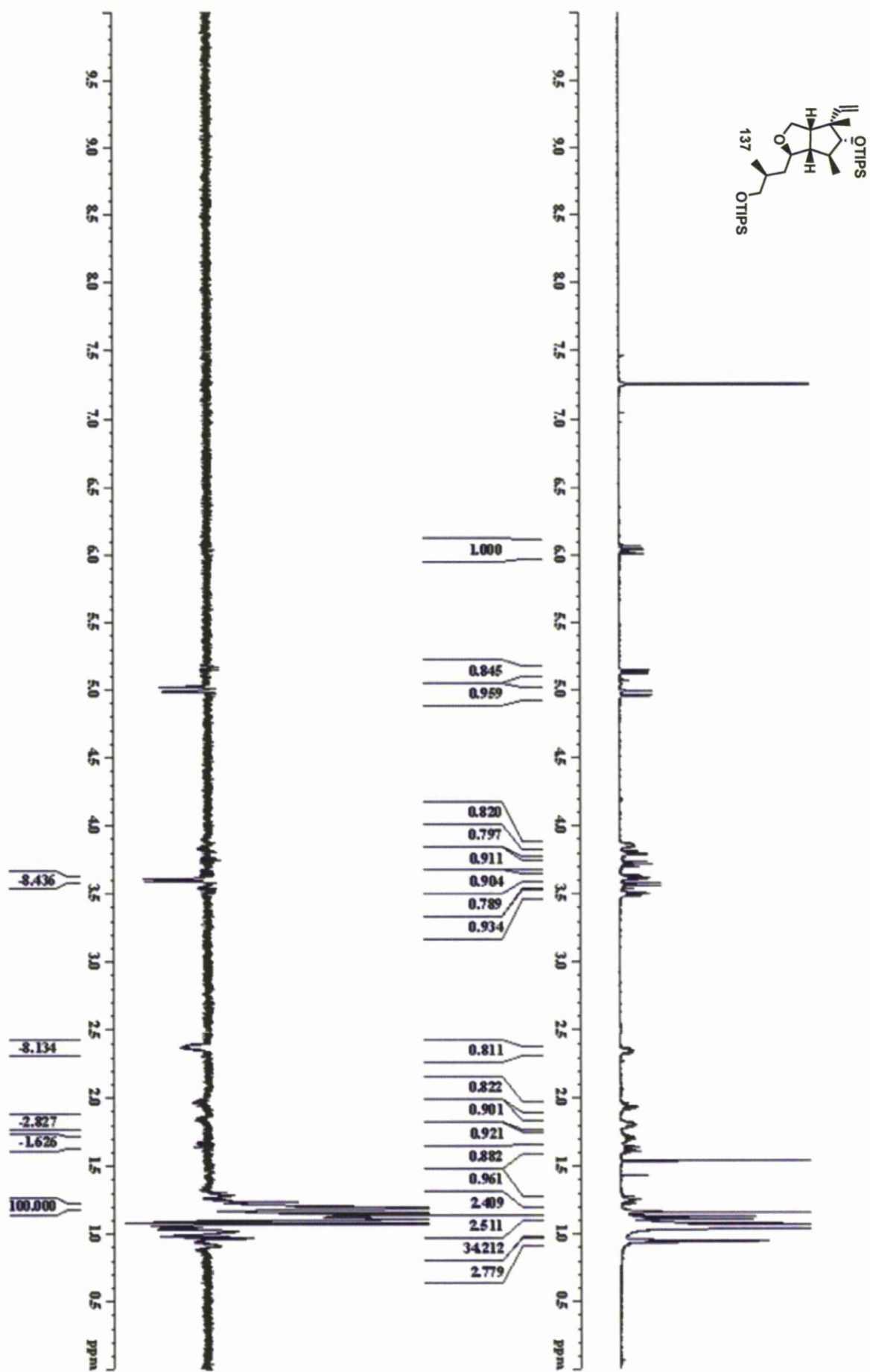


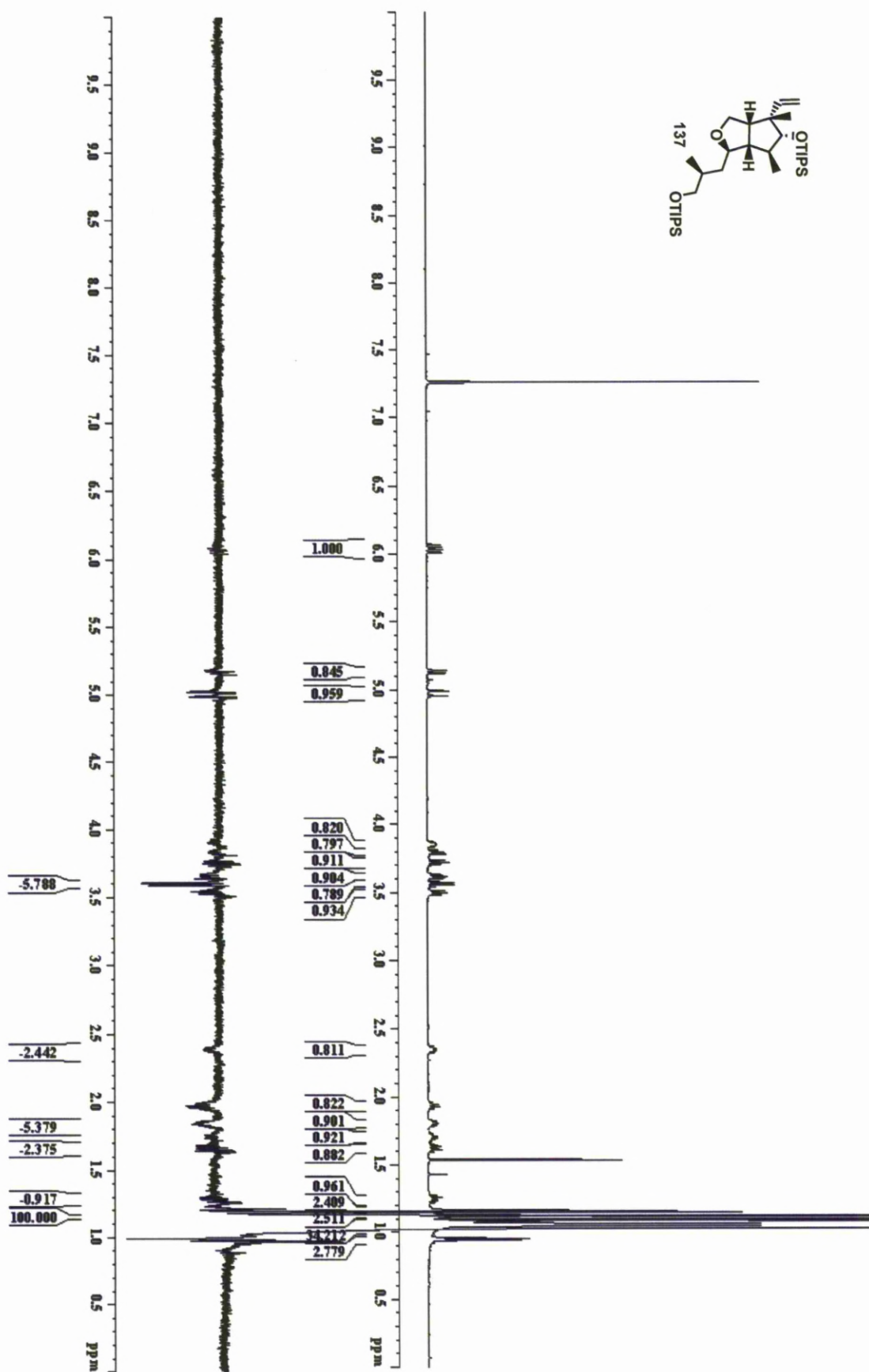












Chapter 3

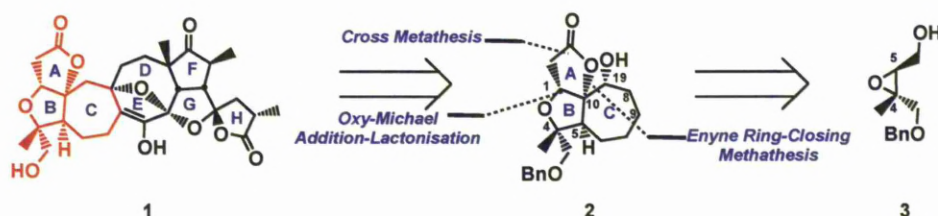
Synthesis of the Western Fragment (B-C Rings) of Lancifodilactone G

3.1 Introduction

3.1.1 Previous Synthetic Work

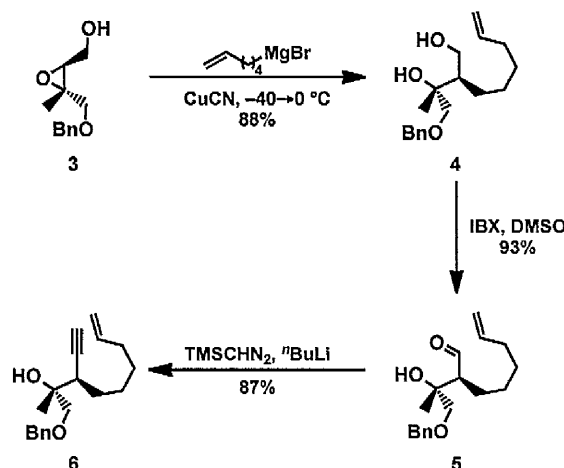
3.1.1.1 The Paquette Approach

In 2008, Paquette and co-workers reported the first synthetic route towards the tricyclic ABC ring network of Lancifodilactone G **1**.¹ As illustrated in Scheme 3.1, the construction of the 5,5-*cis*-fused bicyclic skeleton of the ABC subunit was accomplished by a diastereoselective oxy-Michael lactonisation sequence, whereas the 7-membered C ring was realised *via* an enyne ring-closing metathesis reaction (RCM).



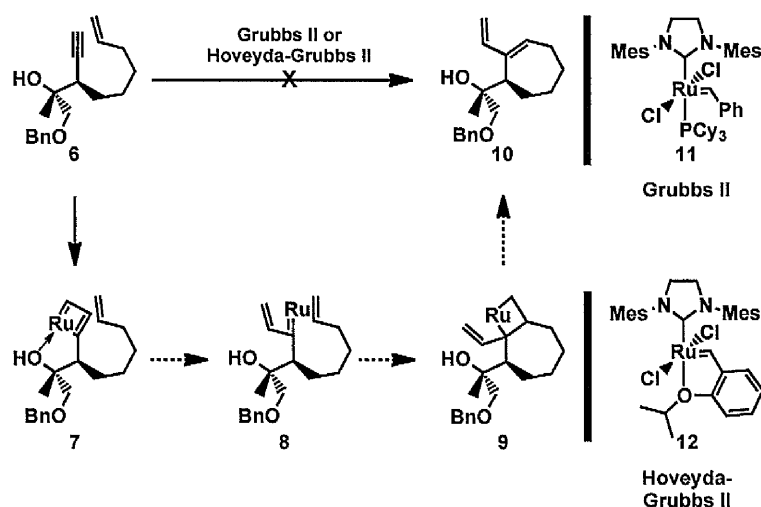
Scheme 3.1 Paquette's Retrosynthetic Analysis.

The epoxy alcohol **3** was initially subjected to a regioselective epoxide opening reaction with the organocuprate derived from 5-hexenylmagnesium bromide, to furnish the desired diol **4** in excellent yield (Scheme 3.2). The primary alcohol **4** was oxidised to aldehyde **5**, and then homologated to the terminal alkyne **6** using the modified Colvin rearrangement reaction, employing trimethylsilyldiazomethane and *n*-butyllithium.²



Scheme 3.2 *Synthesis of Hydroxyl Enyne 6.*

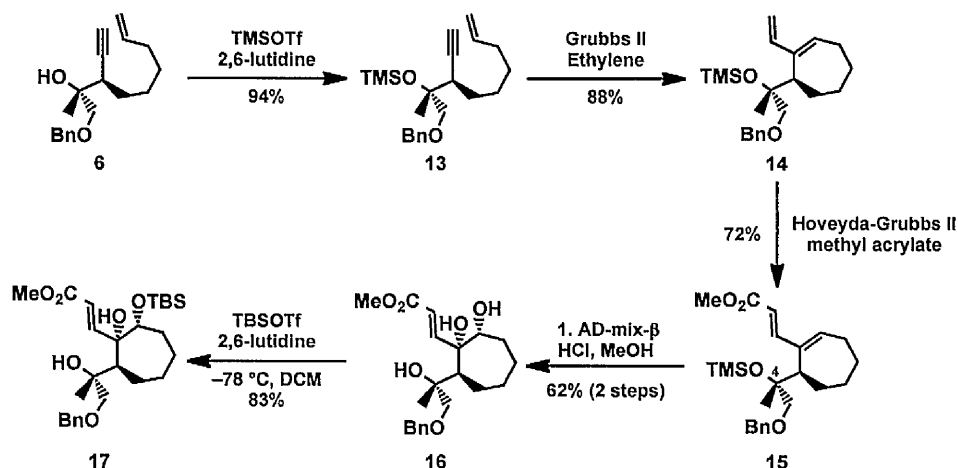
With enyne **6** in hand, the key RCM reaction was probed using Grubbs II **11** and Hoveyda-Grubbs II **12** catalysts. Surprisingly, all attempts to obtain the desired diene **10** provided only recovered starting material. As outlined in Scheme 3.3, the failure of the metathesis reaction was attributed to the formation of a stable vinyl alkylidene species **7**,



Scheme 3.3 *Attempted RCM of Enyne 6.*

which has the free alcohol complexed to the metal centre, was attributed to the inhibition of the metathesis propagation and recycling step *via* **8** and **9**.¹ In order to circumvent this problem, the hydroxyl group was protected as a TMS ether **13** in excellent yield (Scheme 3.4). Interestingly, treatment of TMS protected enyne **13** with catalyst **11** furnished the 7-membered diene **14** in 88% yield. Following the successful RCM reaction of **13**, the vinylogous ester required for the key intramolecular oxy-conjugate addition/lactonisation

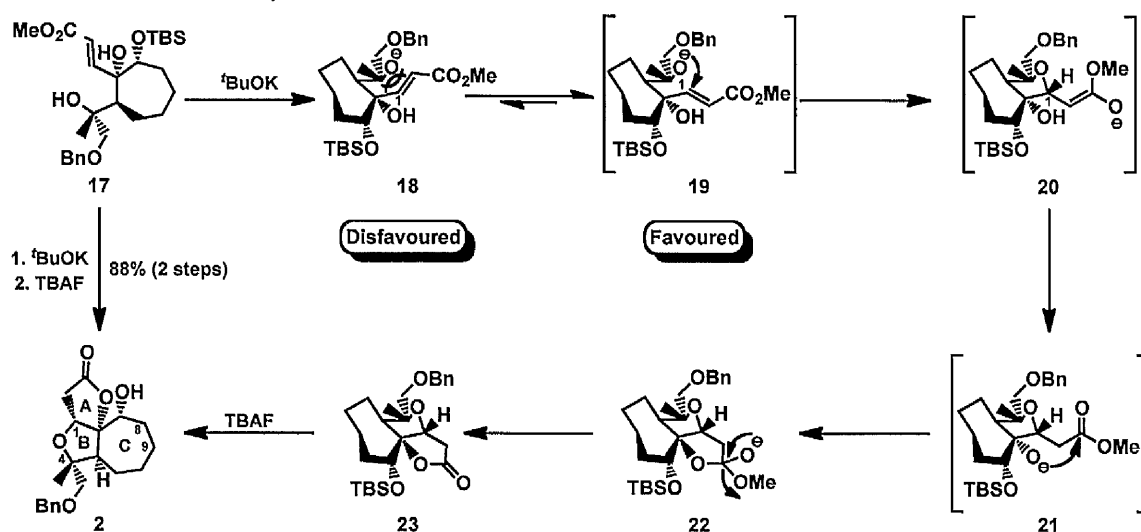
sequence was installed using ruthenium-catalysed cross metathesis between diene **14** and methyl acrylate, which proceeded in 72% yield and with excellent *E/Z*-selectivity ($\geq 20 : 1$). In the ensuing step, the internal alkene in **15** was chemoselectively dihydroxylated and the



Scheme 3.4 *Synthesis of Diol 17.*

tertiary alcohol at C4 was unveiled under standard protodesilylation conditions to generate the requisite triol **16** in 62% overall yield. Finally, chemoselective protection of the secondary alcohol in **16** provided the key intermediate **17** for the conjugate-addition lactonisation/reaction.

Scheme 3.5 delineates the completion of the synthesis of ABC subunit **2** of lancifodilactone **G 1**.¹ The pivotal oxy-Michael/lactonisation reaction was triggered using potassium *tert*-butoxide, which facilitated the installation of the C1 stereocentre with



Scheme 3.5 *Completion of the Western Fragment.*

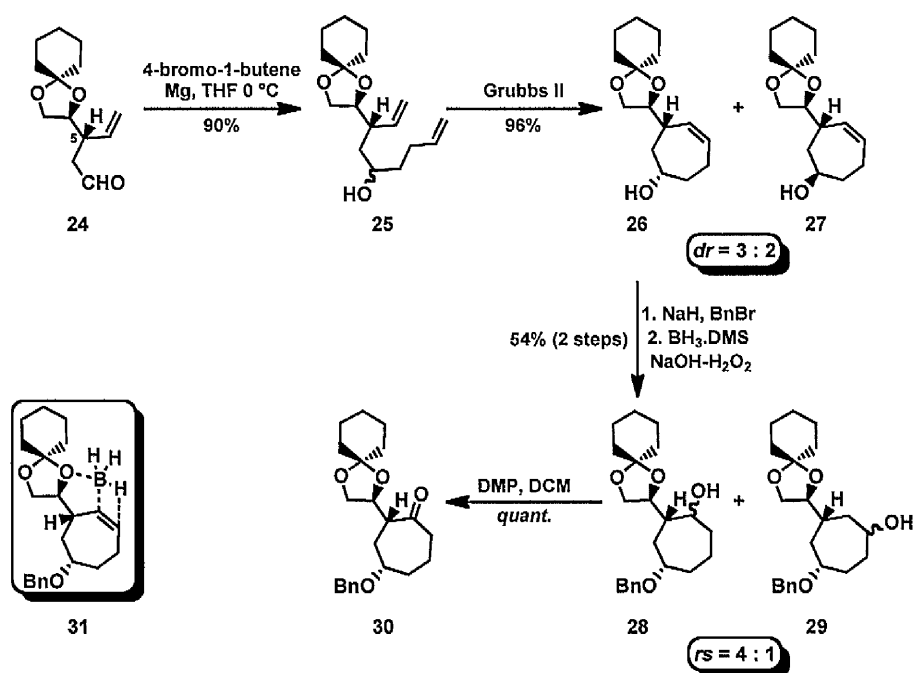
excellent diastereoselectivity under thermodynamically controlled conditions. The initial deprotonation of the tertiary alcohol **17** was postulated to give rise to an equilibrium mixture of conformers **18** and **19**. The favourable pseudoequatorial disposition of the acrylate side chain in **19** renders the alkene moiety susceptible to the nucleophilic attack by the tertiary alkoxide thus enabling the cascade reaction to siphon off *via* intermediate **21** by a lactonisation reaction to furnish the tricyclic lactone **23**. The stereochemical orientation of the acrylate side chain in the conformer **19** is eventually equilibrated to afford **20**, which accounts for the *R*-configuration at C1. Fluoride mediated desilylation of the crude product **23** afforded the desired fragment **2** in 88% overall yield.

In conclusion, the Paquette group accomplished their synthesis of this truncated fragment in 11 linear steps with 19% overall yield. The synthesis successfully identifies and overcomes the problems in the enyne RCM reaction and highlights the oxy-Michael/lactonisation sequence for the diastereoselective construction of A ring of the western fragment. However, it is important to note that the western fragment prepared by Paquette does not completely map onto the natural product due to the lack of appropriate functionality at C8 and C9, which is critical for the successful union of western and eastern fragments for assembly of the 8-membered, ring in lancifodilactone **G 1**.

3.1.1.2 The Ghosh Approach

The Ghosh group has recently reported a general protocol for the synthesis of the 5-*epi*-ABC core present in lancifodilactone **G** in addition to the other members of the Schisandraceae family starting from the known precursor **24**.⁴ In order to demonstrate the feasibility of their synthetic plan for the construction of the ABC core found in lancifodilactone **G 1** and in the related nortriterpenoids, the group decided to prepare the *ent*-ABC unit from the readily available enantioenriched aldehyde **24** with opposite configuration at C5. Towards this end, compound **24** was treated with 4-butenylmagnesium

bromide to afford 3 : 2 mixture of inseparable carbinols **25** in 90% yield (Scheme 3.6). The dienyln alcohol **25** was subjected to RCM reaction to furnish a mixture of cycloheptenols **26** and **27** in excellent yield. The major isomer **26** was separated by column

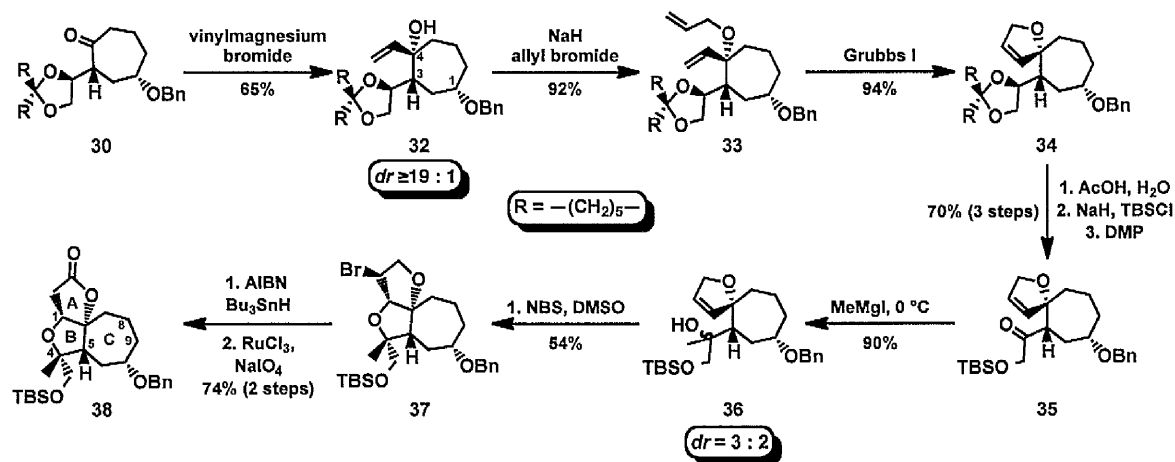


Scheme 3.6 *Synthesis of Cycloheptenone Derivative 30.*

chromatography and the minor diastereoisomer was converted to **26** *via* a Mitsunobu reaction. Alcohol **26** was protected as a benzyl ether using standard conditions and the resulting unsymmetrical cycloheptene derivative was subjected to the regioselective hydroboration-oxidation sequence to generate a mixture of alcohols **28** and **29** in 54% overall yield with 4 : 1 regioselectivity favouring **28**. The regioselectivity in the hydroboration reaction was rationalised *via* the borane adduct **31**, which presumably formed from the coordination of the Lewis acidic borane to the homoallylic oxygen followed by the addition of the B-H unit to the proximal end of the alkene to give the major regioisomer **28**.

Following the chromatographic separation of compounds **28** and **29**, the cycloheptenol **28** was oxidised to ketone **30** using Dess-Martin periodinane in quantitative yield. The subsequent diastereoselective Grignard addition was anticipated to occur from the α -face through a metal-coordinated chelate of the ketal functionality in **30** (Scheme 3.7). Contrary

to the planned stereochemical course, the 1,2-addition reaction proceeded from the less hindered face opposite to the bulky ketal group, thus generating the undesired allylic alcohol **32** with the alternate stereochemistry at C4, albeit with excellent diastereocontrol. The stereochemical outcome in this reaction could only be ascertained in the later stage after the formation of the tricyclic core using NMR (*vide infra*) and thus significantly impacted their efforts to install the correct stereochemistry at C1, C4 and C5 of the ABC motif of Schisandrane natural products.



Scheme 3.7 Synthesis of C5-*epi*-ABC Subunit **38**.

Following the Grignard addition reaction, the resulting tertiary alcohol **32** was alkylated using allyl bromide to afford diene **33** in 92% yield, which was then transformed to the spiro-dihydrofuran derivative **34** in excellent yield through a RCM reaction (Scheme 3.7). The acetal **34** was converted to the silylated hydroxy ketone **35** using a three-step reaction sequence, which involved acetal deprotection, chemoselective silyl protection of the primary alcohol and Dess-Martin oxidation. Unfortunately, the 1,2-addition of methylmagnesium iodide to ketone **35** provided a 3 : 2 mixture of inseparable alcohols **36** for the key bromo-etherification reaction. Stereoselective bromination of spirocyclic alkenes **36** from the less hindered β -face followed by intramolecular 5-*exo* ring closure of the free hydroxyl group at C4 afforded the desired tricyclic bromide **37** in 54% yield after chromatographic separation from the minor diastereoisomer. Debromination of compound

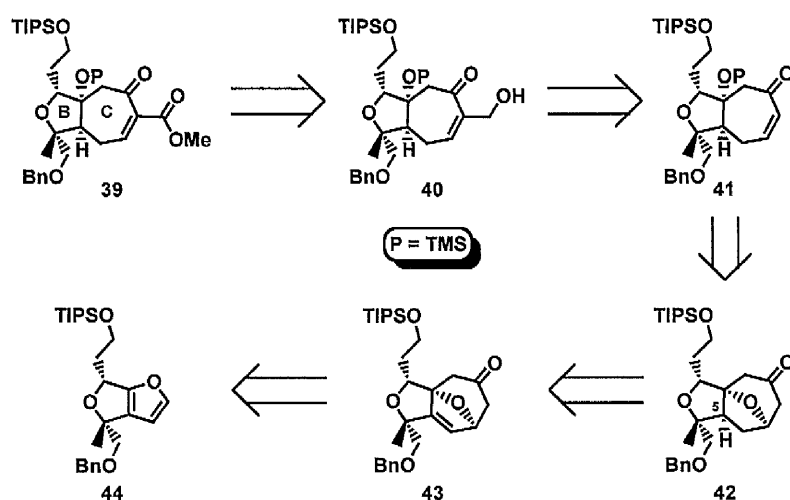
37 under standard radical-mediated reductive conditions furnished the corresponding tricyclic ether in excellent yield. The ruthenium-catalysed oxidation of the tetrahydrofuran ring provided lactone **38** in 74% yield, thereby completing the construction of the western fragment.

In summary, the synthesis of the 5-*epi*-ABC subunit **38** was achieved in 15 steps with 7% overall yield. The synthesis is plagued with poor regio- and stereocontrol and thus relies on tedious chromatographic separation of undesired isomers. More importantly, Ghosh's approach fails to install C1, C4 and C5 stereocentres with the correct relative configuration found in lancifodilactone **1** and in other related nortriterpenoids of Schisandraceae family. Finally, this approach to the ABC core lacks the necessary functionality at C8 and C9 centres to facilitate further elaboration required for the union with the eastern fragment.

3.2 Results and Discussions

3.2.1 Retrosynthetic Analysis

In devising a strategy for the western fragment **39**, we recognized the need to address the two critical aspects in the advanced intermediate: (i) the construction of the fully functionalised *cis*-fused 5,7-ring system that would serve as a suitable intermediate to initiate coupling studies with the eastern fragment, and (ii) the stereocontrolled installation



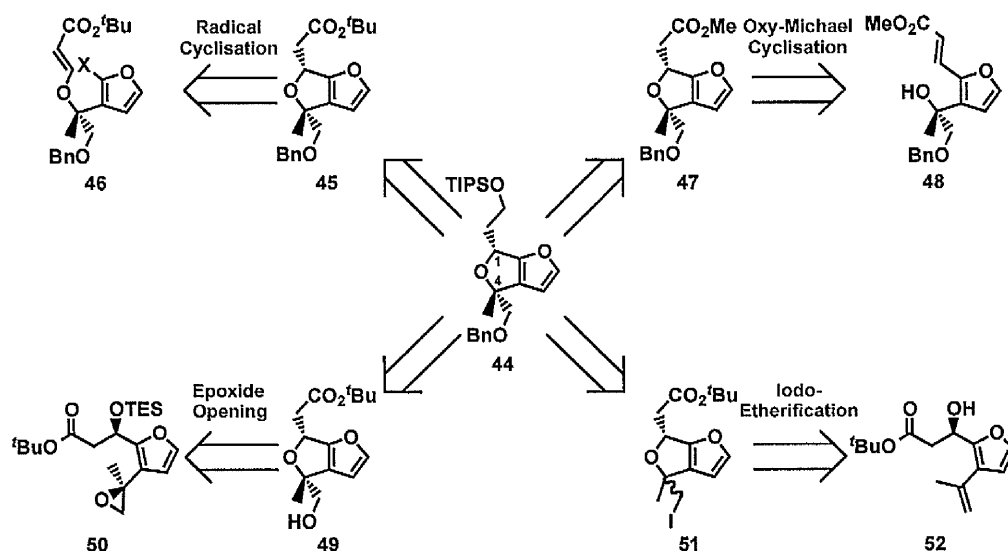
Scheme 3.8 Retrosynthetic Analysis for the Western Fragment.

of the challenging relative stereochemistry in the B ring. The initial strategy for the synthesis of the fully functionalised western fragment is based on the retrosynthetic analysis outlined in Scheme 3.8. The oxidation state adjustment in the bicyclic keto-ester derivative **39** led to the corresponding alcohol derivative **40**, which in turn could come *via* a Baylis-Hillman reaction of the cycloheptenone derivative **41** with formaldehyde.⁵ The bicyclic cycloheptenone **41** was envisaged to arise by an acid or base mediated β -elimination of the bridged C-O bond from the enolate generated after the regioselective deprotonation of the more sterically accessible α -methylene proton in ketone **42**. The tertiary alkoxide resulting from the oxabicyclic ring opening reaction would be protected as the TMS ether in either single-pot or as a two-step reaction sequence. Diastereoselective hydrogenation reaction was anticipated to occur from the less hindered α -face of **43** based on related procedures, to provide access to bicyclic ketone **42** with the requisite stereochemistry at C5.⁶ The key [4+3] cycloaddition of the three-carbon oxyallyl synthon, should be directed by the α -oriented alkyl chains of the 2,3-disubstituted furan derivative **44** to provide required stereochemistry for the cycloadduct **43**.⁷

3.2.2 Attempted Strategies Towards the Synthesis of 2,3-Disubstituted Furan Derivative **44**

The synthesis of 2,3-disubstituted furan derivative **44** required for the key cycloaddition reaction proved extremely challenging. As depicted in Scheme 3.9, four unsuccessful routes were investigated for the synthesis of the fragment **44**, which either furnished the desired product with poor diastereocontrol or failed to undergo cyclisation under the reaction conditions. However, a successful and efficient strategy towards the synthesis of **44** was subsequently realised (*vide infra*) and thus the routes illustrated in Scheme 9 towards **44** were not further investigated.

In the current section, results for the key cyclisation reactions will be summarised in order to highlight the challenges associated with the synthesis of the bicyclic furan derivative **44** (Scheme 3.9).



Scheme 3.9 Attempted Routes Towards the Synthesis of 2,3-Disubstituted Furan **44**.

Our initial strategy for the synthesis of bicyclic furan derivative **44** was based on the Paquette's study,¹ which involves intramolecular oxy-Michael cyclisation of **48** to furnish the 2,3-disubstituted bicyclic furan **47** (*vide supra*). Under thermodynamically-controlled reaction conditions, we anticipated that the 5-*exo-trig* oxy-Michael cyclisation of **48** would preferentially proceed *via* the favoured transition state **53**, which is devoid of A^{1,3}-type allylic strain to afford **47** with high diastereocontrol (Figure 3.1). In order to expeditiously

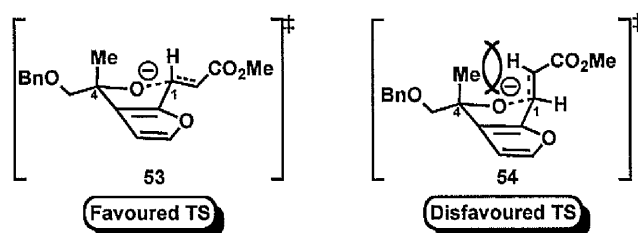
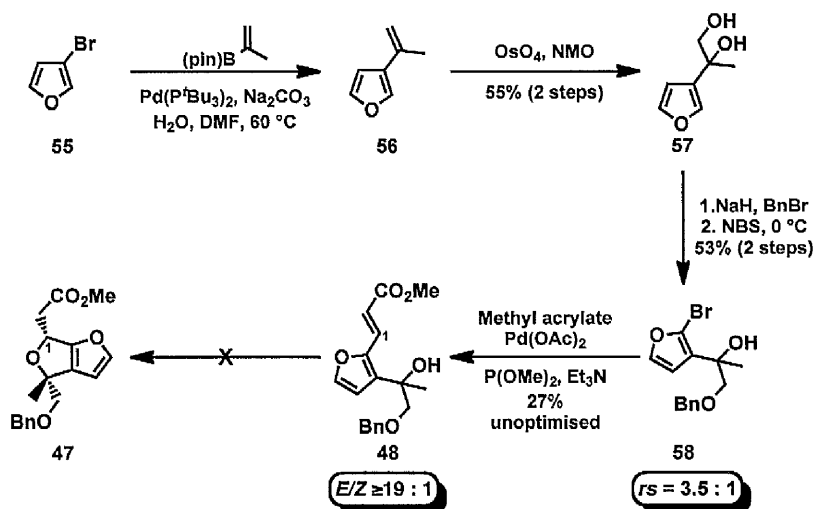


Figure 3.1 Transition States for Oxy-Michael Cyclisation of *Rac*-**48**.

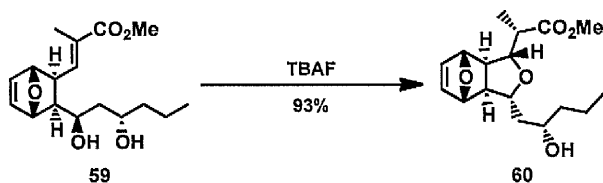
determine the feasibility of this strategy, the reaction was initially carried out with *rac*-**48**, which was prepared in 5 steps from the commercially available 3-bromo furan **55** (Scheme 3.10). The Suzuki-Miyaura cross-coupling reaction of **55** with isoprenyl pinacol boronic ester furnished the volatile isoprenyl furan **56**,⁸ which was subjected to the osmium-catalysed dihydroxylation to afford the diol **57** in 55% overall yield. Chemoselective benzylation of the primary alcohol in compound **57** under standard conditions provided the

hydroxy furan derivative, which was carried forward in the regioselective bromination reaction to afford 2-bromo furan **58** in 53% overall yield, with a poor regiocontrol of 3 : 1 (by ^1H NMR).⁹ The intermolecular Heck reaction of bromide **58** with methyl acrylate delivered the desired hydroxy- α,β -unsaturated ester **48** for the intramolecular conjugate addition reaction with excellent *E/Z* selectivity, albeit with low yield.¹⁰



Scheme 3.10 Attempted Intramolecular Oxy-Michael Cyclisation of **48**.

All attempts to form the oxygen-carbon (C1) bond in the presence of catalytic or excess amounts of standard bases either provided recovered starting material or facilitated an intermolecular *trans*-esterification reaction with KO^tBu . Even under forcing conditions, such as strong base (LiHMDS), polar solvents and at elevated temperature, the starting material remained unchanged. A possible reason for the failure to observe the desired cyclisation in **48** can be attributed to the extended conjugation of the double bond between the furyl ring and the ester functionality, which deactivates the Michael acceptor to the intramolecular 1,4-addition. Interestingly, there are examples for the oxy-Michael cyclisation reported for the synthesis of a similar 5,5-bicyclic framework that contains a hydroxyl tetrahydrofuranyl moiety bearing a vinylogous ester side chain (Scheme 3.11).¹¹



Scheme 3.11 Intramolecular Oxy-Michael Cyclisation of **59**.

Based on the studies in the area of intramolecular radical cyclisation developed within the group,¹² an alternate strategy was devised for the synthesis of bicyclic furan derivative **45** (Scheme 3.9). The transition states that were invoked for the oxy-Michael cyclisation reaction to predict the stereochemical outcome of the major isomer could also be

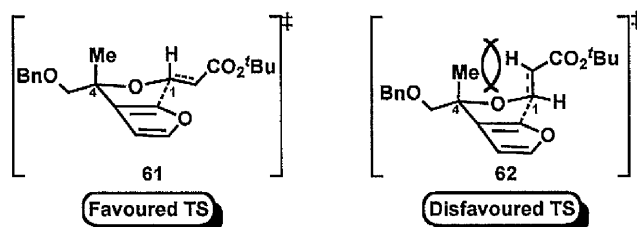
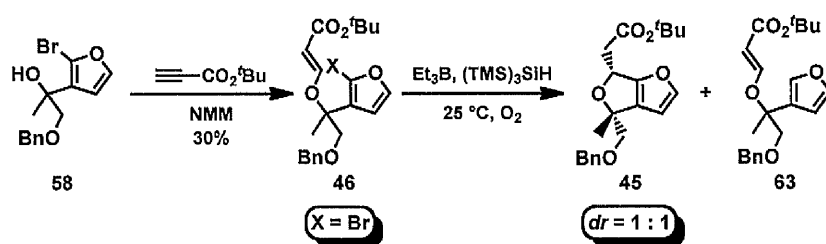


Figure 3.2 Transition States for the 5-*exo-trig* Radical Cyclisation of *Rac*-**46**.

extended to the 5-*exo-trig* radical cyclisation of *rac*-**46** with the caveat that the bond formation in this case is between the radical generated from the 2-bromo furan and C1 of the vinylogous ester side chain (Figure 3.2). Notably, a free energy difference of 0.27 kcal/mol was computed using the Spartan software between the *cis*- and the *trans*-isomer of **45**, which translates to very little difference in energy between the two isomers. However, since this is a kinetic process, there was envisioned to be significant difference in the two transition states.

The vinylogous carbonate **46** required for the radical cyclisation reaction was prepared using standard conditions employing *tert*-butyl propiolate and *N*-methyl morpholine (Scheme 3.12). Treatment of the *rac*-**46** with various radical reducing agents with triethylborane as radical initiator at room temperature, furnished a 1 : 1 mixture of *cis*- and *trans*-isomers of **45** along with significant amounts of inseparable non-cyclised reduced

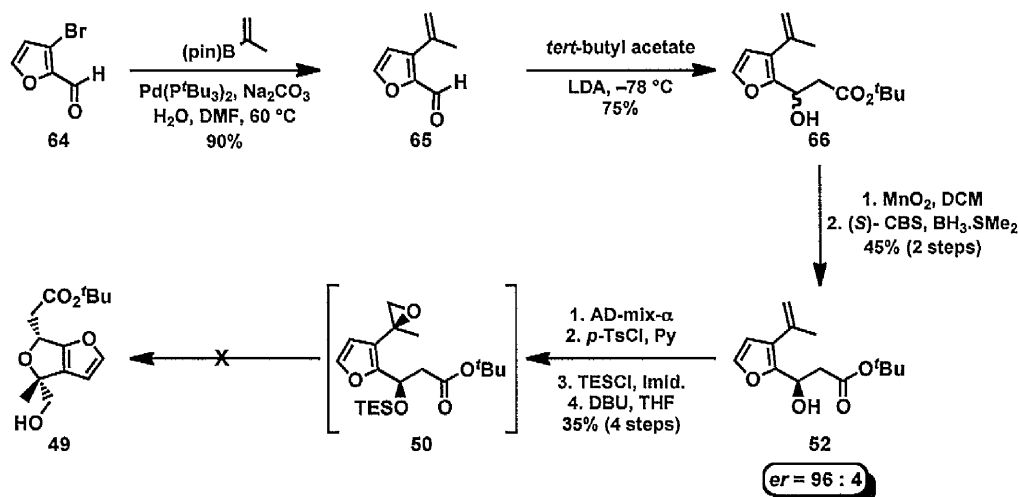
product **63**.¹² Despite undertaking extensive optimisation studies to improve the outcome of the reaction, the level of stereocontrol could not be improved, which is consistent with an early transition state that is more reactant than product-like.



Scheme 3.12 Intramolecular Radical Cyclisation of **46**.

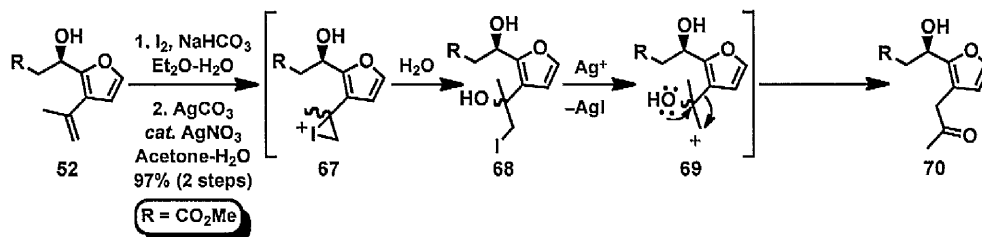
In light of the problem with the installation of the dihydrofuran ring, we elected to examine an intramolecular S_N2 -type epoxide opening reaction of epoxy furan **50** after unveiling the hydroxyl group at C4 to give **49** (Scheme 3.9). The synthesis of epoxy furan **50** required for this strategy is outlined in the Scheme 3.13. The Suzuki-Miyaura cross-coupling reaction of the known bromide **64** under the analogous reaction conditions of **55** (*vide supra*) afforded 3-isoprenyl-2-formyl furan **65** in excellent yield.⁸ The acetate-aldol reaction of the aldehyde **65** using *tert*-butyl acetate in conjunction with *in situ* formed lithium diisopropylamide furnished the racemic mixture of β -hydroxy ester **66** in 75% yield.¹³ While the task of oxidising the secondary furylic alcohol **66** was achieved in moderate yield using manganese dioxide, the CBS reduction of the corresponding ketone facilitated the formation of the enantioenriched hydroxyl centre in **52** in 45% overall yield and with 92% enantiomeric excess (by HPLC).¹⁴ Installation of the epoxy functional group in **50** turned out to be onerous since the direct stereoselective epoxidation of the 1,1-disubstituted alkenes was problematic. Hence, a 4-step sequence was employed for the synthesis of the requisite epoxide, which involved Sharpless dihydroxylation,¹⁵ chemoselective tosylation of the primary alcohol, selective silyl protection of the less hindered secondary alcohol and S_N2 -type ring closure of the tertiary alcohol to afford **50** as a single diastereoisomer (by ^1H NMR) in 35% overall yield. However, the epoxy furan **50** was

prone to decomposition during the chromatographic purification, which impeded scale-up. Nevertheless, small quantities of epoxy furan **50** could still be secured from each iteration to probe the critical epoxide-opening reaction. Several Lewis and protic acids were screened to affect the desired cyclisation, which either led to the extensive decomposition of the epoxide **50** or generated multiple side products in the reaction.



Scheme 3.13 Attempted Intramolecular Epoxide Opening Reaction of **50**.

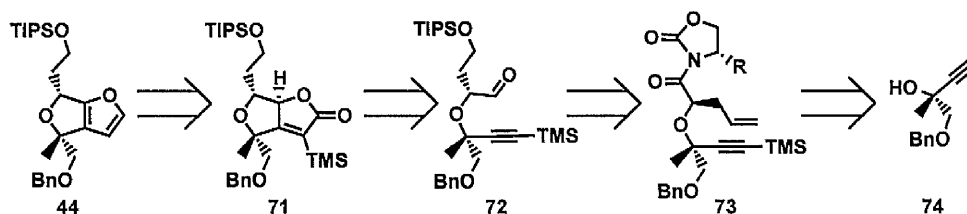
The instability of the epoxide **50** and the tosylated precursor prompted the examination of iodo-etherification reaction of the 1,1-disubstituted alkene **52**, which was expected to furnish the iodide **51** as a mixture of *cis*- and *trans*-isomers. Surprisingly, the iodonium ion **67** formed under the standard iodo-etherification conditions underwent intermolecular ring-opening reaction with water to furnish 1 : 1 mixture of **68** which rearranged to the undesired furyl ketone **70** in excellent yield presumably *via* intermediate **69** in the presence of silver salts (Scheme 3.14).



Scheme 3.14 Attempted Intramolecular Iodo-Etherification Reaction of **52**.

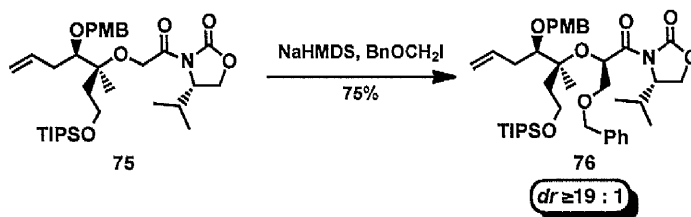
3.2.3 Revised Strategy Towards the Synthesis of 2,3-Disubstituted Furan 44

The problems with the stereoselective construction of 2,3-disubstituted furan derivative **44** using classical intramolecular cyclisation reactions prompted the investigation of a different strategy. We envisioned the formation of the furan ring after the installation of the dihydrofuran functionality, from the bicyclic butenolide **71**, which in principle could be transformed to the furan **44** by hydride reduction of the lactone in **71** followed by the



Scheme 3.15 Revised Route Towards 2,3-Disubstituted Furan Derivative **44**.

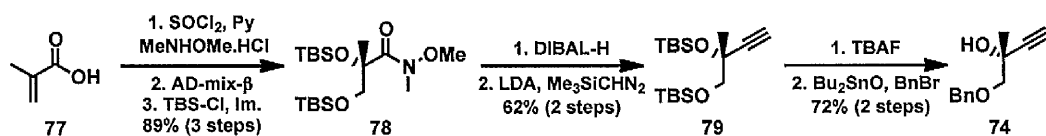
elimination of the resulting lactol (Scheme 3.15). Encouragingly, there are related examples, which sequentially employ DIBAL-H and protic acid for the construction of monocyclic and 5,6-bicyclic furan derivatives.¹⁶ This strategy would avoid the problematic 5-*exo* cyclisation strategy, since the bicyclic lactone **71** would arise from the hetero Pauson-Khand of the alkynyl aldehyde **72** with a molybdenum-carbonyl complex.¹⁷ The key ether bond in **72** would be derived from a simple alkylation followed by allylation in accord with the work of Crimmins using the Evans' chiral auxiliary (Scheme 3.16).¹⁸ The acyclic ether is then easily derived from the propargylic alcohol **74**, which can be prepared from the 1,2-enantiomerically enriched diol derivative in one step.¹⁹



Scheme 3.16 Crimmins Alkylation Reaction of **75**.

3.2.4 Synthesis of 2,3-Disubstituted Bicyclic Furan Derivative 44

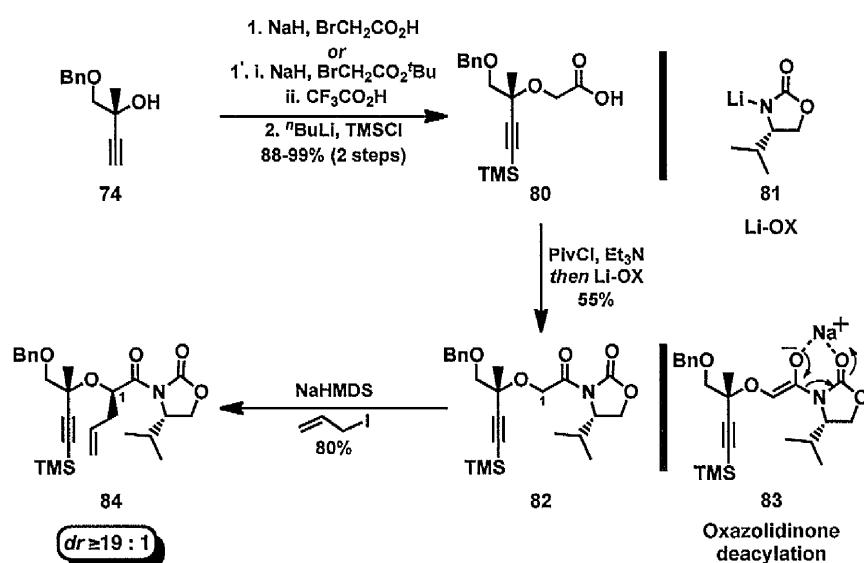
The multigram preparation of the enantiomerically pure propargylic alcohol **74** for the synthesis of 2,3-disubstituted furan **44** was achieved using a scalable sequence illustrated in Scheme 3.17.¹⁹ The synthesis commenced with a 3-step elaboration of commercially available methacrylic acid **77** to the Weinreb amide **78** in 89% overall yield, which involves acid chloride formation followed by conversion to the Weinreb amide and Sharpless asymmetric dihydroxylation of the 1,1-disubstituted alkene and subsequent protection of the resulting diol as the *bis*-silyl ether provided **78**. Since the Sharpless asymmetric reaction was known to provide the requisite diol with excellent enantioselectivity,¹⁹ we decided to determine the enantiomeric excess of the reaction at a later stage upon introduction of the chiral auxiliary for the Crimmins' alkylation reaction (*vide infra*). Reduction of the amide **78** using DIBAL-H furnished the corresponding aldehyde, which was subsequently subjected to



Scheme 3.17 Synthesis of Alkynyl Alcohol Derivative **74**.

one-carbon homologation with the anion derived from trimethylsilyldiazomethane to provide the terminal alkyne **79** in 62% overall yield.² Fluoride-mediated deprotection of the *bis*-silyl ether **79** delivered the known diol,¹⁹ which was chemoselectively benzylated to afford the hydroxyl benzyl ether **74** in 72% overall yield.²⁰ The selective protection deserves a special mention since the chemoselective benzylation reaction of primary versus tertiary alcohol was problematic using sodium hydride and benzyl bromide. This reaction furnished mono- and dibenzylated compounds along with the recovered starting material, whereas, preforming the 1,2-stannylidene with dibutyltin oxide by the azeotropic removal of water followed by addition of the requisite electrophile led to the selective alkylation of the primary alcohol ($\geq 19 : 1$ by ^1H NMR).

Having successfully completed the construction of the alkyne **74**, the tertiary alcohol was alkylated using sodium hydride and excess bromoacetic acid to afford the desired alkynyl carboxylic acid derivative which was silylated with *n*-butyllithium and TMS-Cl in 88-99% yield (Scheme 3.18).¹⁸ Attempted allylation of the **82** after the installation of the auxiliary provided the allyl derivative in excellent yield and selectivity. However, the silyl protection was not reproducible on a multigram scale due to the contamination of the alkylated product with excess bromoacetic acid that was inseparable from the carboxylic acid derivative. Hence a two-step procedure was devised for the large-scale synthesis of **80**,

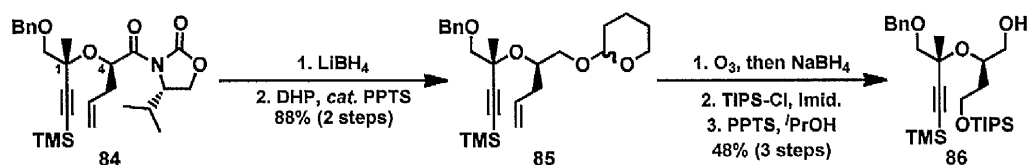


Scheme 3.18 Synthesis of Glycolate **84**.

which involved the initial alkylation reaction with *tert*-butylbromoacetic ester followed by TFA promoted ester hydrolysis. The *N*-acylation of the Evans' chiral auxiliary was achieved in 55% yield, by the treatment of lithiated oxazolidinone **81** with the mixed anhydride generated *in situ* from the acid **80** using pivaloyl chloride ($\geq 19 : 1$ by ^1H NMR). The C1 stereogenic centre in the western fragment was installed with complete diastereocontrol through a β -face selective alkylation of the sodium enolate **83** with allyl iodide to furnish allyl derivative **84** in 80% yield.¹⁸ The reaction is dependent on the order of addition of sodium amide base, in addition to the time allowed for enolisation. For instance, the optimal

conditions involved the addition of a solution of **82** to NaHMDS followed by the addition of allyl iodide, which was freshly purified with neutral alumina. If the enolate was allowed to form over extended periods, large amounts of free oxazolidinone were formed, presumably from the deacylation of enolate **83**.

The remaining sequence prior to the pivotal hetero PK reaction involved oxidation state adjustment of the amide and the alkene at C4 (Scheme 3.19). The reductive removal of the chiral auxiliary in **84** was accomplished with LiBH₄ and the resulting primary alcohol was protected as the tetrahydropyranyl ether **85** in 88% overall yield. The diastereomeric mixture of THP epimers (1 : 1) were not fully characterised, due to the difficulty in their separation. Nonetheless, the newly formed functional groups in the following reactions were easily detected by the characteristic signal in the ¹H NMR and IR spectra and hence, these

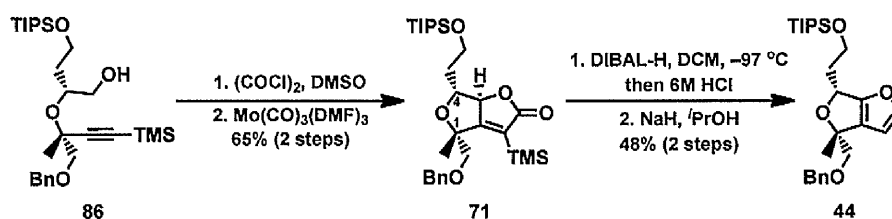


Scheme 3.19 Elaboration of Enyne **84** to Alcohol **86**.

intermediates were taken forward in the synthesis without further analysis. Chemoselective ozonolysis of the terminal alkene **85** followed by a reductive work-up using NaBH₄ furnished the primary alcohol, which was converted to the corresponding triisopropylsilyl ether under standard conditions. This was followed by the cleavage of the THP protecting group using a combination of PPTS and 2-propanol to unveil the hydroxymethylene derivative **86** as a single diastereoisomer in 48% overall yield.

Oxidation of the primary alcohol **86** using Swern conditions provided the aldehyde, which was used in the key cyclocarbonylation reaction without purification to minimise epimerisation (Scheme 3.20). Treatment of the aldehyde with freshly prepared Mo(CO)₃(DMF)₃ furnished the bicyclic butenolide **71** in 65% overall yield as a single *exo*-diastereoisomer.¹⁷ The stereochemical assignments in the tetrahydrofurnyl ring of the

bicyclic lactone **71** were corroborated using the nOe enhancement of C3 methyl group upon irradiating the proton at C4 (Appendix 3.8.1). Although the exact mechanism of this remarkable transformation has not yet been reported, the initial step is believed to be the displacement of the labile DMF ligands on the molybdenum complex by the alkynyl aldehyde.²¹ The resulting organomolybdenum species is speculated to undergo oxidative cyclisation, migratory insertion of CO followed by reductive elimination in a similar manner to related transition-metal mediated PK reactions to furnish the bicyclic butenolide.



Scheme 3.20 *Synthesis of 2,3-Disubstituted Furan 44.*

Having accomplished the synthesis of the bicyclic lactone **71**, we turned our attention towards the conversion of lactone to bicyclic furan derivative **44**. After examining several reaction conditions, sequential hydride reduction at $-97\text{ }^{\circ}\text{C}$ followed by the elimination of the resulting lactol using hydrochloric acid, afforded the desired bicyclic 2,3,4-trisubstituted furan derivative in 72% overall yield.¹⁶ The reaction temperature and solvent were critical parameters for the overall success of the reaction, since the hydride reduction at $-78\text{ }^{\circ}\text{C}$ afforded the undesired 1,2-diol as a result of over reduction of the lactone **71**. Exhaustive efforts to convert the 1,2-diol to the furan **44** through the selective oxidation of the diol to the hydroxy aldehyde led to the decomposition of the aldehyde. Interestingly, a similar transformation has been reported for the construction of the homologous 6,5-bicyclic furan derivative.²² Although the hydride reduction also worked efficiently in THF, the acid-mediated elimination of the lactol led to concomitant deprotection of the primary triisopropylsilyl protecting group. Since dichloromethane and water are not miscible, the lactol elimination is presumed to proceed cleanly to the bicyclic furan **44** without

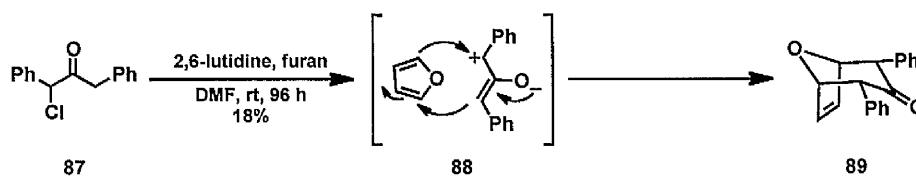
desilylation. Gratifyingly, the challenging 2,3-disubstituted furan **44** was prepared in 48% overall yield after chemoselective C-Si deprotection in the 2,3,4-trisubstituted furan derivative using freshly prepared sodium isopropoxide.

In this section, we have described our efforts for the synthesis of 2,3-disubstituted furan **44** required for the key [4+3] cycloaddition reaction. A brief coverage of the [4+3] cycloaddition reaction will be given in the following section.

3.3 An Overview on Diastereoselective [4+3] Cycloaddition Reactions of Furans for the Synthesis of 8-Oxabicycles

Cycloaddition reactions represent a powerful method for the convergent and stereoselective synthesis of medium-sized carbocycles. While 1,3-dipolar and Diels-Alder cycloaddition reactions have been traditionally employed in the preparation of five- and six-membered rings, respectively, the higher order [4+3] variant has emerged as a powerful tool in the straightforward construction of seven-membered carbocycles that are commonly found in many classes of biologically active natural products.

The [4+3] cycloaddition is electronically homologous to the Diels-Alder reaction. The reaction can formally be deemed as a cycloaddition of a $2\pi(3C)$ allyl cation across a $4\pi(4C)$ diene component in a concerted or step-wise manner depending upon the nature of reacting diene and dienophile. Since the first reported trapping of oxyallyl cation derived from chloroketone **87** by furan in 1962 by Fort (Scheme 3.21),²³ the reaction has undergone



Scheme 3.21 [4+3] Cycloaddition Reaction of Chloroketone **87**.

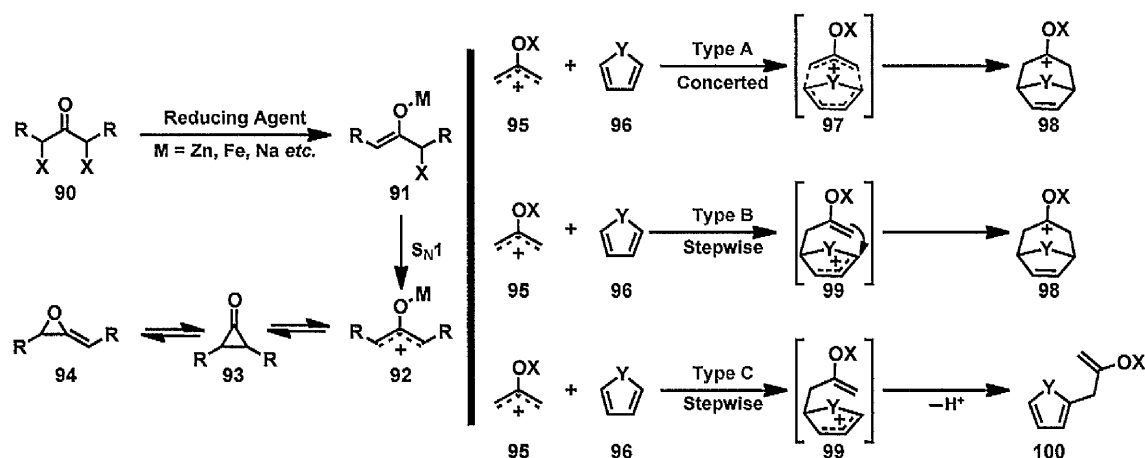
tremendous advancements over the past five decades in a quest to improve the overall efficiency of this important transformation. This section provides a brief overview on the diastereoselective intermolecular cycloaddition of furans (4C) with oxyallyl cations and other closely related $2\pi(3C)$ reactants for the synthesis of oxabicycles.²⁴ The survey will also

highlight the utility of this methodology in the context of its application to the total synthesis of complex natural products.

3.3.1 Oxyallyl Cations Generated from the Reduction of Polyhalogenated Ketones

Following the initial work of Fort and later by Cookson in the area of [4+3] cycloaddition reactions,^{23,25} Hoffmann undertook an exhaustive study to demonstrate that α, α' -dihaloketones provide a convenient *in situ* route to 2-oxyallyl cations.^{24l,o} The reaction involves a two-electron reduction of the dihalogenated ketone **90** by a low valent metal followed by an S_N1-type ionisation of the halide from the resulting metal enolate **91** to generate oxyallyl cation **92** (Scheme 3.22). The oxyallyl species **92** is considered to be labile in its zwitterionic form and is thought to convert to the less reactive isomers **93** and **94** unless it is trapped with a suitable diene or solvent. However, the electrophilic character of the oxyallyl cation can be further enhanced either by increasing the covalent character of the metal-oxygen bond in **92** or *via* cation stabilisation using electron-donating substituents. Hence, the efficiency of a substrate and the mechanism of any particular [4+3] cycloaddition depends on, (i) the nature of the enolate formed in the reaction, (ii) the nucleophilicity of diene, (iii) the electronic property of a substituent on the oxyallyl species, and, (iv) the reaction solvent.^{24f} As outlined in Scheme 3.22, Hoffmann classified the intermolecular [4+3] cycloaddition with dihaloketone into three categories to explain the results with different substrates. Concerted cycloaddition reactions are categorised as Type A. These reactions tend to deliver superior results with electron-rich dienes that undergo electrophilic substitution reaction in the presence of highly reactive oxyallyl cations. Typical conditions for Type A reaction involve NaI in conjunction with stoichiometric copper, which is believed to generate less electrophilic sodium-enolate **97** (X = Na). This is therefore likely to proceed *via* a concerted mechanism due to lower charge build-up in the oxyallyl moiety (Scheme 3.22). Type B and Type C reactions follow a stepwise mechanism due to the high ionic character of the oxyallyls, which leads to a common intermediate **99**. The Fe₂(CO)₉

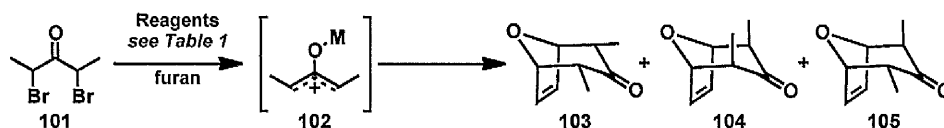
promoted cycloaddition with dibromoketones developed by Noyori, provides a good example of a Type B reaction. The iron-oxyallyls derived in this reaction are more electrophilic than the corresponding zinc or sodium enolate, which can be attributed to the



Scheme 3.22 Types of [4+3] Cycloaddition Reactions.

greater covalent character of iron-oxygen bond to promote the reaction with poorly nucleophilic dienes in a stepwise manner. The second step in Type B reactions gives rise to the desired cycloadduct **98** whereas Type C reactions are favoured with electron-rich dienes that involve the loss of a proton in the second step to furnish **100**, which is an electrophilic substitution reaction.

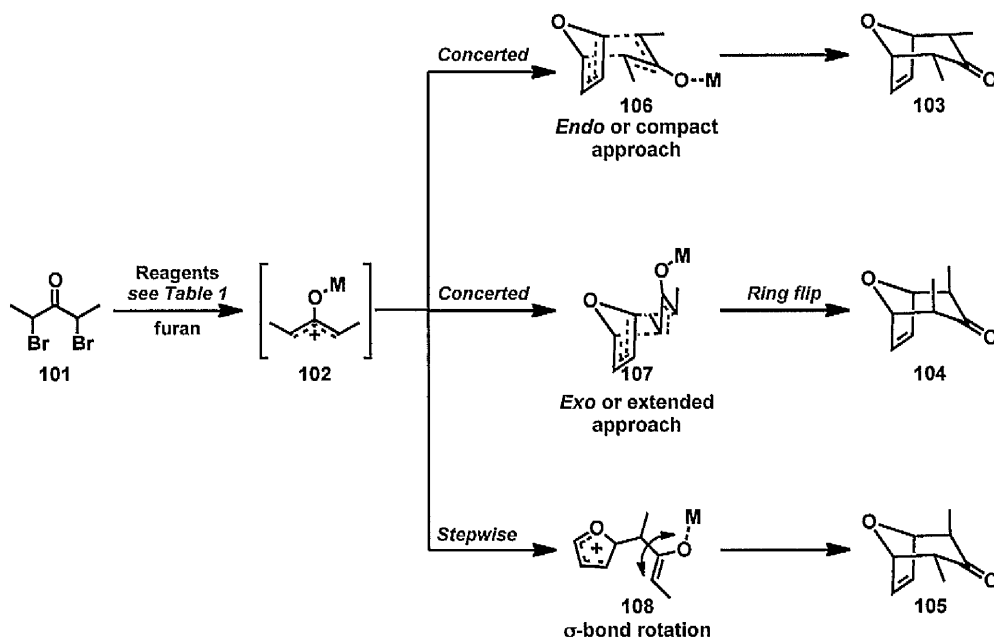
In an analogous manner to the way the course of the [4+3] cycloaddition reaction can be altered based on the reductant, the stereochemical outcome can also be manipulated through the judicious choice of reagents.^{24k} As tabulated in Table 3.1, the cycloaddition



Entry	Reagents	Yield	103 : 104 : 105
1	NaI, Cu	80	95 : 05 : 00
2	Zn-Cu	85	81 : 10 : 09
3	Fe ₂ (CO) ₉	90	44 : 00 : 56

Table 3.1 Reagent Controlled [4+3] Cycloaddition Reaction.

reaction of sodium oxyallyl **102** ($M = \text{Na}$) derived from 2,4-dibromopentanone **101** furnished cycloadducts **103**, **104** and **105** in a diastereomeric ratio of 95 : 5 : 0 (Table 3.1, Entry 1), whereas the zinc oxyallyl **102** ($M = \text{Zn}$) and iron oxyallyl **102** ($M = \text{Fe}$) provided the cycloadducts **103**, **104** and **105** with reduced and somewhat complementary selectivity (81 : 10 : 9 and 44 : 0 : 56) (Table 3.1, Entries 2 and 3). Hoffmann proposed that the metal

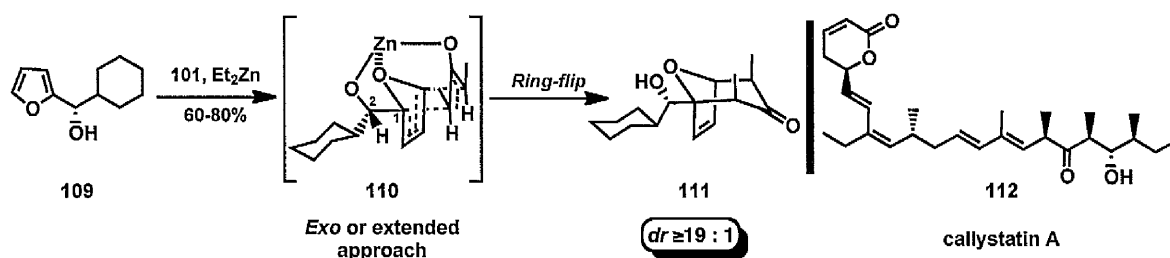


Scheme 3.23 Proposed Models for the [4+3] Cycloaddition Reaction.

bound oxyallyl cation **102** formed after the reduction of **101** adopts a more stable W-configuration as shown in Scheme 3.23. In the concerted pathway, the reaction proceeds either *via* an *endo* (compact) **106** or an *exo* (extended) **107** transition state leading to products **103** and **104** respectively. In the scenario of a stepwise mechanism as in the reaction using $\text{Fe}_2(\text{CO})_9$, **105** is formed from the loss of stereochemical integrity of the dienophile, due to the carbon–carbon bond rotation in **108**. It is also worth noting that the diastereoselectivity in the concerted mechanism favours the formation of *endo*- over the *exo*-isomer, presumably due to the secondary orbital interactions, a phenomenon also observed in the homologous [4+2] Diels-Alder reaction.

Complementary to the *endo*-selectivity observed in the concerted [4+3] cycloaddition reactions of furans, Lautens and co-workers reported an intermolecular [4+3] cycloaddition

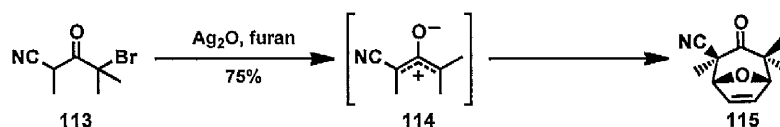
between the 2-hydroxyfuryl derivative **109** and dibromoketone **101** in the presence of diethylzinc to provide a chelate and furnish the *exo*-cycloadduct **111** with high levels of diastereoselectivity (Scheme 3.24).^{26a} The unusual facial selectivity was rationalised using the transition state **110**, wherein the zinc alkoxide formed after the deprotonation of furyl alcohol **109** by diethylzinc, chelates with the W-shaped oxyallyl cation, thereby restricting free rotation around the C1-C2 bond. In the subsequent step, the intramolecular



Scheme 3.24 Diastereoselective [4+3] Cycloaddition Reaction of **109**.

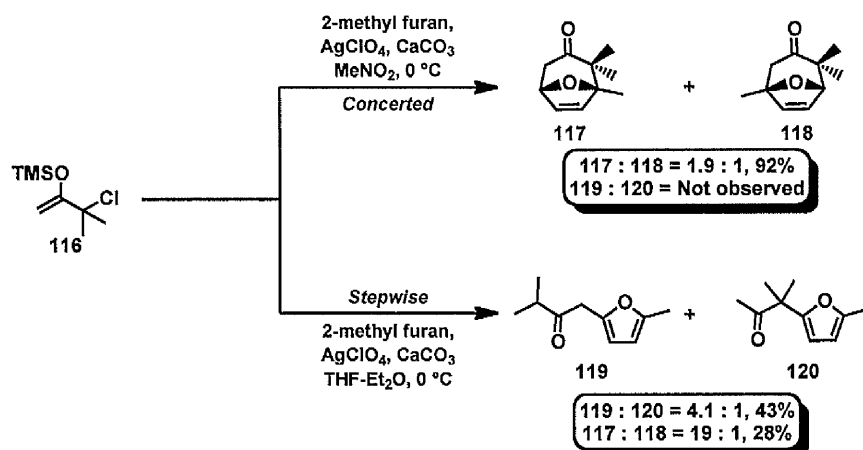
cycloaddition occurs from the opposite side of the bulky cyclohexyl group *via* an extended transition state to generate the boat conformer, which spontaneously undergoes ring-flip to the chair **111** with *syn*-diaxial methyl substituents. Ring-opening of oxabicyclo **111** provides the polypropionate unit in callystatin A **112**.^{26b}

In a related study, Mann demonstrated that oxyallyl cations could be derived from α -bromoketones under basic conditions by employing a silver salt with triethylamine.²⁷ Fohlisch *et. al.* later showed that treatment of more acidic bromo oxonitrile **113** with silver oxide provided the cycloadduct **115** in satisfactory yield, albeit the reaction was rather limited in scope (Scheme 3.25).²⁸



Scheme 3.25 [4+3] Cycloaddition Reaction of Bromo Oxonitrile **113**.

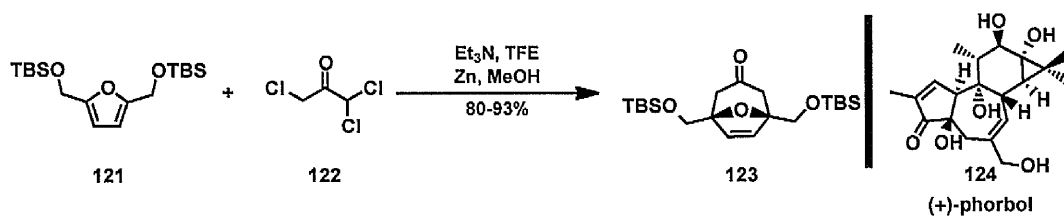
Halogenated silyl enol ethers also provide suitable precursors to the oxyallyl cation. Shimizu and co-workers reported the [4+3] cycloaddition reaction using a silver salt to initiate the formation of a dienophile from the TMS enol ether **116** (Scheme 3.26).²⁹ This study demonstrated that the outcome of the [4+3] cycloaddition reaction is dependent on the nature of the solvent. For example, polar solvents such as nitromethane afford regioisomeric mixture of cycloadducts **117** and **118** in excellent yield, whereas ethereal solvents furnish the electrophilic substitution products **119** and **120** in 42% yield, along with



Scheme 3.26 Solvent Effect in the [4+3] Cycloaddition Reaction of **116**.

the desired oxabicycles **117** and **118** in low yield, but with excellent regioselectivity (Scheme 3.26). The divergent reaction course of **116** is consistent with a concerted pathway (Type A) in polar solvent and a stepwise mechanism (Type C) in a less polar solvent.

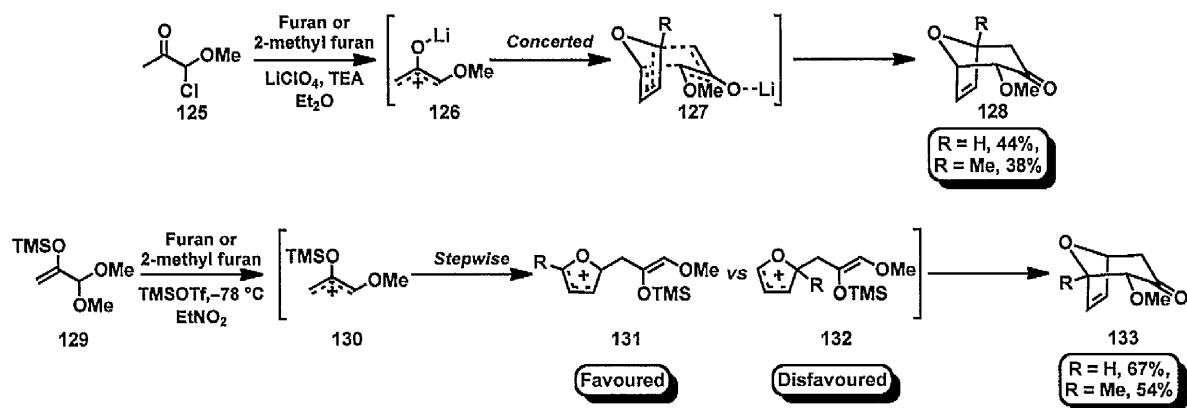
Fohlisch demonstrated a particularly facile method for generating oxyallyl cations from 1,1,3-trichloroacetone and 1,1,3,3-tetrachloroacetone using either triethylamine or NaTFE.^{6,30} Reduction of chlorinated cycloadduct using activated zinc provides the requisite cycloadduct **123** in excellent yield. This method works efficiently on multigram scale and was utilised in the total synthesis of (+)-phorbol **124** by Cha group and co-workers (Scheme 3.27).³¹



Scheme 3.27 [4+3] Cycloaddition Reaction of **121** With TCA **122** in TFE.

3.3.2 [4+3] Cycloadditions of Oxygen-Stabilised Oxyallyl Cations

Fohlisch and co-workers were also the first to demonstrate the utility of α -alkoxy substituted oxyallyl cations in the stereoselective construction of 8-oxabicycles,³² as outlined in Scheme 3.28. Treatment of the α -chloromethoxy ketone **125** with lithium perchlorate and furan provided access to cycloadduct **128** (R = H) with $\geq 19 : 1$ diastereoselectivity. Unsymmetrical dienes, such as 2-methylfuran, also delivered the corresponding cycloheptenone derivative **128** (R = Me) with excellent regio- and diastereoselectivity, albeit in low overall yield.

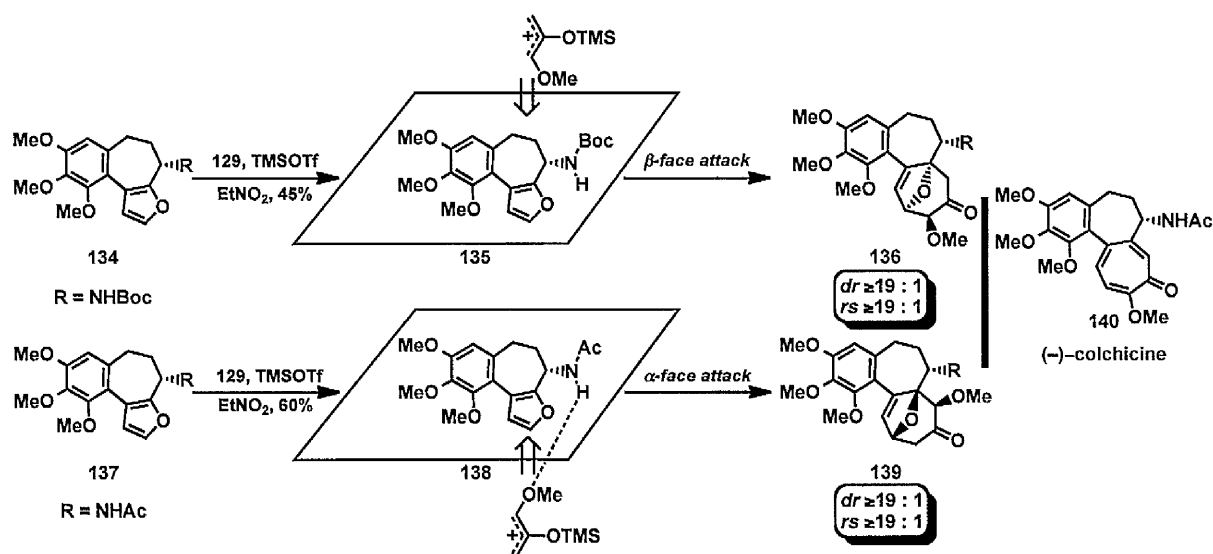


Scheme 3.28 Base and Lewis Acid mediated [4+3] Cycloaddition Reactions.

In a related study, Albizati reported the formation of trialkylsilyloxy cations from the nonhalogenated precursor **129** using Lewis acid, which undergoes a regio- and diastereoselective cycloaddition with furan and 2-methyl furan in moderate to good yield (Scheme 3.28).³³ Interestingly, the regiochemical outcome in the reaction with 2-methyl furan was divergent to that of Fohlisch's reaction (*vide supra*). Hence, the formation of 2,3- and 2,5-disubstituted cycloadducts can be controlled using either acid or base. These results

suggest that the initially formed lithium oxyallyl species **126** engaged the furan derivative selectively from the least hindered sites leading to the cycloadduct **128**. In contrast, the more electrophilic trimethylsilyloxy oxyallyl cation **130** participates in a stepwise cycloaddition with electron-rich furans to furnish the 2,3-disubstituted cycloadduct **133** through a favoured cationic intermediate **131** that is stabilised by the electron-donating methyl substituent.^{24a}

The applicability of this strategy for the regioselective synthesis of functionalised oxabicycles was nicely illustrated in the total synthesis of (–)-colchicine **140**.^{7b-d} As depicted in Scheme 3.29, the [4+3] cycloaddition reaction between the tricyclic furan **137** and oxyallyl cation generated from the silyl enol derivative **129** provided the undesired *exo*-adduct **139** as a single compound in 60% yield. The stereochemical outcome was ascribed to a possible hydrogen bonding interaction between the acetamide N-H proton and the

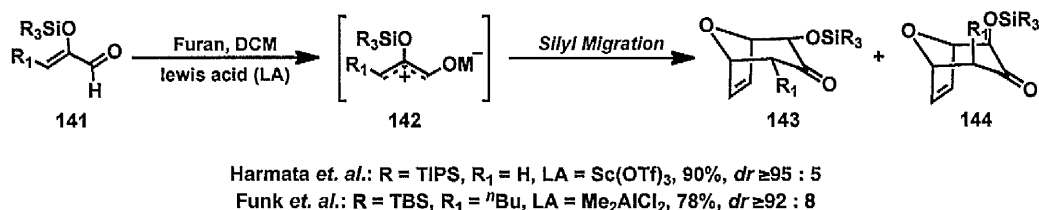


Scheme 3.29 [4+3] Cycloaddition in the Synthesis of (–)-Colchicine **140**.

methoxy moiety of the oxyallyl species. Interestingly, the *N*-methyl derivative was completely unreactive under analogous reaction conditions, whereas the *N*-Boc delivered the desired *endo*-cycloadduct **136** in excellent regio- and diastereoselectivity resulting from the addition of W-shaped oxyallyl species from the less hindered β -face of the furan **135**. This subtle difference was attributed to the *N*-Boc derivative being a weaker hydrogen donor. In the context of our synthetic approach for the western fragment of Lancifodilactone **1**, the

α -oriented alkyl side chains in the bicyclic furan derivative **44** was anticipated to exert a similar directing influence on the incoming oxyallyl cation, which could favour the formation of the oxabicycle **43** with high diastereocontrol.

In 1982, Sasaki reported an alternative method for generating the oxyallyl species **142** from silyloxy acrolein **141**.^{34d} Harmata^{34c} and Funk^{34b} independently disclosed the [4+3] cycloaddition of this silyloxy acrolein derivative **141** with furan, which furnished improved yield and diastereoselectivity for the construction of 8-oxabicycles (Scheme 3.30).

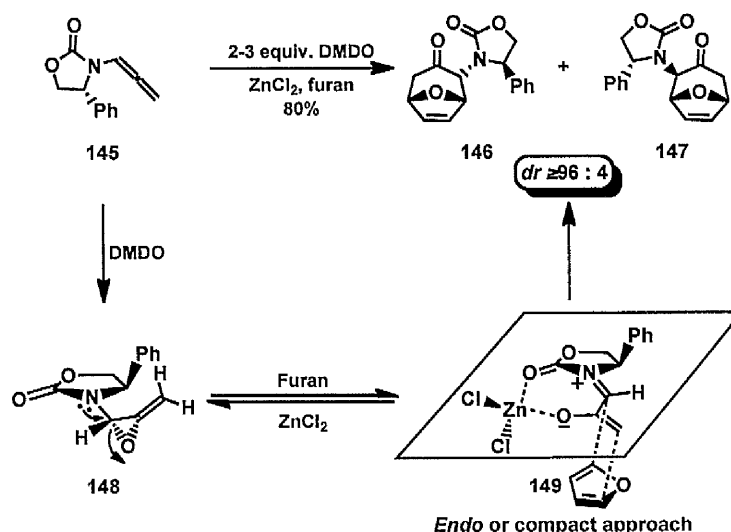


Scheme 3.30 [4+3] Cycloaddition of Silyloxy Acrolein **141**.

The reaction warrants further investigation since studies by Davies group indicates that the cycloadduct **143** could also arise from an acid catalysed tandem Diels-Alder/ring expansion reaction of **141** with furan.^{34a}

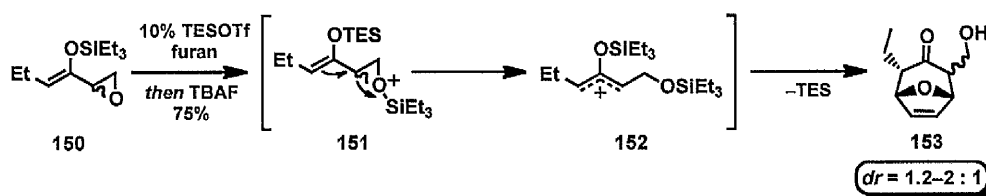
3.3.3 [4+3] Cycloadditions of Oxyallyl Cations Derived From Epoxides

Hsung and co-workers first described the [4+3] cycloaddition reaction of nitrogen stabilised oxyallyl cation **149** with furan to furnish the *endo*-cycloadduct **146** with excellent diastereoselectivity (Scheme 3.31).³⁵ The zwitterionic intermediate **149** was generated in the reaction *via* epoxidation of the allenamide **145** using DMDO to form allene oxide **148**, which affords the conformationally rigid oxyallyl zinc chelate **149** in the presence of ZnCl₂. The chiral environment provided by the oxazolidinone in **149** directs the attack of the diene from the less hindered β -face. The utility of this methodology was highlighted by the formation of enantiomerically pure 1,2-amino alcohols *via* the reduction of cycloadduct **146** in three steps.³⁵ However, the limited scope with respect to the diene component and the necessity for a ten-fold excess of furan limits any applications to the natural product synthesis.



Scheme 3.31 [4+3] Cycloaddition of Amidoallene **145**.

In a related study, Chiu *et. al.* used epoxy enol triethylsilanes **150** as the oxyallyl cation precursor for the intermolecular [4+3] cycloaddition reaction with the unsubstituted



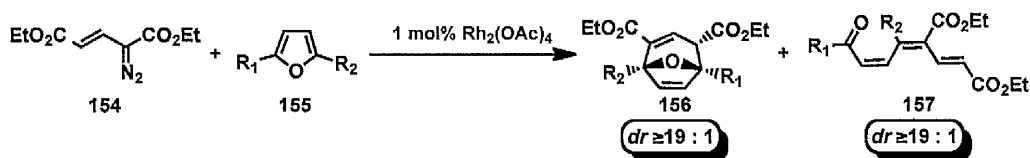
Scheme 3.32 [4+3] Cycloaddition of Epoxy Enolsilane **150** and Furan.

furan.³⁶ As shown in Scheme 3.32, the TES protected oxyallylic species **152** was generated on exposure of oxirane **150** to catalytic TESOTf to afford the desired oxabicyclic **153** epimeric at the hydroxymethylene group. Gratifyingly, the intramolecular variant of this reaction provides improved diastereocontrol and substrate scope.²⁷

3.3.4 Rhodium(II)-Catalysed [4+3] Cycloadditions of VinylCarbenoids

In 1985, Davies and co-workers demonstrated the first example of a rhodium(II)-stabilised vinylcarbenoid, which was formed from the vinyl diazomethane **154**, to undergo a stereospecific [4+3] cycloaddition with furan to furnish functionalised *endo*-cycloadduct **156**.^{37a,b} The reaction also generated the undesired triene **157** with high levels of stereospecificity depending on the nature of the furan **155** (Table 3.2). The *endo*-

stereospecificity for the cycloadduct **156** was initially attributed to transition state outlined by Hoffmann for the oxyallyl cycloaddition reaction (Scheme 3.33).^{37a} Hence, the

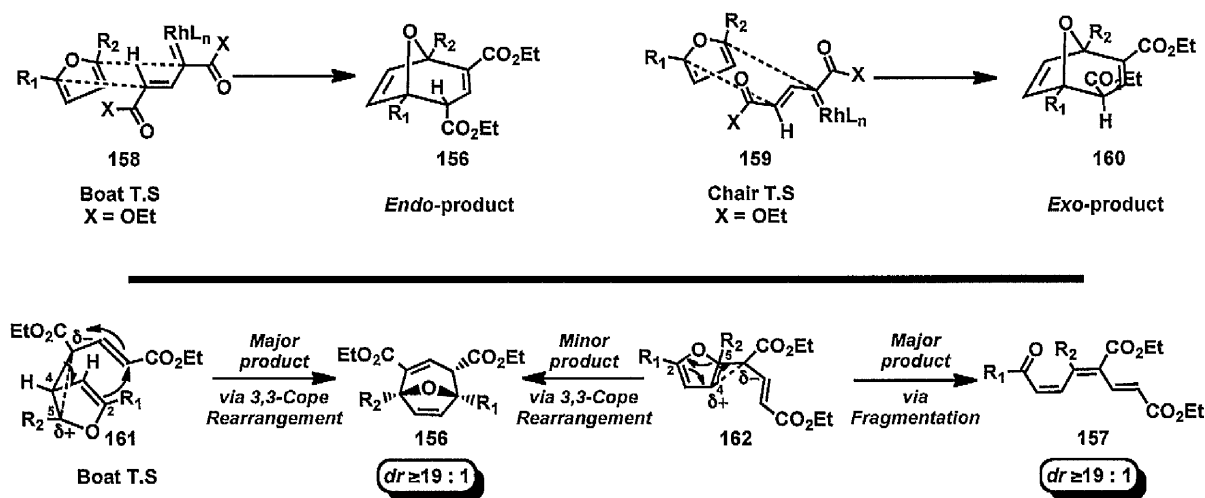


Entry	R_1	R_2	Yield (%)	
			156	157
1	H	H	62	26
2	Me	H	8	74
3	OMe	H	0	92
4	Me	Me	74	0

Table 3.2 [4+3] Cycloaddition between Furan Derivative and Vinyl diazomethane.

reaction between the rhodium carbenoid and **155** was suggested to proceed *via* concerted mechanism, which favoured the boat-like transition state **158** over the chair **159** due to stabilising secondary orbital interactions (Scheme 3.33). However, this did not fully explain the stereospecificity and the product distribution in the reaction with various furan derivatives (Table 3.2, Entry 1-4). Consequently, an alternative mechanism involving a tandem cyclopropanation of furan followed by a [3,3]-Cope rearrangement of the resulting *cis*-divinylcyclopropane **161** was proposed to explain the diastereoselective formation of cycloadduct **156** (Scheme 3.33).³⁸ The excellent diastereocontrol observed in the [4+3] cycloaddition reaction is attributed to a highly stereoselective cyclopropanation process leading to *cis*-divinylcyclopropane **161** (*vide infra*), which then undergoes the Cope rearrangement *via* a stereodefined boat-type transition state to furnish **156**. The triene formation can also be readily rationalised considering the substitution pattern on furan derivatives. The initial cyclopropanation step can give rise to two dipolar intermediates **161** or **162** depending on the site of attack of rhodium-bound vinylcarbenoid on the substituted furan. Generally, furans with electron-donating groups at the 2-position favour attack of the metal-stabilised vinylcarbenoid at 5-position, which stabilises the developing positive

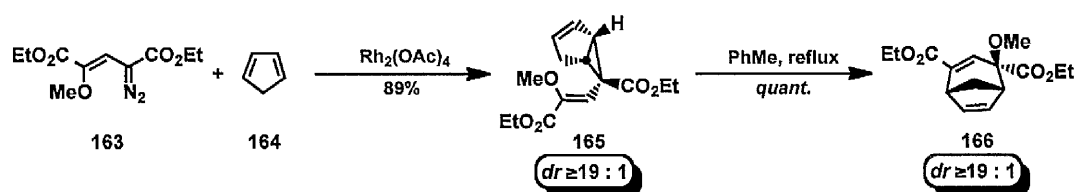
charge at the 4-position. This in turn makes the furyl cyclopropane derivative **162** prone to ring-opening resulting in the stereospecific formation of triene **157** in competition with the



Scheme 3.33 Mechanisms for Rh(II)-Catalysed [4+3] Cycloaddition of Vinylcarbenoid.

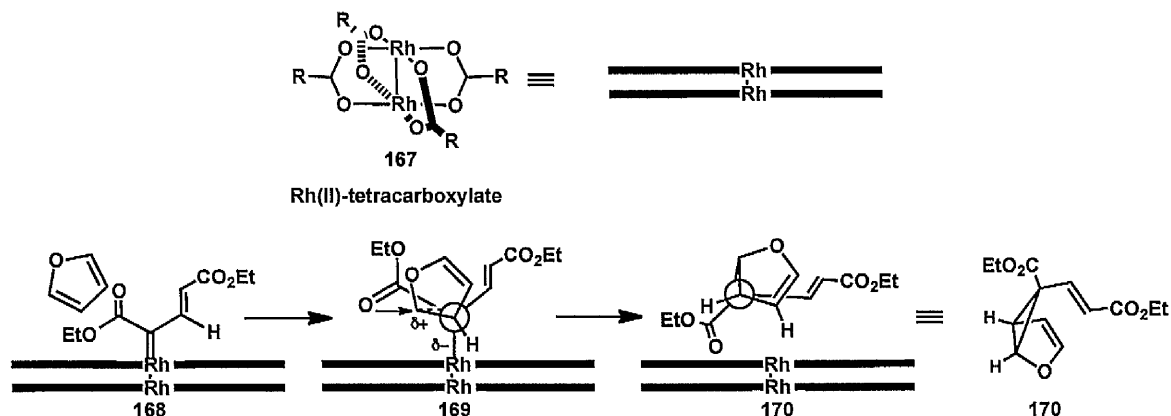
divinylcyclopropane rearrangement to afford **156** (Table 3.2, Entry 1 vs 2-3). In contrast, the undesired reaction pathway is suppressed when the bond formation at the 4-position is more advanced as in **161**, which favours the Cope rearrangement to the desired cycloadduct **156**. This mode of attack is thought to explain the result with 2,5-dimethyl furan, since the initial attack of vinylcarbenoid is likely to occur from the less hindered 4-position (Table 3.2, Entry 4) followed by a concerted nonsynchronous cyclopropanation to provide the cycloadduct **156** via the zwitterionic transition state **161** ($R_1 = R_2 = \text{Me}$).³⁸

The proposed mechanism of tandem cyclopropanation-Cope-rearrangement for the rhodium(II)-catalysed [4+3] cycloaddition of vinyl diazomethane and diene was further supported by the isolation of the sterically congested *cis*-divinyl derivative **165** which is resistant to rearrangement at ambient temperature. Nevertheless, prolonged heating of **165** in boiling toluene furnished the desired cycloadduct **166** as a single diastereoisomer in quantitative yield (Scheme 3.34).³⁹



Scheme 3.34 [4+3] Cycloaddition of Vinyl diazocarbene **163** and Cyclopentadiene **164**.

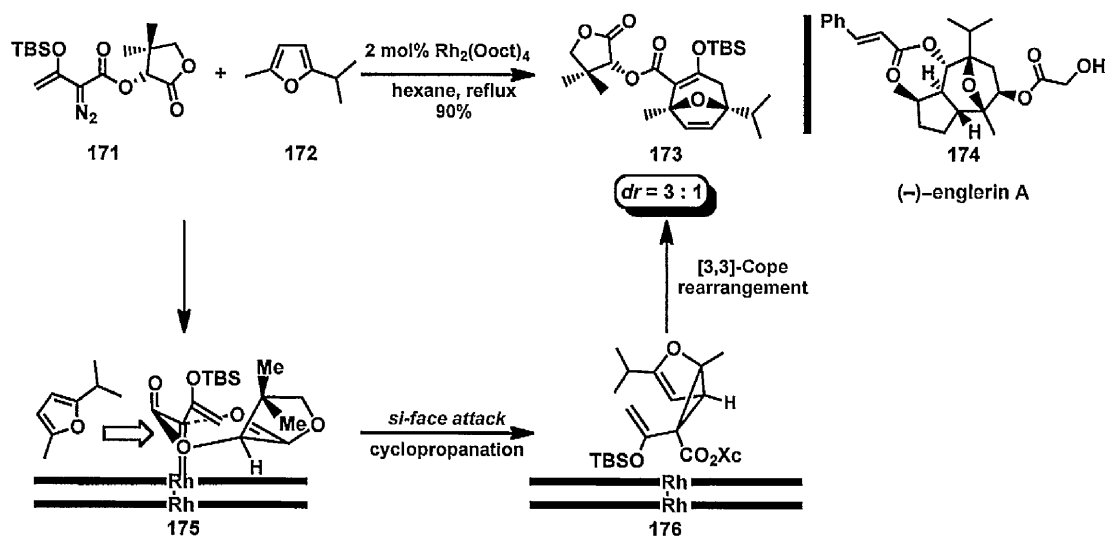
A key to the success of this particular [4+3] cycloaddition reaction is the cyclopropanation reaction, to provide the diastereoselective *cis*-divinyl cyclopropane.⁴⁰ The model for the rhodium(II)-catalysed stereoselective cyclopropanation of furan as well as for the related acyclic dienes is based on the model proposed by Doyle for the metal-catalysed cyclopropanation of alkenes.^{40c} As depicted in Scheme 3.35, the furan derivative approaches the vinylcarbenoid **168** side-on in a concerted nonsynchronous manner from the side of the



Scheme 3.35 Model for the Stereoselectivity in the Cyclopropanation Step.

ester functionality. The reaction proceeds *via* **169**, wherein the developing positive charge at the α -position of furan is stabilised by the lone-pair of electrons on the oxygen of the ester side-chain. The outward rotation of the furan ring for the cyclopropanation results in a *cis*-orientation of the two divinyl groups. It is worthy to note that the cyclic alkene is more reactive to initial cyclopropanation compared to its acyclic counterpart due to the free rotation of C-C bond that exists in the latter, which creates a non-bonding interactions between the vinyl group and the steric bulk of the rhodium(II) catalyst.

The synthetic utility of the rhodium(II)-triggered [4+3] cycloaddition was highlighted in the total synthesis of (–)-englerin A **174** by Theodorakis and co-workers (Scheme 3.36).⁴¹ Treatment of furan derivative **172** with the rhodium-stabilised vinylcarbenoid generated from **171** furnished the desired oxatricyclic derivative **173** in 90% yield with 3 : 1 diastereoselectivity. The (*R*)-pentalactone group in **171** serves as a chiral auxillary to block the *re*-face of the rhodium-bound vinylcarbenoid as illustrated in the transition state **175**,



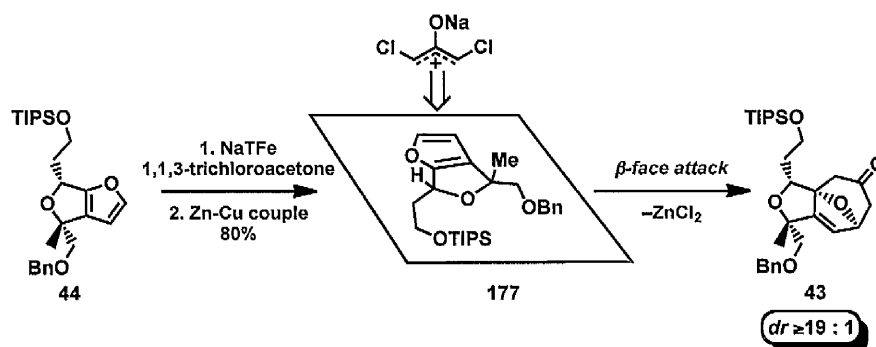
Scheme 3.36 [4+3] Cycloaddition in the Total Synthesis of (–)-Englerin A **174**.

where the α -hydroxy carbonyl oxygen coordinates with the electrophilic carbene carbon to form a rigid six-membered chair conformer and the five-membered lactone points away from the catalyst wall to minimise steric interactions.^{40a} The major diastereoisomer in the cyclopropanation step thus emerges from initial *si*-face nucleophilic attack of furan to the rhodium carbenoid complex. It is likely that a more bulky chiral auxillary would improve the diastereocontrol in this reaction.

3.4 Diastereoselective [4+3] Cycloaddition Reaction

3.4.1 Substrate-Controlled [4+3] Cycloaddition Reaction

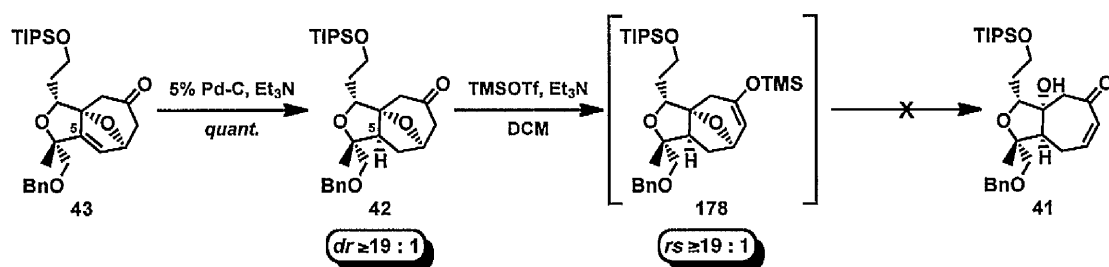
The completion of the bicyclic furan **44** provided an opportunity to examine the key diastereoselective [4+3] cycloaddition reaction (Scheme 3.37). Treatment of the bicyclic furan **44** with the oxyallyl cation generated from 1,1,3-trichloroacetone under the conditions reported by Fohlisch and co-workers, furnished the chlorinated cycloadducts which had a strong characteristic absorption for the electrophilic carbonyl group in the IR



Scheme 3.37 Diastereoselective Synthesis of Tricycle **43**.

spectra ($\nu = 1751 \text{ cm}^{-1}$). Direct dechlorination using zinc-copper couple provided the desired oxabicyclic **43** in 80% yield with excellent diastereocontrol ($\geq 19 : 1$ by ^1H NMR).^{7a} The stereochemical course in the diastereoselective addition of the oxyallyl moiety to furan **44** is consistent with the delivery from the less hindered β -face, as depicted in the model **177**.

Scheme 3.38 illustrates the attempted conversion of the bridged ketone to the α,β -unsaturated version. The C5 stereocentre in the cycloadduct **42** was readily installed by the hydrogenation of the trisubstituted alkene **43** in quantitative yield and with excellent diastereocontrol ($\geq 19 : 1$ by ^1H NMR), using Pd/C poisoned with excess triethylamine to prevent the concurrent debenzylolation in **43**. The next stage of the synthesis was ring-opening of the oxa bicyclic ether bridge in **42** via regioselective enolisation of the sterically accessible methylene unit α to the keto group. Although, the desired enolate formation



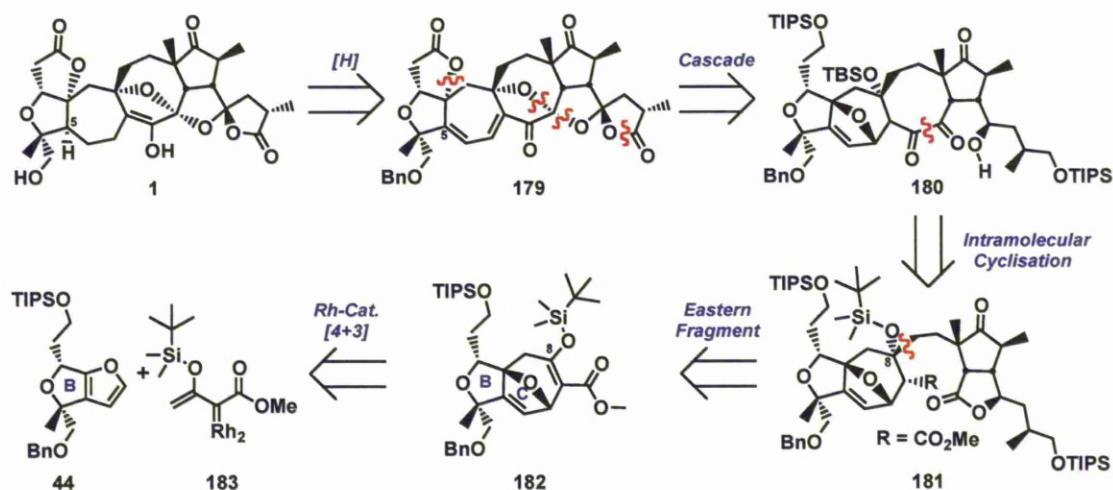
Scheme 3.38 *Diastereoselective Hydrogenation Reaction and Attempted Ring-Opening of 42.*

proceeded uneventfully with excellent levels of regioselectivity to furnish **178** ($\geq 19 : 1$ by ^1H NMR), all efforts to accomplish the Lewis acid mediated β -elimination ring-opening of the C-O bond from either the trimethylsilyl enol ether **178** or from the enolate failed to deliver the cycloheptenone derivative **41**. The unexpected failure of **178** to undergo ring opening of the bridged ether can presumably be attributed to the poor alignment of p-orbitals of the enolate with the sigma orbitals of alkoxy group linked to the β -carbon.

3.4.2 Revised End Game Strategy For Lancifodilactone G

In light of the failure of the oxabicyclic **42** to undergo ring opening of bridged ether, we revised the end game for the total synthesis of Lancifodilactone G **1** (Scheme 3.39). The revised strategy takes maximum advantage of structural topography of the intermediates for the stereocontrolled installation of stereogenic centres *en route* to the natural product **1**. Molecular modeling of the octacyclic diene **179** indicates the hydrogenation reaction should be diastereoselective and facilitate the reductive cleavage of the primary benzyl group. As previously mentioned, **179** could be obtained from the pentacyclic intermediate **180** under biomimetic oxidative cyclisation conditions which will now involve a lactonisation reaction in the western unit *via* ring-opening of dihydrofuran moiety by the carboxylate side chain formed after the removal of the primary TIPS group (*vide supra*). The construction of the 8-membered ring in **180** would involve an acyloin condensation reaction between the resident lactone and ester in **181**, in accordance with the earlier strategy (*vide supra*). The cross-coupling of the eastern with the western subunit **182** is envisioned to proceed from the β -

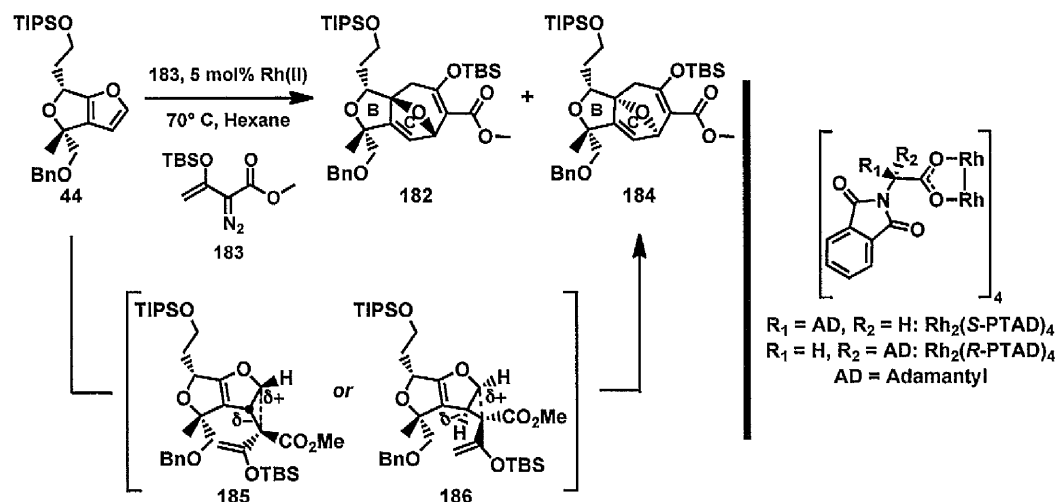
face of the oxatricycle **182** either by a 1,4-radical addition of the eastern fragment to the vinylogous ester or by a 1,2-organometallic addition after transforming **182** to the keto-hydroxymethylene. The fully functionalised 5,7-membered subunit **182** was anticipated to come directly from a catalyst-controlled rhodium-catalysed [4+3] cycloaddition reaction with the bicyclic furan **44** and vinyl carbenoid **183** in accordance with the method reported by Davies and co-workers.^{40a,b}



Scheme 3.39 Revised End Game Strategy for Lancifodilactone G 1.

3.4.3 Catalyst-Controlled [4+3] Cycloaddition Reaction

The revised synthesis of fully functionalised western fragment is outlined in Scheme 3.40. The pivotal rhodium(II)-catalysed [4+3] cycloaddition reaction was triggered by the slow addition of diazoester **183** to a solution of bicyclic furan **44** and $\text{Rh}_2(\text{S-PTAD})_4$ (Table 3.3, Entry 1), which furnished the desired tricycle **182** in 76% yield with excellent regio-



Scheme 3.40 Rhodium(II)-Catalysed [4+3] Cycloaddition Reaction of Bicyclic Furan **44**.

and diastereoselectivity (by ^1H NMR). The relative configuration in **182** was tentatively assigned based on the diastereoselective reaction of **44** using achiral rhodium(II) catalyst, which furnished the opposite diastereoisomer **184** in 74% yield with 7 : 1

Entry	Catalyst Rh(II)	Time (hr)	d.r. (182 : 184)	Yield ^a (%)
1	$\text{Rh}_2(\text{S-PTAD})_4$	1.5	$\geq 19 : 1$	76
2	$\text{Rh}_2(\text{Oct})_4$	1.5	1 : 7	74
3	$\text{Rh}_2(\text{R-PTAD})_4$	2.5	1 : 4	ND ^b

^aIsolated yield of the major isomer. ^bIncomplete conversion.

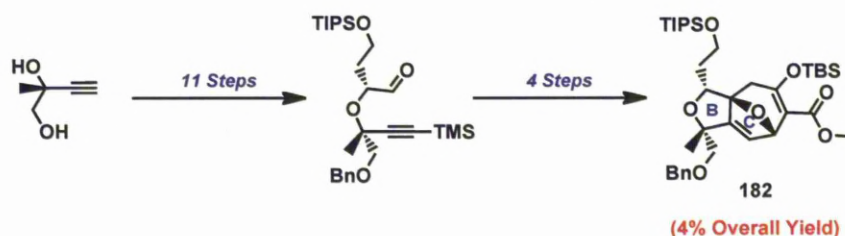
Table 3.3 Rhodium(II)-Catalysed [4+3] Cycloaddition Reaction of Bicyclic Furan **44**.

diastereoselectivity (Table 3.3, Entry 2). The stereo-determining cyclopropanation step in this reaction is anticipated to proceed from the less hindered β -face of the bicyclic furan **44** leading to *cis*-divinyl cyclopropane **186**, which is followed by a stereospecific Cope

rearrangement to furnish **184**. Surprisingly, the cycloaddition reaction catalysed by $\text{Rh}_2(R\text{-PTAD})_4$ delivered the oxa-tricycle **184** with lower selectivity ($dr = 4 : 1$) and required longer reaction time compared to its antipode **182**, suggesting a mismatch case between the chiral catalyst and **44** (Table 3.3, Entry 1-2 vs 3). Notably, the catalyst-controlled [4+3] cycloaddition transformation provides a strategic route for the construction of both diastereoisomers **182** and **184** in good yield and selectivity depending on the achiral or chiral rhodium(II) employed in the reaction. Although it is critical at this stage to unambiguously determine the relative stereochemistry of cycloadducts **182** and **184** using X-ray crystallography, further studies towards the union of western and eastern fragment should not be hampered after having secured access to intermediates **182** and **184**.

3.5 Conclusion

In conclusion, we have completed the synthesis of the western fragment (B-C rings) in 15 steps (longest linear sequence) and in 4% overall yield from the literature known compound (Scheme 3.41). This study successfully incorporates the diastereoselective [4+3] cycloaddition reaction for the rapid construction of the oxa-tricyclic motif of the western



Scheme 3.41 Summary and Outlook.

fragment **182**. The synthesis also features a hetero Pauson-Khand reaction employed in the construction of bicyclic butenolide **71** *en route* to the key bicyclic furan derivative **44**. In the following Chapter 4, preliminary studies towards the second-generation construction of the western fragment will be disclosed, which have the potential to expedite the synthesis of the BC subunit **182**.

3.6 Experimental

3.6.1 General

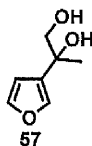
All reactions were performed in oven-dried (125 °C) or flame-dried glassware under an inert atmosphere of nitrogen or argon. Syringes were oven-dried (125 °C) and then cooled in a desiccator. The following reaction solvents were dried using an alumina column solvent system: toluene (PhMe), diethyl ether (Et₂O) and dichloromethane (DCM) were dried over alumina column solvent system using the method of Grubbs.⁴² The following reaction solvents were distilled from the indicated drying agents: tetrahydrofuran (THF) (sodium, benzophenone), hexanes (CaH₂), benzene (PhH) (sodium) and acetonitrile (MeCN) (CaH₂). Triethyl amine (Et₃N) was distilled from CaH₂. Brine refers to a saturated solution of NaCl. All starting material and reagents were purchased from Acros, Aldrich, Alfa Aesar, Fluka, and Strem chemical companies and were used without further purification unless noted otherwise.

Analytical thin layer chromatography (TLC) was performed on Merck 60 F₂₅₄ precoated silica-gel plates. Visualization was accomplished with a UV light and/or a KMnO₄, or *p*-anisaldehyde solution. Flash column chromatography (FCC) was performed by the method of Still with Merck Silica-gel 60 (230-400 mesh). Solvents for extraction and FCC were technical grade. Reported solvent mixtures for both TLC and FCC were volume/volume mixtures. Infrared spectra (IR) were obtained on a Perkin-Elmer spectrum one series FTIR spectrophotometer. Peaks are reported in cm⁻¹ with the following relative intensities: s (strong), m (medium), w (weak). The Liverpool University Mass Spectroscopy Centre and EPSRC National Spectrometry Centre, Swansea, recorded Mass spectra. High-resolution electron-impact electrospray (ESI) mass spectra were obtained on a Micromass LCT Mass spectrometer LTQ Orbitrap XL. The specific rotation was measured with a PerkinElmer Model 343 Plus polarimeter.

^1H -NMR and ^{13}C -NMR were recorded on a Bruker DRX-500 MHz NMR spectrometer in the indicated deuterated solvents. For ^1H -NMR, CDCl_3 and C_6D_6 were set to 7.26 ppm (CDCl_3 singlet) and 7.16 (C_6D_6 singlet) respectively and for ^{13}C -NMR, CDCl_3 and C_6D_6 were set to 77.16 ppm (CDCl_3 center of triplet) and 128.06 ppm (C_6D_6 center of triplet) respectively. All values for ^1H -NMR and ^{13}C -NMR chemical shifts for deuterated solvents were obtained from Cambridge Isotope Labs. Data are reported in the following order: chemical shift in ppm (δ) (multiplicity, which are indicated by br (broadened), s (singlet), d (doublet), t (triplet), q (quartet), quint (quintet), m (multiplet)); assignment of 2nd order pattern, if applicable; coupling constants (J , Hz); integration. All ^{13}C -NMR spectra were reported using the descriptor (o) and (e) referring to whether the peak is odd or even, respectively, and correlate to an attached proton test (ATP) experiment.

3.6.2 Experimental Procedures

2-(Furan-3-yl)propane-1,2-diol



To a suspension of $\text{Pd}(\text{P}^t\text{Bu}_3)_4$ (0.072 g, 0.14 mmol) and sodium carbonate (0.90 g, 8.51 mmol) in DMF (14 mL) was added 3-bromofuran **55** (0.50 g, 3.40 mmol), isopropenylboronic acid pinacol ester (0.48 g, 2.84 mmol), and water (0.15 mL) at room temperature. The reaction mixture was heated at 70 °C for 12 hours before diluting with diethyl ether and water. The reaction mixture was partitioned with diethyl ether and the phases were separated. The combined organic phases were dried with MgSO_4 , concentrated under *vacuo* and used directly in the next step.

To a solution of crude alkene **56** (0.31 g, 2.84 mmol) and *N*-methylmorpholine *N*-oxide (0.67 g, 5.72 mmol) in 4 : 1 acetone- H_2O (10 mL) was added osmium tetroxide (1.60 mL,

0.079 mmol, 0.05 M in water) at room temperature and stirred for 12 hours. The reaction mixture was quenched with saturated aqueous sodium thiosulphate and diluted with brine. The reaction mixture was partitioned with ethyl acetate and the phases were separated. The combined organic phases were dried with MgSO_4 and concentrated under *vacuo* and purified by flash chromatography (70-100% EtOAc-hexanes as eluent) to give the title compound **57** (0.22 g, 55%) as a colourless oil.

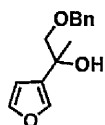
^1H NMR (500 MHz, CDCl_3) δ 7.43-7.42 (m, 1H), 7.41-7.40 (m, 1H), 6.37-6.36 (m, 1H), 3.77 (br t, $J = 4.7$ Hz, 1H), 3.70 (d, A of AB, $J_{AB} = 11.0$ Hz, 1H), 3.58 (d, B of AB, $J_{AB} = 11.0$ Hz, 1H), 2.52 (br s, 1H), 1.50 (s, 3H).

^{13}C NMR (125 MHz, CDCl_3) δ 143.57 (o), 139.16 (o), 130.44 (e), 108.55 (o), 71.27 (e), 70.71 (e), 25.47 (o).

IR (Neat) 3378 (br, s), 2977 (w), 2929 (m), 2870 (w), 1503 (w), 1457 (w), 1376 (w), 1164 (m), 1046 (s), 1024 (m), 876 (m).

HRMS (ESI, $[\text{M}]^+$) calcd for $\text{C}_7\text{H}_{10}\text{O}_3$ 142.0624, found 142.0623.

1-(Benzyloxy)-2-(furan-3-yl)propan-2-ol



To a solution of diol **57** (0.056 g, 3.93 mmol) in DMF (12 mL) at 0 °C was added sodium hydride (0.19 g, 4.71 mmol, 60% in oil) in a single portion. After stirring for 20 minutes, benzyl bromide (0.61 mL, 0.87 mmol) and TBAI (0.15 g, 0.39 mmol) were sequentially added and the reaction mixture was warmed to room temperature and stirred for 4 hours. The heterogeneous solution was then cooled to 0 °C and quenched by slow addition of water. The reaction mixture was partitioned with diethyl ether and the phases were separated. The combined organic phases were dried with MgSO_4 and concentrated under

vacuo and purified by flash chromatography (50% Et₂O-hexanes as eluent) to give the title compound (0.78 g, 85%).

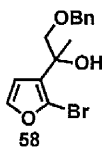
¹H NMR (500 MHz, CDCl₃) δ 7.41-7.40 (m, 1H), 7.38-7.30 (m, 6H), 6.39 (dd, *J* = 1.7, 0.8 Hz, 1H), 4.60 (s, 2H), 3.58 (d, A of AB, *J*_{AB} = 9.1 Hz, 1H), 3.49 (d, B of AB, *J*_{AB} = 9.1 Hz, 1H), 2.85 (br s, 1H), 1.50 (s, 3H).

¹³C NMR (125 MHz, CDCl₃) δ 142.99 (o), 138.87 (o), 137.99 (e), 130.79 (e), 128.55 (o), 127.88 (o), 127.77 (o), 108.77 (o), 77.93 (e), 73.61 (e), 70.30 (e), 26.07 (o).

IR (Neat) 3434 (br, w), 2922 (w), 2855 (w), 1499 (w), 1454 (m), 1370 (w), 1095 (s), 1021 (s), 875 (s).

HRMS (ESI, [M + Na]⁺) calcd for C₁₄H₁₆O₃Na 255.0997, found 255.1000.

1-(Benzyloxy)-2-(2-bromofuran-3-yl)propan-2-ol



To a solution of furanyl alcohol (0.15 g, 0.64 mmol) in DMF (13 mL) at 0 °C was added freshly recrystallized *N*-bromosuccinimide (0.12 g, 0.64 mmol). The reaction mixture was stirred for 2 hours at 0 °C whereupon, saturated aqueous NaHCO₃ (5 mL) and water (5 mL) was added. The reaction mixture was partitioned with diethyl ether and the phases were separated. The combined organic phases were dried with MgSO₄ and concentrated under *vacuo* and purified by flash chromatography (50% Et₂O as eluent) to give 2-bromofuran **58** (0.13 g, 62%) as a mixture of inseparable regioisomers (*rs* = 3.5 : 1 by ¹H NMR).

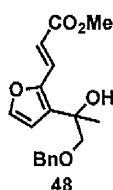
¹H NMR (500 MHz, CDCl₃) δ 7.37-7.28 (m, 6H), 6.47 (d, *J* = 2.0 Hz, 1H), 4.58 (s, 2H), 3.74 (d, A of AB, *J*_{AB} = 9.2 Hz, 1H), 3.53 (d, B of AB, *J*_{AB} = 9.2 Hz, 1H), 2.94 (s, 1H), 1.51 (s, 3H).

^{13}C NMR (125 MHz, CDCl_3) δ 143.32 (o), 137.85 (e), 128.51 (o), 128.19 (e), 127.87 (o), 127.76 (o), 117.51 (e), 112.33 (o), 76.28 (e), 73.49 (e), 70.57 (e), 24.95 (o).

IR (Neat) 3453 (br, w), 2979 (w), 2862 (w), 1495 (m), 1454 (m), 1369 (m), 1158 (m), 1087 (s), 890 (s), 736 (s).

HRMS (ESI, $[\text{M} + \text{Na}]^+$) calcd for $\text{C}_{14}\text{H}_{15}\text{O}_3\text{Na}^{79}\text{Br}$ 333.0102, found 333.0116, (ESI, $[\text{M} + \text{Na}]^+$) calcd for $\text{C}_{14}\text{H}_{15}\text{O}_3\text{Na}^{81}\text{Br}$ 335.0082, found 335.0098.

(*E*)-Methyl 3-(3-(1-(benzyloxy)-2-hydroxypropan-2-yl)furan-2-yl)acrylate



A flame dried 25 mL flask was charged with palladium acetate (0.087 g, 0.39 mmol) under argon. 2-bromofuranyl alcohol **58** (0.20 g, 0.64 mmol) in DMF (1.6 mL) was added to the reaction flask followed by methyl acrylate (0.70 mL, 7.71 mmol), triethylamine (0.45 mL, 3.21 mmol) and trimethyl phosphite (0.091 mL, 0.77 mmol). The reaction mixture was warmed to 110° C and stirred for 3 hours (TLC control) before diluting with diethyl ether and water. The reaction mixture was partitioned with diethyl ether and the phases were separated. The combined organic phases were dried with MgSO_4 , concentrated under *vacuo* and purified by silica-gel chromatography (20-25% EtOAc-hexanes as eluent) to give hydroxy- α,β -unsaturated ester **48** (0.055 g, 27%) as a brown oil.

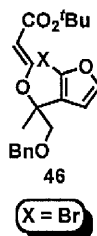
^1H NMR (500 MHz, C_6D_6) δ 8.53 (d, $J = 15.8$ Hz, 1H), 7.16-7.07 (m, 5H), 6.78 (d, $J = 1.8$ Hz, 1H), 6.73 (d, $J = 15.8$ Hz, 1H), 5.88 (d, $J = 1.9$ Hz, 1H), 4.14 (d, A of AB, $J_{AB} = 12.1$ Hz, 1H), 4.11 (d, B of AB, $J_{AB} = 12.1$ Hz, 1H), 3.44 (s, 3H), 3.20 (d, A of AB, $J_{AB} = 9.0$ Hz, 1H), 3.13 (d, B of AB, $J_{AB} = 9.1$ Hz, 1H), 2.42 (s, 1H), 1.27 (s, 3H).

^{13}C NMR (125 MHz, C_6D_6) δ 167.37 (e), 147.27 (e), 143.27 (o), 138.34 (e), 133.79 (e), 132.58 (o), 128.66 (o), 128.35 (o), 115.71 (o), 111.84 (o), 77.96 (e), 73.41 (e), 71.87 (e), 51.17 (o), 26.98 (o).

IR (Neat) 3483 (br, w), 2931 (w), 2861 (w), 1702 (s), 1630 (m), 1454 (m), 1435 (m), 1267 (m), 1167 (s), 1096 (s), 985 (m), 736 (s).

HRMS (ESI, $[\text{M} + \text{Na}]^+$) calcd for $\text{C}_{18}\text{H}_{20}\text{O}_5\text{Na}$ 339.1208, found 339.1219.

(*E*)-*tert*-Butyl 3-((1-(benzyloxy)-2-(2-bromofuran-3-yl)propan-2-yl)oxy)acrylate



To a stirred solution of 2-bromofuranyl alcohol **58** (0.10 g, 0.32 mmol) and *tert*-butyl propiolate (0.22 g, 1.74 mmol) in dry CH_2Cl_2 (1 mL) at room temperature was added *N*-methylmorpholine (0.19 mL, 1.74 mmol). The reaction mixture was stirred for 2 days at room temperature whereupon, the solvent was evaporated under *vacuo*. Purification of the residue by silica-gel column chromatography (20% Et_2O -hexanes as eluent) gave vinylogous carbonate **46** (0.042 g, 30%) as a pale yellow oil.

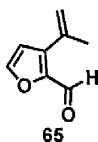
^1H NMR (500 MHz, C_6D_6) δ 7.90 (d, $J = 12.0$ Hz, 1H), 7.19-7.06 (m, 5H), 6.71 (d, $J = 2.2$ Hz, 1H), 5.96 (d, $J = 2.1$ Hz, 1H), 5.79 (d, $J = 12.1$ Hz, 1H), 4.23 (d, A of AB, $J_{AB} = 12.2$ Hz, 1H), 4.18 (d, B of AB, $J_{AB} = 12.2$ Hz, 1H), 3.49 (d, A of AB, $J_{AB} = 10.1$ Hz, 1H), 3.41 (d, B of AB, $J_{AB} = 10.1$ Hz, 1H), 1.43 (s, 3H), 1.41 (s, 9H).

^{13}C NMR (125 MHz, C_6D_6) δ 167.06 (e), 157.91 (o), 144.01 (o), 138.33 (e), 128.63 (o), 127.80 (o), 124.98 (e), 120.20 (e), 112.71 (o), 102.16 (o), 80.03 (e), 75.19 (e), 73.51 (e), 28.38 (o), 22.39 (o).

IR (Neat) 2865 (w), 2857 (w), 1699 (s), 1637 (s), 1454 (m), 1367 (m), 1120 (s), 1103 (s), 1052 (m), 734 (s).

HRMS (ESI, $[M + Na]^+$) calcd for $C_{21}H_{25}O_5Na^{79}Br$ 459.0783, found 459.0778, (ESI, $[M + Na]^+$) calcd for $C_{21}H_{25}O_5Na^{81}Br$ 461.0763, found 461.0744.

3-(Prop-1-en-2-yl)furan-2-carbaldehyde



To a suspension of $Pd(P^tBu_3)_4$ (0.32 g, 0.63 mmol) and sodium carbonate (4.01 g, 37.9 mmol) in DMF (51 mL) was added 3-bromo-2-furaldehyde **64** (2.21 g, 12.62 mmol), isopropenylboronic acid pinacol ester (2.54 g, 15.14 mmol), and water (0.68 mL) at room temperature. The reaction mixture was heated at 70 °C for 12 hours before diluting with diethyl ether and water. The reaction mixture was partitioned with diethyl ether and the phases were separated. The combined organic phases were dried with $MgSO_4$, concentrated under *vacuo* and purified by column chromatography (30-40% Et_2O -hexanes as eluent) to afford **65** as a yellow oil (1.55 g, 90%).

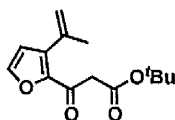
1H NMR (500 MHz, $CDCl_3$) δ 9.76 (d, $J = 0.6$ Hz, 1H), 7.59 (dd, $J = 1.7, 0.6$ Hz, 1H), 6.58 (d, $J = 1.8$ Hz, 1H), 5.35-5.34 (m, 1H), 5.37-5.36 (m, 1H), 2.15-2.14 (m, 3H).

^{13}C NMR (125 MHz, $CDCl_3$) δ 177.57 (o), 147.12 (o), 139.80 (e), 134.58 (e), 131.31 (e), 119.31 (e), 112.44 (o), 23.07 (o).

IR (Neat) 2920 (w), 2866 (w), 1664 (s), 1421 (m), 1366 (s), 1258 (m), 891 (s), 778 (s).

HRMS (ESI, $[M - H]^+$) calcd for $C_8H_7O_2$ 135.0441, found 135.0439.

tert-Butyl 3-oxo-3-(3-(prop-1-en-2-yl)furan-2-yl)propanoate



To a stirred solution of diisopropylamine (1.42 mL, 9.94 mmol) in THF (22 mL), *n*-butyllithium (3.98 mL, 9.94 mmol, 2.5M in hexanes) was added at 0 °C and stirred at same

temperature for 20 minutes followed by 20 minutes at room temperature. The reaction mixture was cooled to $-78\text{ }^{\circ}\text{C}$ and *tert*-butyl acetate (1.22 mL, 9.03 mmol) in THF (5.4 mL) was added dropwise. The resulting solution was stirred at the same temperature for 2 hours whereupon, furaldehyde **65** (1.23 g, 9.03 mmol) in THF (5.4 mL) was added. After stirring at $-78\text{ }^{\circ}\text{C}$ for another 1.5 hours, the reaction was quenched by addition brine. The reaction mixture was partitioned with ethyl acetate and the phases were separated. The combined organic phases were dried with MgSO_4 and concentrated under *vacuo* and purified by flash chromatography (10-20% EtOAc-hexanes as eluent) to give the β -hydroxy ester **66** (1.70 g, 75%) as a yellow oil.

In a 100 mL flask charged with flame dried 4Å molecular sieves (0.60 g), a solution of alcohol **66** (0.96 g, 3.80 mmol) in CH_2Cl_2 (7.6 mL) was added and stirred at room temperature for 5 minutes. To the reaction mixture was added activated manganese dioxide (5.83 g, 57.00 mmol) in a single portion and the resulting black suspension was stirred vigorously at room temperature for 12 hours whereupon, the reaction mixture was filtered over celite aided by CH_2Cl_2 . The reaction mixture was concentrated under *vacuo* and purified by flash chromatography (5% EtOAc-hexanes as eluent) to afford β -keto ester (0.57 g, 60%) as a pale yellow oil.

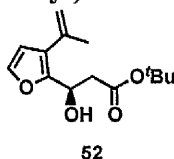
^1H NMR (500 MHz, CDCl_3) δ 7.45 (d, $J = 1.7\text{ Hz}$, 1H), 6.51 (d, $J = 1.7\text{ Hz}$, 1H), 5.41-5.40 (m, 1H), 5.29-5.28 (m, 1H), 3.79 (s, 2H), 2.12-2.11 (m, 3H), 1.43 (s, 9H).

^{13}C NMR (125 MHz, CDCl_3) δ 182.45 (e), 166.51 (e), 146.46 (e), 144.61 (o), 136.03 (o), 135.53 (o), 117.88 (e), 114.37 (o), 81.46 (e), 47.61 (e), 27.76 (o), 22.40 (o).

IR (Neat) 2979 (w), 1732 (s), 1678 (s), 1560 (m), 1480 (m), 1368 (m), 1257 (m), 1142 (s), 1096 (m), 886 (m).

HRMS (ESI, $[\text{M} + \text{Na}]^+$) calcd for $\text{C}_{14}\text{H}_{18}\text{O}_4\text{Na}$ 273.1103, found 273.1106.

(*R*)-tert-Butyl 3-hydroxy-3-(3-(prop-1-en-2-yl)furan-2-yl)propanoate



A flame-dried 100 ml RBF was charged with β -keto ester (0.60 g 2.39 mmol) in THF (12 ml). The vessel was cooled to $-10\text{ }^{\circ}\text{C}$ and (*S*)-methyl-CBS-oxazaborolidine (4.79 mL, 4.79 mmol, 1M in toluene) was added. Borane-methyl sulfide complex (0.46 mL, 4.79 mmol) was slowly added over 5 minutes. The reaction stirred for 3.5 hours at this temperature before being slowly quenched with 2 mL of methanol. The reaction was warmed to room temperature, and after the majority of gas evolution subsided, the reaction was diluted with water (20 mL) and ethyl acetate (20 mL). The reaction mixture was partitioned with ethyl acetate and the phases were separated. The combined organic phases were dried over MgSO_4 and concentrated under *vacuo* to afford the crude oil. Purification by flash chromatography over silica-gel (20% EtOAc-hexanes as eluent) furnished the allylic alcohol **52** as a colourless oil (0.45 g, 75%). The enantiomeric ratio was determined to be 96 : 4 by HPLC (Chiralcel AD-H, 2% *i*-PrOH in hexane, 254 nm, flow rate 0.5 mL/min, $22\text{ }^{\circ}\text{C}$): (*R*)-isomer t_R 35.57 min (major), (*S*)-isomer t_R 38.14 min (minor).

$[\alpha]_D^{20} -19.5$ ($c = 0.49$, CHCl_3).

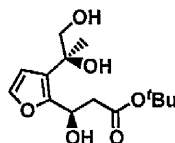
^1H NMR (500 MHz, CDCl_3) δ 7.20 (d, $J = 1.8$ Hz, 1H), 6.27 (d, $J = 1.9$ Hz, 1H), 5.14-5.11 (m, 1H), 5.03-5.02 (m, 1H), 4.99-4.98 (m, 1H), 3.30 (br d, $J = 2.1$ Hz, 1H), 2.91 (dd, A of ABX, $J_{AB} = 16.6$ Hz, $J_{AX} = 9.4$ Hz, 1H), 2.57 (dd, B of ABX, $J_{AB} = 16.6$ Hz, $J_{BX} = 3.7$ Hz, 1H), 1.95-1.94 (m, 3H), 1.36 (s, 9H).

^{13}C NMR (125 MHz, CDCl_3) δ 171.53 (e), 149.30 (e), 141.27 (o), 135.98 (e), 124.50 (e), 114.42 (e), 110.39 (o), 81.38 (e), 62.62 (o), 40.66 (e), 28.03 (o), 23.13 (o).

IR (Neat) 3426 (br, w), 2977 (w), 1726 (m), 1634 (w), 1368 (m), 1257 (m), 1150 (s), 1033 (m), 891 (m).

HRMS (ESI, $[\text{M} + \text{Na}]^+$) calcd for $\text{C}_{14}\text{H}_{20}\text{O}_4\text{Na}$ 275.1259, found 275.1256.

(*R*)-*tert*-Butyl 3-(3-((*S*)-1,2-dihydroxypropan-2-yl)furan-2-yl)-3-hydroxypropanoate



To a suspension of (DHQ)₂PHAL (0.009 g, 0.011 mmol), K₂Os₂(OH)₄ (0.004 g, 0.011 mmol), K₃Fe(CN)₆ (1.14 g, 3.45 mmol) and K₂CO₃ (0.48 g, 3.45 mmol) in a solution of *t*-BuOH/H₂O (11.6 mL, 1 : 1) was added 3-isoprenyl furan **52** (0.29 g, 1.15 mmol) at 0 °C overnight. The reaction mixture was stirred for 24 hours at same temperature (TLC control). The reaction mixture was quenched with saturated aqueous sodium thiosulphate solution (10 ml) and diluted with ethyl acetate. The reaction mixture was partitioned with ethyl acetate and the phases were separated. The combined organic phases were dried over MgSO₄ and concentrated under *vacuo* to afford the crude oil. Purification by flash chromatography over silica-gel (70-100% EtOAc-hexanes as eluent) furnished the triol as a colourless oil (0.23 g, 70%).

$[\alpha]_D^{20} +14.07$ (c = 0.28, CHCl₃).

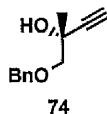
¹H NMR (500 MHz, CDCl₃) δ 7.25 (d, *J* = 1.9 Hz, 1H), 6.21 (d, *J* = 1.8 Hz, 1H), 5.34 (dd, *J* = 8.3, 4.9 Hz, 1H), 4.33 (br s, 1H), 4.22 (br s, 1H), 3.69 (d, A of AB, *J*_{AB} = 11.1 Hz, 1H), 3.58 (d, B of AB, *J*_{AB} = 11.1 Hz, 1H), 2.94 (dd, A of ABX, *J*_{AB} = 16.7 Hz, *J*_{AX} = 8.4 Hz, 1H), 2.84 (dd, B of ABX, *J*_{AB} = 16.7 Hz, *J*_{BX} = 4.9 Hz, 1H), 2.48 (br s, 1H), 1.48 (s, 3H), 1.44 (s, 9H).

¹³C NMR (125 MHz, CDCl₃) δ 171.58 (e), 150.69 (e), 140.59 (o), 125.75 (e), 110.33 (o), 81.40 (e), 72.46 (e), 70.69 (e), 64.14 (o), 40.98 (e), 28.06 (o), 25.93 (o).

IR (Neat) 3386 (br, w), 2980 (w), 1719 (w), 1368 (w), 1151 (m), 1025 (m), 907 (s), 728 (s).

HRMS (ESI, [M + Na]⁺) calcd for C₁₄H₂₂O₆Na 309.1314, found 309.1308.

(R)-1-(Benzyloxy)-2-methylbut-3-yn-2-ol



Diol¹⁹ (5.12 g, 51.10 mmol) and Bu₂SnO (15.18 g, 61.05 mmol) was dissolved in dry toluene (170 mL) and was refluxed using a Dean-Stark condenser for 6 hours. Benzyl bromide (6.69 mL, 56.30 mmol) and TBAI (4.72 g, 12.79 mmol) were added and the reaction mixture was further refluxed for further 16 hours. After cooling allowing the reaction mixture to room temperature, the crude solution was directly purified by column chromatography (20% EtOAc-hexanes as eluent) to afford **74** as a pale yellow oil (8.80 g, 90%).

$[\alpha]_D^{20} +10.3$ (c = 0.64, CHCl₃).

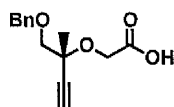
¹H NMR (500 MHz, CDCl₃) δ 7.38-7.29 (m, 5H), 4.69 (d, A of AB, J_{AB} = 12.2 Hz, 1H), 4.65 (d, B of AB, J_{AB} = 12.1 Hz, 1H), 3.56 (d, A of AB, J_{AB} = 9.2 Hz, 1H), 3.42 (d, B of AB, J_{AB} = 9.2 Hz, 1H), 2.88 (s, 1H), 2.46 (s, 1H), 1.47 (s, 3H).

¹³C NMR (125 MHz, CDCl₃) δ 137.74 (e), 128.53 (o), 127.90 (o), 127.80 (o), 86.21 (e), 77.28 (e), 73.60 (e), 71.69 (e), 67.20 (e), 25.91 (o).

IR (Neat) 3422 (br, w), 3288 (w), 2933 (w), 2111 (w), 1454 (m), 1095 (s), 737 (m).

HRMS (CI, [M + NH₄]⁺) calcd for C₁₂H₁₈O₂N 208.1332, found 208.1333.

(R)-2-((1-(Benzyloxy)-2-methylbut-3-yn-2-yl)oxy)acetic acid



To a suspension of sodium hydride (0.58 g, 14.59 mmol, 60% in oil) and bromoacetic acid (0.87 g, 6.25 mmol) (freshly passed through neutral alumina aided by ethyl acetate) in 5 : 1 THF : DMF (37 mL) at 0 °C was carefully added a solution of tertiary alcohol **74** (0.397 g,

2.09 mmol) in DMF (1 mL). The reaction mixture was warmed to room temperature and further stirred for 12 hours. The heterogeneous solution was then cooled to 0 °C and quenched by slow addition of water. The organic layer was separated and the aqueous layer was washed with ethyl acetate (3 X 10 mL). The aqueous layer was acidified with 2N HCl and partitioned with ethyl acetate. The aqueous layer was back extracted with ethyl acetate (3 X 10 mL) and the combined organic phases were dried over MgSO₄ and concentrated in *vacuo* to afford the crude acid. The brown oil was passed through a pad of silica aided by ethyl acetate to afford the carboxylic acid as a yellow oil (0.46 g, 88%).

2-Step procedure:

To a suspension of sodium hydride (1.79 g, 44.80 mmol, 60% in oil) and *tert*-butyl bromoacetic ester (13.10 g, 67.2 mmol) in 5 : 1 THF-DMF (75 mL) at 0 °C was carefully added a solution of tertiary alcohol **74** (4.26 g, 22.39 mmol) in THF (5 mL). The reaction mixture was warmed to room temperature and further stirred for 12 hours. The heterogeneous solution was then cooled to 0 °C and quenched by slow addition of water. The reaction mixture was partitioned with ethyl acetate and the phases were separated. The combined organic phases were dried over MgSO₄ and concentrated under *vacuo* to afford the crude oil. Purification by flash chromatography over silica gel (5% EtOAc-hexanes as eluent) afforded the alkynyl ester as a colourless oil (6.75 g, 99%), which was directly used in the next step

To a solution of alkynyl *tert*-butyl ester (6.75 g, 22.18 mmol) in CH₂Cl₂ (44 mL) was added trifluoroacetic acid (42.7 mL) at room temperature. After stirring for 4 hours at room temperature, the reaction mixture was azeotroped with toluene (3 X 10 mL) on the rotary evaporator to yield a brown oil. The crude acid was passed through a pad of silica aided by ethyl acetate to afford the carboxylic acid as a brown oil (5.50 g, 90%).

$[\alpha]_D^{20} +9.0$ (c = 0.87, CHCl₃).

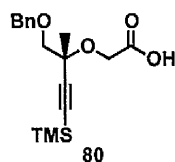
¹H NMR (500 MHz, CDCl₃) δ 7.39-7.29 (m, 5H), 4.69 (d, A of AB, J_{AB} = 12.1 Hz, 1H), 4.64 (d, B of AB, J_{AB} = 12.1 Hz, 1H), 4.37 (d, A of AB, J_{AB} = 17.2 Hz, 1H), 4.24 (d, B of AB, J_{AB} = 17.1 Hz, 1H), 3.58 (d, A of AB, J_{AB} = 10.0 Hz, 1H), 3.52 (d, B of AB, J_{AB} = 10.0 Hz, 1H), 2.63 (s, 1H), 1.48 (s, 3H).

¹³C NMR (125 MHz, CDCl₃) δ 174.03 (e), 137.07 (e), 128.68 (o), 128.18 (o), 127.99 (o), 81.10 (e), 76.59 (e), 75.07 (e), 74.76 (e), 73.73 (e), 63.18 (e), 24.37 (o).

IR (Neat) 3277 (br, w), 2917 (w), 2113 (w), 1729 (s), 1454 (m), 1356 (m), 1205 (m), 1104 (s), 739 (m).

HRMS (ESI, [M + Na]⁺) calcd for C₁₄H₁₆O₄Na 271.0946, found 271.0948.

((*R*)-2-((1-(Benzyloxy)-2-methyl-4-(trimethylsilyl)but-3-yn-2-yl)oxy)acetic acid



In a flame dried 250 ml round bottom flask equipped with a magnetic stirring bar, acid (4.7 g, 18.93 mmol) was dissolved in THF (115 ml) and cooled to -78 °C. To the colorless solution *n*-butyllithium (17.04 ml, 42.6 mmol, 2.5M in hexanes) was added dropwise. The resulting yellow slurry was stirred for 10 minutes before chlorotrimethylsilane (7.52 ml, 58.90 mmol) was added dropwise at -78 °C and the reaction was allowed to warm to room temperature over 1.5 hours. The yellow solution was further stirred at room temperature for 1 hour before being quenched by the addition of 2N HCl. The reaction mixture was partitioned with ethyl acetate and the phases were separated. The combined organic phases were dried with MgSO₄ and concentrated under *vacuo* and purified by flash chromatography (100% EtOAc as eluent) to give the title compound **80** (6.05 g, quant.) as a colourless oil.

$[\alpha]_D^{20} +14.5$ (c = 0.50, CHCl₃).

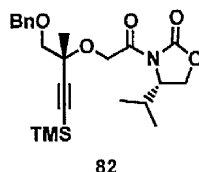
¹H NMR (500 MHz, CDCl₃) δ 7.39-7.29 (m, 5H), 4.68 (d, A of AB, J_{AB} = 12.3 Hz, 1H), 4.65 (d, B of AB, J_{AB} = 12.3 Hz, 1H), 4.35 (d, A of AB, J_{AB} = 17.1 Hz, 1H), 4.20 (d, B of AB, J_{AB} = 17.1 Hz, 1H), 3.56 (d, A of AB, J_{AB} = 10.0 Hz, 1H), 3.50 (d, B of AB, J_{AB} = 10.0 Hz, 1H), 1.45 (s, 3H), 0.18 (s, 9H).

¹³C NMR (125 MHz, CDCl₃) δ 173.58 (e), 137.26 (e), 128.60 (o), 128.08 (o), 127.88 (o), 102.22 (e), 93.81 (e), 75.23 (e), 75.07 (e), 73.58 (e), 63.16 (e), 24.37 (o), -0.26 (o).

IR (Neat) 2958 (br, w), 2171 (w), 1731 (s), 1454 (w), 1250 (m), 1102 (m), 842 (s), 759 (m).

HRMS (ESI, [M + Na]⁺) calcd for C₁₇H₂₄O₄NaSi 343.1342, found 343.1356.

(*S*)-3-(2-(((*R*)-1-(Benzyloxy)-2-methyl-4-(trimethylsilyl)but-3-yn-2-yl)oxy)acetyl)-4-isopropylloxazolidin-2-one



In a flame dried 250 ml round bottom flask equipped with a magnetic stirring bar, acid **80** (6.40 g, 19.97 mmol) and triethylamine (3.06 mL, 21.97 mmol) was dissolved in THF (56 mL). The solution was cooled to -78 °C, and pivaloyl chloride (2.48 mL, 2.43 mmol) was added dropwise. After stirring ten minutes at -78 °C, the reaction was warmed to 0 °C for 1 hour followed by recooling to -78 °C. In a flame dried 100 mL, (*S*)-(-)-4-isopropyl-2-oxazolidinone (3.10 g, 23.97 mmol) was dissolved THF (43 ml). After cooling to -78 °C, *n*-butyllithium (9.59 ml, 23.97 mmol, 2.5M in hexanes) was added dropwise. The reaction was allowed to stir for 20 minutes at -78 °C. The lithiated oxazolidinone was then cannulated into the mixed anhydride followed by warming to 0 °C for 1 hour. The reaction was quenched with saturated NH₄Cl. The solution was extracted twice with ethyl acetate, and the combined organic extracts were dried over MgSO₄, concentrated under *vacuo* and purified by flash chromatography (20-25% EtOAc-hexanes as eluent) to provide imide **82** (4.75 g,

55%).

$[\alpha]_D^{20} +53.9$ ($c = 0.36$, CHCl_3).

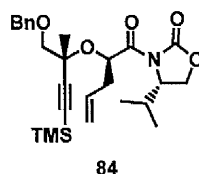
^1H NMR (500 MHz, CDCl_3) δ 7.38-7.26 (m, 5H), 5.19 (d, A of AB, $J_{AB} = 18.1$ Hz, 1H), 4.70 (d, B of AB, $J_{AB} = 18.1$ Hz, 1H), 4.63 (d, A of AB, $J_{AB} = 12.3$ Hz, 1H), 4.54 (d, B of AB, $J_{AB} = 12.3$ Hz, 1H), 4.22 (ddd, $J = 8.6, 3.6, 3.1$ Hz, 1H), 4.10 (dd, A of ABX, $J_{AB} = 9.2$ Hz, $J_{AX} = 3.1$ Hz, 1H), 3.87 (app. t, $J = 8.8$ Hz, 1H), 3.62 (d, A of AB, $J_{AB} = 9.9$ Hz, 1H), 3.59 (d, B of AB, $J_{AB} = 9.9$ Hz, 1H), 2.41-2.35 (m, 1H), 1.52 (s, 3H), 0.87 (d, $J = 7.0$ Hz, 3H), 0.82 (d, $J = 6.9$ Hz, 3H), 0.19 (s, 9H).

^{13}C NMR (125 MHz, CDCl_3) δ 170.38 (e), 153.91 (e), 138.47 (e), 128.37 (o), 127.43 (o), 126.98 (o), 104.09 (e), 91.96 (e), 76.37 (e), 74.60 (e), 72.93 (e), 66.05 (e), 64.06 (e), 58.14 (o), 28.13 (o), 24.42 (o), 17.89 (o), 14.59 (o), -0.12 (o).

IR (Neat) 2962 (w), 2171 (w), 1780 (s), 1719 (m) 1388 (m), 1250 (m), 1206 (m), 1120 (m), 842 (s), 760 (m).

HRMS (ESI, $[\text{M} + \text{Na}]^+$) calcd for $\text{C}_{23}\text{H}_{33}\text{NO}_5\text{NaSi}$ 454.2026, found 454.2043.

(*S*)-3-((*R*)-2-(((*R*)-1-(Benzyloxy)-2-methyl-4-(trimethylsilyl)but-3-yn-2-yl)oxy)pent-4-enoyl)-4-isoproploxazolidin-2-one



In a flame dried, 200 ml round bottom flask equipped with a magnetic stirring bar was taken sodium hexamethyldisilazide (14.92 mL, 14.92 mmol, 1M in THF) in THF (59 mL). The solution was cooled to -78 °C and *N*-glycolyl oxazolidinone **82** (4.6 g, 10.66 mmol) in THF (59 mL) was added dropwise. After addition, the solution was stirred at -78 °C for 30 minutes after which time allyl iodide (4.87 mL, 53.3 mmol) (freshly passed through a pad of neutral alumina) was added dropwise. The solution was further stirred at same temperature

for 10 minutes whereupon, the reaction flask was placed in a $-45\text{ }^{\circ}\text{C}$ bath. After stirring for 30 minutes, the reaction mixture was quenched with brine (10 mL). The reaction mixture was partitioned with ethyl acetate and the phases were separated. The combined organic phases were dried with MgSO_4 and concentrated under *vacuo* and purified by flash chromatography (10-20% EtOAc-hexanes as eluent) to give the title compound **84** (4.0 g, 80%).

$$[\alpha]_{\text{D}}^{20} +56.3 \text{ (c = 0.87, CHCl}_3\text{)}.$$

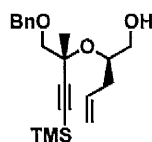
^1H NMR (500 MHz, CDCl_3) δ 7.37-7.27 (m, 5H), 5.97-5.89 (m, 2H), 5.12 (dq, $J = 17.4, 1.5$ Hz, 1H), 5.09-5.06 (m, 1H), 4.52 (d, A of AB, $J_{AB} = 12.3$ Hz, 1H), 4.39 (d, B of AB, $J_{AB} = 12.3$ Hz, 1H), 3.99 (ddd, $J = 8.6, 3.8, 3.1$ Hz, 1H), 3.78 (dd, A of ABX, $J_{AB} = 8.9$ Hz, $J_{AX} = 3.0$ Hz, 1H), 3.63 (d, A of AB, $J_{AB} = 9.6$ Hz, 1H), 3.50 (d, B of AB, $J_{AB} = 9.6$ Hz, 1H), 2.96 (app. t, $J = 8.8$ Hz, 1H), 2.53-2.45 (m, 1H), 2.33-2.27 (m, 1H), 2.23-2.16 (m, 1H), 1.47 (s, 3H), 0.77 (d, $J = 7.0$ Hz, 3H), 0.75 (d, $J = 6.9$ Hz, 3H), 0.24 (s, 9H).

^{13}C NMR (125 MHz, CDCl_3) δ 173.21 (e), 153.40 (e), 138.70 (e), 134.10 (o), 128.60 (o), 127.41 (o), 126.17 (o), 117.51 (e), 104.60 (e), 92.24 (e), 78.23 (e), 74.58 (o), 74.37 (e), 72.36 (e), 63.17 (e), 57.95 (o), 38.52 (e), 28.28 (o), 25.35 (o), 17.90 (o), 14.82 (o), -0.06 (o).

IR (Neat) 2963 (w), 2173 (w), 1779 (s), 1714 (m), 1386 (m), 1249 (m), 1204 (s), 1120 (m), 1098 (m), 872 (m), 840 (s).

HRMS (ESI, $[\text{M} + \text{Na}]^+$) calcd for $\text{C}_{26}\text{H}_{37}\text{NO}_5\text{NaSi}$ 494.2339, found 494.2328.

(*R*)-2-(((*R*)-1-(Benzyloxy)-2-methyl-4-(trimethylsilyl)but-3-yn-2-yl)oxy)pent-4-en-1-ol



To a solution of alkylated glycolate **84** (3.89 g, 8.24 mmol) and methanol (0.66 mL, 16.47 mmol) in THF (82 mL) was added lithium borohydride (8.24 mL, 16.47 mmol, 2M in THF)

dropwise at 0 °C. The reaction mixture was stirred at 0 °C for 30 minutes followed by 2.5 hours at room temperature after which the reaction mixture was quenched with methanol (10 mL) and brine (5 mL). The reaction mixture was partitioned with EtOAc and the phases were separated. The combined organic phases were dried with MgSO₄ and concentrated under *vacuo* and purified by flash chromatography (10% EtOAc-hexanes as eluent) to give the title compound (2.5 g, 88%) as a colourless oil.

$[\alpha]_D^{20} +9.4$ (c = 0.43, CHCl₃).

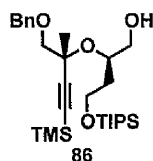
¹H NMR (500 MHz, CDCl₃) δ 7.37-7.28 (m, 5H), 5.81-5.73 (m, 1H), 5.08-5.02 (m, 2H), 4.65 (d, A of AB, J_{AB} = 12.0 Hz, 1H), 4.51 (d, B of AB, J_{AB} = 12.0 Hz, 1H), 3.98-3.93 (m, 1H), 3.73 (d, A of AB, J_{AB} = 10.2 Hz, 1H), 3.61-3.54 (m, 1H), 3.46-3.40 (m, 2H), 3.33 (d, B of AB, J_{AB} = 10.2 Hz, 1H), 2.51-2.45 (m, 1H), 2.26-2.20 (m, 1H), 1.49 (s, 3H), 0.16 (s, 9H).

¹³C NMR (125 MHz, CDCl₃) δ 137.17 (e), 134.07 (o), 128.28 (o), 127.77 (o), 127.73 (o), 117.04 (e), 104.88 (e), 90.84 (e), 75.23 (o), 73.76 (e), 73.15 (e), 72.67 (e), 64.90 (e), 37.62 (e), 25.60 (o), -0.32 (o).

IR (Neat) 3476 (br, w), 2958 (w), 2169 (w), 1640 (w) 1250 (m), 1091 (m), 1064 (m), 841 (s), 760 (m).

HRMS (ESI, [M + Na]⁺) calcd for C₂₀H₃₀O₃NaSi 369.1862, found 369.1866.

(*R*)-2-(((*R*)-1-(Benzyloxy)-2-methyl-4-(trimethylsilyl)but-3-yn-2-yl)oxy)-4-((triisopropylsilyl)oxy)butan-1-ol



Tetrahydropyranyl ether (0.70 g, 1.184 mmol) was dissolved in 2-propanol (59 mL). Pyridinium-*p*-toluenesulphonate (0.15 g, 0.59 mmol) was added and the reaction was heated to 50 °C. After 9 hours, the mixture was quenched with triethylamine (2 mL) and

concentrated under *vacuo*. The crude oil was purified by flash chromatography (10% EtOAc-hexanes as eluent) to give the alcohol **86** (0.45 g, 75%) as a colorless oil.

$[\alpha]_D^{20} +2.0$ (c = 0.46, CHCl₃).

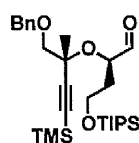
¹H NMR (500 MHz, CDCl₃) δ 7.35-7.28 (m, 5H), 4.65 (d, A of AB, J_{AB} = 12.1 Hz, 1H), 4.54 (d, B of AB, J_{AB} = 12.1 Hz, 1H), 4.08-4.04 (m, 1H), 3.81-3.69 (m, 3H), 3.66 (d, A of AB, J_{AB} = 10.1 Hz, 1H), 3.52 (ddd, J = 11.6, 7.3, 4.3 Hz, 1H), 3.37 (d, B of AB, J_{AB} = 10.1 Hz, 1H), 3.34 (dd, J = 8.7, 4.3 Hz, 1H), 1.95-1.89 (m, 1H), 1.80-1.73 (m, 1H), 1.48 (s, 3H), 1.12-1.06 (m, 21H), 0.16 (s, 9H).

¹³C NMR (125 MHz, CDCl₃) δ 137.71 (e), 128.52 (o), 127.88 (o), 127.86 (o), 105.54 (e), 90.90 (e), 74.77 (e), 74.25 (o), 73.44 (e), 73.13 (e), 65.72 (e), 60.17 (e), 36.56 (e), 25.52 (o), 18.14 (o), 11.99 (o), -0.13 (o).

IR (Neat) 3477 (br, w), 2942 (m), 2865 (m), 2168 (w), 1463 (w) 1251 (m), 1095 (s), 880 (m), 843 (s), 734 (m).

HRMS (ESI, $[M + Na]^+$) calcd for C₂₈H₅₀O₄NaSi₂ 529.3145, found 529.3148.

(*R*)-2-(((*R*)-1-(Benzyloxy)-2-methyl-4-(trimethylsilyl)but-3-yn-2-yl)oxy)-4-((triisopropylsilyl)oxy)butanal



In a flame-dried under an argon atmosphere, oxalyl chloride (0.095 mL, 1.09 mmol) was dissolved in CH₂Cl₂ (6.8 mL). The reaction mixture was cooled to -78 °C before DMSO (0.15 mL, 2.17 mmol) was added dropwise. After stirring for 20 minutes at -78 °C, alcohol **86** (0.34 g, 0.68 mmol) in CH₂Cl₂ (6.8 mL) was added dropwise. The white slurry was stirred 20 min at -78 °C before triethylamine (0.47 mL, 3.39 mmol) was added slowly. After the addition was complete the solution was allowed to warm to room temperature in 1.5 hours before being diluted in diethyl ether (10 mL). The reaction mixture was partitioned

with Et₂O and the phases were separated. The combined organic phases were dried with MgSO₄ concentrated under *vacuo* and passed through a pad of silica to afford the title compound as a colourless oil which was immediately used in the hetero Pauson-Khand reaction.

$$[\alpha]_D^{20} +23.2 \text{ (c = 0.41, CHCl}_3\text{)}.$$

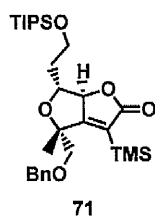
¹H NMR (500 MHz, CDCl₃) δ 9.75 (d, *J* = 2.1 Hz, 1H), 7.34-7.28 (m, 5H), 4.62 (s, 2H), 4.38 (ddd, *J* = 6.7, 5.6, 2.0 Hz, 1H), 3.85 (app. dt, *J* = 10.0, 6.1 Hz, 1H), 3.75 (app. dt, *J* = 10.0, 6.2 Hz, 1H), 3.55 (s, 2H), 1.89-1.82 (m, 2H), 1.47 (s, 3H), 1.10-1.03 (m, 21H), 0.15 (s, 9H).

¹³C NMR (125 MHz, CDCl₃) δ 205.74 (o), 138.23 (e), 128.45 (o), 127.69 (o), 127.63 (o), 105.23 (e), 92.34 (e), 76.56 (o), 76.43 (e), 74.48 (e), 73.50 (e), 58.80 (e), 35.57 (e), 24.12 (o), 18.13 (o), 12.03 (o), -0.26 (o).

IR (Neat) 2943 (w), 2866 (m), 2172 (w), 1732 (m) 1464 (w), 1251 (m), 1098 (s), 882 (m), 842 (s), 732 (m).

HRMS (ESI, [M + Na]⁺) calcd for C₂₈H₄₈O₄NaSi₂ 527.2989, found 527.2968.

(4*R*,6*R*,6*aS*)-4-((Benzyloxy)methyl)-4-methyl-6-(2-((triisopropylsilyl)oxy)ethyl)-3-(trimethylsilyl)-6,6*a*-dihydrofuro[3,4-*b*]furan-2(4*H*)-one



Freshly prepared Mo(CO)₃(DMF)₃ (0.26 g, 0.64 mmol) was charged in a flame-dried flask under an argon atmosphere. A solution of aldehyde (0.32 g, 0.64 mmol) in THF (32 mL) was added dropwise and the resulting brown reaction mixture was stirred at room temperature for 15 minutes. The reaction mixture was passed through a pad of silica aided

by ethyl acetate and concentrated under *vacuo*. The crude brown oil was purified by flash chromatography (10% EtOAc-hexanes as eluent) to afford the bicyclic lactone **71** (0.22 g, 65%, 2 steps) as a colourless oil.

$[\alpha]_D^{20}$ -105.1 ($c = 0.74$, CHCl_3).

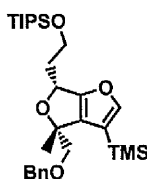
$^1\text{H NMR}$ (500 MHz, CDCl_3) δ 7.36-7.27 (m, 5H), 4.88 (d, $J = 9.6$ Hz, 1H), 4.65 (d, A of AB, $J_{AB} = 12.4$ Hz, 1H), 4.47 (d, B of AB, $J_{AB} = 12.4$ Hz, 1H), 3.87-3.84 (m, 2H), 3.65 (ddd, $J = 9.6, 7.3, 4.9$ Hz, 1H), 3.59 (d, A of AB, $J_{AB} = 10.2$ Hz, 1H), 3.56 (d, B of AB, $J_{AB} = 10.5$ Hz, 1H), 2.14-2.04 (m, 1H), 2.01-1.90 (m, 1H), 1.39 (s, 3H), 1.11-1.01 (m, 21H), 0.24 (s, 9H).

$^{13}\text{C NMR}$ (125 MHz, CDCl_3) δ 186.68 (e), 177.93 (e) 137.77 (e), 128.58 (o), 127.96 (o), 127.75 (o), 125.07 (e), 87.61 (o), 80.77 (e), 74.38 (e), 74.28 (o), 73.62 (e), 59.30 (e), 36.74 (e), 23.68 (o), 18.13 (o), 12.01 (o), -0.73 (o).

IR (Neat) 2943 (m), 2865 (m), 1753 (s) 1632 (w) 1463 (w), 1249 (m), 1100 (s), 882 (m), 841 (s), 735 (m).

HRMS (ESI, $[\text{M} + \text{Na}]^+$) calcd for $\text{C}_{29}\text{H}_{48}\text{O}_5\text{NaSi}_2$ 555.2938, found 555.2940.

(2-(((4*R*,6*R*)-4-((Benzyloxy)methyl)-4-methyl-3-(trimethylsilyl)-4,6-dihydrofuro[3,4-*b*]furan-6-yl)ethoxy)triisopropylsilane



To a solution of bicyclic lactone **71** (0.051 g, 0.096 mmol) in CH_2Cl_2 (1.9 mL) was added DIBAL-H (0.19 mL, 0.19 mmol, 1M in hexane) dropwise at -97°C . The reaction mixture was stirred at -97°C for 1.15 hours after which the reaction mixture was quenched with 6N HCl (0.41 mL). The biphasic solution was warmed to room temperature and further stirred for 1.30 hours. The reaction mixture was partitioned with CH_2Cl_2 and the phases were

separated. The combined organic phases were dried with MgSO_4 and concentrated under *vacuo* and purified by flash chromatography (5% EtOAc-hexanes as eluent) to give the title compound (0.036 g, 72%) as a colourless oil.

$[\alpha]_D^{20} -17.7$ ($c = 0.21$, CHCl_3).

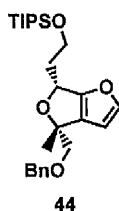
^1H NMR (500 MHz, CDCl_3) δ 7.34-7.25 (m, 5H), 7.20 (s, 1H), 5.15 (t, $J = 6.4$ Hz, 1H), 4.63 (d, A of AB, $J_{AB} = 12.4$ Hz, 1H), 4.56 (d, B of AB, $J_{AB} = 12.4$ Hz, 1H), 3.92-3.86 (m, 2H), 3.56 (d, A of AB, $J_{AB} = 10.1$ Hz, 1H), 3.49 (d, B of AB, $J_{AB} = 10.1$ Hz, 1H), 2.05-1.93 (m, 2H), 1.47 (s, 3H), 1.11-1.01 (m, 21H), 0.17 (s, 9H).

^{13}C NMR (125 MHz, CDCl_3) δ 159.67 (e), 152.06 (o), 138.52 (e), 131.60 (e), 128.39 (o), 127.80 (o), 127.57 (o), 115.77 (e), 83.73 (e), 77.05 (e), 73.46 (e), 72.61 (o), 59.92 (e), 39.60 (e), 24.45 (o), 18.15 (o), 12.07 (o), -0.10 (o).

IR (Neat) 2943 (m), 2865 (m), 1463 (w), 1367 (w), 1249 (m), 1101 (s), 1064 (m), 882 (m), 838 (s), 752 (m).

HRMS (ESI, $[\text{M} + \text{Na}]^+$) calcd for $\text{C}_{29}\text{H}_{48}\text{O}_4\text{NaSi}_2$ 539.2989, found 539.2993.

(2-((4*R*,6*R*)-4-((Benzyloxy)methyl)-4-methyl-4,6-dihydrofuro[3,4-*b*]furan-6-yl)ethoxy) triisopropylsilane



To the solution of 3-trimethylsilyl substituted furan derivative (0.01 g, 0.019 mmol) in DMF (0.19 mL) was added 2-propanol (7.16 μL , 0.093 mmol) and sodium hydride (0.0039 g, 0.097 mmol, 60% in oil) sequentially at room temperature. The reaction mixture was stirred for 30 minutes after which the reaction mixture was quenched with water (1 mL). The reaction mixture was partitioned with diethyl ether and the phases were separated. The combined organic phases were dried with MgSO_4 and concentrated under *vacuo* and

purified by flash chromatography (5% EtOAc-hexanes as eluent) to afford bicyclic furan **44** (0.0058 g, 67%) as a colourless oil.

$[\alpha]_D^{20} +4.5$ (c = 0.58, CHCl₃).

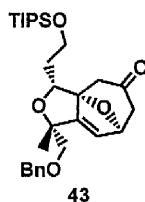
¹H NMR (500 MHz, CDCl₃) δ 7.47-7.28 (m, 6H), 6.26 (d, J = 1.3 Hz, 1H), 5.17 (t, J = 6.4 Hz, 1H), 4.59 (d, A of AB, J_{AB} = 12.5 Hz, 1H), 4.56 (d, B of AB, J_{AB} = 12.4 Hz, 1H), 3.88 (t, J = 6.6 Hz, 2H), 3.52 (d, A of AB, J_{AB} = 9.5 Hz, 1H), 3.49 (d, B of AB, J_{AB} = 9.5 Hz, 1H), 1.98 (q, J = 6.5 Hz, 2H), 1.47 (s, 3H), 1.11-1.05 (m, 21H).

¹³C NMR (125 MHz, CDCl₃) δ 158.69 (e) 147.04 (o), 138.73 (e), 128.87 (e), 128.43 (o), 127.57 (o), 127.54 (o), 106.17 (o), 82.92 (e), 77.64 (e), 73.56 (e), 73.31 (o), 59.91 (e), 39.66 (e), 24.44 (o), 18.16 (o), 12.15 (o).

IR (Neat) 2942 (m), 2865 (m), 1463 (m), 1367 (w), 1102 (s), 1069 (m), 994 (m), 882 (m), 733 (m).

HRMS (ESI, $[M + Na]^+$) calcd for C₂₆H₄₀O₄NaSi 467.2594, found 467.2604.

(1*R*,3*R*,3*aR*,7*S*)-1-((Benzyloxy)methyl)-1-methyl-3-(2-((triisopropylsilyl)oxy)ethyl)-3,4,6tetrahydro-3*a*,7-epoxycyclohepta[*c*]furan-5(1*H*)-one



In a flame-dried under an argon atmosphere, furan **44** (0.001 g, 0.022 mmol) was dissolved in 2,2,2-trifluoroethanol (0.23 mL). To the reaction mixture was added NaTFE (0.07 mL, 0.139 mmol, 2M in TFE) at room temperature over an hour and the solution was further stirred at ambient temperature for 2 hours (TLC control) after which the reaction mixture was quenched with water (1 mL). The reaction mixture was partitioned with EtOAc and the phases were separated. The combined organic phases were dried with MgSO₄ and concentrated under *vacuo* and was redissolved in methanol saturated with ammonium

chloride (0.45 mL). To the reaction mixture Zn-Cu couple (0.053 g) was added in a single portion and the suspension was stirred for 24 hours at room temperature. The reaction mixture was filtered over a pad of celite aided with ethyl acetate and concentrated under *vacuo*. The crude oil was purified by silica-gel chromatography (20% EtOAc-hexanes as eluent) to afford cycloadduct **43** (0.009 g, 80%) as a colourless oil with $\geq 19 : 1$ diastereoselectivity (by ^1H NMR).

$[\alpha]_{\text{D}}^{20} +30.7$ ($c = 0.45$, CHCl_3).

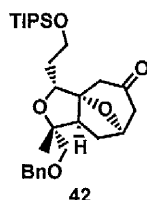
^1H NMR (500 MHz, CDCl_3) δ 7.36-7.27 (m, 5H), 5.96 (d, $J = 2.0$ Hz, 1H), 5.28 (dd, $J = 4.8, 1.5$ Hz, 1H), 4.59 (d, A of AB, $J_{AB} = 12.1$ Hz, 1H), 4.54 (d, B of AB, $J_{AB} = 12.2$ Hz, 1H), 4.07 (dd, $J = 8.8, 5.3$ Hz, 1H), 3.80 (t, $J = 6.5$ Hz, 2H), 3.43 (s, 2H), 2.90 (d, A of AB, $J_{AB} = 16.3$ Hz, 1H), 2.83-2.76 (m, 2H), 2.41 (d, B of AB, $J_{AB} = 16.3$ Hz, 1H), 1.86-1.80 (m, 1H), 1.75-1.69 (m, 1H), 1.35 (s, 3H), 1.08-1.03 (m, 21H).

^{13}C NMR (125 MHz, CDCl_3) δ 204.99 (e), 156.76 (e), 138.31 (e), 128.54 (o), 127.78 (o), 127.63 (o), 123.19 (o), 93.66 (e), 86.08 (o), 77.42 (e), 77.22 (o), 77.12 (e), 73.73 (e), 59.81 (e), 51.53 (e), 45.63 (e), 35.17 (e), 23.58 (o), 18.19 (o), 11.90 (o).

IR (Neat) 2927 (m), 2865 (m), 1721 (m), 1455 (w), 1100 (s), 1070 (m), 882 (m), 754 (s).

HRMS (ESI, $[\text{M} + \text{Na}]^+$) calcd for $\text{C}_{29}\text{H}_{44}\text{O}_5\text{NaSi}$ 523.2856, found 523.2869.

(1*R*,3*R*,3*aR*,7*R*,8*aS*)-1-((Benzyloxy)methyl)-1-methyl-3-(2-((triisopropylsilyl)oxy)ethyl)hexahydro-3*a*,7-epoxycyclohepta[*c*]furan-5(1*H*)-one



Cycloadduct **43** (0.009 mg, 0.018 mmol) was dissolved in ethyl acetate (0.36 mL). To the reaction mixture, triethylamine (0.11 mL) followed by 5% Pd-C was added under argon in a single portion and the suspension was stirred at room temperature for 3 hours. The reaction

mixture was filtered over celite aided by ethyl acetate and concentrated under *vacuo* to afford cycloadduct **42** (0.009 g, quant.) as a colourless oil with $\geq 19 : 1$ diastereoselectivity (by ^1H NMR).

$[\alpha]_D^{20} +21.1$ ($c = 0.35$, CHCl_3).

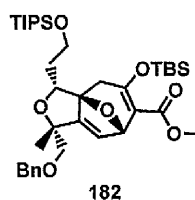
^1H NMR (500 MHz, CDCl_3) δ 7.35-7.28 (m, 5H), 4.70 (app. t, $J = 6.4$ Hz, 1H), 4.54 (d, A of AB, $J_{AB} = 11.9$ Hz, 1H), 4.48 (d, B of AB, $J_{AB} = 12.0$ Hz, 1H), 3.97 (dd, $J = 6.7, 5.5$ Hz, 1H), 3.89-3.84 (m, 1H), 3.83-3.78 (m, 1H), 3.42 (d, A of AB, $J_{AB} = 9.2$ Hz, 1H), 3.37 (d, B of AB, $J_{AB} = 9.2$ Hz, 1H), 2.68 (d, A of AB, $J_{AB} = 15.5$ Hz, 1H), 2.62 (dd, $J = 16.3, 5.7$ Hz, 1H), 2.37-2.34 (m, 2H), 2.29 (d, $J = 16.2$ Hz, 1H), 2.24-2.19 (m, 1H), 1.94-1.87 (m, 3H), 1.28 (s, 3H), 1.09-1.04 (m, 21H).

^{13}C NMR (125 MHz, CDCl_3) δ 206.76 (e), 138.24 (e), 128.49 (o), 127.84 (o), 127.80 (o), 92.78 (e), 81.87 (e), 76.80 (o), 76.18 (o), 74.53 (e), 73.62 (e), 60.42 (e), 56.03 (o), 49.81 (e), 48.18 (e), 34.33 (e), 32.45 (e), 25.20 (o), 18.18 (o), 12.11 (o).

IR (Neat) 2925 (m), 2865 (m), 1721 (m), 1463 (m), 1097 (s), 1075 (s), 882 (m), 735 (m).

HRMS (ESI, $[\text{M} + \text{Na}]^+$) calcd for $\text{C}_{29}\text{H}_{46}\text{O}_5\text{NaSi}$ 525.3012, found 525.3007.

(1*R*,3*R*,3*aS*,7*S*)-methyl-1-((Benzyloxy)methyl)-5-((*tert*-butyldimethylsilyl)oxy)-1-methyl-3-(2-((triisopropylsilyl)oxy)ethyl)-1,3,4,7-tetrahydro-3*a*,7-epoxycyclohepta[*c*]furan-6-carboxylate



In a flame-dried under an argon atmosphere, furan **44** (0.013 mg, 0.029 mmol) and $\text{Rh}_2(\text{S-PTAD})_4$ (0.0028 mg, 1.46 μmol) were dissolved in hexane (1.5 mL). To the reaction mixture was added diazoester (0.011 mg, 0.044 mmol) in hexane (1.5 mL) at 70 $^\circ\text{C}$ over an hour and the solution was further stirred at same temperature for 15 minutes (TLC control). The

reaction mixture was passed through a pad of silica aided by ethyl acetate and concentrated under *vacuo* to afford a green oil. Purification by flash chromatography (10% EtOAc-hexanes as eluent) to afforded cycloaduct **182** (0.015 g, 76%) as a colourless oil with $\geq 19 : 1$ diastereoselectivity (by ^1H NMR).

$[\alpha]_{\text{D}}^{20} -21.5$ (c = 0.69, CHCl_3).

^1H NMR (500 MHz, CDCl_3) δ 7.34-7.26 (m, 5H), 6.19 (d, $J = 2.1$ Hz, 1H), 5.55 (d, $J = 1.9$ Hz, 1H), 4.58 (d, A of AB, $J_{AB} = 12.9$ Hz, 1H), 4.49 (d, B of AB, $J_{AB} = 12.9$ Hz, 1H), 4.10 (dd, $J = 9.0, 4.3$ Hz, 1H), 3.88-3.79 (m, 2H), 3.72 (s, 3H), 3.38 (d, A of AB, $J_{AB} = 10.0$ Hz, 1H), 3.34 (d, B of AB, $J_{AB} = 10.0$ Hz, 1H), 2.60 (d, A of AB, $J_{AB} = 17.4$ Hz, 1H), 2.45 (d, B of AB, $J_{AB} = 17.4$ Hz, 1H), 1.93-1.86 (m, 1H), 1.83-1.75 (m, 1H), 1.31 (s, 3H), 1.21-1.04 (m, 21H), 0.92 (s, 9H), 0.19 (s, 3H), 0.14 (s, 3H).

^{13}C NMR (125 MHz, CDCl_3) δ 165.45 (e), 158.66 (e), 155.50 (e), 138.22 (e), 129.04 (o), 128.46 (o), 127.69 (o), 113.67 (e), 92.75 (e), 85.71 (o), 78.63 (e), 75.78 (o), 75.22 (e), 73.26 (e), 60.10 (e), 51.00 (o), 33.01 (e), 32.66 (e), 25.74 (o), 23.90 (o), 18.44 (e), 18.19 (o), 12.14 (o), -3.42 (o), -3.53 (o).

IR (Neat) 2930 (m), 2864 (m), 1720 (m), 1686 (m), 1617 (m), 1463 (w), 1369 (m), 1206 (s), 1099 (s), 902 (m), 829 (m), 782 (m), 733 (m).

HRMS (ESI, $[\text{M} + \text{Na}]^+$) calcd for $\text{C}_{37}\text{H}_{60}\text{O}_7\text{NaSi}_2$ 695.3775, found 695.3779.

3.7 References

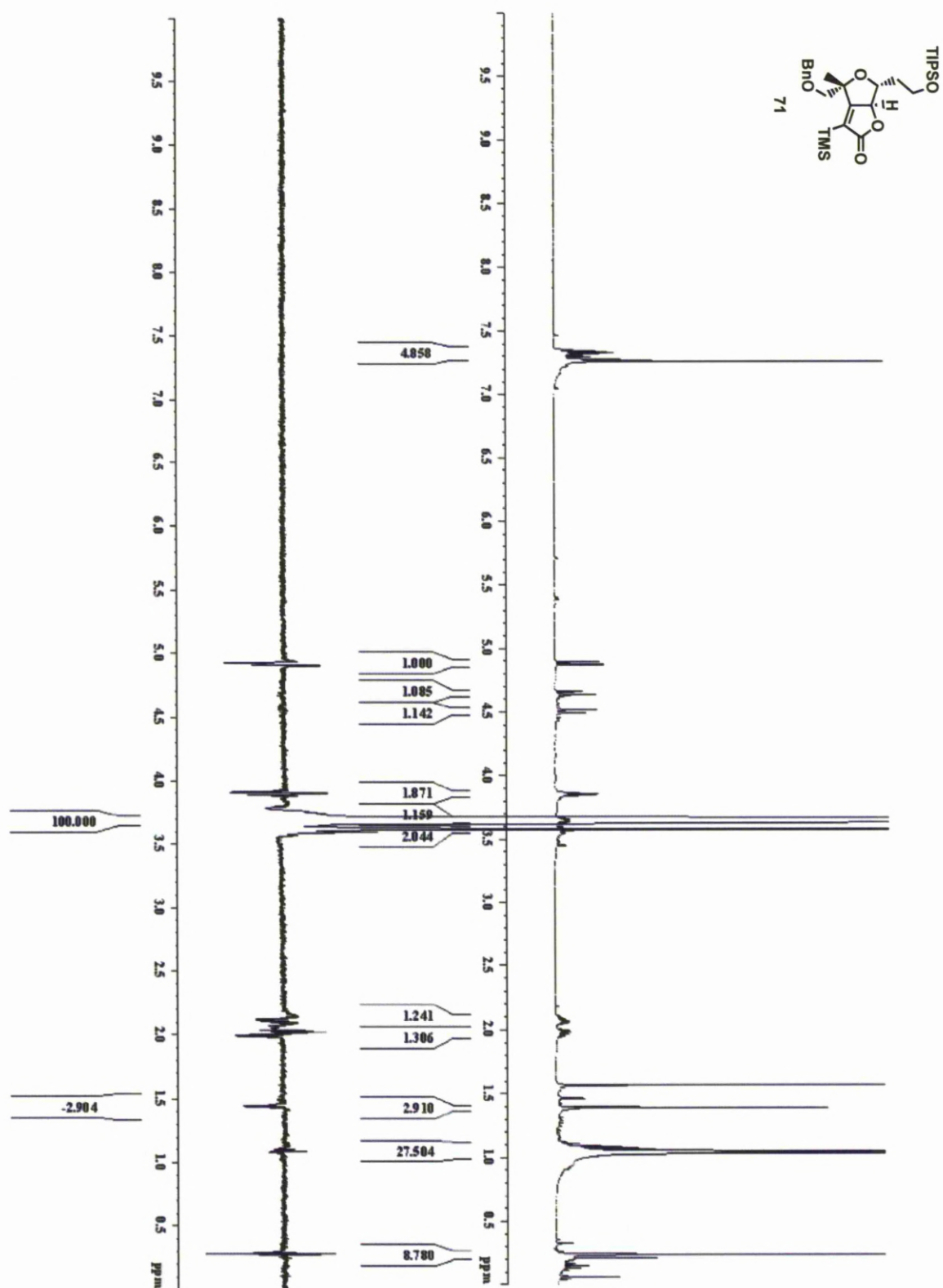
- 1 Paquette, L. A.; Lai, K. W. *Org. Lett.* **2008**, *10*, 2111, and references cited therein.
- 2 (a) Miwa, K.; Aoyama, T.; Shioiri, T. *Synlett* **1994**, 107. (b) Colvin, E. W.; Hamill, B. J. *J Chem Soc Chem Comm* **1973**, 151.
- 3 Kolb, H. C.; Vannieuwenhze, M. S.; Sharpless, K. B. *Chem. Rev.* **1994**, *94*, 2483.
- 4 Maity, S.; Matcha, K.; Ghosh, S. *J. Org. Chem.* **2010**, *75*, 4192.
- 5 Imagawa, H.; Saijo, H.; Kurisaki, T.; Yamamoto, H.; Kubo, M.; Fukuyama, Y.; Nishizawa, M. *Org. Lett.* **2009**, *11*, 1253.
- 6 Fohlich, B.; Flogaus, R.; Henle, G. H.; Sendelbach, S.; Henkel, S. *Eur. J. Org. Chem.* **2006**, 2160.
- 7 (a) Wright, D. L.; Whitehead, C. R.; Sessions, E. H.; Ghiviriga, I.; Frey, D. A. *Org. Lett.* **1999**, *1*, 1535, and pertinent references cited therein. (b) Lee, J. C.; Cha, J. K. *J. Am. Chem. Soc.* **2001**, *123*, 3243. (c) Lee, J. C.; Cha, J. K. *Tetrahedron* **2000**, *56*, 10175. (d) Lee, J. C.; Jin, S. J.; Cha, J. K. *J. Org. Chem.* **1998**, *63*, 2804.
- 8 Miyaura, N.; Suzuki, A. *Chem. Rev.* **1995**, *95*, 2457.
- 9 Sparks, S. M.; Chen, C. L.; Martin, S. F. *Tetrahedron* **2007**, *63*, 8619.
- 10 Kwok, T. J.; Virgilio, J. A. *Org. Process Res. Dev.* **2005**, *9*, 694, and pertinent references cited therein.
- 11 Mandville, G.; Girard, C.; Bloch, R. *Tetrahedron Asymmetry* **1997**, *8*, 3665.
- 12 (a) Evans, P. A.; Raina, S.; Ahsan, K. *Chem. Commun.* **2001**, 2504. (b) Evans, P. A.; Manangan, T.; Rheingold, A. L. *J. Am. Chem. Soc.* **2000**, *122*, 11009.
- 13 Zhou, X. F.; Wu, W. Q.; Liu, X. Z.; Lee, C. S. *Org. Lett.* **2008**, *10*, 5525.
- 14 Corey, E. J.; Helal, C. J. *Angew. Chem. Int. Ed.* **1998**, *37*, 1987.
- 15 Kolb, H. C.; Vannieuwenhze, M. S.; Sharpless, K. B. *Chem. Rev.* **1994**, *94*, 2483.
- 16 (a) Vassilikogiannakis, G.; Margaros, I.; Montagnon, T.; Stratakis, M. *Chem.-Eur. J.* **2005**, *11*, 5899. (b) Takikawa, H.; Ueda, K.; Sasaki, M. *Tetrahedron Lett.* **2004**, *45*, 5569.
- 17 Adrio, J.; Carretero, J. C. *J. Am. Chem. Soc.* **2007**, *129*, 778.
- 18 (a) Crimmins, M. T.; Zuccarello, J. L.; Cleary, P. A.; Parrish, J. D. *Org. Lett.* **2006**, *8*, 159. (b) Crimmins, M. T.; Emmitte, K. A.; Katz, J. D. *Org. Lett.* **2000**, *2*, 2165.
- 19 Knight, D. W.; Qing, X. *Tetrahedron Lett.* **2009**, *50*, 3534.
- 20 Martinelli, M. J.; Nayyar, N. K.; Moher, E. D.; Dhokte, U. P.; Pawlak, J. M.; Vaidyanathan, R. *Org. Lett.* **1999**, *1*, 447.

- 21 Yu, C. M.; Hong, Y. T.; Lee, J. H. *J. Org. Chem.* **2004**, *69*, 8506.
- 22 Yang, Y. K.; Choi, J. H.; Tae, J. *J. Org. Chem.* **2005**, *70*, 6995.
- 23 Fort, A. W. *J. Am. Chem. Soc.* **1962**, *84*, 2620.
- 24 For reviews on [4+3] cycloaddition reactions, see: (a) Harmata, M. *Chem. Commun.* **2010**, *46*, 8904. (b) Harmata, M. *Chem. Commun.* **2010**, *46*, 8886. (c) Harmata, M. *Adv. Synth. Catal.* **2006**, *348*, 2297. (d) Niess, B.; Hoffmann, H. M. R. *Angew. Chem. Int. Ed.* **2005**, *44*, 26. (e) Hartung, I. V.; Hoffmann, H. M. R. *Angew. Chem. Int. Ed.* **2004**, *43*, 1934. (f) Harmata, M. *Acc. Chem. Res.* **2001**, *34*, 595. (g) Cha, J. K.; Oh, J. *Curr. Org. Chem.* **1998**, *2*, 217. (h) Rigby, J. H.; Pigge, F. C. *Org. React.* **1997**, *51*, 351. (i) Harmata, M. *Tetrahedron* **1997**, *53*, 6235. (j) Hosomi, A.; Tominaga, Y. in *Comprehensive Organic Synthesis* (Eds.: Trost, B. M.; Fleming), Pergamon, Oxford, **1991**, Vol. 5, p. 593-615. (k) Mann, J. *Tetrahedron* **1986**, *42*, 4611. (l) Hoffmann, H. M. R. *Angew. Chem. Int. Ed.*, **1984**, *96*, 1. (m) Noyori, R.; Hayadawa, Y. *Org. React.* **1983**, *29*, 163. (n) Noyori, R. *Acc. Chem. Res.* **1979**, *12*, 61. (o) Hoffmann, H. M. R. *Angew. Chem. Int. Ed.*, **1973**, *12*, 819.
- 25 Cookson, R. C.; Nye, M. J.; Subrahmanyam, S. *J. Chem. Soc. C.* **1967**, 473.
- 26 (a) Lautens, M.; Aspiotis, R.; Colucci, J. *J. Am. Chem. Soc.* **1996**, *118*, 10930. (b) Lautens, M.; Stammers, T. A. *Synthesis* **2002**, 1993.
- 27 Mann, J.; Usmani, A. A. *J. Chem. Soc. Chem. Comm.* **1980**, 1119.
- 28 (a) Fohlsch, B.; Herter, R.; Wolf, E.; Stezowski, J. J.; Eckle, E. *Chem. Ber.* **1982**, *115*, 355. (b) Fohlsch, B.; Wolf, E. *J. Chem. Res. S* **1983**, 166.
- 29 Shimizu, N.; Tanaka, M.; Tsuno, Y. *J. Am. Chem. Soc.* **1982**, *104*, 1330.
- 30 (a) Fohlsch, B.; Gehrlach, E.; Geywitz, B. *Chem. Ber.* **1987**, *120*, 1815. (b) Fohlsch, B.; Gehrlach, E.; Stezowski, J. J.; Kollat, P.; Martin, E.; Gottstein, W. *Chem. Ber.* **1986**, *119*, 1661.
- 31 Lee, K.; Cha, J. K. *J. Am. Chem. Soc.* **2001**, *123*, 5590.
- 32 Fohlsch, B.; Krimmer, D.; Gehrlach, E.; Kashammer, D. *Chem. Ber.* **1988**, *121*, 1585.
- 33 Murray, D. H.; Albizati, K. F. *Tetrahedron Lett.* **1990**, *31*, 4109.
- 34 (a) Davies, H. M. L.; Dai, X. *J. Am. Chem. Soc.* **2004**, *126*, 2692. (b) Aungst, R. A.; Funk, R. L. *Org. Lett.* **2001**, *3*, 3553. (c) Harmata, M.; Sharma, U. *Org. Lett.* **2000**, *2*, 2703. (d) Sasaki, T.; Ishibashi, Y.; Ohno, M. *Tetrahedron Lett.* **1982**, *23*, 1693.
- 35 Xiong, H.; Hsung, R. P.; Berry, C. R.; Rameshkumar, C. *J. Am. Chem. Soc.* **2001**, *123*, 7174.
- 36 Chung, W. K.; Lam, S. K.; Lo, B.; Liu, L. L.; Wong, W. T.; Chiu, P. *J. Am. Chem. Soc.* **2009**, *131*, 4556.
- 37 (a) Davies, H. M. L.; Clark, D. M.; Alligood, D. B.; Eiband, G. R. *Tetrahedron* **1987**, *43*,

4265. (b) Davies, H. M. L.; Clark, D. M.; Smith, T. K. *Tetrahedron Lett.* **1985**, 26, 5659.
- 38 Leahy, D. K.; Evans, P. A. in *Modern Rhodium-Catalyzed Organic Reactions* (Ed.: Evans, P. A.), Wiley-VCH: Weinheim, **2005**, Ch. 14, pp 301-337.
- 39 Davies, H. M. L.; Smith, H. D.; Korkor, O. *Tetrahedron Lett.* **1987**, 28, 1853.
- 40 (a) Lian, Y. J.; Miller, L. C.; Born, S.; Sarpong, R.; Davies, H. M. L. *J. Am. Chem. Soc.* **2010**, 132, 12422. (b) Davies, H. M. L.; Ahmed, G.; Churchill, M. R. *J. Am. Chem. Soc.* **1996**, 118, 10774, and pertinent references cited therein. (c) Doyle, M. P.; Bagheri, V.; Wandless, T. J.; Harn, N. K.; Brinker, D. A.; Eagle, C. T.; Loh, K. L. *J. Am. Chem. Soc.* **1990**, 112, 1906.
- 41 Xu, J.; Caro-Diaz, E. J. E.; Theodorakis, E. A. *Org. Lett.* **2010**, 12, 3708.
- 42 Pangborn, A. B.; Giardello, M. A.; Grubbs, R. H.; Rosen, R. K.; Timmers, F. J. *Organometallics* **1996**, 15, 1518.

3.8 Appendix

3.8.1 One-Dimensional ^1H -nOe Data: Proof of Relative Configuration for Compound 71



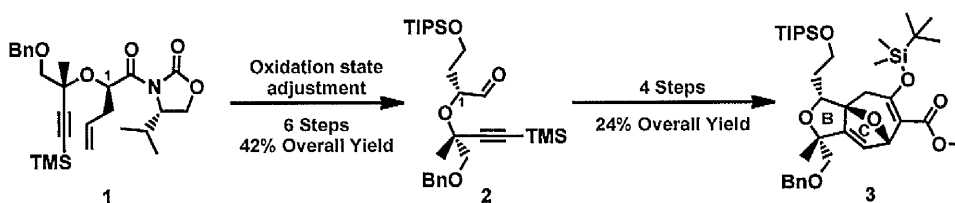


Chapter 4

Model Study for the Second-Generation Synthesis of the Western Fragment and Plans for the Completion of the Synthesis of Lancifodilactone G

4.1 Second-Generation Strategy for the Western Fragment

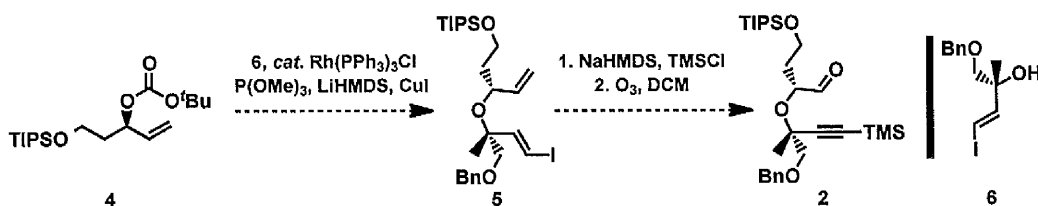
In Chapter 3, we described a highly selective and high-yielding allylation of *N*-acyl oxazolidinone to prepare the glycolate intermediate **1**, which was transformed to the fully functionalised western fragment **3** (Scheme 4.1). However, the conversion of **1** to aldehyde **2** was particularly cumbersome, due to the excessive oxidation state manipulation of the C1 side chain. In order to increase the overall efficiency of the synthesis of the western fragment, we sought to develop a convergent synthetic route for the preparation of **2**.



Scheme 4.1 *First-Generation Synthesis of the Western Fragment.*

Previous studies within the Evans group have demonstrated the merit of the rhodium-catalysed allylic substitution for carbon-carbon and carbon-heteroatom bond construction with a variety of pronucleophiles.¹ Hence, we envisaged that an alternative approach would involve a stereospecific construction of **5**, which would employ the regio- and stereospecific rhodium(I)-catalysed allylic etherification reaction of the allylic carbonate **4** with the tertiary alcohol **6** (Scheme 4.2) in accordance with previous studies.² Base-mediated elimination of the vinyl iodide **5** and *in situ* protection of the resulting terminal alkyne,³ and

chemoselective oxidative cleavage of the monosubstituted alkene would provide the alkynyl aldehyde **2** utilised in our first approach in a more expeditious manner. This strategy provides an opportunity to accomplish a rapid construction of the western fragment of lancifodilactone **G** in 8 longest linear sequence from a known carbonate precursor.⁴



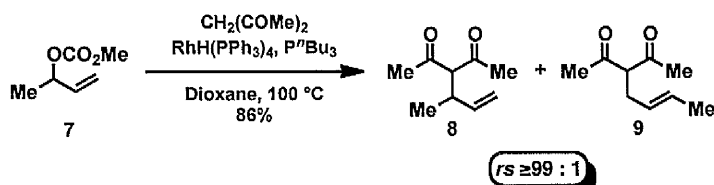
Scheme 4.2 *Second Generation Plan for the Western Fragment.*

One of the unique features in the mechanism of the rhodium(I)-catalysed allylic alkylation is the highly regiospecific nature of the reaction.⁵ The following section will cover the mechanistic aspects of the rhodium(I)-catalysed allylic alkylation with pronucleophiles.⁶

4.2 Development and Mechanism of Rhodium(I)-catalysed Allylic Substitution Reaction

4.2.1 Regiospecificity

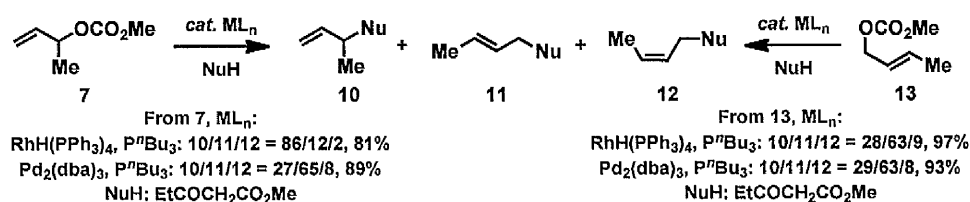
The foundation for Evans' work in the area of regioselective rhodium(I)-catalysed allylic alkylation was laid by Tsuji and co-workers on the regiospecific rhodium-catalysed allylation with carbon nucleophiles using unsymmetrical allylic carbonates under neutral conditions (Scheme 4.3).⁷ The study involved the use of tri-(*n*-butyl) phosphine, which was critical for achieving high yield and turnover in this transformation.



Scheme 4.3 *Tsuji's Regiospecific Allylic Substitution Reaction.*

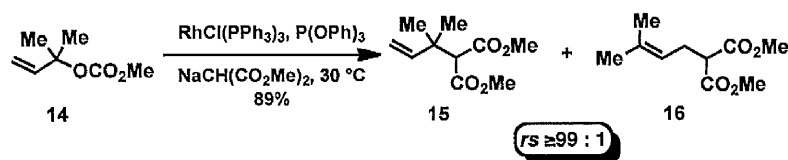
The reaction has a particularly unusual regiospecificity wherein, the branched allylic carbonate **7** predominantly favoured branched product **10** and the isomeric linear carbonate

13 furnished the linear product **11/12** as a mixture of *E/Z*-geometric isomers (Scheme 4.4). Hence, the reaction displayed a memory effect wherein the alkylation could be directed to the either allylic terminus depending on the position of the allylic leaving group. Comparative study with the analogous palladium-catalysed version of the reaction revealed an interesting contrast, in which the same ratio of branched to linear products were obtained regardless of isomeric carbonate employed (Scheme 4.4). These results suggest that rhodium-catalysed allylic alkylation does not proceed through a fluxional π -allyl organorhodium intermediate, but instead proceeds *via* a σ -allyl organorhodium complex as first proposed by Tsuji.^{6,7}



Scheme 4.4 Metal Effect on Regiospecific Allylic Substitution Reaction.

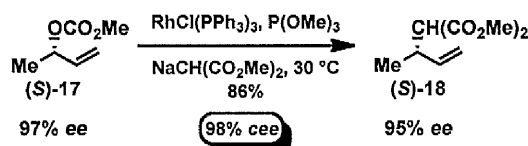
Nearly 14 years after Tsuji's seminal report, Evans and Nelson revisited the rhodium-catalysed allylic substitution reaction and showed that a triorganophosphite-modified Wilkinson's catalyst facilitated the construction of ternary and quaternary allylic products starting from secondary and tertiary allylic carbonates with excellent regioselectivity (Scheme 4.5).^{5,8} The report also outlined the role of triorganophosphites to increase the reaction rate in addition to enhancing regioselectivity. It was hypothesised that the increased π -accepting nature of the triorganophosphite additive promoted alkylation at the more substituted terminus through enhancing the charge build up in the transition state.



Scheme 4.5 Evans' Regioselective Allylic Substitution Reaction.

4.2.2 Enantiospecificity

In an effort to garner insight into the mechanism and explain the high regioselectivity, Evans and Nelson probed the stereospecific manifold of the rhodium(I)-catalysed allylic substitution reaction.⁵ It was thought that if the reaction were to proceed through a σ -allyl metal intermediate, the alkylation of the enantiomerically enriched allylic carbonate (*S*)-**17** should afford a racemic product. However, treatment of the enantiomerically enriched acyclic allylic carbonate (*S*)-**17** under the optimal conditions furnished the allylic alkylation product (*S*)-**18** in 86% yield (98% *cee*), with net retention of absolute configuration (Scheme 4.6).

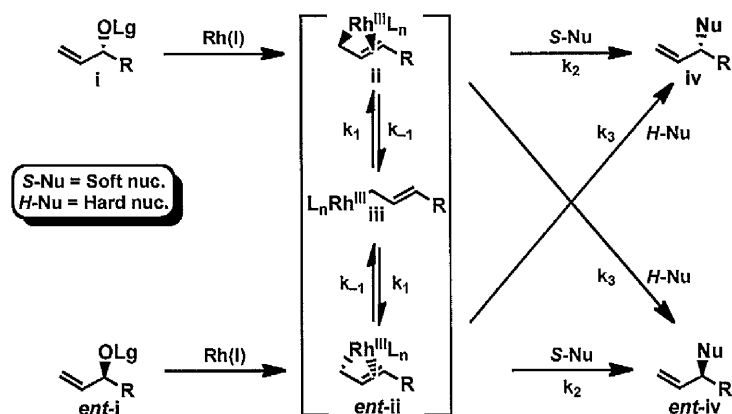


Scheme 4.6 *Enantiospecific Allylic Substitution Reaction.*

Hence the high selectivities observed in the rhodium(I)-catalysed allylic substitution reaction was rationalised by invoking a configurationally stable *enyl* or ($\sigma + \pi$) allyl intermediate, which contains discrete σ - and π -components in the same metal-allyl intermediate. The complex is presumably 18 electron, which prevents facile π - σ - π isomerisation through ligand exchange and thus facilitates the stereospecific allylic alkylation.^{5,6}

Scheme 4.7 illustrates the proposed working model for the observed regio- and stereospecificity in the rhodium(I)-catalysed allylic substitution reaction for different pronucleophiles.^{5,6} The initial complexation of rhodium(I) to the alkene **i** (or *ent-i*) followed by S_N2' oxidative addition of rhodium is thought to furnish the *enyl* intermediate **ii** (or *ent-ii*). The regio- and enantiospecific S_N2' displacement by soft or stabilised nucleophiles (pK_a < 25) can lead to enantiomerically enriched **iv** (or *ent-iv*) provided the initial *enyl* intermediate **ii** (or *ent-ii*) does not isomerise to the achiral organorhodium **iii** via π - σ - π

isomerisation ($k_2 \gg k_1$ or k_{-1}). Alternatively, direct attack of a hard or unstabilised nucleophile ($pK_a > 25$) on the metal centre followed by reductive elimination can also lead to the product of inversion *ent-iv* (or *iv*) with high levels of stereospecificity, if $k_3 \gg k_2$.⁹

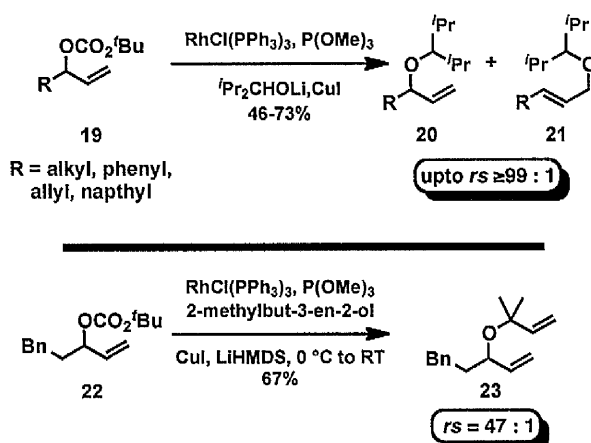


Scheme 4.7 Origin of Stereospecificity in the Allylic Substitution Reaction.

4.3 Rhodium(I)-Catalysed Allylic Etherification

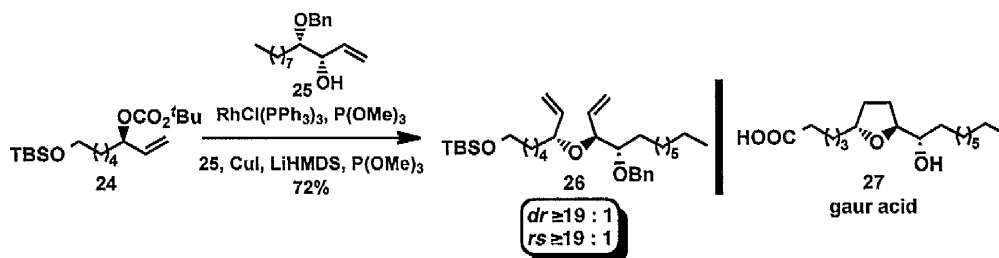
4.3.1 Background

Evans and Leahy extended the rhodium(I)-catalysed allylic substitution reaction to the cross-coupling of unsymmetrical allylic alcohol derivative **19** with secondary and or tertiary alcohols to afford the corresponding acyclic ethers **20** with excellent levels of regioselectivity (Scheme 4.8).² The reaction required transmetallation of the alkali metal alkoxide with a copper(I) halide salt, which was necessary to soften the basic character of the metal alkoxide. During the optimisation study, it was found that the *tert*-butoxycarbonate leaving group was crucial to obtaining high chemical yield, which suppressed the competitive trans-esterification of the leaving group, by the nucleophile. The reaction was compatible with a variety of allylic carbonate derivatives and surprisingly proceeded well with tertiary alcohols, which generally behave as excellent bases and promote elimination under classical alkylation conditions (Scheme 4.8).



Scheme 4.8 Rhodium(I)-Catalysed Allylic Etherification of Secondary and Tertiary Alcohols.

Evans and co-workers also demonstrated that the nature of copper(I) salt employed in the reaction had significant bearing on the stereospecificity of the etherification.^{2,10} In additional studies the group also showed that modification of the copper(I) alkoxide with trimethylphosphite can increase the rate of nucleophilic attack of the organorhodium intermediate prior to the π - σ - π isomerisation, thereby dramatically enhancing the stereospecificity of the etherification. For example, this was utilised in a 7-step synthesis of gaur acid **27** (Scheme 4.9).¹¹

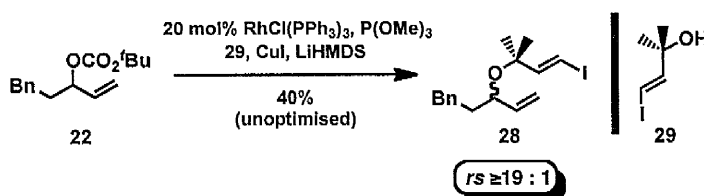


Scheme 4.9 Role of Excess Phosphite in the Rhodium(I)-Catalysed Allylic Etherification.

4.3.2 Rhodium(I)-Catalysed Etherification: Model Study

In order to investigate the key rhodium-catalysed etherification reaction, the allylic carbonate **22** and the allylic alcohol **29** were selected to determine feasibility (Scheme 4.10).^{2,12} Treatment of *in situ* formed copper alkoxide generated from alcohol **29** with trimethyl phosphite modified Wilkinson's catalyst furnished the diene **28** in moderate yield and with excellent regioselectivity (by ^1H NMR).² Since it is important at this stage to

determine the stereospecificity in the etherification reaction, we decided to further improve the efficiency of the allylic substitution reaction employing carbonate **4** and alcohol **6** (Scheme 4.2).

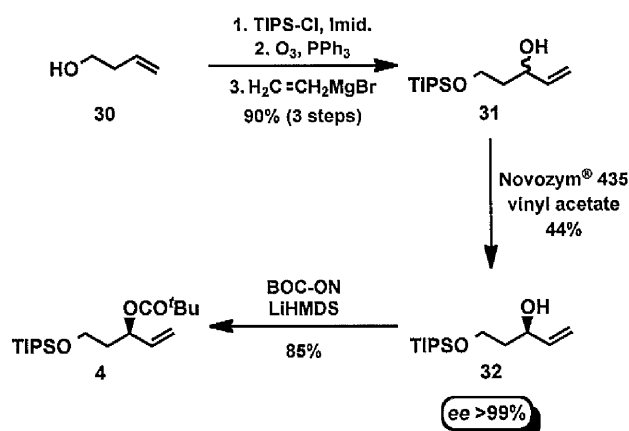


Scheme 4.10 Synthesis of Model Compound **28** Via Rhodium(I)-Catalysed Etherification Reaction.

4.4 Future Studies

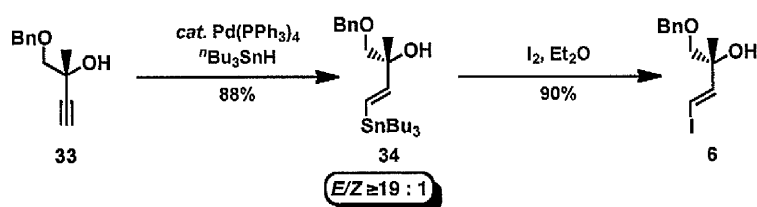
4.4.1 Second-Generation Synthesis of the Western Fragment

The synthesis of allyl carbonate **4** commenced from commercially available homoallylic alcohol **30**, which was converted to a known racemic allylic alcohol **31** using 3-step sequence involving primary silyl protection, ozonolysis of the terminal alkene and Grignard addition to the resulting aldehyde (Scheme 4.11).⁴ Enzymatic kinetic resolution of **31** employing lipase and vinyl acetate furnished the enantiomerically enriched allylic alcohol **32** in 44% yield and with excellent enantiomeric excess (by HPLC).¹³ Subsequent conversion of the secondary alcohol **32** to the *tert*-butoxycarbonate derivative **4** was achieved in 85% yield.



Scheme 4.11 Synthesis of Carbonate **4**.

The tertiary alcohol counterpart required for the rhodium(I)-catalysed allylic etherification reaction was prepared from the propargyl alcohol **33** that was previously used in our first generation synthesis. Palladium-catalysed hydrostannylation of alkyne **33**



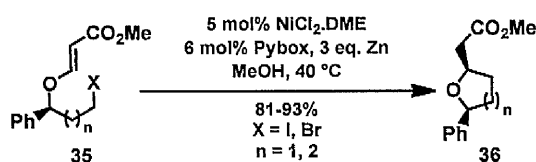
Scheme 4.12 *Synthesis of Tertiary Alcohol 6.*

provided vinyl stannane **34** in 88% yield and with excellent *E/Z* selectivity (by ^1H NMR). Iodination of **34** under standard conditions furnished the vinyl iodide **6** in 90% yield (Scheme 4.12).

As outlined in Scheme 4.2, future work on the coupling of tertiary alcohol **6** with carbonate **4** will involve probing catalyst loading, reaction concentration and modification of the copper alkoxide with phosphite in order to achieve high chemical yield and stereospecificity in the allylic etherification reaction. Conversion of the vinyl iodide **5** to aldehyde **2** (Scheme 4.2) is expected to complete the second-generation synthesis of the western fragment **3**.

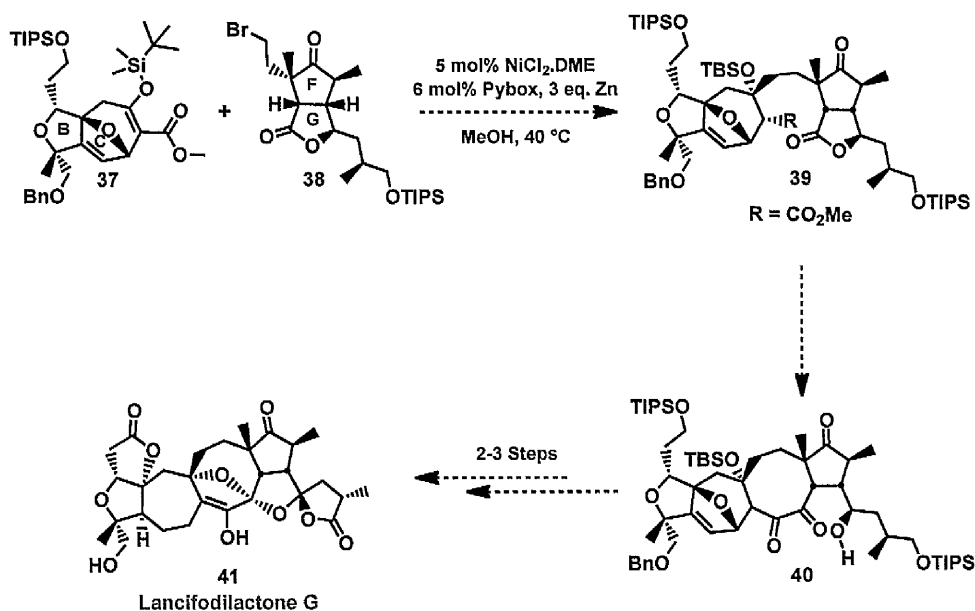
4.4.2 End Game Strategy

With advanced intermediates **37** and **38** in hand, we are at a stage to investigate the end game strategy for lancifodilactone **G 41** (Scheme 4.14). Our initial consideration for the coupling of eastern and western fragments will be the diastereoselective addition of the primary radical generated from the bromide **38** to the tricyclic- β -silyloxy acrylate **37** using conditions developed by Lee and co-workers (Scheme 4.13).¹⁴ It is likely that the 1,4-



Scheme 4.13 *Nickel(II)-Catalysed Radical Cyclisation Reaction of 35.*

addition would be sterically driven from the less hindered β -face of oxatricycle **37**, thereby furnishing **39** with high levels of diastereocontrol (Scheme 4.14). This approach is also anticipated to disfavour the elimination of the β -silyloxy moiety in **37**. In an event that radical addition is unsuccessful, an alternative strategy in the form of 1,2-organozinc addition to the keto hydroxymethylene derived after the deprotection of the silyl enol ester **37** followed by the hydride reduction of the ester side chain would be employed, which again is anticipated to proceed in a diastereoselective manner for the reasons described above. Acyloin condensation between the ester and lactone in **39** can directly lead to octacyclic diketone **40**. Finally, the biomimetic spiroketalisation/lactonisation cascade of **40** would provide a highly convergent total synthesis of lancifodilactone G **41** in 14-15 steps, which will determine the absolute stereochemistry and facilitate studies on the origin of the enol functionality.



Scheme 4.14 End Game for Lancifodilactone G **41**.

4.5 Experimental

4.5.1 General

All reactions were performed in oven-dried (125 °C) or flame-dried glassware under an inert atmosphere of nitrogen or argon. Syringes were oven-dried (125 °C) and then cooled in a desiccator. The following reaction solvents were dried using an alumina column solvent system: toluene (PhMe), diethyl ether (Et₂O) and dichloromethane (DCM) were dried over alumina column solvent system using the method of Grubbs.¹⁵ The following reaction solvents were distilled from the indicated drying agents: tetrahydrofuran (THF) (sodium, benzophenone), hexanes (CaH₂), benzene (PhH) (sodium) and acetonitrile (MeCN) (CaH₂). Triethyl amine (Et₃N) was distilled from CaH₂. Brine refers to a saturated solution of NaCl. All starting material and reagents were purchased from Acros, Aldrich, Alfa Aesar, Fluka, and Strem chemical companies and were used without further purification unless noted otherwise.

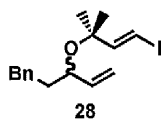
Analytical thin layer chromatography (TLC) was performed on Merck 60 F₂₅₄ precoated silica-gel plates. Visualization was accomplished with a UV light and/or a KMnO₄, or *p*-anisaldehyde solution. Flash column chromatography (FCC) was performed by the method of Still with Merck Silica-gel 60 (230-400 mesh). Solvents for extraction and FCC were technical grade. Reported solvent mixtures for both TLC and FCC were volume/volume mixtures. Infrared spectra (IR) were obtained on a Perkin-Elmer spectrum one series FTIR spectrophotometer. Peaks are reported in cm⁻¹ with the following relative intensities: s (strong), m (medium), w (weak). The Liverpool University Mass Spectroscopy Centre and EPSRC National Spectrometry Centre, Swansea, recorded Mass spectra. High-resolution electron-impact electrospray (ESI) mass spectra were obtained on a Micromass LCT Mass spectrometer and LTQ Orbitrap XL. The specific rotation was measured with a PerkinElmer Model 343 Plus polarimeter.

¹H-NMR and ¹³C-NMR were recorded on a Bruker DRX-500 MHz NMR

spectrometer in the indicated deuterated solvents. For ^1H -NMR, CDCl_3 and C_6D_6 were set to 7.26 ppm (CDCl_3 singlet) and 7.16 (C_6D_6 singlet) respectively and for ^{13}C -NMR, CDCl_3 and C_6D_6 were set to 77.16 ppm (CDCl_3 center of triplet) and 128.06 ppm (C_6D_6 center of triplet) respectively. All values for ^1H -NMR and ^{13}C -NMR chemical shifts for deuterated solvents were obtained from Cambridge Isotope Labs. Data are reported in the following order: chemical shift in ppm (δ) (multiplicity, which are indicated by br (broadened), s (singlet), d (doublet), t (triplet), q (quartet), quint (quintet), m (multiplet)); assignment of 2nd order pattern, if applicable; coupling constants (J , Hz); integration. All ^{13}C -NMR spectra were reported using the descriptor (o) and (e) referring to whether the peak is odd or even, respectively, and correlate to an attached proton test (ATP) experiment.

4.5.2 Experimental Procedures

(*E*)-(3-((4-Iodo-2-methylbut-3-en-2-yl)oxy)pent-4-en-1-yl)benzene



Trimethyl phosphite (0.038 mL, 0.32 mmol) was added directly to a red suspension of Wilkinson's catalyst (0.074 mg, 0.08 mmol) in anhydrous THF (1.5 mL) then heated to 30 °C, under an atmosphere of argon. The catalyst was allowed to form over *ca.* 15 minutes resulting in a light yellow homogeneous solution. Lithium hexamethyldisilyl azide (0.70 mL, 0.70 mmol, 1.0M solution in THF) was added dropwise to a suspension of copper(I) iodide (0.14 g, 0.74 mmol, previously dried *in vacuo* at 160 °C then pyrolyzed in the dark immediately before use) and tertiary alcohol **29** (0.16 g, 0.74 mmol) in anhydrous THF (2.2 mL) under an atmosphere of argon and the anion was allowed to form over *ca.* 2 minutes until a homogeneous solution was obtained. The catalyst and the alkoxide solutions were then cooled with stirring to 0 °C, and the former was then added *via* Teflon® cannula to the copper alkoxide solution. The allylic carbonate **22** (0.095 g, 0.36 mmol) was then added *via* a tared 500 μL gastight syringe to the catalyst/alkoxide mixture, and the reaction was

allowed to slowly warm to room temperature over *ca.* 18 hours (TLC control) resulting in a tan heterogeneous solution. The reaction mixture was filtered through silica gel and washed with ethyl ether, and the filtrate concentrated under *vacuo* to afford a crude oil. Purification by flash chromatography (eluting with 1-2% diethyl ether/hexanes) furnished diene **28** as a colorless oil (0.058 mg, 45%).

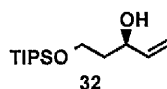
¹H NMR (500 MHz, CDCl₃) δ 7.33-7.20 (m, 5H), 6.61 (d, A of AB, *J*_{AB} = 14.8 Hz, 1H), 6.23 (d, B of AB, *J*_{AB} = 14.8 Hz, 1H), 5.85 (ddd, *J* = 17.3, 10.5, 6.8 Hz, 1H), 5.17-5.12 (m, 2H), 3.90 (app. q, *J* = 6.5 Hz, 1H), 2.72-2.61 (m, 2H), 1.90-1.83 (m, 1H), 1.81-1.74 (m, 1H), 1.30 (s, 3H), 1.29 (s, 3H).

¹³C NMR (125 MHz, CDCl₃) δ 152.60 (o), 142.25 (e), 141.57 (o), 128.50 (o), 125.88 (o), 114.90 (e), 78.36 (e), 76.35 (o), 74.15 (o), 38.67 (e), 31.85 (e), 26.74 (o), 26.45 (o).

IR (Neat) 2977 (w), 2925 (w), 1601 (w), 1455 (w) 1380 (w), 1241 (m), 1134 (m), 1042 (m), 921 (m), 749 (m), 698 (s).

HRMS (ESI, [M + Na]⁺) calcd for C₁₆H₂₁ONa¹²⁷I 379.0535, found 379.0527.

(*R*)-5-((Triisopropylsilyl)oxy)pent-1-en-3-ol



To a solution of (*RS*)-**31** (2.95 g, 11.39 mmol) in toluene (23 mL) were added vinyl acetate (0.98 g, 11.39 mmol) and Novozym® 435 (0.25 g). The reaction mixture was stirred at ambient temperature for 4 days after which the reaction mixture was filtered on a sintered glass funnel. Concentration of the filtrate followed by purification by flash chromatography (5-10% diethyl ether in hexanes as eluent) furnished the desired (*R*)-**32** as a colourless oil (44%, 1.30 g). The enantiomeric excess was determined to be >99% by HPLC after converting (*R*)-**32** to the corresponding benzoyl ester derivative (Chiralcel AD-H, 0.5% *i*-PrOH in hexane, 254 nm, flow rate 0.5 mL/min, 22 °C): (*R*)-isomer *t*_R 9.95 min (major), (*S*)-

isomer t_R 11.25 min (minor).

$[\alpha]_D^{20} -10.1$ ($c = 0.34$, CHCl_3).

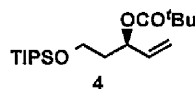
$^1\text{H NMR}$ (500 MHz, CDCl_3) δ 5.89 (ddd, $J = 17.1, 10.4, 5.4$ Hz, 1H), 5.30 (dt, $J = 17.1, 1.6$, Hz, 1H), 5.12 (dt, $J = 10.6, 1.5$, Hz, 1H), 4.42-4.38 (m, 1H), 4.00 (ddd, $J = 10.1, 5.7, 4.4$ Hz, 1H), 3.91 (ddd, $J = 10.2, 7.8, 4.1$ Hz, 1H), 3.57 (br s, 1H), 1.83-1.72 (m, 2H), 1.14-1.05 (m, 21H).

$^{13}\text{C NMR}$ (125 MHz, CDCl_3) δ 140.65 (o), 114.16 (e), 72.65 (o), 62.54 (e), 38.34 (e), 17.99 (o), 11.79 (o).

IR (Neat) 3413 (br, w), 2943 (m), 2866 (m), 1463 (m) 1383 (w), 1100 (m), 991 (m), 882 (s).

HRMS (ESI $[\text{M} + \text{H}]^+$) calcd for $\text{C}_{14}\text{H}_{31}\text{O}_2\text{Si}$ 259.2088, found 259.2090.

(*R*)-5-((Triisopropylsilyl)oxy)pent-1-en-3-yl pivalate



The allylic alcohol **32** (0.81 g, 3.12 mmol) was dissolved in anhydrous tetrahydrofuran (30 mL) and cooled with stirring to 0 °C. Lithium bis(trimethylsilyl)amide (3.12 mL, 3.12 mmol 1.0M solution in THF) was added dropwise at 0 °C, followed by the addition of BOC-ON (1.54 g, 6.24 mmol) in a single portion. The reaction was stirred until the allylic alcohol was consumed 6 hours at room temperature after which, the reaction was quenched by addition of saturated NH_4Cl solution with rapid stirring for 12 hours. The reaction mixture was partitioned between diethyl ether and saturated aqueous NH_4Cl and the phases were separated. The combined organic phases solution were dried with MgSO_4 , filtered and concentrated under *vacuo* to afford a crude oil. Purification by flash chromatography (3-5% diethyl ether in hexanes as eluent) furnished the desired allylic carbonate **4** as a colourless oil (85%, 0.95 g).

$[\alpha]_D^{20} +11.1$ ($c = 0.89$, CHCl_3).

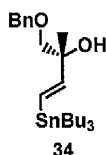
¹H NMR (500 MHz, CDCl₃) δ 5.82 (ddd, *J* = 17.2, 10.5, 6.7 Hz, 1H), 5.31-5.27 (m, 1H), 5.24-5.17 (m, 2H), 3.78 (ddd, *J* = 10.0, 7.8, 5.5 Hz, 1H), 3.74-3.70 (m, 1H), 1.91 (app. ddt, *J* = 13.8, 8.4, 5.4 Hz, 1H), 1.85-1.78 (m, 1H), 1.47 (s, 9H), 1.10-1.00 (m, 21H).

¹³C NMR (125 MHz, CDCl₃) δ 152.86 (e), 136.56 (o), 116.84 (e), 81.81 (e), 74.86 (o), 59.12 (e), 37.50 (e), 27.84 (o), 18.07 (o), 11.98 (o).

IR (Neat) 2943 (m), 2867 (m), 1742 (s), 1463 (m) 1368 (m), 1254 (s), 1166 (s), 1104 (s), 882 (m).

HRMS (ESI, [M + Na]⁺) calcd for C₁₉H₃₈O₄NaSi 381.2437, found 381.2431.

(*R,E*)-1-(Benzyloxy)-2-methyl-4-(tributylstannyl)but-3-en-2-ol



Tri-*n*-butyltin hydride (0.14 mL, 0.53 mmol) was added dropwise at room temperature to a solution of alkyne **33** (0.10 g, 0.53 mmol), and Pd(PPh₃)₄ (0.03 g, 0.026 mmol) in THF (1 mL). The reaction mixture was stirred for 2 hour at room temperature after which it was concentrated under *vacuo* to afford a crude oil. Purification by flash chromatography (5-10% diethyl ether in hexanes as eluent) furnished the desired vinyl stannane **34** as a colourless oil (88%, 0.22 g) with excellent *E/Z* selectivity (≥19 : 1 by ¹H NMR).

[α]_D²⁰ +6.3 (*c* = 0.76, CHCl₃).

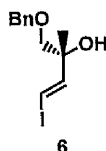
¹H NMR (500 MHz, CDCl₃) δ 7.37-7.28 (m, 5H), 6.31-5.95 (m, 2H), 4.57 (s, 2H), 3.39 (d, A of AB, *J*_{AB} = 9.0 Hz, 1H), 3.35 (d, B of AB, *J*_{AB} = 9.0 Hz, 1H), 2.48 (s, 1H), 1.56-1.47 (m, 6H), 1.33-1.28 (m, 6H), 1.26 (s, 3H), 0.90-0.86 (m, 15H).

¹³C NMR (125 MHz, CDCl₃) δ 151.78 (o), 138.28 (e), 128.44 (o), 127.71 (o), 127.60 (o), 125.74 (o), 77.38 (e), 74.18 (e), 73.44 (e), 29.15 (e), 27.35 (e), 24.58 (o), 13.82 (o), 9.52 (e).

IR (Neat) 3453 (br, w), 2955 (s), 2923 (m), 1603 (w), 1454 (m), 1376 (w), 1096 (s), 991 (m), 734 (m), 696 (s).

HRMS (ESI, $[M + Na]^+$) calcd for $C_{24}H_{42}O_2Na^{116}Sn$ 501.2100, found 501.2086, (ESI, $[M + Na]^+$) calcd for $C_{24}H_{42}O_2Na^{118}Sn$ 503.2099, found 503.2089, (ESI, $[M + Na]^+$) calcd for $C_{24}H_{42}O_2Na^{120}Sn$ 505.2104, found 505.2093.

(*R,E*)-1-(Benzyloxy)-4-iodo-2-methylbut-3-en-2-ol



To a solution of **34** (0.18 g, 0.36 mmol) in diethyl ether (1.8 ml), iodine (2.18 mL, 0.44 mmol, 0.2M in diethyl ether) was added at 0 °C. After stirring for an hour at 0 °C followed by an hour at room temperature, the reaction mixture was quenched with saturated sodium thiosulphate solution (5 mL). The reaction mixture was diluted with diethyl ether and the phases were separated. Combined organic phases were dried on $MgSO_4$, filtered and concentrated under *vacuo* to afford a crude oil. Purification by flash chromatography (30% diethyl ether in hexanes as eluent) furnished the desired vinyl iodide **6** as a yellow oil (90%, 0.11 g).

$[\alpha]_D^{20} +5.2$ (c = 0.52, $CHCl_3$).

1H NMR (500 MHz, $CDCl_3$) δ 7.38-7.30 (m, 5H), 6.59 (d, A of AB, $J_{AB} = 14.5$ Hz, 1H), 6.42 (d, B of AB, $J_{AB} = 14.5$ Hz, 1H), 4.57 (app. t, $J = 12.4$ Hz, 2H), 3.37 (d, A of AB, $J_{AB} = 9.1$ Hz, 1H), 3.32 (d, B of AB, $J_{AB} = 9.1$ Hz, 1H), 2.57 (s, 1H), 1.25 (s, 3H).

^{13}C NMR (125 MHz, $CDCl_3$) δ 149.61 (o), 137.71 (e), 128.59 (o), 127.98 (o), 127.81 (o), 76.90 (o), 76.44 (e), 75.42 (e), 73.55 (e), 24.26 (o).

IR (Neat) 3433 (br, w), 3064 (w), 2858 (w), 1602 (w), 1453 (m), 1201 (m), 1090 (s), 944 (m), 736 (m).

HRMS (CI, $[M + Na]^+$) calcd for $C_{22}H_{15}O_2Na^{127}I$ 341.0015, found 341.0019.

4.6 References

- 1 For reports on rhodium(I)-catalysed allylic substitution reactions from the Evans group, see: (a) Evans, P. A.; Clizbe, E. A. *J. Am. Chem. Soc.* **2009**, *131*, 8722. (b) Evans, P. A.; Qin, J.; Robinson, J. E.; Bazin, B. *Angew. Chem. Int. Ed.* **2007**, *46*, 7417. (c) Evans, P. A.; Lawler, M. J. *Angew. Chem. Int. Ed.* **2006**, *45*, 4970. (d) Evans, P. A.; Lawler, M. J. *J. Am. Chem. Soc.* **2004**, *126*, 8642. (e) Evans, P. A.; Leahy, D. K. *J. Am. Chem. Soc.* **2003**, *125*, 8974. (f) Evans, P. A.; Robinson, J. E.; Moffett, K. K. *Org. Lett.* **2001**, *3*, 3269. (g) Evans, P. A.; Robinson, J. E. *J. Am. Chem. Soc.* **2001**, *123*, 4609. (h) Evans, P. A.; Kennedy, L. J. *J. Am. Chem. Soc.* **2001**, *123*, 1234. (i) Evans, P. A.; Kennedy, L. J. *Tetrahedron Lett.* **2001**, *42*, 7015. (j) Evans, P. A.; Leahy, D. K. *J. Am. Chem. Soc.* **2000**, *122*, 5012. (k) Evans, P. A.; Kennedy, L. J. *Org. Lett.* **2000**, *2*, 2213. (l) Evans, P. A.; Robinson, J. E.; Nelson, J. D. *J. Am. Chem. Soc.* **1999**, *121*, 6761.
- 2 Evans, P. A.; Leahy, D. K. *J. Am. Chem. Soc.* **2002**, *124*, 7882.
- 3 Hillier, M. C.; Price, A. T.; Meyers, A. I. *J. Org. Chem.* **2001**, *66*, 6037.
- 4 Vettel, S.; Vaupel, A.; Knochel, P. *J. Org. Chem.* **1996**, *61*, 7473.
- 5 Evans, P. A.; Nelson, J. D. *J. Am. Chem. Soc.* **1998**, *120*, 5581.
- 6 Leahy, D. K.; Evans, P. A. in *Modern Rhodium-Catalyzed Organic Reactions* (Ed.: Evans, P. A.), Wiley-VCH: Weinheim, **2005**, Ch. 14, pp 301-337.
- 7 Tsuji, J.; Minami, I.; Shimizu, I. *Tetrahedron Lett.* **1984**, *25*, 5157.
- 8 Evans, P. A.; Nelson, J. D. *Tetrahedron Lett.* **1998**, *39*, 1725.
- 9 Evans, P. A.; Uraguchi, D. *J. Am. Chem. Soc.* **2003**, *125*, 7158.
- 10 Evans, P. A.; Leahy, D. K.; Slieker, L. M. *Tetrahedron Asymmetry* **2003**, *14*, 3613.
- 11 Evans, P. A.; Leahy, D. K.; Andrews, W. J.; Uraguchi, D. *Angew. Chem. Int. Ed.* **2004**, *43*, 4788.
- 12 Morrill, C.; Grubbs, R. H. *J. Org. Chem.* **2003**, *68*, 6031.
- 13 Singh, O. V.; Han, H. S. *Org. Lett.* **2007**, *9*, 4801.
- 14 Kim, H.; Lee, C. *Org. Lett.* **2011**, *13*, 2050.
- 15 Pangborn, A. B.; Giardello, M. A.; Grubbs, R. H.; Rosen, R. K.; Timmers, F. J. *Organometallics* **1996**, *15*, 1518.